The oceanographic variability along the North Atlantic margins through the last 2000 yrs: climatic impacts and forcing mechanisms reconstructed from high-resolution diatom records

Dissertation zur Erlangung des Doktorgrades der Naturwissenschaften

im Fachbereich Geowissenschaften der Universität Bremen

Vorgelegt von

Isabelle Martins Gil

Bremen, Mai 2006

Tag des Kolloquiums:
30.06.06

Gutachter :
1. Herr Prof. Dr. Dierk Hebbeln
2. Frau Dr. Fátima Abrantes

Prüfer:
1. Herr Prof. Dr. G. Bohrmann
2. Herr Prof. Dr. K.- U. Hinrichs

Erklärung

Hiermit versichere ich, dass ich

1. die Arbeit ohne unerlaubte fremde Hilfe angefertigt habe,

2. keine anderen als die von mir angegebenen Quellen und Hilfsmittel benutz habe und

3. die den benutzten Werken wörtlich oder inhaltlich entnommenen Stellen als solche kenntlich gemacht habe.

Bremen, den 15. Mai 2006

Isabelle Martins Gil

Acknowledgments

I am deeply grateful to my two supervisors, Priv. Doz. Dr. Dierk Hebbeln (University of Bremen) and Dr. Fatima Abrantes (INETI – Marine Geology Department, Lisbon). Their guidance, support and suggestions have without any doubt contributed to the realization of this thesis. I also thank them for their capacity to find time when deadlines got hot.
I am thankful to Priv. Doz. Dr. Dierk Hebbeln for accepting me as a Ph. D. student and for very helpful advices that helped me to progress and to conclude this thesis.
I am also deeply thankful to Dr. Fatima Abrantes for all her support, her encouraging enthusiasm, friendship and her availability. I also thank her to offer me the chance to board on oceanographic cruises.
I would also like to express my gratitude to Prof. Dr. Gerold Wefer, the head of the Department of Geosciences at the University of Bremen, for welcoming me at the department as a Ph. D. student.
Special thank also to Dr. Lloyd Keigwin for offering me the possibility to work with the material from the Laurentian fan and for his support with quick feedbacks while writing the paper.

I thank Apolónia Inês for all the support in the preparation of the diatom samples at the laboratory of the Marine Geology Department (Lisbon) and her special care. Special thanks to Antje Voelker for interesting and important initial conversations about data; and to Margarida Henriques when solving administrative issue. Thanks are also due to the colleagues of the Marine Geology Department (Lisbon) and of the University of Bremen for their support.
Special "obrigada" to Emilia Salgueiro for her continuous support and company while being in Bremen. Also special acknowledgments to Fontes Mil-Homens family to have been such a reliable and comfortable support during those last years, and especially to Nuno.
"Vielen dank" to Ulrich Alt-Epping for his friendship and also for his practical help while in Bremen, facilitating my stays and making them fun. I would like also to express my gratitude to Silvia Hess and Stefan Rothe for the very warm welcoming into their home and their continuous moral support that helped me to end this thesis with the best conditions.

Special "obrigada" and "merci" to the ones that always accompanied and encouraged the major steps of my life, my family and the "old" friends from Paris, and especially Elodie Cassan for her availability to support me during all those years.

Finally, I would like to dedicate this work to my parents for their continuous support and to have always encouraged all my choices throughout my life. Their strength, optimism and unusual experiences in life have been always an example that incited me to progress. I also thank my sister Stéphanie for her support.

This work has been supported by the European Union through funding of the project HOLSMEER - Late Holocene Shallow Marine Environments of Europe (EVK2-CT-2000-00060) and Ph D. grant (SFRH/BD/18317/2004) awarded by the Portuguese Foundation for Science and Technology (FCT-MCES).

To the ones that will read more than this page, I wish a pleasant reading.

Contents

SUMMARY

Several locations along the North Atlantic margins are investigated to provide high-resolution paleoceanographic reconstructions based on diatom records for the last 2000 yrs: the Tagus pro-delta (SW Portuguese margin, Lisbon latitude), the Skagerrak (NE North Sea) and the Laurentian deep sea fan (South of Newfoundland). At present, through ocean/atmosphere feedbacks, surface ocean changes in the North Atlantic are closely linked to the atmospheric circulation. This link is specifically described by the North Atlantic Oscillation (NAO), which is defined by the NAO index describing the difference in air pressure at sea level between the Azores high and the Iceland low. The NAO is considered as the main climatic factor controlling the northeastward heat flux associated with the Gulf Stream, the wind pattern and the distribution of the precipitation over the North Atlantic realm. Paleoenvironmental reconstructions attempt mainly to evaluate the role of this forcing mechanism through the late Holocene.

Present day oceanographic studies of the sites investigated here indicate certain relationships between the NAO index signal and oceanographic conditions. During NAO negative phases, precipitation over the Iberian Peninsula increase, the bottom currents in the Skagerrak increase, and the waters over the Laurentian fan warm. In contrast, during NAO positive phases, the coastal upwelling affecting the western Portuguese coast, activated by northerly and westerly winds is intensified and more Atlantic water is injected into the Skagerrak. No specific water temperature signal over the Laurentian fan is described for NAO negative phase.

The high sedimentation rates at all sites allow the acquisition of high-resolution paleoenvironmental records. Diatom and phytolith records are used to assess the paleoceanographic changes in different ways: at the Tagus pro-delta, the combination of the proxies helps to identify major flooding of the Tagus river and the intensity and occurrence of upwelling; at Skagerrak, diatoms track the prevalence of the currents based on salinity changes; over the Laurentian fan, diatoms clearly mark the different water masses based on temperature changes.

The major climatic periods of the last 2000 yrs, the Dark Ages (DA), the Medieval Warm Period (MWP) and the Little Ice Age (LIA), are identifiable in the sedimentary sequences of all

sites. Difference in the precise timing of the beginning and the end of those periods can result from dating uncertainties, but also because the time propagation of the oceanic anomalies lead them to be asynchronous. Over the Laurentian fan, the DA, MWP and the LIA are registered at AD 250 – 550, AD 550 – 1550 and AD 1550 – 1850, respectively. The studies from the Skagerrak and the Tagus pro-delta place the DA between AD 475 and 675, whereas the LIA began around AD 1125 at the Skagerrak and AD 1150 at the Tagus pro-delta. Those two periods, generally considered as cold, correspond to diatom dissolution stages in the Skagerrak and to a local warming of the surface waters over the Laurentian fan. Diatom dissolution is likely due to a strengthening of the bottom currents surely associated to increased storminess at Skagerrak. Warming over the Laurentian fan is likely due to a northward migration of the Warm Slope Water Current in response to an intensification of the Labrador Current. At the Tagus pro-delta, the paleoceanographic response differs for the two cold periods: while during the DA coastal upwelling was probably intensified, during the LIA there are strong indications for an increase in the Tagus River input. The warmer MWP is marked by an increased upwelling at AD 900 at the Tagus pro-delta and improved diatom preservation likely associated to the inflow of more saline waters at the Skagerrak. Finally, at the Laurentian fan, the MWP is marked by diatom evidence of ice-drift around AD 1150.

The NAO appears as a forcing mechanism over the North Atlantic realm through the last 2000 yrs, as the main oceanographic and related climatic events revealed by these reconstructions correspond to NAO-type situations, with periods recorded as cold / harsher climate over Western Europe and corresponding to a local warming over the Laurentian fan attributed to NAO negative-like conditions. This is in agreement for the LIA, but not for the DA, when the oceanic response at the Tagus pro-delta is not in phase with the others locations. Such a discrepancy shows that the NAO mechanism by itself is not sufficient to explain all the observed oceanographic variability. The response of the oceanographic systems can vary and the NAO, as an almost hemispheric-wide indicator of the atmospheric setting may not explain more local variations. The Tagus pro-delta is more directly influenced by the Azores high (being even located at an extreme location), and the NAO index expresses a gradient between air pressure cells reflecting their position and strength, but does not necessarily consider their extension. This could explain the discrepancy found in the Tagus pro-delta record.

Another climatic mechanism presenting some imprints over the Laurentian fan is solar forcing. The centennial frequencies and timing of the cooling indicated by the diatom record over the Laurentian fan suggest a higher sensitivity of the upper surface layer to external forcing, such as solar activity. In fact, the cooling events indicated by the diatom record correspond to changes in solar activity (although not all the major changes in solar activity are marked on the diatom record) and the frequencies of 104 and 203 yrs in diatom abundance are in the range of the well-known solar cycles of Gleissberg and de Vries-Suess.

In summary, changes in oceanic circulation associated with the NAO and solar forcing appear to be the main factors influencing the diatom records at the investigated sites through the latest Holocene.

Finally, diatom analyses have been limited by silica dissolution at the Skagerrak and especially at the Tagus pro-delta. However, at the Tagus pro-delta, higher resolution (biennial resolution) analyses of recent sediments (~ the last 100 yrs) are compared to instrumental data, i.e., the measured Tagus River flow and the upwelling index. The comparison between diatom and instrumental records are in good agreement and demonstrate the reliability of diatoms to trace major upwelling and flooding events. Although, the dissolution affecting the diatoms in the older sediments is obvious, it appears that minor peaks in diatom abundance are still marking major upwelling events.

The results obtained from the sites appeal for more records from the North Atlantic margin to improve the paleoceanographic reconstruction over the last 2000 yrs, considering that the "extreme" position of some sites could imply a response different from the one expected from the general climatic setting. Besides, it would provide high-resolution diatom data series to investigate the periodicity of climatic variability associated to solar cycles of different time length.

CHAPTER 1:

General introduction

1. Motivation and main objectives

There is an increasing need for high-resolution records to investigate the short-term climate variability, at decadal and centennial time-scales. Instrumental records of climatic variability are limited in time to the last ~150 years, and proxy records from high-sedimentation rate sites in the ocean are needed to compensate this lack of instrumental data, since a better understanding of past climate change will serve the ability to predict future climate changes.

The North Atlantic Ocean is a key-site of the global climate-ocean system, with its wide meridional connection between the Atlantic and the Arctic oceans (Meincke, 2002) and its large scale oceanic circulation dominated by the deep-water formation in the northern North Atlantic initiating the thermohaline circulation. Salinity changes in the North Atlantic today could lead to abrupt climate changes, with a freshening of this part of the Atlantic reducing or even suppressing the northward heat transport involved in this process and, subsequently, also the formation of deep-water. The paleoceanographic and paleoclimatic variability of the North Atlantic region is recorded at several time scales, with different frequency bands. Millennial and centennial scale variability has been revealed by the study of North Atlantic sediment records (Bond *et al*., 1997, 2001; Black *et al*., 2004), and tree-rings (Ogurtsov *et al*., 2002). The main forcings invoked are the internal variability of the climate system itself and / or the action of external forcing. During the Holocene, millennial-scale Bond cycles are supposedly driven by external solar forcing and, as a consequence, ice sheets around the northern North Atlantic started melting under positive forcing (Bond *et al*., 1997, 2001). Accordingly to Schulz and Paul (2002), a periodicity of 900 yrs recorded in the Greenland ice-cores (in the range of the periodicity found by Bond *et al*. (1997), taking into account the dating uncertainty of 500 yrs) is due to a negative salinity anomaly in the northern North Atlantic, caused by a reduction in northward heat transport that resulted in the generation of cold spells. Besides, a cyclicity of ~1500 yrs is also found in the bottom current strength in the deep North Atlantic (Bianchi and McCave, 1999).

The North Atlantic thermohaline circulation also appears to be affected by a cycle of 512 yrs seen in the atmospheric ^{14}C concentration (Stuiver and Braziunas, 1993). The centennial-scale solar cyclicity, as the Suess-De Vries cycle (Suess and Linick, 1990) of roughly 208-212 yrs, and the Gleissberg cycle (Gleissberg, 1944) of 88 yrs (having probably a wider frequency band), have also been identified in marine sediment records (Hodell *et al*., 2001; Black *et al*., 2004;

Roth and Reijmer, 2005). At present, the frequencies of the North Atlantic climate variability (short term variability) are rather associated to atmospheric changes, such as the North Atlantic Oscillation – NAO (Hurrell, 1995; Hurrell and VanLoon, 1997; Hurrell *et al*., 2001), the Atlantic Multidecadal Oscillation – AMO (Delworth and Mann, 2000), the Arctic Oscillation – AO (Thompson and Wallace, 1998) and the Quasi-Biennale Oscillation – QBO (Baldwin *et al*., 2001).

Although marine sediments as paleoarchives are imperfect recorders of climate signals compared to tree-ring or coral records (because they are affected by the depositional environment, bioturbation and age control uncertainties), they still have the advantage of containing several proxies that bring different and complementary information about e.g. the surface water conditions and, thus, strengthen the interpretation of the paleorecords. The main aim of this study is to provide high-resolution diatom records and contribute to the reconstruction of paleoenvironmental changes in the North Atlantic realm during the last 2000 yrs.

2. Study areas

Three key-sites from the North Atlantic realm have been selected to investigate past oceanic and climatic variability: the Tagus pro-delta (SW Portuguese margin, Lisbon latitude), the Skagerrak (NE-North Sea) and the Laurentian fan (South of Newfoundland). Through ocean-atmosphere feedbacks, the oceanographic circulation of the North Atlantic is an important regulator of the climate along its margins. The Gulf Stream and its extension, the North Atlantic drift, transport heat northward. Strong heat flux corresponds to warm and wet climate in northern Europe. At the opposite, a weaker and more longitudinal heat flux, lead to increasing precipitation on the Iberian Peninsula (Lamb and Peppler, 1987). The heat flux strength is assessed by the NAO (North Atlantic Oscillation). The NAO index (Hurrell *et al*., 2001) is defined by the difference between subpolar-low surface pressure (south and east Greenland) and subtropical high surface pressure (near Azores). At present, all investigated sites are under the influence of a wind pattern which depends on the air pressure cells over the North Atlantic (the Azores high and the Icelandic low). The Tagus pro-delta and the Skagerrak are directly under this climatic pattern, while the water temperature over the Laurentian fan depends mainly on the

strength and orientation of the Gulf Stream and Labrador Current. Each site reveals specific oceanographic features in response to the atmospheric forcing.

The Portuguese margin is affected by seasonal upwelling (from late May to September), instigated by northerly winds associated to the Azores high. Besides, the Tagus outflow depends on the precipitation over the Iberian Peninsula.

The Skagerrak is the deepest part of the Norwegian Trench, but the bathymetry is still relatively shallow (around 300 m water depth and a maximum of 700 m) and the intensity of the currents is sensitive to wind stress and climate changes. The sediment distribution at the sampling site is governed by the Jutland Current, which transports high salinity waters from the North Atlantic including some coastal waters northeastward. At the opposite, the Baltic current crossing the Kattegat channel transports brackish waters westward into the North Sea.

Finally, the Laurentian fan is on the pathway of waters from clearly opposite origins: a minor bifurcation of the Gulf Stream, the Warm Slope Water Current (WSWC) and the cold water from the Arctic and Labrador Seas. At Present, surface water temperature changes over this site are as large as 10ºC and results from the competing influence of those opposite water masses.

The comparison of the paleoceanographic changes at all these sites through the last 2000 yrs will contribute to our understanding of the overall surface water circulation in the North Atlantic.

3. Diatoms, a proxy for paleoenvironmental changes of the last 2000 yrs

3.1 Diatoms

Diatoms are photosynthetic organisms, and as such their habitat is restricted to the photic zone of the ocean, where light and nutrients are the main factors defining their existence. They depend on the conditions of the upper part of the water column and they can be used as paleoenvironmental recorders, as they thrive in waters of a wide range of salinity (from fresh to saline) and temperatures. The variety of diatom species reflects the diversity of the environmental conditions. The main environmental conditions (salinity and temperature) are possibly quantified by the application of transfer functions.

3.2 The Main Climatic Changes of the last 2000 yrs

The main climatic events of the last 2000 yrs (mainly an alternating sequence of cold and warm periods) are reflected in the history of Human society, as their denomination shows: the Roman Warm Period (RWP), the Dark Ages (DA), the Medieval Warm Period (MWP) and the Little Ice Age (LIA). The timing of these periods varies, but it is generally admitted that they had a worldwide expression (Jones *et al.*, 2001; Broecker, 2001).

Records of the RWP are scarce and appear in few studies (Bianchi and McCave, 1999; Mc Dermot *et al*., 2001). The RWP is supposed to have culminated around AD 100 and it is traced in continental and marine records between BC 320 and AD 380 (Hass, 1996). This climatic optimum is followed by a deterioration of the climate, the DA, centered ~ AD 500 – 600 (Keigwin and Pickart, 1999; Bianchi and McCave, 1999; Mikkelsen and Kjuipers, 2001).

The following warm interval, the MWP is often compared to the 20th century warming, to evaluate the impact of anthropogenic activities on climate. Although the MWP was not continuously warm (Grove, 2001), the atmospheric circulation during the medieval times brought greater changes in precipitation than in temperature and it appears like a widespread hydrological anomaly occurring between AD 900 to 1300 (Grove, 2001). Such anomalies were registered at different European locations, but also in California and Patagonia (Grove, 2001; Stine, 1994). As the dominant pattern could not be described by temperature changes alone, it has been suggested to call this period the "Medieval Climatic Anomaly" (Stine, 1994; Bradley *et al*., 2003).

Finally, the LIA is one of the coldest periods of the last ~10 000 cal yrs (Bradley *et al*., 2003). It is marked by major glacier advances (Grove, 2001), but marine evidences are also numerous (Jones *et al.*, 2001). The LIA was under way in the 13th and 14th centuries, culminated during the 17th and 18th centuries and ended around AD 1900 (Grove, 2001; Jones *et al.*, 2001).

3.3 Main climatic forcings

Besides the internal variability of the climatic system itself, the climate is also subject to external forcings. Orbital, solar and volcanic forcings and events (e.g. sudden meltwater outbreaks) are the most important. At the time scale of the records presented here, the orbital forcing (Milankovitch cycles) does not play any role.

Changes in solar insolation since the mid-Holocene appear to be the largest perturbation in radiative forcing since the Laurentian and Fennoscandian ice sheets disappeared (Schmidt *et al*., 2004). Variations in solar activity are slight, but evidences for sun / climate connections are numerous and argue for an impact of solar forcing on the Earth´s climate (Rind, 2002). In fact, imprints of the well-known solar cycles often appear in several proxy records indicating a stronger impact of decadal solar forcing over the continents than over the ocean (Rind, 2002). In addition, the feedbacks of the climate system can have stronger effects than the forcing itself. Solar forcing variability appears to interfere with the atmospheric circulation, as a downward shift of the balance of the AO corresponds to cold temperatures over Europe (Shindell *et al*., 2003).

The major effect of the volcanic activity on climate is related to the emission of dust into the stratosphere, which reduces the solar insolation leading to a wide cooling. For example, the eruption of the Tambora in AD 1815 was followed by a "year without summer" (Briffa *et al*., 1998). However, the short residence time of dust in the stratosphere makes those cooling events limited in time.

4. Material and methods

4.1 Material

Considering the geological time scale, the investigated period is quite short. The materials studied are mainly multicores and box-cores (Fig. 1). Multicoring and box-coring are the most accurate techniques to collect undisturbed surface sediments. On very high sedimentation rate areas, as at the Tagus pro-delta, and the Skagerrak, gravity and piston cores are required to get records spanning the last 2000 years.

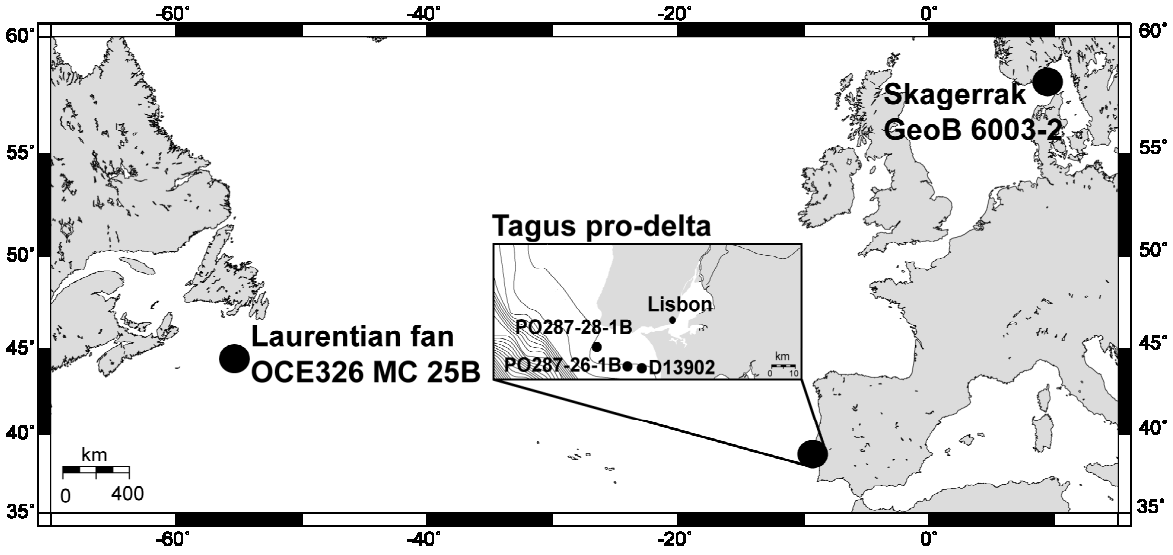

Fig. 1: Map showing the cores location

Core GeoB6003-2 (gravity core) from the Skagerrak was collected during RV Meteor cruise M-45/5 in 1999 from 312 m water depth. D13902 (piston core), PO287-26-1B and PO287-28-1B (box-cores) were collected in the Tagus pro-delta during the RV Discovery 249 and the RV Poseidon PALEO 1 cruises, from 90, 96 and 105 m water depth, respectively. Multicore OCE326MC25B was retrieved from the Laurentian deep sea fan in July 1998, on board the R/V Oceanus from 3890 m water depth.

The multicore and the box-cores were sampled and studied every centimeter, the Skagerrak core has a sampling interval of five centimeter, and the sampling of D13902 is of one centimeter, but the resolution used for this study varies between one and five centimeters.

4.2 Methods

Diatoms: sample preparation and analysis procedure

Diatoms and others siliceous components are extracted from around 1 g of bulk sediment, after calcium carbonate removal using HCl and organic matter oxidation using H_2O_2, according to the method of Abrantes *et al.* (2005). An aliquot of sample is dried on cover slips (Battarbee, 1973), which are mounted on microscope slides. Diatoms are counted and identified at 1000 X magnification, using the counting protocol of Schrader and Gersonde (1978) and Abrantes

(1988). At least 300 specimens per sample are identified to define the diatom assemblage in the Skagerrak and Laurentian fan cores. For the box-cores from the Tagus pro-delta, because the diatom abundance is lower, the number of specimens identified was ≥100, a number considered sufficient for micropaleontology studies by Fatela and Taborda (2002). The diatom amount within the sediments is expressed as Diatom Accumulation Rate (DAR), as number of valves per cm^2/yr, following Abrantes (1988).

The mean diatom diameter is calculated for the species *Paralia sulcata* (Ehrenberg) Cleve and 50 valves are measured. To estimate the general diatom preservation state, the fellowing ratio was used: percentage of poorly preserved valves / (percentage of well preserved valves + percentage of poorly preserved valves) [for a single species] (Abrantes, 1991). In the same way, it is possible to calculate a semi-quantitative temperature index to assess changes in SST: (% cold water diatom species) / (% warm water diatom species + % cold water diatom species). A decrease in the index values indicates increasing temperatures and the diatoms belonging to the genus *Chaetoceros* are excluded in the ratio calculation.

Phytoliths

Phytoliths are an additional proxy of fresh water run-off used in the study of the Tagus pro-delta cores. Phytoliths are silica bodies produced by plants via the deposition of dissolved silica within or between plant cells. Their occurrence in marine sediments indicates a direct influence of continental deposits, as they reach the oceanic domain mainly via river discharge or by wind transport. The identification and classification of opal phytoliths is based on their shape, indicating if they come from tall (Panicoid) or short (Chloridoid) grasses (Twiss *et al*., 1969). The relative abundance of different phytolith morphotypes provides therefore information about continental moisture (vegetation related to dry or wet climate), while their total abundance is considered to be related to precipitation intensity and river flow strength (e.g. flooding). Phytoliths are counted and identified from the same slides prepared for the diatom analyses.

Fe XRF measurements

For the Tagus pro-delta and Skagerrak cores, Fe content was measured by the Bremen CORTEX scanner, a non-destructive XRF system for spliced sediment cores (Jansen *et al*., 1998).

Organic carbon content

The organic carbon content has been measured in the multicore from the Laurentian fan and in the material from the Tagus pro-delta. It is an indicator for primary productivity in the ocean surface waters (Wefer, *et al*., 1999). For its determination, 1cm^3 of bulk sediment has been dried, milled and processed on a CHN-932 LECO elemental analyzer. Organic carbon is calculated by the difference between total carbon and inorganic carbon determined in the same set of samples, before and after being subject to combustion for 8 hours through a predefined stepwise increase temperature up to 400˚C. Analyses are performed on two 1 mg replicates per level.

Spectral analyses

Any periodicity observed in paleorecords provides information to describe and understand the climate variability, what is of special interest in trying to predict future climate development. Specific computer programs have been created to respond to the specificity of paleo data that can be unevenly spaced in time, and to estimate the red-noise background. To analyze the DAR record of the Laurentian fan, the freeware program REDFIT (Schultz and Mudelsee, 2002) has been used.

Age models

The elaboration of age models for such high-resolution and recent sequences is quite a challenge, as the uncertainties of the individual dates can be larger than the sampling resolution. ^{210}Pb and ^{14}C are the most accurate techniques for age model elaboration in such subrecent marine sediments. For ^{210}Pb data, the age error limits are more restricted than for ^{14}C, and the ^{210}Pb profile in the top sediment indicates also if the upper part of the piston or gravity core is really recovered, and it permits to estimate the disturbance / bioturbation of the top part of the core.

For the long-cores and the Laurentian fan multicore, ^{14}C datings on carbonated shells and/or forminifera tests are used as the basis for the age models. Concerning the age models of the Tagus pro-delta box-cores, ^{210}Pb dating, data and ^{14}C datings at the base of the box-cores are in agreement.

5. Main results

5.1 Quantitative diatom analyses—a faster cleaning procedure

Abrantes, F., Gil, I., Lopes, C., Castro, M., 2005

Deep-Sea Research I, 52: 189-198

In view to reduce the time of sample preparation for quantitative diatom analyses, six cleaning procedures were compared to the standard technique used at the INETI-DGM Laboratory. Statistical analyses of the results demonstrated that methods using centrifugation must be eliminated. The chosen procedure is specific in using a non-dried sample dispersed before the chemical attack.

5.2 Diatom as upwelling and river discharge indicators at the Portuguese margin: instrumental data linked to proxy information

Gil, I. M., Abrantes, F., Hebbeln, D.

will be submitted

The river input and the upwelling occurrence and intensity at the Tagus pro-delta is reconstructed for the last ~100 years, based on diatom and phytolith quantitative and qualitative analyses in two box-cores. Proxy records are compared to instrumental data.

Quantitative analyses are performed every centimeter and the age model reveals a roughly biennial time resolution. Results confirm that diatom abundance, and in particular spores of the genus *Chaetoceros*, are good tracers of upwelling intensity. The Tagus river discharge, and in particular the major historic flooding events are well recorded by the abundance of fresh water diatoms and phytoliths. Despite the dissolution affecting biogenic silica in the sediment of this area, the results obtained demonstrate that diatoms are an accurate recorder of upwelling events and river discharge.

5.3 Shallow-marine sediment cores record climate variability and earthquake activity off Lisbon (Portugal) for the last 2000 years

Abrantes, F., Lebreiro, S., Rodrigues, T., Gil, I., Bartels-Jónsdóttir, H., Oliveira, P., Kissel, C, Grimalt, J.O., 2005

Quaternary Science Reviews, 24: 2477-2494

Based on a multiproxy study of the Tagus pro-delta sediment cores, the river input and upwelling occurrence for the last 2000 yrs has been investigated. Besides diatom records, other proxy data have been used: XRF, MST, grain-size and organic carbon measurements, benthic and planktonic foraminifera analysis, and alkenone analysis. A SST variability of 2ºC on a century scale confirms the identification of the MWP and LIA. The presence of freshwater diatoms during the LIA is accompanied by fine-sediment deposition and high *n*-alkane concentrations, reinforcing the diatom indication of increased river discharge for that period. During the MWP, presence of upwelling related diatoms point to increased productivity as well as benthic and planktic foraminifera abundances, while the proxies for river discharge, mean-grain size, magnetic susceptibility, Fe, *n*-alkanes and *n*-alcohols indicate a drier continental climate.

Besides, the sedimentary record presents indications of regional earthquake activity. A major peak in magnetic susceptibility is associated to AD 1755 Lisbon earthquake, which was accompanied by a tsunami and that can explain the loss of 39 cm of sediment, representing 355 years of record and most of the LIA.

5.4 Last two millennia coastal hydrographic and climate changes in the Atlantic Iberian margin (Tagus Prodelta and Muros Ria)

Lebreiro, S., Frances, G., Abrantes, F., Diz, P., Bartels-Jónsdóttir, H., Stroynowski, Z., Gil, I., Pena, L., Rodrigues, T., Nombela, Alejo, Briffa, K., Jones, P., Harris

The Holocene (in press)

The multiproxy study of the Tagus pro-delta is compared with the records from Muros Ría, an area from the NW Iberian margin also characterized by high sedimentation rates. The two areas are comparable only from AD 1150 onwards, because the Muros Ría shows strictly local dynamics until this date. Since AD 1150 the entrance of warmer, oceanic waters caused more intense bottom ventilation in the outer Ría, very likely due to reinforced upwelling. A “suboxic” event, indicative of water stagnation, occurred in the inner Ría around AD 500-700, not noticed in the outer Ría nor the Tagus pro-delta. However, the diatom record points to increased upwelling at the Tagus pro-delta at that time. The last century warming is differently recorded in both areas. The relationship between NAO and the paleoenvironmental variability at the Tagus pro-delta is opposite to the Galician area during the MWP and the LIA. Besides, solar activity is

also an important factor affecting the hydrography in the Tagus area, and the primary production and organic carbon degradation processes in the Muros Ría.

5.5. The North Atlantic Oscillation forcing through the last 2000 years: spatial variability as revealed by high-resolution marine diatom records from N and SW Europe

Gil, I. M., Abrantes, F., Hebbeln, D.

Marine Micropaleontology (in press)

Based on diatom and phytolith records and XRF-Fe measurements from marine sediment cores from the Skagerrak and the Tagus pro-delta, environmental changes are reconstructed for the last 2000 years, focusing on the regional response to changing NAO forcing.

At the Skagerrak, the cold periods of the DA and LIA corresponded to marked diatom dissolution stages, whereas at the Tagus pro-delta the DA were associated with increased diatom production and possible upwelling, and the onset of the LIA corresponded to enhanced flow of the Tagus River. During the MWP, better diatom preservation in the Skagerrak, related to stronger advection of salty Atlantic waters is paralleled by dominant upwelling conditions at the Tagus pro-delta. The comparison of the sites suggests that changes in the marine systems of the Tagus pro-delta and the Skagerrak are mainly explained if NAO is used as an analog. However the different inferred behaviors for the two cold periods at the Tagus pro-delta demonstrate that the NAO is not sufficient to explain the climatic variability at a regional scale.

5.6. Late Holocene coastal hydrographic and climate changes in the eastern North Sea

Hebbeln, D., Knudsen, K. L., Gyllencreutz, R., Kristensen, Klitgaard-Kristensen, Backman, J., Scheurle, C., Jiang, H., Gil, I., Smelror, Jones, P., Sejrup, H.

The Holocene (in press)

Multiproxy studies of Skagerrak's cores and other sites of high-deposition in the North Sea area are compared. Salinity changes are quantified by using diatom transfer functions. A marked environmental shift taking place between AD 700 and AD 1100 with the most pronounced changes occurring at AD 900 is recorded in all the sites. This change is due to an enhanced advection of Atlantic waters to the North Sea, marking the beginning of the MWP. The increase in bottom current strength (unprecedented going back to 1000 BC) indicates major circulation

and productivity changes. During the LIA, the bottom current strength remains at a high level, probably forced by the atmospheric circulation.

5.7. 1750 yrs of rapid oceanographic changes over the Laurentian fan (South of Newfoundland) as revealed by high resolution diatom record

Gil, I. M., Keigwin, L. D., Abrantes, F., Hebbeln, D.

Submitted to Paleoceanography

Diatom analyses have been performed along a sedimentary sequence recovered from the Laurentian deep-sea fan spanning the last 1750 years. The results confirm the occurrence of warm spells between 1750 and 1100 yr BP (DA) and between 500 and 150 yr BP (LIA), most likely due to a northward migration of the Warm Slope Water Current. The diatom assemblages reveal additional major coolings centered around 800 yr BP and 300 yr BP, while the contribution of *N. pachyderma* (s), a cold water planktonic foraminifera species, does not indicate any significant change, suggesting that the cooling events revealed by the diatoms were limited to the near surface water layer. Besides, the timing of the cooling events overlaps major opposite changes in solar activity, the Medieval Maximum and the Maunder Minimum and the diatom record indicates that it occurred in different ways. While the cold event at ~ 800 yr BP appears to be associated with some ice drift related waters from the Gulf of St Lawrence, the cold event at ~ 300 yr BP was preceded by an increase in productivity generated by the presence of a water front between cold nutrient rich water (supplied by a more intense Labrador Current) and more saline WSWC. Finally, the diatom record presents centennial-scale variability, which is in the range of well-known centennial-scale solar cycles. The diatom record shows that the upper surface layers are quite sensitive to solar forcing, even not all the major changes for the studied period are recorded by the diatom.

REFERENCES

Abrantes, F., 1988. Diatoms assemblages as upwelling indicators in surface sediments off Portugal. Marine Geology, 85: 15-39.

Abrantes, F., 1991. Increased upwelling off Portugal during the last glaciation: diatom evidence. Marine Micropaleontology, 17: 285-310.

Abrantes, F., Gil, I., Lopes, C., Castro, M., 2005. Quantitative diatom analyses-a faster cleaning procedure. Deep-Sea Research I, 52: 189-198.

Baldwin, M. P., Gray, L. J., Dunkerton, T. J., Hamilton, K., Haynes, P. H., Randel, W. J., Holton, J. R., Alexander, M. J., Hirota, I., Horinouchi, T., Jones, D. B. A., Kinnersley, J. S., Marquardt, C., Sato, K., Takahashi, M., 2001. The quasi-biennial oscillation, Reviews of Geophysics, 39: 179-229.

Battarbee, R.W., 1973. A new method for estimation of absolute microfossil numbers with reference especially to diatoms. Limnology and Oceanography, 18: 647-652.

Bianchi, G.G., McCave, N., 1999. Holocene periodicity in North Atlantic climate and deep-ocean flow south of Iceland. Nature, 397: 515-517.

Black, D.E., Thunell, R.C., Kaplan, A., Peterson, L.C., Tappa, E.J., 2004. A 2000-year record of Caribbean and tropical North Atlantic hydrographic variability. Paleoceanography, 19(2): doi:10.1029/2003PA000982.

Bond, G., Showers, W., Cheseby, M., Lotti, R., Almasi, P., deMenocal, P., Priore, P., Cullen, H., Hajdas, I., Bonani, G., 1997. A pervasive millenial-scale cycle in North Atlantic Holocene and glacial climates. Science, 278(5341): 1257-1266.

Bond, G., Kromer, B., Beer, J., Muscheler, R., Evans, M. N., Showers, W., Hoffmann, S., Lotti-Bond, R., Hajdas, I., Bonani, G., 2001. Persistent solar influence on north Atlantic climate during the Holocene. Science, 294(5549): 2130-2136.

Bradley, R.S., Hughes, M. K., Diaz, H. F., 2003. Climate in Medieval Time. Science, 302(5644): 404-405.

Briffa, K.R., Jones, P. D., Schweingruber, F. H.; Osborn, T. J., 1998. Influence of volcanic eruptions on Northern Hemisphere summer temperature over the past 600 years. Nature, 393: 450-455.

Broecker, W.S., 2001. Was the Medieval Warm Period global? Science, 291(5508): 1497-1499.

Delworth, T.L., Mann, M.E., 2000. Observed and simulated multidecadal variability in the Northern Hemisphere. Climate Dynamics, 16(9): 661-676.

Fatela, F., Taborda, R., 2002. Confidence limits of species proportions in microfossil assemblages. Marine Micropaleontology, 45: 169-174.

Gleissberg, W., 1944. A secular change in the shape of the spot-frequency curve. The Observatory, 65: 244.

Grove, J., 2001. The onset of the LIA. In: P.D. Jones, Ogilvie, A. E. J., Davies, T. D., Briffa, K. R. (Editors), History and Climate - Memories of the Future? Kluwer Academic/Plenum Publishers, New York, pp. 153-186.

Hass, H.C., 1996. Northern Europe climate variations during the late Holocene: evidence from marine Skagerrak. Palaeogeography, Palaeoclimatology, Palaeoecology, 123: 121-145.

Hodell, D.A., Brenner, M., Curtis, J.H., Guilderson, T., 2001. Solar forcing of drought frequency in the Maya lowlands. Science, 292(5520): 1367-1370.

Hurrell, J.W., 1995. Decadal trends in the North Atlantic Oscillation: Regional temperatures and precipitation. Science, 269(5224): 676-679.

Hurrell, J.W., VanLoon, H., 1997. Decadal variations in climate associated with the North Atlantic Oscillation. Climatic Change, 36(3-4): 301-326.

Hurrell, J.W., Kushnir Y., Visbeck M., 2001. The North Atlantic Oscillation. Science, 291(5504): 603-605.

Jansen, J.H.F., Van der Gaast, S. J., Koster, B., Vaars, A. J., 1998. CORTEX, a shipboard XRF-scanner for element analyses in split sediment cores. Marine Geology, 151: 145-153.

Jones, P. D., Mann, M. E., 2004.Climate over past millennia. Reviews of Geophysics, 42, doi:10.1029/2003RG000143.

Jones, P.H., Osborn, T. J., Briffa, K. R., 2001. The evolution of climate over the last Millenium. Science, 292(5517): 662-667.

Keigwin, L.D., Pickart, R. S., 1999. Slope water current over the Laurentian Fan on interannual to millenial time scales. Science(5439), 286: 520-523.

Lamb, P.J., Peppler R. A., 1987. North Atlantic Oscillation: Concept and an Application. Bulletin American Meteorological Society, 68 (10): 1218-1225.

McDermott, F., Mattey, D.P.,Hawkesworth, C., 2001. Centennial-scale holocene climate variability revealed by a high-resolution speleothem delta O-18 record from SW Ireland. Science, 294(5545): 1328-1331.

Meincke, J., 2002. Climate dynamics of the North Atlantic and NW-Europe: an observation-based overview. In: G. Wefer, Berger, W. H., Behre, K. E., Jansen, E. (Editors), Climate developement and History of the North Atlantic realm. Springer-Verlag, Berlin Heidelberg, pp. 25-40.

Mikkelsen, N., Kuijpers, A., 2001. Natural climate variations in a geological perspective. Gads Forlag., Copenhagen.

Ogurtsov, M.G., Kocharov, G. E., Lindholm, M., Merilainen, J., Eronen, M., Nagovitsyn, Y. A., 2002. Evidence of solar variation in tree-ring-based climate reconstructions. Solar Physics, 205(2): 403-417.

Rind, D., Shindell, D., Perlwitz, J., Lerner, J., Lonergan, P., Lean, J., McLinden, C., 2004. The relative importance of solar and anthropogenic forcing of climate change between the Maunder Minimum and the present. Journal of Climate, 17: 906-929.

Rind, D., 2002. The sun's role in climate variations. Science, 296: 673-677.

Roth, S., Reijmer, J.J.G., 2005. Holocene millennial to centennial carbonate cyclicity recorded in slope sediments of the Great Bahama Bank and its climatic implications. Sedimentology, 52(1): 161-181.

Schmidt, G.A., Shindell, D.T., Miller, R.L., Mann, M.E., Rind, D., 2004. General circulation modelling of Holocene climate variability. Quaternary Science Reviews, 23(20-22): 2167-2181.

Schrader, H.J., Gersonde, R., 1978. Diatoms and Silicoflagellates. Utrecht Micropaleontological Bulletin, 17: 129-176.

Schultz, M., Mudelsee, M., 2002. REDFIT: estimating the red-noise spectra directly from unevenly spaced paleoclimatic time series. Computers and Geosciences, 28: 421-426.

Schultz, M., Paul, A., 2002. Holocene climate variabilitty on centennial-to-millenial time scales: Climate records from the North-Atlantic realm. In: G. Wefer, Berger, W. H., Behre, K. E., Jansen, E. (Editors), Climate developement and History of the North Atlantic realm. Springer-Verlag, Berlin Heidelberg, pp. 41-54.

Shindell, D. T., Schmidt, G. A., Miller, R. L., Mann, M. E., 2003. Volcanic and solar forcing of climate change during the preindustrial era. Journal of Climate, 16: 4094-4107.

Stine, S., 1994. Extreme and Persistent drought in California and Patagonia during Medieval Time. Nature, 369(6481): 546-549.

Stuiver, M., Braziunas, T. F., 1993. Sun, ocean, climate and atmospheric $^{14}CO_2$: an evaluation of causal and spectral relationships. The Holocene, 3, 4: 289-305.

Suess, H.E., Linick, T.W., 1990. The C-14 Record in Bristlecone-Pine Wood of the Past 8000 Years Based on the Dendrochronology of the Late C.W. Ferguson. Philosophical Transactions of the Royal Society of London Series A-Mathematical Physical and Engineering Sciences, 330(1615): 403-412.

Thompson, D.W.J., Wallace, J.M., 1998. The Arctic Oscillation signature in the wintertime geopotential height and temperature fields. Geophysical Research Letters, 25(9): 1297-1300.

Twiss, P.C., Suess, E., Smith, R. M., 1969. Morphological classification of grass phytoliths. Soil Science Society of America Proceedings, 33: 109-115.

Wefer, G., Berger, W. H., Bijma, J., Fischer, G., 1999. Clues to ocean History: a brief overview of proxies. In: G. Fischer, Wefer, G. (Editors), Use of proxies in paleoceanography: examples from the South Atlantic. Springer-Verlag, Berlin Heidelberg, pp. 1-68.

CHAPTER 2:

Quantitative diatom analyses—a faster cleaning procedure

Abrantes, F., Gil, I., Lopes, C., Castro, M.,

*Deep-Sea Research I, 52: 189-198 (*2005*)*

Available online at www.sciencedirect.com
SCIENCE DIRECT®
DEEP-SEA RESEARCH PART I
Deep-Sea Research I 52 (2005) 189–198 www.elsevier.com/locate/dsr

Instruments and Methods

Quantitative diatom analyses—a faster cleaning procedure

F. Abrantes [a*], I. Gil [a], C. Lopes [a, b], M. Castro [c]

[a] Departamento de Geologia Marinha, Instituto National de Engenharia, Technologia e Inovação-INETI, Aptdo. 7586, Estrada da Portela, Alfragide 2721, Portugal

[b] College of Oceanic and Atmospheric Sciences, Oregon State University, USA

[C] Centro de Ciencias do Mar, Universidade do Algarve, Portugal

Received 13 June 2003; accepted 27 May 2004 Available online 11 November 2004

Abstract

Laboratory techniques employed for cleaning marine sediments for quantitative diatom analyses are time consuming and expensive. In an attempt to reduce preparation time, the method in use in our laboratory, has been compared to six other different methods, which derive from Barron's procedure for rapid sample preparation at sea.

Based on the statistical analyses of the results all the methods in which centrifugation was used, were eliminated. From the two methods that did not show differences from the control method, the cleaner and better preservation of the diatom specimens observed in the slides produced by method M2 lead us to elect this procedure as the best. This method distinguishes itself from other techniques in using of a non-dried sample dispersed before the chemical attack.

Keywords: Diatoms; Cleaning procedure; Quantitative analyses; Paleoproductivity; Paleoceanography; Paleoclimatology

*Corresponding author. Tel.: +351 21470 5535; fax: +351 21471 9018.
E-mail address: fatima.abrantes@ineti.pt (F. Abrantes).

1. Introduction

Diatoms constitute the basis of the food chain and are the dominant phytoplankton in the most productive regions of the world's oceans, the upwelling areas (both coastal and equatorial). In papers recently published, Falkowsky (Falkowski *et al*., 1998; Falkowski, 2002) calls the attention for the importance that phytoplankton and diatoms in particular may have in climate

regulation in the future as major players in the sequestration of CO_2 from the atmosphere. The need to understand their distribution, abundance and species composition in past oceans, as well as their relation/reaction to past climate change is therefore, of primary importance. At present, coring technology is capable of retrieving long sedimentary sequences from marginal regions with sedimentation rates high enough to resolve past climate variability at a decadal scale. However, current laboratory preparation methodologies, quantitative microscopic counting, and observation techniques are very laborious and time-consuming and prevent diatomists from fulfilling the need of simultaneously obtaining long and high-resolution diatom records. A number of procedures have been employed to clean siliceous microfossils (cf. Schrader and Schuette, 1968; Schrader and Gersonde, 1978; Fenner, 1982; Scherer, 1994). Abrantes (1988) has combined and adapted Fenner's cleaning procedure (Fenner, 1982) with Battarbee's technique for quantitative slide preparation (Battarbee, 1973). The method has been successfully used in several distinct diatom studies over the last several years (cf. Abrantes, 1988; Nave *et al*., 2001). However, the cleaning procedures for clay and/or organic carbon-rich sediments, keep samples in the laboratory for long periods of time, with the danger of loss of siliceous material by dissolution during preparation. In an attempt to reduce the laboratory preparation time, Barron's procedure for rapid sample preparation at sea (Barron, 1985) was used as the basis for the new approaches. In order to control the representativeness of the concentration/absolute abundances of microfossils as estimated from sample aliquots, marker microspheres (ECRC divinylbenzene microsphere solution) were added to a set of 25 samples randomly selected from the samples/areas under study at the INETI's Marine Geology Laboratory.

This paper presents the results obtained with the tests of various laboratory methods, as well as with the test of the counting procedure, and, proposes a new, faster and more efficient laboratory methodology.

2. Materials and methods

2.1. Sample cleaning procedures

Seven different methods were tested on a single sample (GeoB 6003-1 35–36 cm). The differences introduced are restricted to the cleaning methodology; all other phases of the quantitative estimation were maintained, according with the routine protocol. One of the methods, the control, followed the cleaning procedure used routinely until now (Abrantes, 1988)

and the other 6 consisted in modifications of the rapid procedure (Barron, 1985).

2.1.1. The control method—control

The method in use in our laboratory (Abrantes, 1988) is a follow up of the method of Fenner (1982) and includes the following steps:

- Weight a known volume of sample (about 2 cc), dry over night at 40 °C and weight again.
- Place the material in 250 ml beakers and attack for carbonate and organic matter destruction with 25 ml 10% hydrochloric acid (HCl) and 25 ml 35% hydrogen peroxide (H_2O_2–110 V). Let the reaction take place at room temperature, when finished, put the beakers over a hotplate at 120 °C until reaction stops.
- Add distilled water and leave to settle for about 8 h and then gently remove the excess liquid (correspondent to a 9 cm height) with the help of a vacuum pump. Repeat this operation until the solution has a neutral pH.
- To remove the clay fraction, fill the beakers with a 0.5% sodium pyrophosphate solution and leave for 8 h, then remove the excess liquid of the suspension with the help of a vacuum pump. Add distilled water, let rest for another 8 h and gently remove excess liquid with the help of a vacuum pump. Repeat sodium pyrophosphate/ distilled water washing until no clay remains in suspension.

2.1.2. New methods

The new methods followed from modifications of the rapid cleaning procedure proposed by Barron (1985) for fast sample preparation at sea, and start with a bulk non-dried sediment sample:

2.1.2.1. Method 1—M1 (Barron's laboratory procedure)

- Weight about 1 g of bulk sediment and place it in 50 ml centrifuge tubes.
- Attack carbonate with 25 ml 10% HCl.
- Decant excess acid.
- Attack organic matter with 25 ml 30% H_2O_2.
- Clean off excess acid and H_2O_2 through centrifuging 2 min at 1200 rpm with distilled water.

- Decant liquid, wash in distilled water and repeat washing/centrifuging 3 times.
- For clay dispersion and remotion, put the solution in a 250 ml beaker, add a 0.5% sodium pyrophosphate solution and leave for 8 h. Gently wash sodium pyrophosphate solution with the help of a vacuum pump, add distilled water, let rest for another 8 h, and wash excess liquid with the help of a vacuum pump. Repeat sodium pyrophosphate/distilled water washing until no/little clay remains in suspension.

2.1.2.2. Method 2—M2

- Weigh about 1 g of bulk sediment and place it in 250 ml beakers.
- Promote clay dispersion by adding a 0.33% calgon water softener (Calgon contains sodium phosphate and sodium carbonate) and let sample rest over night or by about 12 h.
- Attack organic matter with 25 ml 30% H_2O_2.
- Attack carbonate with 25 ml 10% HCl.
- After reaction cease, clean off excess acid and H_2O_2 by decanting liquid, wash in distilled water and repeat decantation until clays start to be in suspension.
- For clay cleaning, add distilled water, let rest for 8 h and decant remnant. Repeat distilled water washing until no clay remains in suspension.

2.1.2.3. Method 3—M3 (Barron's procedure for rapid cleaning at sea+clay cleaning)

- Weight about 1 g of bulk sediment and place it in 50 ml centrifuge tubes.
- Attack carbonate with 25 ml 10% HCl.
- After reaction ceases and no material is in suspension decant excess acid.
- Attack organic matter with 25 ml 30% H_2O_2.
- Clean off excess acid and H_2O_2 through centrifuging at 1200 rpm/2 min with distilled water.
- Decant liquid, wash in distilled water and repeat washing/centrifuging 3 times.
- For clay cleaning, shake residue with 0.5% sodium pyrophosphate centrifuge twice at 1200 rpm/2 min. Then shake residue with distilled water and centrifuge 3 times at 1200 rpm/ 2 min.

2.1.2.4. Method 4—M4 (same as 1 without centrifuge)

- Weight about 1 g of bulk sediment and place it in 250 ml beakers.

- Attack carbonate with 25 ml 10% HCl.
- Attack organic matter with 25 ml 30% H_2O_2.
- Clean off excess acid and H_2O_2 by decanting liquid, wash in distilled water and repeat decantation until clays start to be in suspension.
- For clay cleaning add a 0.5% sodium pyrophosphate solution and let rest for 8 h. Gently wash sodium pyrophosphate solution with the help of a vacuum pump, add distilled water, let rest for another 8 h, and wash excess liquid with the help of a vacuum pump. Repeat sodium pyropho-sphate/distilled water washing until no clay remains in suspension.

2.1.2.5. Method 5—M5

- Same as Control method.
- Clay cleaning in centrifuge tubes (less height implies faster settling of particles and less than 8 h waiting time between washes).

2.1.2.6. Method 6—M6 (same as 2 with centrifuge)

- Weigh about 1 g of bulk sediment and place it in 50 ml centrifuge tubes.
- Promote clay deflocculation by adding a 0.33% Calgon solution and let sample rest over night or by about 12 h.
- Attack organic matter with 25 ml 30% H_2O_2.
- Attack carbonate destruction with 25 ml 10% HCl.
- Clean off excess acid and H_2O_2 through centrifuging 2 min at 1200 rpm with distilled water.
- Decant liquid, wash in distilled water and repeat washing/centrifuging 3 times.
- For clay cleaning add a 0.5% sodium pyrophosphate solution and leave for 8 h. Gently wash sodium pyrophosphate solution with the help of a vacuum pump, add distilled water, leave for another 8 h, and wash excess liquid with the help of a vacuum pump. Repeat sodium pyrophosphate/distilled water washing until no clay remains in suspension.

2.2. Slide preparation

For slide preparation, a known volume of the solution resultant of any of the preparation procedures is poured in the ‘‘Battarbee circular evaporation tray’’ (Battarbee, 1973) after stirring the solution for homogenization. Then, the plate is let to rest in an undisturbed environment to allow particles to settle randomly into the four 20 mm diameter cover slips placed in the evenly spaced wells made on the tray floor (Fig. 2 in Battarbee, 1973). When evaporation is complete and cover slips are dry, cover slips are removed and mounted on slides with Permount mounting medium.

3. Diatom quantification

Quantification of diatoms is done at 1000 x s magnification using a Nikon microscope with differential interference contrast (DIC) illumination. Quantitative abundance estimates of the several groups considered (centric diatoms, pennate diatoms, freshwater diatoms, *Chaetoceros* resting spores, fragments of centric diatoms, fragments of pennate diatoms) are based on the median value obtained for each group/variable from the counting of 100 random fields of view on 3 replicate slides for each sample. For the quantitative estimation all groups lying within each field of view are counted, and the 100 fields of view observed per slide are distributed as shown in Fig. 1. With this counting method, and knowing the area of each microscopic field of view, the absolute number of diatom valves per g of sediment can be calculated as follows:

$$\text{No. valves/g} = ((N*(S/s))*(V/v))/W,$$

where N is the median of the number of valves counted in 100 fields of view in the three replicate slides, S is the area of the evaporation tray, s is the area of the slide counted, V is the volume of solution in the beaker, v is the volume of solution put into the evaporation tray, W is the weight of raw sample, and (S/s) is a constant for each microscope.

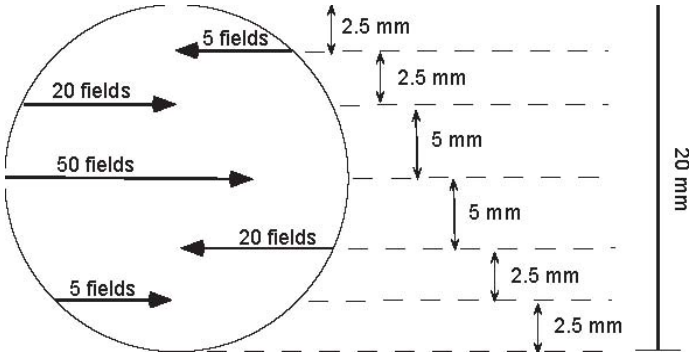

Fig. 1. Representation of the distribution on the slide of the 100 fields of view observed for the quantitative estimation of all groups.

The counting procedure and definition of counting units followed those of Schrader and Gersonde (1978).

Twenty-two fractions of the sample were obtained, 4 were processed according with the control method and the other 18 were separate in six groups of 3 per each of the new methods. For each fraction four slides were prepared according to Battarbee's plate method (1973). Three slides were counted and the median of the counts for each parameter (log transformed) constituted the basic data for the statistical analysis.

3.1. How represenatitive of real abundances are the estimated diatom concentrations?

The fact that only a known volume aliquot of the sample solution is put to dry rather than the total sample, may raise questions relatively to the representativeness of the concentrations of microfossils absolute abundances estimated from these aliquots. Besides, the different laboratory methodologies were to be evaluated on the basis of statistical analysis of the median values resultant from the counts of aliquots, we needed to test the reliability of our slide preparation and counting procedures. To do so, we have randomly selected 25 samples from different locations and variable diatom abundances (Table 1). Each sample was now prepared according to the control method and after the last wash, that is, right before pouring the solution into the plates, each sample was spiked with microsphere markers following Battarbee and Kneen (1982). The known microsphere concentration solution used was the ECRC divinylbenzene microsphere solution. The volume of solution added to each sample was calculated on the basis of the sample initial weight according to the ECRC instructions, and pipeted after 1 min sonication, to guaranteee homogenization of the microsphere solution.

4. Statistical analysis

A test of homogeneity of variances was done prior to deciding which group comparison tests should be used. The Leven's test for homogeneity of variances (Snedecor and Cochran, 1980) showed that two of the dependent variables considered did not have homogenous variances (p-value <0.05) (Table 2). The methods were therefore compared using a non-parametric technique, the Kruskal–Wallis test (Table 2) (Hollander and Wolfe, 1973). For the variables showing significant differences for the method used (p-value <0.05), all possible combinations of two methods were compared using the Wilcoxon test for two independent samples (Hollander and Wolfe, 1973). The same test was used for comparing the control method and the new method considered the best in terms of the qualitative evaluation.

The preliminary data exploration of microsphere addition for the estimation of microfossils concentration in the sample, suggested a correlation between the concentration with the order of sample preparation. A Sperman correlation test was used to test microsphere concentration and order of the sample.

All statistical analysis was done using the software SAS (SAS Ins., 2000).

Table 1
List of samples spiked with marker microspheres (ECRC divinylbenzene microsphere solution)

Sample ID	Sequence No.	Geographic location
LEG 175 1083D 4H-2W (32–34 cm)	1	SW Africa (ODP LEG 175)
LEG 175 1083D 4H-2W (132–134 cm)	2	SW Africa (ODP LEG 175)
LEG 175 1083D 3H-3W (92–94 cm)	3	SW Africa (ODP LEG 175)
GeoB M4241-11 (87–89 cm)	4	NW Africa–Canary Islands
GeoB M4241-11 (91–93 cm)	5	NW Africa–Canary Islands
LEG 175 1083D 3H-4W (2–4 cm)	6	SW Africa (ODP LEG 175)
LEG 175 1083D 3H-6W (97–99 cm)	7	SW Africa (ODP LEG 175)
LEG 175 1083D 3H-6W (112–114 cm)	8	SW Africa (ODP LEG 175)
LEG 175 1083D 3H-6W (122–124 cm)	9	SW Africa (ODP LEG 175)
LEG 175 1083D 3H-7W (22–24 cm)	10	SW Africa (ODP LEG 175)
LEG 175 1083D 3H-7W (42–44 cm)	11	SW Africa (ODP LEG 175)
LEG 175 1083D 3H-CCW (12–14 cm)	12	SW Africa (ODP LEG 175)
LEG 175 1083D 4H-1W (2–4 cm)	13	SW Africa (ODP LEG 175)
GeoB M4242-5 (47–49 cm)	14	NW Africa–Canary Islands
GeoB M5559-2 (42–44 cm)	15	NW Africa–Canary Islands
GeoB M4242-5 (137–139 cm)	16	NW Africa–Canary Islands
GeoB M4242-5 (142–144 cm)	17	NW Africa–Canary Islands
GeoB M4242-5 (87–89 cm)	18	NW Africa–Canary Islands
GeoB M4242-5 (462–464 cm)	19	NW Africa–Canary Islands
GeoB M4242-5 (472–474 cm)	20	NW Africa–Canary Islands
GeoB M4242-5 (382–384 cm)	21	NW Africa–Canary Islands
LEG 175 1083D 3H-3W (107–109 cm)	22	SW Africa (ODP LEG 175)
GeoB M4241-11 (137–139 cm)	23	NW Africa–Canary Islands
GeoB M4242-5 (58–59 cm)	24	NW Africa–Canary Islands
LEG 175 1083D 4H-2W (97–99 cm)	25	SW Africa (ODP LEG 175)

5. Results

5.1. Sample cleaning procedures

The first important result is that all 6 tested methods allow a reduction in laboratory preparation time of at least 2 weeks (Table 3). The abundances estimated for the groups considered in each replicate of the 7 methods utilized, the control method plus the 6 new tested methodologies are available on request (Electronic Supplement Table).

5.2. Slide preparation and diatom quantification

The results of the test to the reliability of the slide preparation and diatom quantification procedures, are presented in Fig. 2 which shows the estimated vs the range of expected number

of microspheres in each sample. The range of expected numbers was calculated from the volume of microsphere solution added to each sample and the estimated number based on the counting procedure described in Section 3 (diatom quantification). With the exception of 7 samples (3, 6, 7, 8, 9, 23, 25), the median of the estimated number, used as the accepted concentration, are within the expected limits.

Table 2
p-values associated with the Leven's test for homogeneity of variance and the Kruskal–Wallis test

Variables	Leven's	Kruskal–Wallis
Centric	0.0846	0.1105
Pennate	0.0943	0.1199
Fragments centric	0.0426	0.0635
Fragments pennate	0.3047	0.1201
Spores	0.6414	**0.0408**
Total diatoms	0.0480	0.0932

Centric—centric diatoms; Pennate—pennate diatoms; Fragments centric—fragments of centric diatoms; Fragments pennate—fragments of pennate diatoms; Spores—resting spores mainly of the genus *Chaetoceros*; Tot diatoms—Sum of centric and pennate diatoms.

5.3. Statistical analysis

The results of Leven's test for homogeneity of variance, and the Kruskal–Wallis test for methods comparison are presented in Table 2. Only for spores, the overall comparison of the 7 methods was significant. For this variable, pairwise comparisons of all possible combinations of the methods were done using the Wilcoxon test. The results are shown in Table 4.

From the microscopic observation of all samples prepared (3 slides for each three replicates of the 6 methods, and three slides for each of the four replicates of the control method, in a total of 66 slides), it became clear that the slides produced by test method 2 were cleaner in aspect and diatom valves showed better preservation. The control and method 2 were compared for all variables considered using the Wilcoxon test (Table 5) and none of the comparisons was significantly different (*p*-values ranging from 0.16 to 0.72).

Table 3
Comparison of the 7 methods main procedures and laboratory preparation time

Method	Sample dry	Sample dispersion	Chemical attack (with centrifuge)	Clay cleanning (with centrifuge)	Total time (days)
Control	Yes	No	No	No	25
M1	No	No	Yes	No	7
M2	No	Yes	No	No	5
M3	No	No	Yes	Yes	1
M4	No	No	No	No	7
M5	No	No	No	Yes	1
M6	No	Yes	Yes	No	5

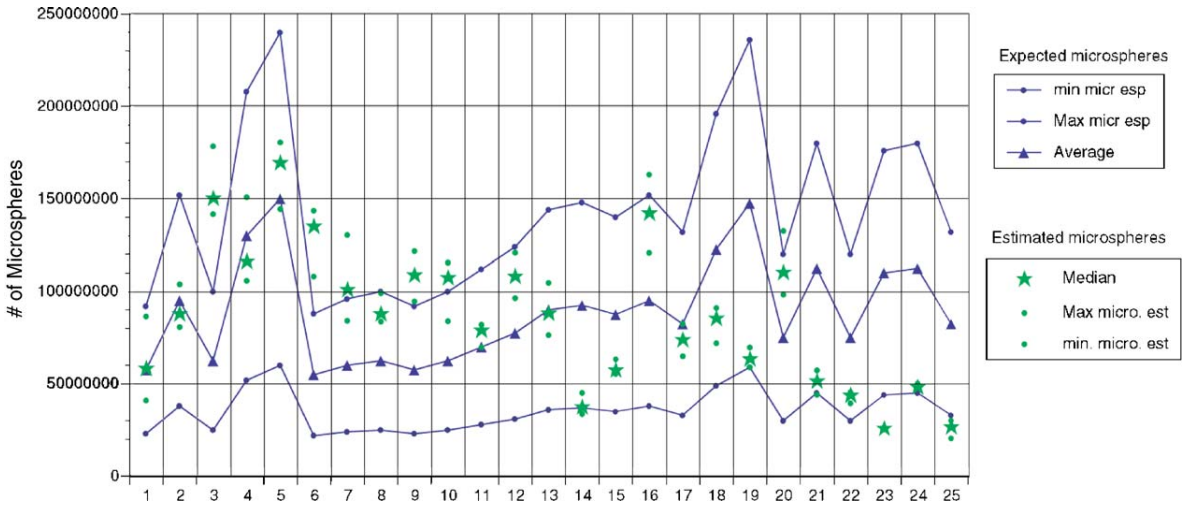

Fig. 2. Comparison of the expected and estimated number of microspheres. Maximum and minimum expected values are calculated based on the concentration of marker microspheres in the solution indicated by the producing company. Estimated value is the median value of the three counted slides for each sample.

Table 4
Table showing the combinations of method with significant differences with respect to the variable spores

	M1	M2	M3	M4	M5	M6
Control						
0.0771		0.1573	**0.0339**	1.000	**0.0339**	0.7237
M1		0.8273	0.2752	0.5637	0.2752	**0.0495**
M2			0.1266	0.1266	0.5637	0.1266
M3				0.0833	0.8273	**0.0495**
M4					0.0833	1.0000
M5						**0.0495**

Method M2 and M4 did not show any differences when compared with all the other methods. Comparisons were made using the Wilcoxon test, the *p*-value of the test is shown in the cells. Significance considered for *p*-value <0.05 (values in bold).

6. Discussion and conclusions

Paleoceanographic and paleoproductivity reconstructions based on diatoms, impose the calculation of diatom accumulation rates. For that to be achieved, diatom abundances have to be determined in a quantitative way and density and porosity of the sediment has to be known. This requires a known volume of sample to be dried, resulting in the ‘‘cooking’’ of the clay component of the sediment and consequently making dispersal of sediment and removal of the organic matter difficult, often requiring more than one H_2O_2 attack. Given that sediment density and porosity can nowadays be estimated through automatic and continuous non-invasive measurement systems, such as the GRAPE system (Ortiz and Rack, 1999) available in multisensor tracks (MST) and used in most coring campaigns, cleaning procedures can now be done without drying the samples. This is the main difference between the control method and the new tested methods, a difference that appears to be of great importance, given that it reduces the time needed for sample preparation from 25 to 5 days at the most.

Table 5
Comparison of the control method with M2

Variable	*p* Value
Centric	0.6067
Pennate	0.1366
Fragments centric	0.4375
Fragments pennate	0.7749
Spores	0.8057
Totaldiatoms	0.4041

Comparisons were made using the Wilcoxon test.

6.1. Slide preparation and diatom quantification

Given that the methods comparison is based on the various groups concentrations, as estimated from known volume aliquots of the whole solution resultant from the laboratory treatment, we will start by discussing the results of the test used to check its representativeness, that is the addition of a known quantity of marker microspheres to 25 randonmly selected sediment samples with variable diatom abundances (Battarbee and Kneen, 1982).

The results (Fig. 2) show that most estimated numbers (76%) are within the range of expected values confirming Battarbee's settling tray method and slide counting technique as reliable for diatom quantification. However, a closer observation of the graphic, reveals a tendency for the estimated values to decrease between the first and last sample prepared, a tendency that is confirmed when the difference between the estimated and expected average value is calculated (Fig. 3). This difference although not clearly related to the volume of microsphere solution added to the sample (Fig. 4), does show mainly negative values, that is, less microspheres estimated then expected, for the small volumes and mainly positive differences for the larger volumes. These results indicate that the ECRC stock solution was not well homogenized at the time it was sampled and increased in microspheres concentration with utilization, meaning that longer sonication time is needed for a better mixing of the microsphere solution before addition to the sample.

6.2. Sample cleaning procedures

From the statistical analysis of the results obtained by all 7 methods (control, plus 6 new

methodologies), significant differences in abundance values were found only with respect to spores and for methods M3, M5 and M6 (Table 4). The group spores corresponds to the resting spores of the genus *Chaetoceros* Ehrenberg that generally dominates diatom assemblages both in the plankton and the sediment record of coastal upwelling areas (cf. Estrada and Blasco, 1985; Abrantes and Moita, 1999; Abrantes *et al*., 2002). As so, it is important to understand the reason behind the observed differences. Spores are heavily silicified and resistant to breakage and dissolution when compared to other diatom species. Its occurrence in higher numbers when the method used for sample preparation includes centrifuging for clay cleaning (M3 and M5), can be interpreted as the result of breakage and/or loss of the more fragile and/or less resistant pennate forms as indicated by the increase in abundance of pennate fragments found for this method. It should also be noted that spores estimated abundance is different between M6 and all the other methods that involve centrifugation (M1, M3, M5), indicating that the spores concentration effect is less important if sample dispersion is done before the chemical attack and centrifuging as in M6. Given the importance of this group in coastal productive areas and the shown tendency to become concentrated by any laboratory preparation method that involves centrifugation, this group should always be counted separately from other diatoms.

Even though methods M1, M3, M5 and M6 are faster due to the use of centrifugation to separate the fraction of interest, the reported differences advice for discontinuation in their use, in particular for diatom quantitative studies.

Of the two methods that showed no difference to the control method, M2 and M4, microscopic observation of the slides showed cleaner samples (easier for microscopic observation) and better preservation of diatom specimens on the slides produced by M2, in which dispersion was done previously to the attack for carbonate and organic carbon destruction, and no centrifugation was applied.

Method M2 is then proposed as the more appropriate for the cleaning of marine sediments when the quantitative estimation of diatom abundance is the objective. Moreover, the use of a method that does not introduce differences in abundance estimation is of extreme importance to allow comparisons to data obtained previously with the methodology identified as Control.

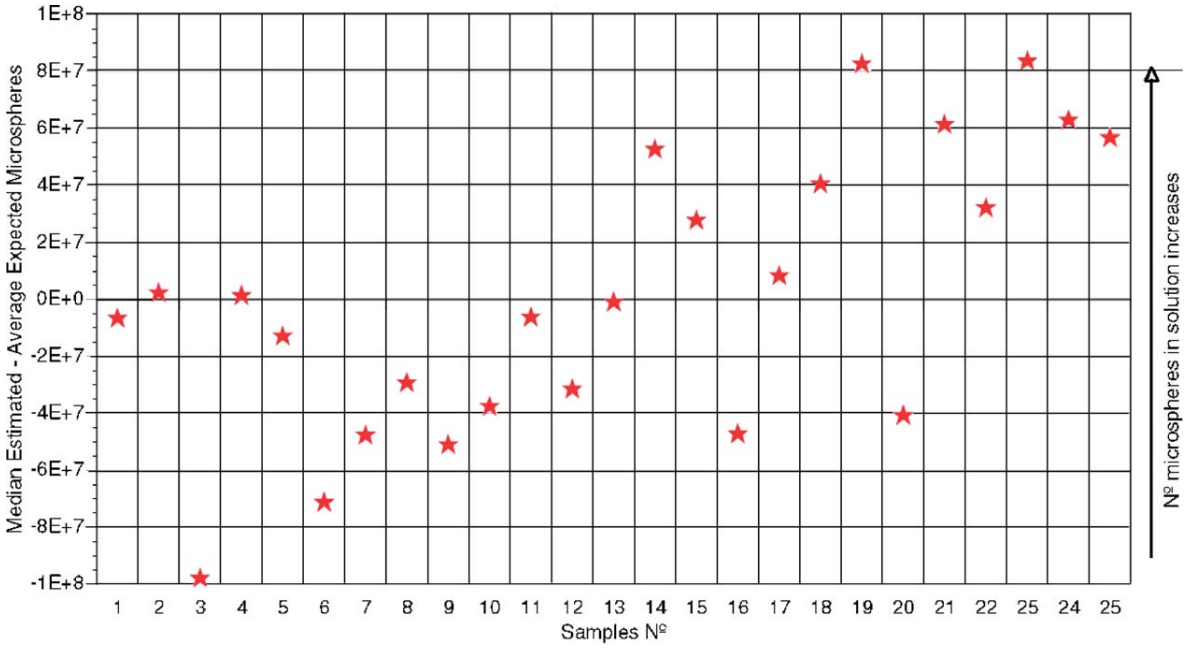

Fig. 3. Difference between the average expected number and the median estimated value, along the sequence of sample preparation.

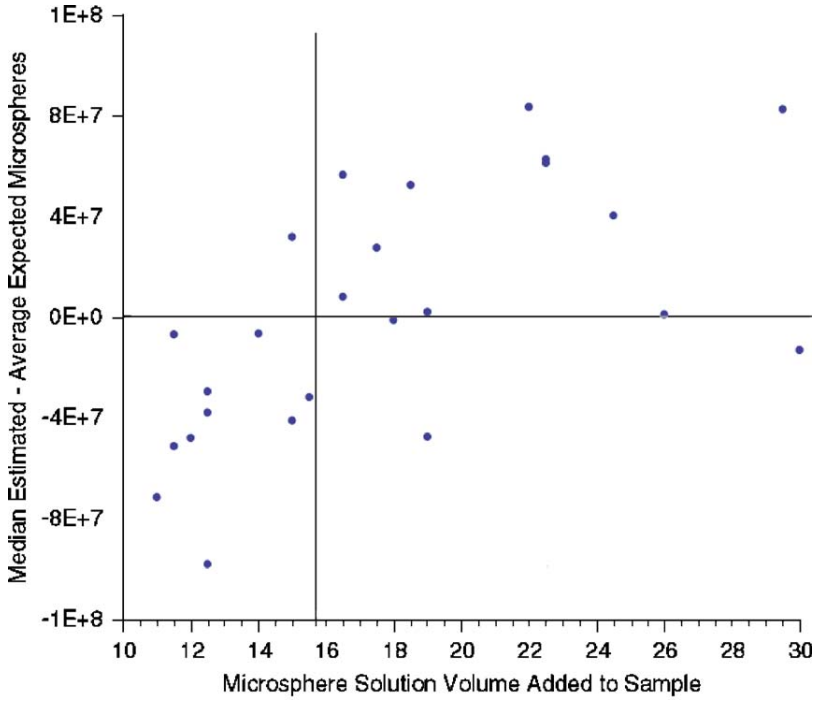

Fig. 4. Difference between the microsphere average expected number and the median microsphere estimated value versus the volume of stock microsphere solution added to the initial sample.

REFERENCES

Abrantes, F., 1988. Diatom assemblages as upwelling indicators in surface sediments in Portugal. Marine Geology 85, 15–39.

Abrantes, F., Moita, T., 1999. Water column and recent sediment data on diatoms and coccolithophorids, off Portugal, confirm sediment record as a memory of upwelling events. Oceanologica Acta 22, 319–336.

Abrantes, F., *et al*., 2002. Fluxes of micro-organisms along a productivity gradient in the Canary Islands region (29 N): implications for paleoreconstructions. Deep-Sea Research II 49, 3599–3629.

Barron, J., 1985. Late eocene to holocene diatom biostratigraphy of the equatorial Pacific Ocean, Deep Sea Drilling Project LEG 85. In: Mayer, L., Theyer, F., *et al*. (Eds.), Initial Reports of the Deep Sea Drilling Project. US Government Printing Office, Washington, pp. 413–456.

Battarbee, R., 1973. A new method for estimating absolute microfossilnumbers with specialreference to diatoms. Limnology and Oceanography 18, 647–653.

Battarbee, R., Kneen, M.J., 1982. The use of electronically counted microspheres in absolute diatom analysis. Limnology and Oceanography 27 (1), 184–188.

Estrada, M., Blasco, D., 1985. Phytoplankton assemblages in coastal upwelling areas. In: Bas, C., Margalef, R., Rubies, P. (Eds.), Simposio InternacionalSobre Las Areas de Afloramiento Mas Importantes DelOeste Africano, (Cabo Blanco y Benguela). Instituto de Investigaciones Pesqueras, Barcelona, pp. 379–402.

Falkowski, P.G., 2002. The ocean's invisible forest. Scientific American 287, 38–45.

Falkowski, P., Barber, R., Smetacek, V., 1998. Biogeochemical controls and feedbacks on ocean primary production. Science 281, 200–206.

Fenner, J., 1982. Diatoms in the Eocene and Oligocene sediments off NW Africa, their stratigraphic and paleogeographic occurrences. Dissertation Thesis, University of Kiel.

Hollander, M., Wolfe, D.A., 1973. Nonparametric Statistical Methods. Wiley, New York, pp. 505.

Nave, S., Freitas, P., Abrantes, F., 2001. Coastal upwelling in the Canary Island region: spatial variability reflected by the surface sediment diatom record. Marine Micropaleontology 42, 1–23.

Ortiz, J., Rack, F., 1999. Non-invasive sediment monitoring methods: current and future tools for high-resolution climate studies. In: Abrantes, F., Mix, A. (Eds.), Reconstructing Ocean History: A Window into the Future. Kluwer Academic publishers, New York. SAS Institute Inc., 2000. SAS Online Doc^{S}, Version 8 (CDROM).

Scherer, R., 1994. A new method for the determination of absolute abundance of diatoms and other silt-sized sedimentary particles. Journal of Paleolimnology 12, 171–179.

Schrader, H., Gersonde, R., 1978. Diatoms and silicoflagellates. Utrecht Micropaleontological Bulletin 17, 129–176.

Schrader, H.-J., Schuette, G., 1968. Marine diatoms. In: Emiliani, C. (Ed.), The Sea. Wiley, New York, pp. 1179–1231.

Snedecor, G.W., Cochran, W.G., 1980. StatisticalMethods. The Iowa State University Press, 507pp

CHAPTER 3:

Diatom as upwelling and river discharge indicators at the Portuguese margin: instrumental data linked to proxy information

Gil, I. M., Abrantes, F., Hebbeln, D.,

will be submitted

Diatom as upwelling and river discharge indicators at the Portuguese margin: instrumental data linked to proxy information

Gil, I. M.[1, 2], Abrantes, F.[1], Hebbeln, D.[2]

[1] Marine Geology Department, National Institute of Engineering, Technology and Innovation, 2721-866 Alfragide, Portugal

[2] MARUM – Center for Marine Environmental Sciences, University of Bremen, Leobener Straße, 28359 Bremen, Germany

Abstract

High-resolution diatom and phytolith quantitative and qualitative analyses are conducted on two box-cores from the Tagus pro-delta (SW Portuguese Margin) in order to confront these common paleoceanographic proxies to instrumental data describing the upwelling regime and the freshwater input of the Tagus River. The western Portuguese margin is affected by seasonal coastal upwelling controlled by northerly winds, and by strong freshwater input through the Tagus River, that is controlled by precipitation over the whole Iberian Peninsula. For both features, upwelling and freshwater input, instrumental data such as river flow and an upwelling index, are available for the last ~100 and 50 yrs, respectively.

Diatoms and phytoliths are used as proxies for salinity and productivity changes, resulting from river input and upwelling variability. Proxy and instrumental records are compared and confirm that diatom abundance, and in particular the genus *Chaetoceros*, trace the main periods of intense upwelling, whereas the fresh water diatoms and the phytoliths trace the major floodings of the Tagus River. Based on such verifications, the proxies can be surely used to reconstruct the paleoenvironment on time scales reaching way beyond the range of instrumental data. The results confirm that, despite the dissolution affecting silica compounds in the water column and in the sediment, diatoms and phytoliths are an accurate recorder of upwelling events and river discharge in this area. Such results have important implications for interpreting high resolution diatom records from non laminated sediments.

Keywords: paleoceanography; diatom; upwelling; river discharge; phytolith; Tagus River

1. Introduction

Climate data series are required to better describe and understand the climatic variability and the forcing behind it, especially in view to predict future climate development. However, instrumental climate data only reach back in time for ~150 yrs (Jones and Mann, 2004), which is by far not enough in order to understand climate dynamics. Thus, to compensate the lack of longer instrumental data time series, other information describing the

(paleo)environment also for older periods are required. Such information is commonly based on proxies, i.e., variables measurable in any kind of paleoarchive that are interpreted as descriptors for the physical environment at any given time. One such paleoarchive are marine sediments, and especially at sites with extremely high sedimentation rates, such proxies can be reasonably correlated with instrumental data to verify the reliability of any given proxy for the reconstruction of older paleoenvironments.

Most of the high resolution proxy records from marine sedimentary sequences are derived from laminated sediments that even can reach a seasonal resolution (Maddison *et al*., 2005). Sites providing such laminated sediments are mostly restricted to lacustrine environments (Gajeski *et al*., 1997; Laird *et al*., 1998) and studies from marine environments are sparse (Roberts *et al*., 2001; Barron *et al*., 2004).

The Tagus pro-delta off Lisbon is a marine environment presenting sediment accumulation rates high enough to be reasonably compared with instrumental data. However, these oxic sediments are affected by bioturbation that probably resulted in a smoothing of the original environmental signals. The site is affected on one hand by strong river input and on the other hand by seasonal coastal upwelling, and both features are documented instrumentally for the last ~100 and 50 yrs, respectively. Therefore, the Tagus pro-delta offers an ideal setting to compare such instrumental data with paleoenvironmental proxies. Two box-cores from this area have been studied here. Both are from slightly different locations (Fig. 1), with box-core PO287-26B (26B) subjected to a more direct influence of the river flow and box-core PO287-28B (28B) being located closer to the area of the upwelling plume. Close to our sampling sites, a submarine sewage outfall has been installed in 1994 and the effluents are released at 40 m depth (Silva *et al.*, 2004), but it does not appear to have a direct influence on the sedimentation at the location of the box cores.

In this study, instrumental data of upwelling intensity as well as river input will be linked to quantitative and qualitative analyses of diatoms and phytoliths preserved in the sediments. Diatoms are microscopic unicellular algae thriving in waters of a wide range of salinity (from fresh to saline). Phytoliths are also microscopic silica bodies produced by terrestrial plants and are transported to the pro-delta via river discharge. Both proxies can be used as indicators for river / fresh water input. In addition, diatom assemblages also can serve as indicators for the coastal upwelling affecting the Portuguese margin (Abrantes, 1988; Abrantes and Moita, 1999; Moita; 2001).

Based on the two box-cores from the Tagus pro-delta, providing a roughly biennial time resolution, diatom and phytolith records have been generated and linked to instrumental

records of freshwater input and coastal upwelling intensity. Besides, the pertinence of very high resolution studies (every centimeter) on non laminated sediments is also considered.

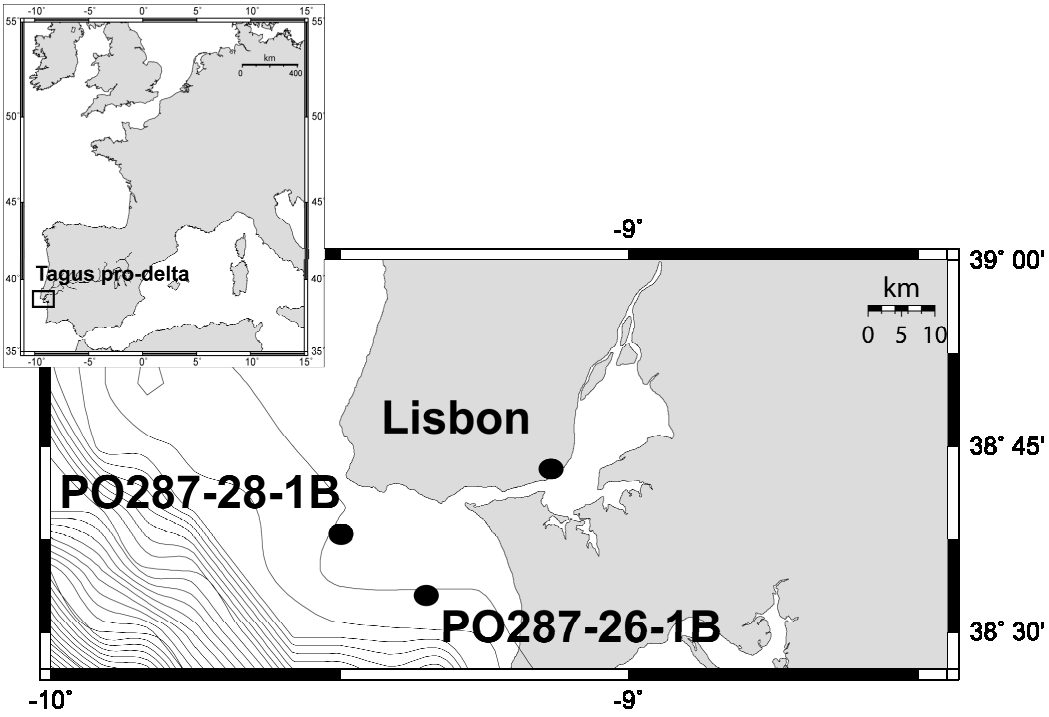

Figure 1: Location map of box-cores PO287-26-1B (26B) and PO287-28-1B (28B)

2. Oceanographic and climatic settings

The wind regime over the Portuguese coast is related to the latitudinal migration of the Azores high-pressure centre, with northeasterly and northerly winds instigating upwelling conditions on the west coast during spring and summer (Fiúza, 1982). During winter, southerly winds appear to prevail and lead to a coastal convergence (Fiúza, 1982). Because of the morphology of the coast at Lisbon latitude (Fig. 1), the upwelled water forms a recurrent plume (Sousa and Bricaud, 1992). During the upwelling season, the southward extension of this plume appears to be related to a coastal jet flowing southward (Sousa, 1986). The extension of the upwelling plume is therefore wind driven and reflected by phytoplankton abundance (Moita *et al*., 2003). Its distribution in and around the upwelling plume in Lisbon bay is asymmetric, with diatoms dominating the upwelling core (in particular *Cylindrotheca closterium* Ehrenberg) and mature oceanic waters (mainly *Proboscia alata* (Brightwell) Sundström) on the outer side of the upwelling plume (Moita *et al*., 2003). Given that the distribution of diatoms depends on the strength of the winds (Moita *et al*., 2003), spatial variability of diatom species distribution through time registered in the

Tagus pro-delta waters should reflect variations in the extension of the upwelling plume (Fig. 2).

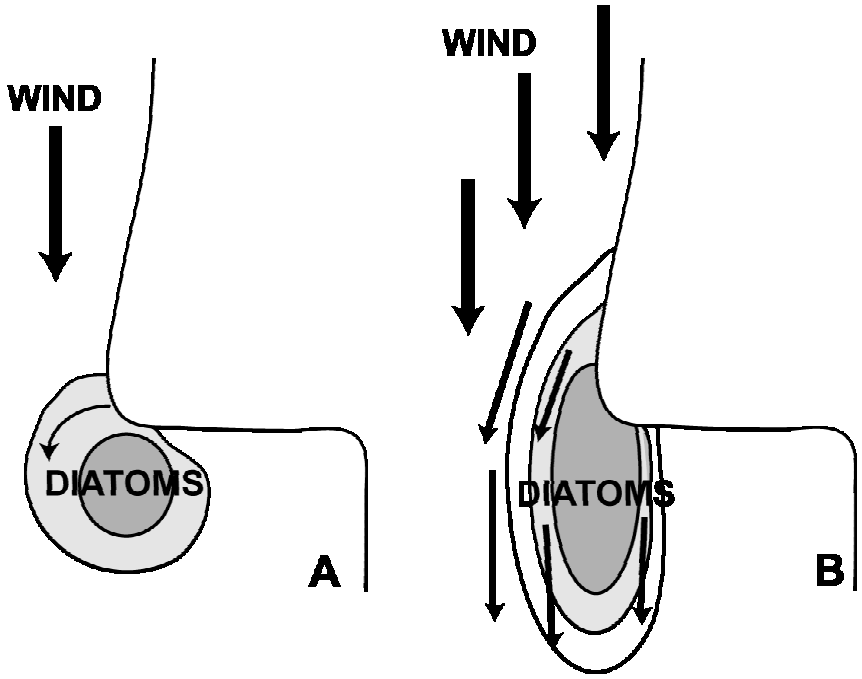

Figure 2: Upwelling plume extension over the Tagus pro-delta and distribution of the diatoms after Moita *et al*. (2003). The thick arrows represent the wind direction and the thin arrows the direction of the surface water circulation. The sketch (a) presents an early stage of the upwelling, while sketch (b) a fully developed upwelling situation, with intensified northerly winds.

Another process that influences sedimentation in the area of the present study is the Tagus river discharge. The Tagus is the longest river of the Iberian Peninsula and the third largest in catchment area and outflow. Its flow is strongly influenced by the precipitation over the entire peninsula (Trigo *et al*., 2002). The distribution of precipitation over the Iberian Peninsula is mainly controlled by the North Atlantic Oscillation – NAO (Lamb and Peppler, 1987; Hurrell, 1995; Hurrell *et al*., 2001). In fact, there is a close correlation between the NAO and the precipitation at a monthly scale (Trigo and da Camara, 2000) and the correlation between the Tagus flow and the NAO index is also clear (Trigo *et al*., 2004; Abrantes *et al*., 2005 (b)).

The description of the precipitation regime over Portugal (Trigo and da Camara, 2000) based on the period between 1946 and 1990 shows that the anticyclonic circulation type prevails throughout the year, except during summer. This circulation type brings only 16% of the precipitation received during winter, while the cyclonic, southwesterly and westerly circulation types deliver all together 62% of the precipitation received. During winter, increased precipitation over the Iberian Peninsula consequently enhances the Tagus river

discharge and this situation corresponds to a negative NAO situation. At the opposite, during summer, northeasterly and northerly winds are reinforced, instigating the coastal upwelling season, a situation that also occurs during NAO positive situations. Besides, all along the year, plumes of pigment-rich waters highlight the enrichment of the waters over the Tagus pro-delta with nutrients due to river discharge (Sousa and Bricaud, 1992).

In brief, upwelling rather occurs in summer, while precipitation is strongest in winter time. Both processes, upwelling and river input, are also closely linked to the atmospheric circulation pattern, allowing to interpret a climatic signal from the paleoceanographic record. The major factors controlling the spring phytoplankton bloom over the Tagus pro-delta are the hydrodynamics (stratified or mixed water column) and the input of nutrients (Cabeçadas, 1999) that can be provided by river discharge or by upwelling.

3. Material and methods

3.1 Material

Box-cores PO287-26-1B (26B) and PO287-28-1B (28B) were collected in the Tagus pro-delta (Fig. 1) in 2001 during Paleo I cruise and retrieved at 96 and 105 m water depth, respectively. The liners 26B (35 cm long) and 28B (37 cm long) were sliced every centimetre and each centineter was analysed for diatoms and phytoliths. The spacing of diatom assemblage identification depends on the diatom abundance in the sediment sample.

3.2 Age model

The age models of the box-cores are based on ^{210}Pb measurements, and ^{14}C dating at the base of each box-core confirm the age of the box-cores interpreted from the ^{210}Pb record. The imprints of bioturbation are revealed by steep slope of the activity profile in the upper part (Appleby and Oldfield, 1992), and by an important major discrepancy in the ^{210}Pb profile of core 28B (Fig. 3). The ^{210}Pb background of the box-cores was assumed to be 47 Bq/kg (Abrantes *et al*., 2005 (b)). The results show a sedimentation rate of 0,47 cm per year in box-core 26B (Fig. 2 and Table 2 in Abrantes *et al*., 2005 (b)) and of 0,7 cm per year in box-core 28B (Fig. 3). That means, core 28B has a 1930-2001 record, while in core 26B, the oldest sample corresponds to 1891.

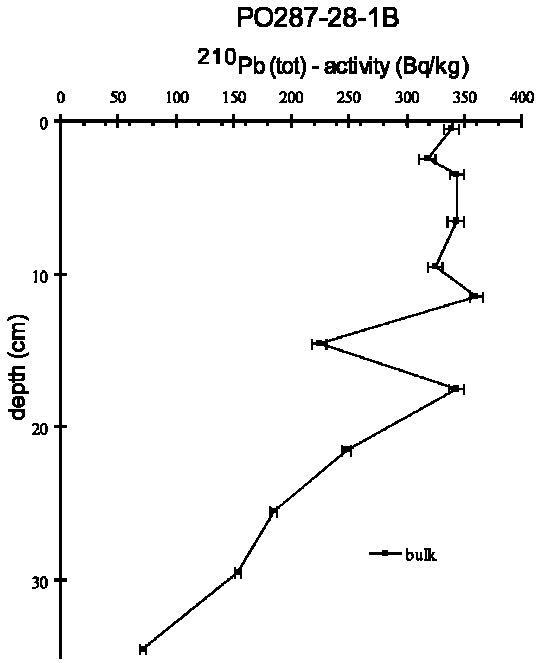

Figure 3: ^{210}Pb measurements in PO287-28-1B from the Tagus pro-delta, off Portugal.

3.3 Proxy data

For diatom and phytolith analysis, carbonates and organic matter have been removed from the sediment using the procedure described by Abrantes *et al*. (2005 (b)). An aliquot of sample is dried on cover slips (Battarbee, 1973), which are mounted on microscope slides. Diatoms are counted and identified at 1000 X magnification, using the counting protocol of Schrader and Gersonde (1978) and Abrantes (1988). The determination of the diatom assemblages is based on the identification of at least 100 valves (Fatela and Taborda, 2002). The diatom amounts within the sediments is expressed as Diatom Accumulation Rate (DAR), number of valves per cm ^{2}/yr, following Abrantes (1988) and applying the following ratio: number of valves (or phytoliths) per gram of dry bulk sediment *x* dry bulk density *x* sedimentation rate. The same is calculated for the phytoliths (PAR), for the diatom genus *Chaetoceros* (CAR), and the fresh water diatoms (FWAR).

3.4 Instrumental data

Tagus flow

The Tagus flow data are provided by INAG (http://www.inag.pt) and the combination of the stations of Santarém (1944-2002) and V. V. Rodão (1901-1974) covers the period between 1901

and 2002. Between 1940 and 1974, the two data series overlap and the average is calculated. The flow is given in cubic decametre (dam^3).

Upwelling index

The annual upwelling index was calculated for a location in the vicinity of the studied site (38.5N; 9.5 W). This index was calculated by L. de Witt from the NOAA following the procedures described at http://las.pfeg.noaa.gov/las/doc/wind_from_pressure.nc.html. This coastal upwelling index is based on the strength of the wind forcing on surface water and based on Ekman's theory of mass transport due to stress wind. This index expresses the amount of upwelled water transported offshore and is expressed in m^3/sec/100 m of coast line.

4. Results

4.1 Diatom and phytolith accumulation rates

In both box-cores, the diatom accumulation rates (DAR) are in the same order of magnitude, between $2.00x10^5$ and $2.98x10^6$ valves/cm^2/yr in core 26B (Fig. 4) and between $7.40x10^4$ and $7.45x10^6$ valves/cm^2/yr in 28B (Fig. 5). The lowest DAR correspond to the deeper parts of the box-cores, and are interpreted as a result of silica dissolution which starts at around 20 cm core depth (at 21 cm in 26B and at 17 cm in 28B).

There are two main periods of higher DAR in 26B, from 1946 to 1962 and from 1975 to 1984. The *Chaetoceros* accumulation rates (CAR) follow roughly the DAR (Fig. 4) along the box-core, however from 1933 to 1946 and at 1994, the DAR registers higher values (peaks), not accompanied by a higher CAR. This pattern also occurred in 1894, 1904 and 1920, though it is much less marked, likely due to stronger silica dissolution.

In 28B, dissolution is more pronounced than in 26B. In contrast to 26B, there is only one period of higher DAR between 1971 and 1983 and a small single peak in 1985. In the lower part of the box-core more affected by silica dissolution, there is a higher DAR between 1938 and 1940. From 1989 to 1995, the DAR increased and became constant until present. Also here the CAR (Fig. 5) follows the DAR and shows higher values from 1973 to 1981 and a slight increase after 1991.

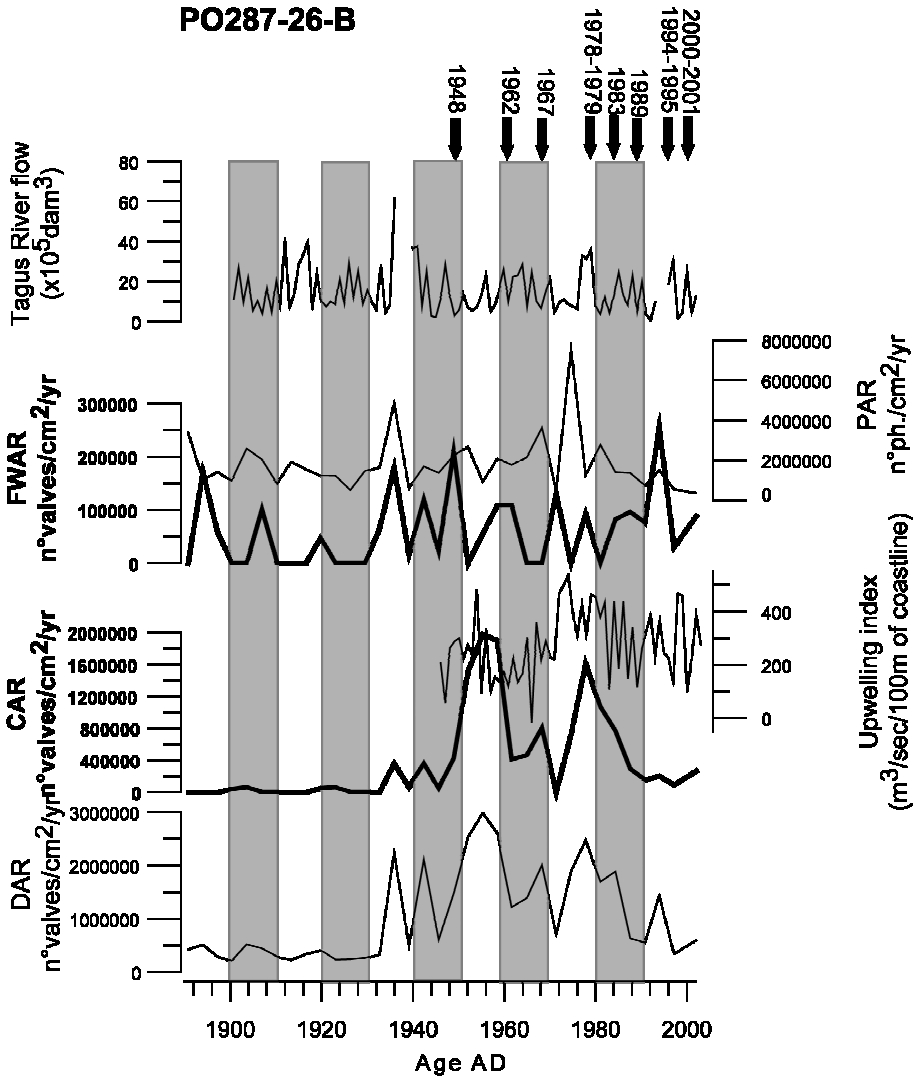

Figure 4: Tagus River flow, Fresh Water Diatom Accumulation Rates (FWAR), Phytolith Accumulation Rates (PAR), *Chaetoceros* Accumulation rates (CAR), Upwelling index and Diatom Accumulation Rates (DAR) in box-core 26B. The arrows indicates the major floodings reported by"Serviço Nacional de Bombeiros e Protecção Civil" –National fire brigades and civil protection (http://www.snbpc.pt) and INAG (http://www.inag.pt).

Although the fresh water diatom accumulation rates (FWAR) are relatively low in both box-cores, they are higher and more constant in core 26B (Fig. 4) than in 28B (Fig. 5). However, highest values are recorded in 28B for 1981 and 1995, with the younger peak also picked up in core 26B.

In 26B, the phytolith accumulation rates (PAR) present little variation in comparison to the FWAR (Fig. 4), however, higher PAR correspond to higher FWAR. The maxima of FWAR

occurred in 1994, 1949, 1936 and 1894 in 26B, and the most important values in PAR occurred in 1975, 1936 (maximum) and 1891, in decreasing order of importance.

In 28B, the highest values in PAR (Fig. 5) are recorded at 1940, between 1945 and 1951, at 1979 and 1995, and the major peaks in FWAR at 1995, 1981 and 1940, in decreasing order of importance.

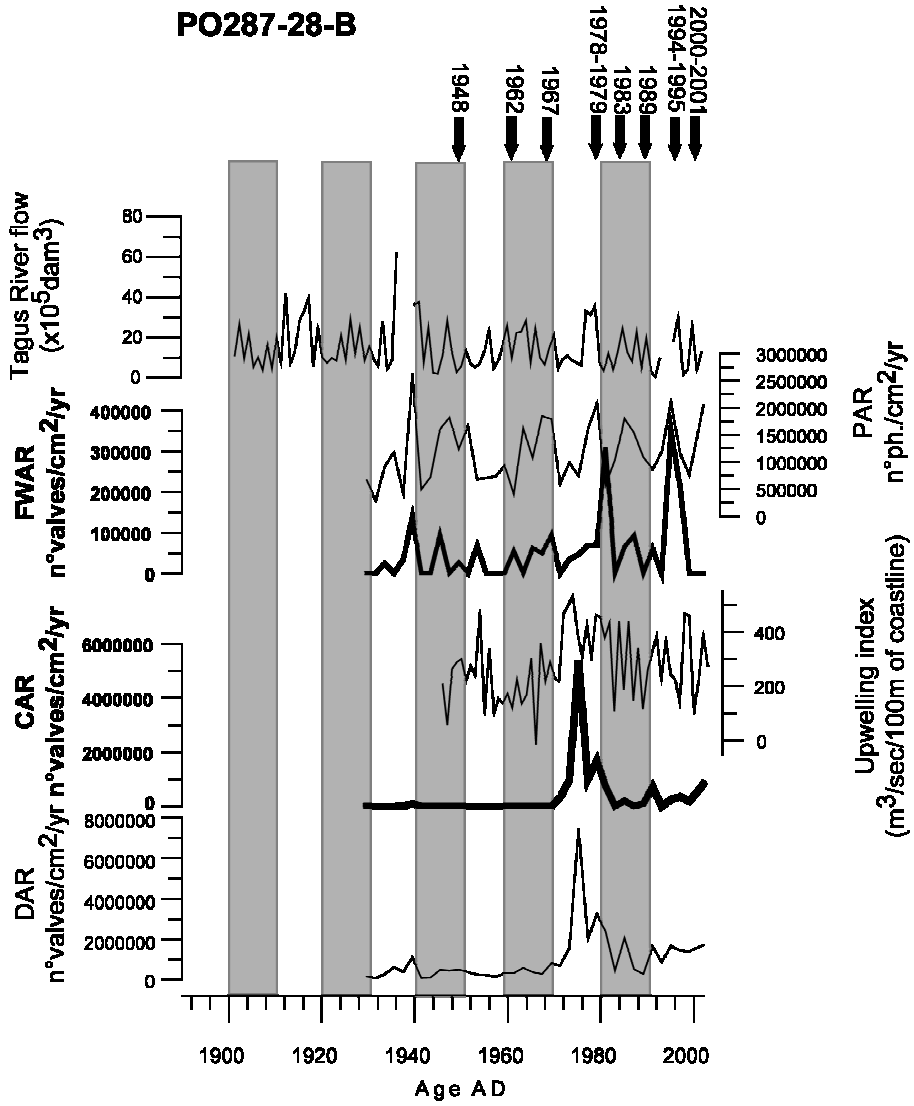

Figure 5: Tagus River flow, Fresh Water Diatom Accumulation Rate (FWAR), Phytolith Accumulation Rates (PAR), *Chaetoceros* Accumulation rates (CAR), Upwelling index and Diatom Accumulation Rates (DAR) in box-core 28B. The arrows indicates the major floodings reported by"Serviço Nacional de Bombeiros e Protecção Civil" –National fire brigades and civil protection (http://www.snbpc.pt) and INAG (http://www.inag.pt).

4.2 Diatom assemblages

Diatoms are preserved better and occur deeper in the sediment in core 26B than in core 28B and the difference in preservation is also reflected by the species diversity: in 26B, there are 168 diatoms species in total, incl. 45 fresh water and 25 brackish water species, while in 28B, 127 diatom species are identified, incl. 30 fresh water and 20 brackish water species. There are also important amounts of spore morphotypes of the diatom genus *Chaetoceros* identified in both box-cores. A complete list of species found in both box-cores is available in the PANGAEA data base under the DOI XXXXXX.

4.3 Instrumental upwelling record

The presented annual upwelling index extends back to 1946. There are three main distinct periods of more persistent intense upwelling: between 1948 and 1956, from 1990 to 1995 and between 1972 and 1986, with the maximum of the record in 1974. In between those two periods, the index is relatively low, but presenting a slight tendency to increase.

4.4 Instrumental Tagus river discharge record

There are three main periods when enhanced higher river flow is recorded in the annual data set: 1912-1917, 1933-1943 (with a maximum in 1936), and 1977-1979. Considering individually the two data series of V.V. Rodão and Santarém for the overlapping period between 1940 and 1974 (not presented here), a fourth period of higher flux at Santarém station is recorded between 1960 and 1963. Data are lacking for the years 1937-1939 and 1994-1995. In addition, there is information on individual flooding events recorded by ”Serviço Nacional de Bombeiros e Protecção Civil” (SNBPC) – National fire brigades and civil protection service (http://www.snbpc.pt) and INAG (http://www.inag.pt). According to their records major floods occurred in 1948, 1962, 1967, 1978-1979, 1983, 1989, 1994-1995 and 2000-2001.

5. Discussion

5. 1 The diatom species preserved in the box-cores

The different diatom species presented in Figure 6 are related to different environments, with *Paralia sulcata* and *Chaetoceros* spp. being related to marine / oceanic environments comprising

characterised by upwelling conditions (Moita, 2001); and *Cyclotella striata* and *Thalassionema nitzschioides*, being associated to coastal environments (Moita, 2001).

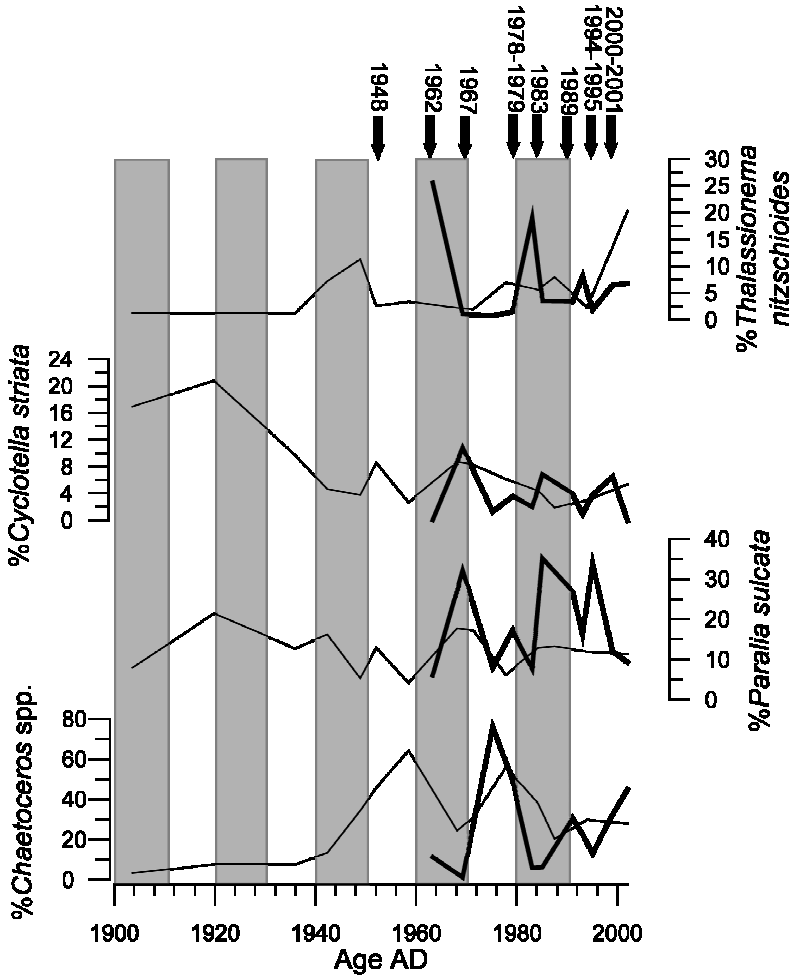

Figure 6: Relative abundances of the most persistent diatom species and groups along box-cores 26B (thin line) and 28B (bold line). The arrows indicates the major floodings reported by"Serviço Nacional de Bombeiros e Protecção Civil" –National fire brigades and civil protection (http://www.snbpc.pt) and INAG (http://www.inag.pt).

The most common species found by Moita *et al*. (2003) in the water column of Lisbon Bay (as *Cylindrotheca closterium or Proboscia alata*) are not found in the box-cores investigated here. These species are weakly silicified and are probably too delicate to resist to silica dissolution in the water column and at the seabed, confirming that parts of the diversity of the original diatom assemblage and also parts of the total diatom accumulation are lost by dissolution in this area (Abrantes and Moita, 1999). However, those diatom species found in the box-cores and related to upwelling were identified all along the Portuguese margin (Moita, 2001), showing that the

diatom assemblage in the sediment, although not reflecting the original assemblage, still serves as a good recorder of the upwelling regime.

5.2 Marine diatoms vs. upwelling index

The upwelling index and CAR records of core 26B present a similar pattern (Fig. 4), although some mismatching between peaks is observed. These may be explained by inaccuracies of the age model that is based on the assumption of a continuous sedimentation rate of 0.47 cm/yr throughout the core, although some variability as e.g. caused by catastrophic floods, as the one in 1979, probably leaded to a short-term enhancement of the sedimentation rate (Vale and Sundby, 1987).

The diatom record of 28B is more affected by silica dissolution and shows less variability and similarity with the upwelling index than the one of 26B. However, the main peak in CAR at 1975 in 28B matches a broad period of more intense upwelling (1972-1986, with a maximum in 1974).

Comparing the DAR records from both box-cores, there is an overlapping period of higher values in common between 1975 and 1984 in 26B and between 1971 and 1983 in 28B as also seen in the CAR records. This period also coincides with high values of the upwelling index recorded for the period 1972 to 1986, thus, confirming that the CAR (and to a lesser extent the DAR) indicates increased productivity resulting from enhanced upwelling.

5.3 Fresh water diatoms/phytoliths vs Tagus River flow

Fresh water diatoms show high accumulation rates in both box-cores in 1936 and 1994 / 1995. 1936 is the year of maximum river flow recorded by the instrumental data. Unfortunately, there are no river flow data for 1994 and 1995. However, according to SNBPC (http://www.snbpc.pt) and INAG (http://www.inag.pt), the Tagus River went out its minor bed in 1995 and 1996. Again, the time offset between the instrumental data and the estimated age of the peaks in the freshwater diatom (and phytolith) records seen in the cores is well within the accuracy of the age model. Other maxima in FWAR are observed in 26B for the year 1948 and in 28B for 1981.

Higher values in PAR in 26B are observed for 1936 and 1975. Whereas the 1936 event matches with high FWAR and maximum Tagus river flow, the 1974 event has no correspondence in FWAR, however, it might be linked to very high river flow recorded for 1978

and 1979. In 28B the 1936 event also sticks out very prominently. In addition, in this core there are several periods with enhanced PAR, as e.g., 1944-1950, 1963-1969, 1978-1979 and 1994 that are not so clearly marked in 26B. The proxy indications of higher river run-off score the main flooding events recorded by the instrumental data and the information provided by SNBPC (http://www.snbpc.pt). Even though the PAR record is similar to the FWAR, it is a better indicator for flooding events in 28B, as the highest values in PAR score the major floodings. However, the PAR signal is less clear than the one of the FWAR by not presenting so distinct peaks, but the FWAR do not record all the floodings. Additionally it appears that due to its off-shore position relatively to 26B, 28B mainly register the largest flooding events because it is precisely during those extreme events under the direct influence of the Tagus flow. In contrast, site 26B is always under river flow influence and it appears that the floodings do not result in a proportional increase in abundance of the fresh water indicators. It explains why the fresh water indicators give a clearer signal at site 28B than at site 26B.

5.4 The productivity record

A comparison of the DAR, CAR and FWAR records can help to discriminate the origin of the productivity (river input or upwelling) in the Tagus pro-delta waters. For both box-cores, the DAR and CAR curves reveal a similar pattern and show that most of the diatoms preserved in the sediments belong to the genus *Chaetoceros*. As the resting spores of this genus are heavily silicified and characteristic of turbulent waters rich in nutrients of upwelling areas (Blasco *et al.*, 1981), it is suggested that the diatom accumulation at the Tagus pro-delta is linked to upwelling events as indeed demonstrated by Moita (2001). This author's results show that along the west Portuguese margin, diatoms dominate the plankton in the water column during upwelling periods.

However, between 1933 and 1946 and in 1994 in 26B, the high values in DAR are not accompanied by high CAR, but correspond instead to a major contribution in fresh water diatoms. This suggests that these increases in diatom productivity in 26B were triggered by river run-off rather than by upwelling. Indeed, the instrumental river flow data confirm that between 1933 and 1943 the Tagus flow was enhanced. Possibly, the weak signal in DAR and FWAR in 28B between 1938 and 1940, when the diatom record is already strongly affected by dissolution, might reflect the same productivity event triggered by higher river discharge. For 1994, the data

from core 26B indicate a similar event with high DAR and FWAR and low CAR. Unfortunately, for that year no instrumental Tagus river flow data are available. However, the SBPC records report about major floodings in 1994 and 1995.

In brief, these observations suggest that the productivity of the Tagus pro-delta waters is mainly forced by upwelling, except when enhanced FWAR and comparatively low CAR provide clear hints for an enhanced productivity forced by river run-off.

Conclusions

The results attest the reliability of the diatom records, although they are strongly, but unequally, affected by the dissolution at the two sites. The diatom and phytolith records are able to register the major flooding events indicated by the instrumental data, at 1936, 1979 and 1995; as well as the most intense upwelling periods that occurred from 1946 to 1962, from 1975 to 1984 and between 1991 and 1994. As the base of the record is affected by dissolution, the oldest period of intense upwelling is only indicated by a slight increase in diatom accumulation rates. Besides, the comparison of the DAR, CAR and FWAR records help to discriminate the origin of the productivity in the Tagus pro-delta waters.

The spatial variability of the upwelling plume is not simple to detect because the diatom species that could have better trace it are not preserved in the sediment. However, the most intense upwelling events indicated by the instrumental data strongly recorded in 28B but not in 26B, can reveal the different hydrographic conditions at both sites, with 28B more influenced by the upwelling plume and 26B by the river plume.

The use of this proxy is limited by its preservation within the sediment, but even in the levels of stronger dissolution in 28B, one can see the evidences for major upwelling events, confirming the use of this proxy for paleoreconstructions. The results of this study present also important implications for interpreting high resolution diatom record from non laminated sediments.

Acknowledgements

This work has been supported by the Fundação para a Ciência e Tecnologia - FCT (BD - 18317/2004) and European Social Fund (ESF) through the 3rd EU Framework Program. We are grateful to Apolonia Inês for laboratory technical support in the sample preparation for diatom at the INETI-Laboratory of Marine Geology, to Mário Mil-Homens for interesting discussion and

to the colleagues of INETI - Marine Geology Department who helped in the box-cores collection during the PALEO I cruise.

APPENDIX

Diatom species found in P0287-26B and PO287-28B.

Species	PO287-26B	PO287-28B
Fresh water		
Achnanthes clevei (Grunow in Cleve et Grunow)	X	X
Achnanthes delicatula (Kützing) Grunow in Cleve et Grunow	X	
Achnanthes lanceolata (Brébisson in Kützing) Grunow in Cleve et Grunow	X	X
Achnanthes minutissima(Kützing)	X	
Amphora copulata (Kützing) Schœman et Archibald	X	
Amphora pediculus (Kützing) Grunow ex Schmidt		X
Aulacoseira ambigua (Grunow in Van Heurck) Simonsen	X	
Aulacoseira distans (Ehrenberg) Simonsen	X	X
Aulacoseira granulata (Ehrenberg) Simonsen	X	X
Caloneis leptostoma (Grunow in Van Heurck) Krammer	X	
Cocconeis placentula (Ehrenberg)	X	X
Cyclostephanos dubius (Fricke in Schmidt) Round		X
Cyclotella atomus (Hustedt)	X	
Cyclotella bodanica (Eulenstein)	X	
Cyclotella choctawatcheeana (Prasad)	X	
Cyclotella comensis (Grunow in Van Heurck)		X
Cyclotella comta (Ehrenberg) Kützing	X	
Cyclotella gamma (Sovereign)	X	
Cyclotella glomerata (Bachmann)	X	
Cyclotella kurdica (Håkanson)	X	X
Cyclotella meneghiana (Kützing)	X	X
Cyclotella ocellata (Pantocsek)	X	X
Cyclotella stelligera (Cleve et Grunow in Cleve) Van Heurck		X
Cymbella affinis (Kützing)	X	X
Diploneis ovalis (Hilse) Cleve	X	
Eunotia pectinalis (Müller) Rabenhorst	X	X
Eunotia sp.	X	X
Eunotia sp. 1	X	
Fragilaria capucina (Desmazières)	X	X
Fragilariforma virescens (Ralfs) Williams et Round		X
Frustulia amphipleuroides(Grunow in Cleve et Grunow) Cleve-Euler	X	
Gomphonema angustum (Agardh)	X	
Gomphonema truncatum (Ehrenberg)	X	
Hantzchia amphioxys (Ehrenberg) Grunow	X	
Luticola mutica (Kützing) Mann	X	
Luticola obligata (Hustedt) Mann		X
Martyana martyi (Héribaud) Round	X	X
Navicula capitata (Ehrenberg)	X	
Nitzschia capitellata (Hustedt)		X
Nitzschia dissipata (Kützing) Grunow	X	X

Nitzschia intermedia (Hantzsch ex Cleve et Grunow)		X
Nitzschia lanceolata (Smith)		X
Nitzschia prolongata (Hustedt)	X	
Pinnularia borealis (Ehrenberg)	X	X
Pinnularia intermedia (Lagerstedt) Cleve	X	
Pseudostaurosira brevistriata (Grunow in Van Heurck) Williams et Round	X	X
Rhopalodia gibba (Ehrenberg) Müller	X	
Sellaphora bacillum (Ehrenberg) Mann	X	
Stauroneis anceps fo. gracilis (Rabenhorst)		X
Stauroneis phoenicenteron (Nitzsch) Ehrenberg	X	X
Staurosira constuens (Ehrenberg)	X	X
Stephanodiscus hantzschii (Grunow)	X	
Synedra rumpens (Kützing)	X	
Synedra ulna (Nitzsch) Ehrenberg	X	X
Tabellaria flocculosa (Roth) Kützing	X	X
Brackish		
Achnanthes brevipes (Agardh)	X	
Achnanthes lilljeborgei (Grunow)	X	X
Amphora exigua (Gregory)		X
Aneumastis tusculus (Ehrenberg) Mann et Stickle	X	X
Bacillaria paxilifer (Müller) Hendey	X	X
Caloneis subsalina (Donkin) Hendey	X	
Catenula adherens (Mereschkowsky) Mereschkowsky	X	
Cocconeis scutellum (Ehrenberg)	X	X
Cocconeis peltoides (Hustedt)	X	
Craticula halophila (Grunow ex Van Heurck) Mann		X
Cyclotella striata (Kützing) Grunow in Cleve et Grunow	X	X
Diploneis elliptica (Kützing) Cleve	X	
Epithemia adnata (Kützing) Rabenhorst	X	X
Epithemia zebra (Ehrenberg) Kützing	X	
Epithemia sp.	X	X
Eunotogramma laevis (Grunow in Van Heurck)	X	X
Navicula digitoradiata (Gregory) Ralfs in Pritchard	X	X
Nitzschia acuminata (Smith) Grunow syn. *Tryblionella acuminata* (Smith)	X	X
Nitzschia fasciculata (Grunow) Grunow in Van Heurck	X	
Nitzschia lacunarum (Hustedt)		X
Nitzschia lanceolata (Smith)	X	
Nitzschia navicularis (Brébisson ex Kützing) Grunow in Cleve	X	X
Nitzschia sigma (Kützing) Smith	X	
Nitzschia sp.	X	X
Opephora olsenii (Møller)		X
Pleurosigma sp.	X	X
Psammodictyon panduriforme (Gregory) Mann	X	X
Staurophora amphyoxis (Gregory) Mann	X	
Staurophora salina (Smith) Mereschkowsky	X	X
Thalassiosira decipiens (Grunow) Jorgensen		X
Other species		
Actinocyclus octanarius (Ehrenberg)	X	
Actinoptychus senarius (Ehrenberg) Ehrenberg	X	X

Amphiprora angustata (Hendey)		X
Amphora binodis(Gregory)	X	
Amphora commutata (Grunow in Van heurck)	X	
Amphora crassa (Gregory)	X	
Amphora crassa (Gregory) var. *exornata* (Janisch)		X
Amphora holsatica (Hustedt)	X	
Amphora laevis (Gregory)	X	X
Amphora proteus (Gregory)	X	X
Amphora spectabilis (Gregory)	X	
Amphora turgida (Gregory)	X	X
Amphora valida (Peragallo)	X	
Amphora sp.		X
Amphora sp. 1		X
Anaulus sp.	X	
Asteromphalus flabellatus (Brébisson) Ralfs in Pritchard	X	
Azpeitia nodulifer (Schmidt) Fryxell et Sims		X
Biddulphia pulchella (Gray)	X	X
Caloneis linearis (Grunow) Boyer	X	
Campylosira cymbelliformis (Schmidt) Grunow ex Van Heurck	X	X
Catacombas gaillonii (Bory) Williams et Round	X	X
Cerataulus radiatus (Roper) Ross	X	X
Chaetoceros diadema (Ehrenberg) Gran	X	X
Chaetoceros wighami (Brightwell)	X	X
Chaetoceros spp.	X	X
Cocconeis costata (Gregory)	X	
Cocconeis disculoides (Hustedt)	X	X
Cocconeis disculus (Schumann) Cleve	X	
Cocconeis grata (Schmidt)	X	
Cocconeis pseudomarginata (Gregory)	X	X
Cocconeis schmidtii (Cleve-Euler)	X	X
Cocconeis stauroneiformis (Smith) Okuno	X	
Cocconeis sp.		X
Coscinodiscus curvatulus (Grunow in Schmidt)	X	X
Coscinodiscus kutzingii (Schmidt)		X
Coscinodiscus marginatus (Ehrenberg)	X	X
Coscinodiscus obscurus (Schmidt)	X	
Coscinodiscus oculus-iridis (Ehrenberg)	X	
Coscinodiscus radiatus (Ehrenberg)	X	X
Coscinodiscus rothii (Ehrenberg) Grunow	X	
Cocsinodiscus sp.		X
Cyclotella sp.		X
Cymatosira belgica (Grunow in van Heurck)	X	X
Delphineis surirella (Ehrenberg) Andrews	X	X
Dimeregramma minor (Gregory) Ralfs in Pritchard	X	
Diploneis bombus (Ehrenberg) Ehrenberg ex Cleve	X	X
Diploneis coffaeiformis (Cleve)	X	
Diploneis constricta (Grunow) Cleve	X	
Diploneis crabro (Ehrenberg) ex Cleve	X	X
Diploneis didyma (Ehrenberg) Cleve	X	X
Diploneis incurvata var. dubia (Hustedt)	X	X
Diploneis smithii (Brébisson ex Smith) Cleve	X	X

Diploneis suborbicularis (Gregory) Cleve	X	
Diploneis sp.	X	
Diploneis sp. 2	X	X
Ditylum brightwellii (West) Grunow ex Van Heurck	X	X
Fallacia forcipata (Greville) Stickle et Mann	X	X
Glyphodesmis distans (Gregory) Grunow in Van Heurck	X	
Grammatophora hamulifera (Kützing)	X	X
Grammatophora marina (Lyngbye) Kützing	X	
Grammatophora oceanica (Ehrenberg)	X	X
Grammatophora oceanica var. *macilenta* (Smith) Grunow	X	X
Grammatophora undulata (Ehrenberg)	X	X
Grammatophora sp.		X
Gyrosigma sp.		X
Leptocylindricus danicus (Cleve)	X	X
Lyrella abrupta (Gregory) Mann	X	
Lyrella atlantica (Schmidt) Mann	X	
Lyrella hennedyi (Smith) Stickle et Mann	X	X
Navicula cancellata (Donkin)	X	X
Navicula directa (Smith) Ralfs in Pritchard	X	X
Navicula palpebralis (Brébisson ex Smith)	X	X
Navicula pennata (Schmidt)		X
Navicula salinarum (Grunow in Cleve in Grunow)	X	
Navicula sp.	X	
Nitzschia angularis (Smith)	X	X
Nitzschia compressa (Bailey) Boyer	X	X
Nitzschia distans (Gregory)	X	
Nitzschia marina (Grunow) Cleve and Grunow	X	X
Odontella aurita (Lyngbye) Agardh	X	
Odontella regia (Schultze) Simonsen	X	X
Opephora gemmata (Grunow) Hustedt	X	X
Paralia sulcata (Ehrenberg) Cleve	X	X
Plagiogramma interruptum (Gregory) Ralfs in Pritchard	X	X
Plagiogramma sp.		X
Plagiotropis vitrea (Smith) Cleve		X
Pleurosigma normanii (Ralfs in Pritchard)	X	
Podosira stelligera (Bailey) Mann	X	X
Psammodiscus nitidus (Gregory) Round et Mann	X	X
Rhizosolenia bergonii (Peragallo)	X	
Rhizosolenia hebetata forma semispina (Hensen) Gran	X	X
Rhizosolenia styliformis (Brightwell)	X	X
Rhizolenia sp.	X	X
Roperia tesselata (Roper) Grunow in Van Heurck	X	X
Stauroneis sp.		X
Surirella fastuosa (Ehrenberg)	X	
Tabularia investiens (Smith) Williams et Round	X	
Thalassionema frauenfeldi (Grunow) Hallegraeff	X	X
Thalassionema nitzschioides (Grunow) Grunow ex Hustedt	X	X
Thalassiosira angulata (Gregory) Hasle	X	X
Thalassiosira diporocyclus (Hasle)	X	X
Thalassiosira eccentrica (Ehrenberg) Cleve	X	X
Thalassiosira gravida (Cleve)		X

Thalassiosira lineata (Jousé)	X	
Thalassiosira nordenskioeldii (Cleve)	X	
Thalassiosira oestrupii (Ostenfeld) Hasle	X	X
Thalassiosira sp. 08	X	X
Thalassiosira sp. 10		X
Thalassiosira symmetrica (Fryxell et Hasle)	X	
Thalassiosira tenera (Proschkina-Lavrenko)	X	X
Toxarium undulatum (Bailey)		X
Trachyneis aspera (Ehrenberg) Cleve	X	X
Trachysphenia australis (Petit in Folin et Perier)	X	
Triceratium alternans (Bailey)	X	X
Tryblionella granulata (Grunow) Mann	X	

REFERENCES

Abrantes, F., 1988. Diatoms assemblages as upwelling indicators in surface sediments off Portugal. Marine Geology, 85: 15-39.

Abrantes, F., Gil, I., Lopes, C., Castro, M., 2005 (a). Quantitative diatom analyses-a faster cleaning procedure. Deep-Sea Research I, 52: 189-198.

Abrantes, F., Lebreiro, S., Rodrigues, T., Gil, I., Bartels-Jonsdottir, H., Oliveira, P., Kissel, C., Grimalt, J. O., 2005 (b). Shallow-marine sediment cores record climate variability and earthquake activity off Lisbon (Portugal) for the last 2000 years. Quaternary Science Reviews, 24: 2477-2494.

Abrantes, F., Moita, M., 1999. Water column and recent sediment data on diatoms and coccolithophorids, off Portugal, confirm sediment record of upwelling events. Oceanologica Acta, 22, 1: 67-84.

Appleby,P.G., Oldfield, F., 1992. Application of ^{210}Pb to sedimentation studies. In: Uranium series disequilibrium (Eds. M. Ivanovich & R.S. Harmon), OUP: 731-778.

Barron, J.A., Bukry, D., Bischoff, J.L., 2004. High resolution paleoceanography of the Guaymas Basin, Gulf of California, during the past 15000 years. Marine Micropaleontology, 50: 185-207.

Battarbee, R.W., 1973. A new method for estimation of absolute microfossil numbers with reference especially to diatoms. Limnology and Oceanography, 18: 647-652.

Blasco, D., Estrada, M., Jones, B.H., 1981. Short Time Variability of Phytoplankton Populations in Upwelling Regions - The Example of Northwest Africa. American Geophysical Union, pp. 339-347.

Cabeçadas, L., 1999. Phytoplankton production in the Tagus estuary (Portugal). Oceanologica Acta, 22(2): 205-214.

Fatela, F., Taborda, R., 2002. Confidence limits of species proportions in microfossil assemblages. Marine Micropaleontology, 45: 169-174.

Fiúza, A., de Macedo, M. E., Guerreiro, M. R., 1982. Climatological Space and Time Variation of the Portuguese Coastal Upwelling. Oceanologica Acta, 5(1): 15.

Gajewski, K., Hamilton, P.B., McNeely, R., 1997. A high resolution proxy-climate record from an arctic lake with annually-laminated sediments on Devon Island, Nunavut, Canada. Journal of Paleolimnology, 17(2): 215-225.

Hurrell, J.W., 1995. Decadal trends in the North Atlantic Oscillation: Regional temperatures and precipitation. Science, 269: 676-679.

Hurrell, J.W., Kushnir Y., Visbeck M., 2001. The North Atlantic Oscillation. Science, 291: 603-605.

Jones, P.D. and Mann, M.E. 2004: Climate over past millennia. *Reviews of Geophysics* 42, doi:10.1029/2003RG000143.

Laird, K.R., Fritz, S.C., Cumming, B.F., 1998. A diatom-based reconstruction of draught intensity, duration, and frequency from Moon Lake, North Dakota: a sub-decadal record of the last 2300 years. Journal of Paleolimnology, 19(2): 161-179.

Lamb, P.J., Peppler R. A., 1987. North Atlantic Oscillation: Concept and an Application. Bulletin American Meteorological Society, 68 (10): 1218-1225.

Maddison, E.J., Pike, J., Leventer, A., Domack, E.W., 2005. Deglacial seasonal and sub-seasonal diatom record from Palmer Deep, Antarctica. Journal of Quaternary Science, 20(5): 435-446.

Moita, M.T., Oliveira, P.B., Mendes, J.C., Palma, A.S., 2003. Distribution of chlorophyll a and *Gymnodinium catenatum* associated with coastal upwelling plumes off central Portugal. Acta Oecologica-International Journal of Ecology, 24: S125-S132.

Moita, M.T.C.d.J.G., 2001. Estrutura, variabilidade e dinâmica do fitoplâncton na costa de Portugal continental. Ph D Thesis, Faculdade de Ciências da Universidade de Lisboa, Lisbon, 272 pp.

Roberts, D., van Ommen, T.D., McMinn, A., Morgan, V., Roberts, J.L., 2001. Late-Holocene East Antarctic climate trends from ice-core and lake-sediment proxies. Holocene, 11(1): 117-120.

Schrader, H.J., Gersonde, R., 1978. Diatoms and Silicoflagellates. Utrecht Micropaleontological Bulletin, 17: 129-176.

.

Silva, S., Re, A., Pestana, P., Rodrigues, A., Quintino, V., 2004. Sediment disturbance off the Tagus Estuary, Western Portugal: chronic contamination, sewage outfall operation and runoff events. Marine Pollution Bulletin, 49(3): 154-162.

Sousa, F.M., 1986. Determinação da temperatura da superficie do mar com satélites, uma aplicação ao oceano costeiro de Portugal (Evaluation of sea surface temperatures with satellites, an application to the Portuguese coastal ocean). unpublished M. Sc. Thesis, Universidade de Lisboa, Lisbon, 127 pp.

Sousa, F.M., Bricaud, A., 1992. Satellite-Derived Phytoplankton Pigment Structures in the Portuguese Upwelling Area. Journal of Geophysical Research-Oceans, 97(C7): 11343-11356.

Trigo, R.M., DaCamara, C. C., 2000. Circulation weather types and their influence on the precipitation regime in Portugal. International Journal of Climatology, 20: 1559-1581.

Trigo, R.M., Osborn, T. J., Corte-Real, J. M., 2002. The North Atlantic Oscillation influence on Europe: climate impacts and associated physical mechanisms. Climate Research, 20: 9-17.

Trigo, R.M., Pozo-Vásquez, D., Osborn, T. J., Castro-Díez, Y., Gámiz-Fortis, S., Esteban-Parra, M. J., 2004. North Atlantic Oscillation influence on precipitation, river flow and water ressources in the Iberian peninsula. International Journal of Climatology, 24: 925-944.

Vale, C., Sundby, B., 1987: Suspended sediment fluctuations in the Tagus estuary on semi-diurnal and fortnightly time scales. Estuarine, Coastal and Shelf Science, 25: 495-508

CHAPTER 4:

Shallow-marine sediment cores record climate variability and earthquake activity off Lisbon (Portugal) for the last 2000 years

Abrantes, F., Lebreiro, S., Rodrigues, T., Gil, I., Bartels-Jónsdóttir, H., Oliveira, P., Kissel, C, Grimalt, J.O.,

Quaternary Science Reviews, 24: 2477-2494 (2005)

ELSEVIER

Available online at www.sciencedirect.com

SCIENCE DIRECT®

QSR

Quaternary Science Reviews 24 (2005) 2477–2494

Shallow-marine sediment cores record climate variability and earthquake activity off Lisbon (Portugal) for the last 2000 years

F. Abrantes[a,*], S. Lebreiro[a], T. Rodrigues[a], I. Gil[a], H. Bartels-Jónsdóttir[a], P. Oliveira[b], C. Kissel[c], J.O. Grimalt[d]

[a] Departamento de Geologia Marinha, INETInovação (former Instituto Geológico e Mineiro), Estrada da Portela-Zambujal, Apartado 7586, 2721-866 Amadora, Portugal

[b] Instituto Nacional de Investigação Agrária e das Pescas (INIAP), Av.Brasilia, 1449-006 Lisboa, Portugal

[c] Laboratoire des Sciences du Climat et de l'Environnement, Unité de recherche mixte CEA/CNRS, Campus du CNRS, Avenue de la Terrasse, Bat12, 91198 Gif-sur-YvetteCedex, France

[d] Department of Environmental Chemistry, Institute of Chemical and Environmental Research(CSIC), Jordi Girona, 18, 08034 Barcelona, Spain

Received 9 January 2004; accepted 18 April 2004

* Corresponding author. Tel.: +351-21470-5535; fax: +351-21471-9018.
E-mail address: fatima.abrantes@ineti.pt (F. Abrantes).

Abstract

Sea Surface Temperature (SST), river discharge and biological productivity have been reconstructed from a multi-proxy study of a high-temporal-resolution sedimentary sequence recovered from the Tagus deposition center off Lisbon (Portugal) for the last 2000 years. SST shows 2 °C variability on a century scale that allows the identification of the Medieval Warm Period (MWP) and the Little Ice Age (LIA).

High Iron (Fe) and fine-sediment deposition accompanied by high *n*-alkane concentrations and presence of freshwater diatoms during the LIA (1300–1900 AD) (Science 292 (2001) 662) suggest augmented river discharge, whereas higher total-alkenone concentrations point to increased river-induced productivity. During the MWP (550–1300 AD) (Science 292 (2001) 662) larger mean-grain size and low values of magnetic susceptibility, and concentrations of Fe, *n*-alkanes, and *n*-alcohols are interpreted to reflect decreased runoff. At the same time, increased

benthic and planktonic foraminifera abundances and presence of upwelling related diatoms point to increased oceanic productivity. On the basis of the excellent match found between the negative phases of the North Atlantic Oscillation (NAO) index and the intensified Tagus River discharge observed for the last century, it is hypothesized that the increased influx of terrigenous material during the LIA reflects a negative NAO-like state or the occurrence of frequent extreme NAO minima. During the milder few centuries of the MWP, stronger coastal upwelling conditions are attributed to a persistent, positive NAO-like state or the frequent occurrence of extreme NAO maxima.

The peak in magnetic susceptibility, centered at 90 cm composite core depth (ccd), is interpreted as the result of the well-known 1755 AD Lisbon earthquake. The Lisbon earthquake and accompanying tsunami are estimated to have caused the loss of 39 cm of sediment (355 years of record—most of the LIA) and the instantaneous deposition of a 19-cm sediment bed.

1. Introduction

Climatic conditions have oscillated over the past 100,000 years, with an average period of about 1500 years (Bond *et al*., 1997). The large millennial-scale abrupt events of the last glacial are clearly recorded on the Portuguese Margin (de Abreu, 2000; Shackleton *et al*., 2000; Voelker *et al*., 2002). The Holocene is also marked by repeating but less severe climate shifts, the most recent of which are the Medieval Warm Period (MWP) and subsequent Little Ice Age (LIA) (Bond *et al*., 1997, 2001).

Primary forcing factors of climate change on millennial and centennial time scales are yet poorly understood. Broecker (2001) hypothesized that recent millennial-scale climatic oscillations are caused by changes in the North Atlantic thermohaline circulation. Variations in solar activity (Stuiver and Braziunas, 1989) have also been suggested as the driver for the North Atlantic cycles (Bond *et al*., 2001). In addition, the North Atlantic Oscillation (NAO) index which describes the steepness of a north–south atmospheric pressure gradient across the North Atlantic Ocean (Hurrell, 1995), has also been pointed as a useful analog for interpreting longer-term climatic conditions observed for the last 2000 years (Keigwin, 1996; Keigwin and Pickart, 1999).

Today, the NAO is believed to dictate climate variability across most of the Northern Hemisphere, especially during wintertime. Defined as the atmospheric sea-level pressure difference between Iceland and Lisbon–Portugal, it is in a positive phase when the meridional

pressure gradient over the North Atlantic is large, due to the enhancement of both pressure centers (the Icelandic low and the Azores high), and in a negative phase when both centers are weakened (Hurrell, 1995). Swings from a positive to a negative phase produce changes in mean wind speed and direction over the Atlantic, seasonal mean heat and moisture transport across the ocean, the path and number of storms, and may also induce significant variations in ocean temperature, heat content, current patterns, and sea ice cover in the Arctic (Hurrell *et al*., 2003). Its largest amplitude anomalies occur near Iceland and across the Iberian Peninsula. Over Iberia, atmospheric storminess and increased precipitation coincide with NAO-negative conditions. The strong north–south atmospheric pressure gradient and strong clockwise flow around the Azores high-pressure center during NAO-positive conditions enhances coastal upwelling conditions. Further insight on the impact of NAO on precipitation over Europe through the analysis of a 40-yr-long global coverage of consistent precipitation-related data was reported by Trigo *et al*. (2002). Results show that cloud cover as well as precipitation anomaly fields (mm/d) for winter months with low NAO index (<-1.0) have high values in the area of the Tagus Basin.

The Tagus is the longest river in the Iberian Peninsula and extreme flood events lead to a major discharge of suspended and bed-load sediments (Vale, 1981). Clayey–silty sediment is transported to the Tagus deposition center on the continental shelf (Monteiro and Moita, 1971). The sediment is characterized by high concentration of organic matter (Gaspar and Monteiro, 1977; Cabeçadas and Brogueira, 1997). Additionally, the Tagus deposition center is influenced by seasonal (May–September) coastal upwelling, mainly by the Cape Roca upwelling filament (Fiuza, 1983, 1984; Sousa and Bricaud, 1992; Sousa, 1995; Abrantes and Moita, 1999; Moita, 2001).

Our objective is to reconstruct a detailed record of river influx and coastal upwelling variability over the last 2000 years, through a multi-proxy study of a sedimentary sequence recovered from the Tagus River prodelta deposition center, off Lisbon (Portugal).

The study of a site directly under the influence of the Azores High Pressure center, does not only enlarge the data network needed to validate climate models on time scales of many decades to centuries, but it also offers new insights into the view of modern NAO conditions as a robust modern analog for decadal to century-scale climate variability.

2. Material and methods

The material used in this study was obtained from core D13902 collected at 38°33.24'N, 9°20.13'W and 90 m water depth. The core was taken during the British Research Vessel (RV) *Discovery* cruise 249 in August-September 2000 using the British long-piston coring system. Box-core PO287-26B and gravity core PO287-26G (38°3.49'N, 9°2.84'W, 96 m water depth) were recovered in May 2002 during the PALEO1 campaign aboard the German RV Poseidon (Fig. 1). The two top liners of core D13902 (189 cm) were half-filled and disturbed, therefore, this material was discarded and a zero depth assigned to the initial 189-cm liner level.

Magnetic susceptibility (MS) of core D13902 and cores PO287-26 (B and G) were measured on a multiparameter logging system at the Southampton Oceanography Center and at Bremen University, respectively. Iron (Fe) concentrations in counts per second (cps) were determined at 1 cm intervals in cores PO287-26 and at 2 cm intervals in core D13902 by X-ray fluorescence core scanning for non-destructive semi-quantitative analysis of major elements at Bremen University (Jansen *et al*., 1998). Paleomagnetic analyses were performed at the Laboratoire des Sciences du Climat et de l'Environnement (LSCE/CNRS) in Gif-sur-Yvette. Continuous analyses were made using U-channels 2 x 2 x 150 cm.

The low-field susceptibility was measured using a 45 mm diameter Bardington coil, which yields 4 cm resolution. The remanent magnetizations were measured using 2G 755-R cryogenic magnetometers within a shielded room at LSCE (Weeks *et al*., 1993). The spatial resolution is similar to the low-field susceptibility resolution (about 4 cm). Anhysteretic Remanent Magnetization (ARM) was imparted along the axis of the U-channel at a translation speed of 1 cm/s using a 100 mT AF in a bias 50 μT DC field (Kissel *et al*., 1999).

Sediments were sliced at 1-cm intervals in 3 sub-cores of the box-core (Table 1) and the gravity and piston cores. Grain size, total carbon, $CaCO_3$, and diatom analysis were performed on all samples from D13902 and PO287-26B. Alkenones, *n*-alkanes, *n*-alcohols, and foraminifera were analyzed every cm in the box-core, every 2 cm in PO287-26G, and at 5–20 cm intervals in the piston core.

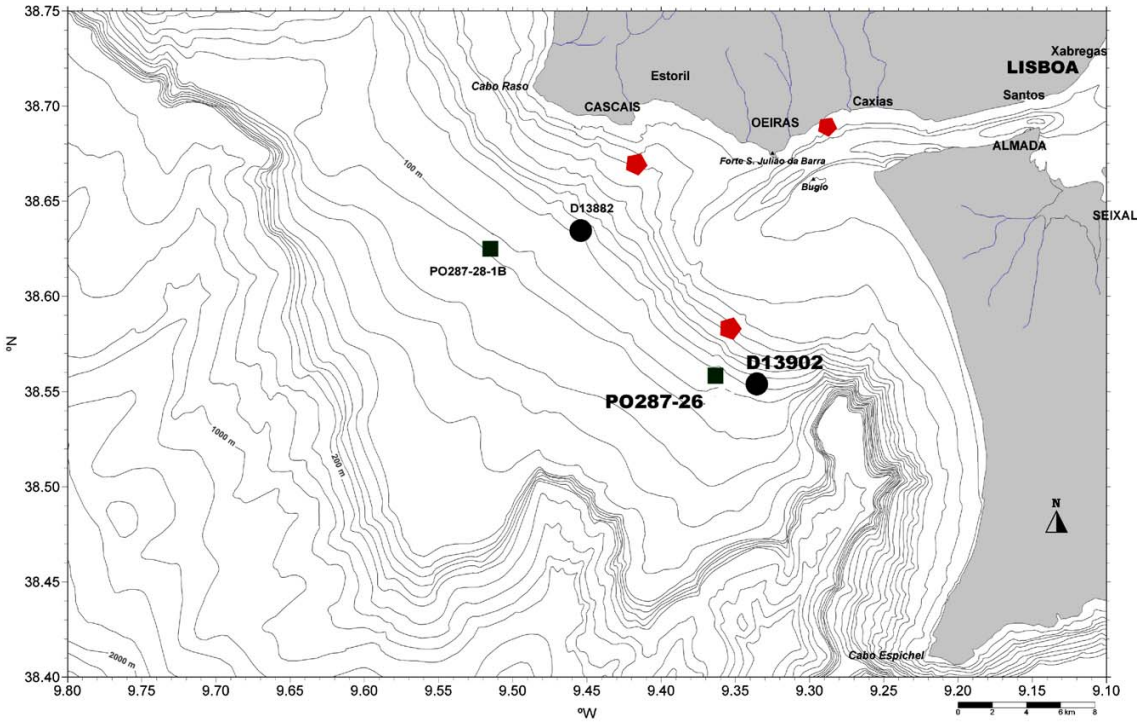

Fig. 1. Detailed bathymetric map of the Tagus Estuary mouth and prodelta with location of the sedimentary sequences used in this work. Bathymetric contour interval is 10 m. Circles correspond to cores recovered on RV Discovery using the long piston coring system of Southampton Oceanographic Center. Squares indicate positions of the gravity and box-cores retrieved aboard RV Poseidon. Pentagons indicate position of pre 1950 shells dated by AMS C-14.

Table 1
Sub-cores of box-core PO287-26B used for the different analysis

Subcore 1	Subcore 2	Subcore 3	Subcore 4
MST XRF	Grain-size $CaCo_3$ Corg Foraminifera Isotopes AMS ^{14}C ^{210}Pb	Diatoms	Alkenones *n*-Alkanes *n*-Alcohols

Grain size analysis was performed on 5–8 cc of sediment with a Coulter LS230 laser instrument. Prior to grain-size analysis, organic matter was removed using peroxide (H_2O_2) and dispersed with sodium hexametaphosphate (0.033 M).

Total carbon content was determined using a CHNS932 LECO elemental analyzer. Three

replicates of dried and homogenized sediment (2 mg) were analyzed per level. The same set of samples was later subjected to combustion for 8 h through a predefined stepwise increase in temperature up to 400 °C to remove organic carbon and re-analyzed for inorganic carbon. The organic carbon content (Corg) was determined by difference between total carbon and inorganic carbon concentration. Data are presented in weight percent (wt%). The relative precision of repeated measurements of both samples and standards was 0.03 wt%.

Oxygen-isotopic compositions were determined on the planktonic foraminifera *Globigerina bulloides* and the benthic species *Uvigerina* sp. 221 on a Finnigan MAT 251 mass spectrometer at Bremen University. The $^{18}O/^{16}O$ ratio is reported in per mil (‰) relative to the Vienna Peedee Belemnite (VPDB) standard. Analytical standard deviation is ±0.07‰.

Alkenones, higher plant *n*-alkanes, and *n*-alcohols were determined on 2 g of homogenized sediment using a Varian 3400 gas chromatograph equipped with a septum programmable injector at the Department of Environmental Chemistry, Institute of Chemical and Environmental Research (CSIC), Barcelona, following the methods described in Villanueva (1996), Villanueva and Grimalt (1997) and Villanueva *et al*. (1997). For SST reconstruction, the $U^{k'}_{37}$ calibration proposed by Müller *et al*. (1998) was used due to its global character. Analytical precision was 0.5 °C.

Benthic foraminifera quantification and assemblage determinations are based on census counts of splits (300 individuals) of the 125-µm fraction, whereas planktonic foraminifera quantification is based on census counts of splits (300 individuals) of the 149 -µm fraction. Benthic foraminifera were classified according to Loeblich and Tappan (1988).

Siliceous microfossil quantification and diatom assemblages determinations followed the methods of Abrantes (1988).

3. Chronology

3.1.Reservoir-effect correction

The site of study is under the influence of the Tagus River, whose waters cross limestone-rich areas. The site is also under the influence of coastal upwelling. Both processes may lead to large reservoir ages (Little, 1993; Goodfriend and Flessa, 1997). In order to better constrain the reservoir correction for the Iberian site, we measured apparent radiocarbon ages on 3 live-collected, pre-bomb mollusk shells from the region (Portuguese King D. Carlos collection

housed at the AquárioVasco da Gama in Lisbon) (Table 2). Analyses were performed at the Aarhus University AMS Laboratory and results indicate that the 400 yr global average is a good reservoir correction value.

3.2. Age model

An age-depth model has been constructed by combining ^{210}Pb dates of the box-core PO278-26B and piston-core D13902 (Table 3) and accelerator mass spectrometry (AMS) ^{14}C dates from the two cores (Table 4). ^{210}Pb analysis was performed on 18 samples (16 box-core and 2 piston-core samples), enabling the assessment of recent mass accumulation rates. The down-core total ^{210}Pb activity profile is shown in Fig. 2. The ^{210}Pb background (^{226}Ra supported ^{210}Pb) of these two core sediments was assumed to be 47 Bq/kg (Becquerel/kg), since this was the value measured in a 760±45 yr BP dated sample (62–63 cm of the D13902 core). The activity profile (Fig. 2) shows an upper interval (12 cm) of slow exponential-downward decline in ^{210}Pb activity, followed by a more rapid decline in the middle (12–60 cm), and a lower interval with constant activity. The steep slope observed for the upper interval of the activity profile is attributed to biological mixing (Appleby and Oldfield, 1992). The two higher-activity values, found at 19 and 23 cm, are associated with relatively lower values in dry bulk density and at the level of a burrow visible on the box-core picture, and were therefore excluded from the model. The accumulation rate (ω) has been calculated using a constant sedimentation model, with no correction for mixing. Compaction was corrected through the dry bulk density values. The model that best fits the data indicates a mass accumulation rate of 0.55 g/cm^2/yr and a sedimentation rate in the order of 0.51 cm/yr (Fig. 2).

Table 2
Results of AMS ^{14}C of Tagus region shells collected alive before 1950. King D. Carlos of Portugal Collection/Vasco da Gama Aquarium

Sample type	Collection site	Collection date	Lat. (°N)	Long. (°W)	Water depth (m)	^{14}C ages (BP)
Bivalve (*Chameliagallina*)	Portugal, Trafaria	16 Sept. 1896	38 °34.4’	09 °21.5’	55	420±38
Bivalve (*Mactrasolida*)	Portugal, Cascais	26 Aug. 1896	38 °40.0’	09 °25.0’	35	477±33
Bivalve (*Mactracorallina*)	Portugal, Dafundo	19 Nov. 1938			10	556±39

AMS ^{14}C analysis was performed on 13 samples (Table 4). In the box-core, at 32–33 cm, the AMS ^{14}C age obtained is 40±25 yr BP, however, if the box-core depth is corrected for compaction during sub-sampling (using the difference in length between the original core and the sub-core), the decompacted depth for this sample is 51.5 cm. Assuming that the top sample corresponds to 2001, the estimated sedimentation rate (SR) is 0.47 cm/yr.

Table 3
Results of ^{210}Pb activity for the Tagus prodelta box and piston cores (PO287-26B and D13902)

Core ID	Spliced depth (cm)	^{210}Pb (tot) (mBq/g)
PO287-26 (0–1 cm)	0.5	296
PO287-26 (2–3 cm)	2.9	299
PO287-26 (4–5 cm)	5.3	283
PO287-26 (6–7 cm)	7.6	271
PO287-26 (9–10 cm)	11.1	221
PO287-26 (11–12 cm)	13.5	217
PO287-26 (11–12 cm)	13.5	224
PO287-26 (14–15 cm)	17.0	151
PO287-26 (14–15 cm)	17.0	158
PO287-26 (16–17 cm)	19.3	216
PO287-26 (16–17 cm)	19.3	211
PO287-26 (19–20 cm)	22.8	216
PO287-26 (19–20 cm)	22.8	217
PO287-26 (24–25 cm)	28.7	131
PO287-26 (29–30 cm)	34.5	116
PO287-26 (34–35 cm)	40.4	74
D13902 (27–28 cm)	75.4	47
D13902 (62–63 cm)	110.9	47

Table 4
Results of AMS dating of the Tagus prodelta box, gravity and piston cores (PO287-26B, PO287-26G and D13902). Ages were reservoir corrected by 400 yr, considering the results presented in Table 1.

Sample ID (cm)	Spliced Depth	Sample Type	^{14}C Age (BP)	Reservoir ^{14}C Age (BP)	Corr Calender Age	Age AD
PO287-26B (32–33 cm)	51.0–52.0	Mollusk shell	440725	40725	51725	1899
D13902 (27–28 cm)	75.4–76.4	Mollusk shell	492739	92739	111739	1839
D13902(31–32cm)	*79.4–80.4*	*Molluskshell*	*2100780*	*1700780*	*1700780*	—
D13902(37–38cm)	*85.4–86.4*	*Molluskshell*	*8955770*	*8555770*	*8555770*	—
D13902(46–47cm)	*94.4–95.4*	*Molluskshell*	*7075750*	*6675750*	*6675750*	—
D13902 (62–63 cm)	110.4–111.4	Mollusk shell	1160745	760745	691745	1259
D13902 (62–63 cm)	110.4–111.4	Turritela	1185740	785740	704745	1246
D13902 (96–97 cm)	144.4–145.4	Mollusk shell	1370745	970745	863740	1087
D13902 (124–125 cm)	172.4–173.4	Shell Fragments	1880780	14807160	1394745	556
D13902 (151–152 cm)	199.4–200.4	Mollusk shell	2007737	1607737	14877160	463
D13902 (199–200 cm)	247.4–248.4	Mollusk shell	2340755	1940755	1885737	65
PO287-26G (86–87 cm)	86.0–87.0	Mollusk shell	545725	145725	1394745	1801

Levels *in italic* correspond to ages not considered for the age model

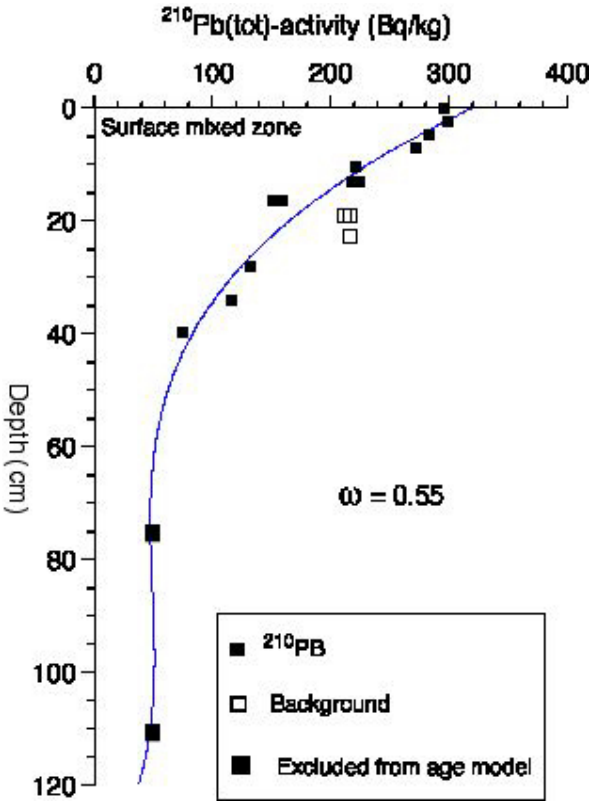

Fig. 2. ^{210}Pb activity (Bq/kg) profile obtained for box-core PO287-26 and top of core D13902.

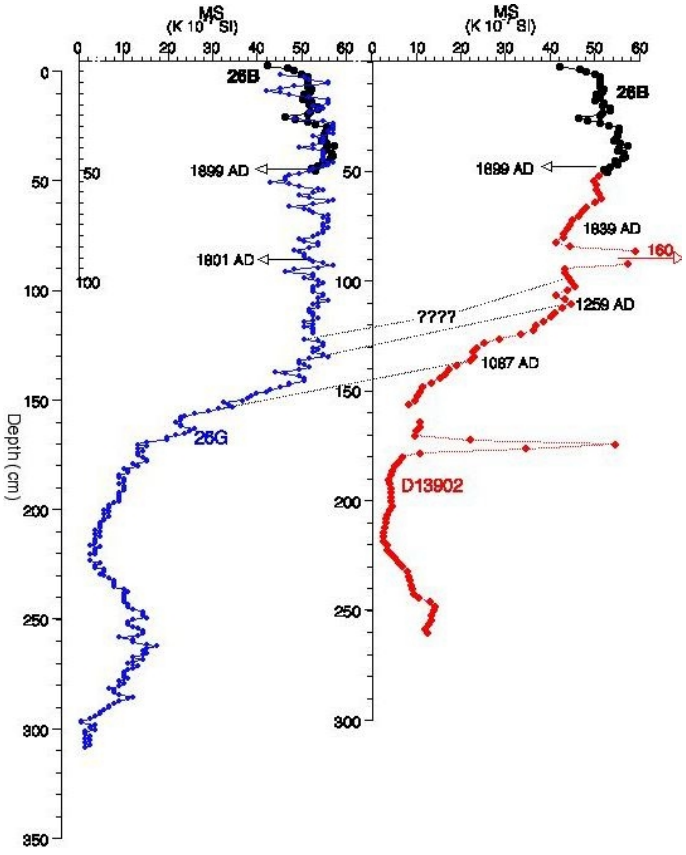

Fig. 3. Correlation between cores PO287-26B and D13902, and PO287-26B and PO287-26G based on the MS (10^{-7}SI) record and AMS ^{14} C dates.

If this sedimentation rate is considered constant down to the next dated level in core D13902, AMS ^{14}Cdated as 92±39 yr BP, then one can estimate that piston core D13902 failed to recover the uppermost 48 cm of the seafloor at this location, a result also indicated by a simple correlation of the MS and $U^{k'}_{37}$ data of both cores, and used to splice the piston with the box-core PO287-26B in order to develop a continuous record throughout the late Holocene (Fig. 3). The sequence of 3 AMS dates, between 95 and 76 cm ccd which deviate considerably from the remaining 9 dates are not included in the age-depth model for core D13902 (Fig. 4) as they are probably related to reworking. Their sedimentological significance will be discussed in Section 4.1. Gravity core PO287-26G was dated by AMS ^{14}C at 86 cm (Table 4), and correlated to the

other two cores as shown in Fig. 3, and used to fill the gap detected in the record of core D13902. AMS ^{14}C ages are corrected for a marine reservoir effect of 400 years, as determined for the area (Section 3.1) and converted to calendar ages and Anno Domini (AD) with the Calib 4.2 program (Stuiver *et al*., 1998).

Sedimentation rate was determined by linear interpolation between all accepted dated points (Fig. 5) and an estimated sedimentation rate of 0.11 cm/yr is found. However, a major change in sedimentation rate is obvious below and above the interval with anomalous older ages, implying a major hiatus and/or change in sedimentation regime at this level.

Consistent with the established sedimentations rates (0.47 cm/yr for box-core, top 75 cm of piston core D13902, and top 100 cm of gravity core 26G, and 0.11 cm/yr for the rest of the piston core and 0.14 cm/yr for the gravity cores (Fig. 5)), a sampling spacing of 1 cm provides a mean temporal resolution of 1.5 yr between 1759 and 2001 AD and 8.4 yr between 1600 and 0 AD.

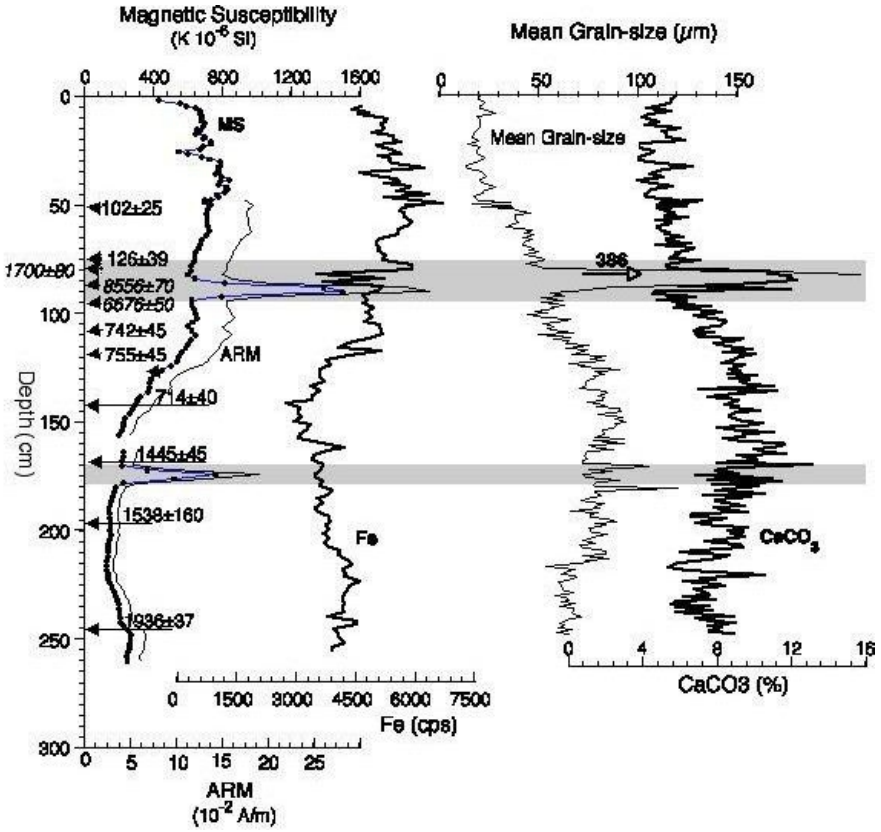

Fig. 4. Magnetic susceptibility, ARM, Fe, grain-size mean, $CaCO_3$ percent abundance, and, radiocarbon chronology versus PO287-26 and D13902 composite depth. Ages as calendar yr BP (2001); MS (10^{-6} SI—full dots) and mean grain-size (μm—open diamonds). Gray bands mark the intervals of high magnetic susceptibility.

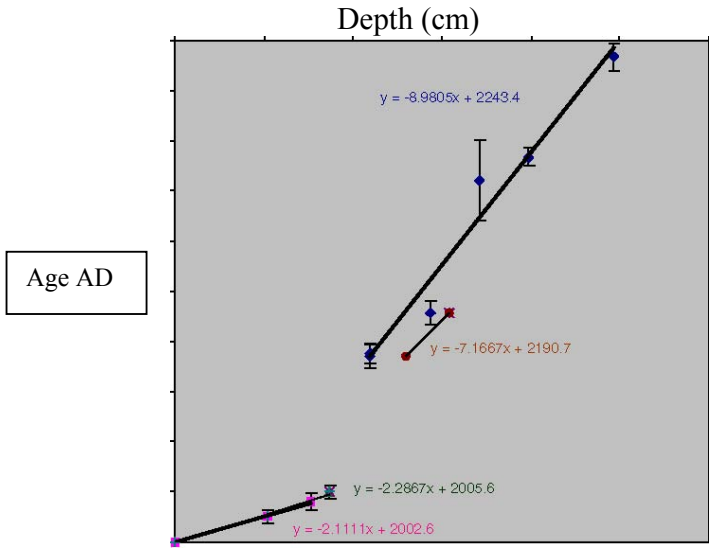

Fig. 5. Age versus depth model for cores PO287-26 and top of core D 13902 based on AMS ^{14}C ages listed in Table 4. Squares correspond to the box-core PO287-26B and top of core D 13902; diamonds represent ages determined for core D13902, triangle represents the age obtained for core PO287-26G, and circles represent the estimated depth for PO287-26G of D13902 dated levels (as in Fig. 3).

4. Results and discussion

4.1.Earthquake activity

MS, ARM, mean grain size, and $CaCO_3$ content along the spliced sequence (box-core PO287-26B and piston-core D13902) are shown in Fig. 4. Extremely high magnetic susceptibility values are coincident with an ARM increase centered at 90 cm ccd, and are followed at ~85 cm ccd by contemporary maxima in mean grain size (up to 386 μm) and in $CaCO_3$ concentration. A smaller maximum in MS and ARM, but no clear increase in mean grain size or in $CaCO_3$, is centered at 174 cm ccd.

The sequence of 3 samples (Table 4) giving ages much older than expected, when all the other dated samples are considered, was found within the 95-to 76-cm ccd interval. This interval coincides with the first abnormally high peaks in magnetic susceptibility and grain size referred to above, which indicates a major event/process that caused reworking of older sequences during a short time interval.

Anomalously old dates are embedded between 1259±45 and 1839±39 AD. This time encompasses 1755 AD, the date of the major earthquake and tsunami felt in the Iberian Peninsula, noted in historical records as the Lisbon earthquake. The earthquake, which had a devastating effect in the Lisbon area, was a multiple event, composed of three shocks (Vilanova

et al., 2003) one of which had an estimated magnitude *M* of 8.7 (Baptista *et al*., 1988a) and modified Mercalli (MM) intensity *X* (Wood and Newmann, 1931 in Vilanova *et al*., 2003). According to historical records, the earthquake was felt as far north as Sweden and Finland, while the tsunami waves reached the Caribbean Sea (Baptista *et al*., 1988b). Eyewitness accounts of the event were compiled and analyzed by de Sousa (1928), in which one can read ''...waves approached Lisbon with an angle from SE to NE, submerging the downtown area of the city and depositing boats on the top of the old town'' (de Sousa, 1928); or yet ''the sea retreated in such a way that for moments the beach was extended to the Torre de S. Julião'' (close to an old fortress located about 15 km from Lisbon on the estuary N margin, Fig. 1).

Although different epicenters have been proposed by different authors, a SE position relative to the SW Portuguese coast is accepted (Machado, 1966; Zitellini, 2001; Terrinha *et al*., 2003; Vilanova *et al*., 2003), corroborating the SE direction of water transport indicated by the above eyewitness report. A southward origin is also indicated by the on-land deposits found mainly in the southern part of Portugal (Andrade, 2002). However, Vilanova *et al*. (2003) defend that the stress changes resulting from the offshore main shock induced the rupture of Lower Tagus Valley Fault (LTVF in Fig. 1 of Vilanova *et al*., 2003) a few minutes after the main shock. This would have resulted in a sequence of high-energy tsunami waves, a tsunami-like wave in the Tagus followed by the arrival of the offshore-generated tsunami, which most likely caused enormous alteration on both the bed of the Estuary and the shallow-shelf area of our cores (90 m water depth). Nevertheless, it is also likely that an instantaneous lag deposit was formed by the deposition of part of the material transported on the flood back of those high-energy waves. According to Dingler and Anima (1981) a sedimentary sequence resulting from artificially generated mass flows produces a deposit similar to the one found in this core (Fig. 4), that is, a level of fine-magnetic grain-size below a much coarser and carbonate rich layer deposited above.

According to the above information and the model of Vilanova *et al*. (2003), the western area of the Tagus prodelta is likely to have received more sediment from the tsunami-like wave generated in the Estuary, whereas a stronger impact by the offshore-generated tsunami wave is likely to have occurred southeastwards of the Tagus estuary mouth. Several cores collected in the area (Fig. 1) were correlated through their magnetic susceptibility records and a few dates (Fig. 6). The records reveal that a general increase in magnetic susceptibility is noticable at all sites, but the strong-magnetic susceptibility peak found in D13902 was not observed in any of the other sites. Spatial comprehensive studies of shallow marine tsunami deposits, such as the

one generated on a shallow marine embayment NW of Java by the Krakatau eruption, have revealed major variability in both the composition and thickness of the tsunamite with lack of a record on the north open-sea facing part of the bay (van der Bergh *et al*., 2003).

The lack of evidence of the tsunami at sites located to the west of the Tagus river mouth, an area certainly more sheltered from the south coming waves is understandable, but the lack of evidence in PO287-26 is suspicious. Visual examination of the archive halves of both cores does not reveal major perturbations in the sediment. The MS measurements for D13902 were repeated on U-channels sampled from the central part of the archive core in order to verify possible liner contamination with downcore sediments through pistonage (upward transport of older material along the core barrel). Those analyses confirmed the occurrence of a major magnetic susceptibility peak and the AMR data validates the existence of an exceptionally high concentration of magnetic minerals in fine-grained sediment with no equivalent record found at the bottom of the core. The relative position of the two southern sites may be the explanation. A closer examination of the local bathymetry shows that site PO287-26 has been recovered from a minor canyon that may have worked as a washout pathway of material towards the deeper Tagus Abyssal Plain, where a major turbidite records the 1755AD earthquake and tsunami (Thomson and Weaver, 1994).

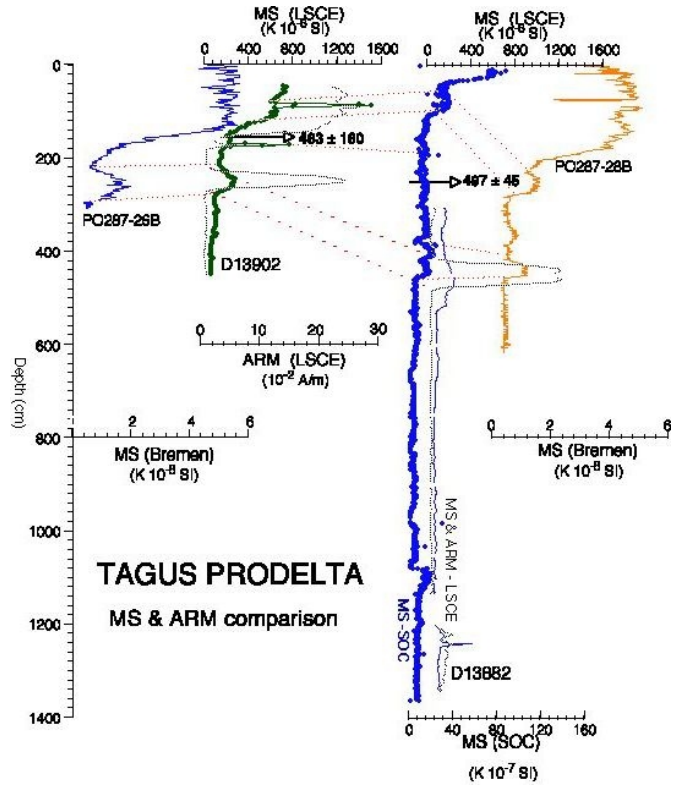

Fig. 6. Magnetic susceptibility and ARM comparison for four cores collected on the Tagus Prodelta and depicted on Fig. 1. (Research Institutions where measurements were preformed: LSCE—Laboratoire des Sciences du Climat et de l'Environnement; SOC—Southampton Ocenographic Center; Bremen—University of Bremen.)

With this hypothesis in mind, the 19 cm of older sediments found in D13902, between 95 and 76 cm ccd, are likely to correspond to an instantaneous deposit of reworked material transported by the high-energy waves during a tsunami. The oldest dated level below the ‘‘tsunamite’’ (110.9 cm ccd) has an age of 1259 AD. If we assume that the sedimentation rate was maintained at 0.11 cm/yr, the estimated age for the last level below the event (95.4 cm ccd) is 1400 AD. Based on the age difference between this level and the year of the tsunami (1755), 355 years of record, about 39 cm of sediment, have been eroded. Even though no clear change in sedimentation pattern is perceived on the MS record of core PO287-26G, from the correlation of the two cores (Figs. 3 and 5), either a major change in SR is implied between 86.5 and 130 cm ccd, or there is a loss of ~22 cm sediment (~160 years of record).

If, on the other hand, one considers a change in sedimentation regime and accepts a drastic decrease in sedimentation rate between 1259 and 1839 AD (Fig. 5), the estimated age limits of the older D13902 sediment sequence become 1515 and 1832 AD, with 1755 AD at 80 cm ccd.

The smaller magnetic susceptibility and ARM maxima centered at 174 cm ccd have an estimated age of 716 AD. In spite of the large number of earthquakes registered in the historical records (Matias/Terrinha, personal communication), no earthquake occurrence is noted between 382 AD and 944 AD. As such, the increasing magnetic susceptibility and ARM may record another earthquake event.

4.2. Climate change

Considering the position of this core relative to the major hydrographic processes that presently characterize the Portuguese margin, we intend to reconstruct both the river input/continental climate variability and productivity/upwelling intensity oscillations throughout the last 2000 years.

4.2.1. Temperature

The SST $U^{k'}_{37}$ record indicates a 4°C variability (14–18 °C) (Fig. 7). From 0 to 200 AD, SST values average 18 °C. Between 200 and 500 AD there is a decrease to ~17 °C followed by a rise to 18 °C at 630 AD. After this date, SST decreases to ~17 °C at 1080 AD. A period of relatively stable temperatures (17 °C) between 1060 and 1200 AD is followed by a minimum at 1365 AD and a new rapid and sharp decrease of 2 °C to ~15 °C by 1600 AD. These temperatures are maintained from 1759 to 1880 AD, with a short duration minima centered at 1860 AD. Since

1900 AD, SST in the Tagus deposition center shows rapid and high amplitude oscillations between 14 °C and 17 °C at a decadal scale (mean 15.5 °C, Standard deviation 0.82°C). The top sample of the box-core sequence gives a temperature of 15 °C.

Instant in situ temperatures reported by Moita (2001) between the summer of 1985 and the winter of 1986 vary between 16 and 14 °C, respectively (Table 5). Furthermore, satellite-derived average SST, calculated from monthly mean values and a time series of data comprising years 1987 to 1999, indicate 15.5 °C for winter, and 19.5 °C for summer temperatures (Table 5).

Alkenones are produced by coccolithophores. The work of Moita (2001) has shown that, in the Tagus pro-delta, coccolithophores dominate the plankton for most of the year, being outcompet by diatoms only during the upwelling season. Given that upwelling is more likely to occur between May and September (Fiuza, 1983, 1984), we expect SST – $U^{k'}_{37}$ will mainly reflect winter to early-spring temperatures. The SST - $U^{k'}_{37}$ temperature calculated from the box-core levels corresponding to this same time interval, is 15 °C, in good agreement with the satellite-derived values, considering the errors of each method.

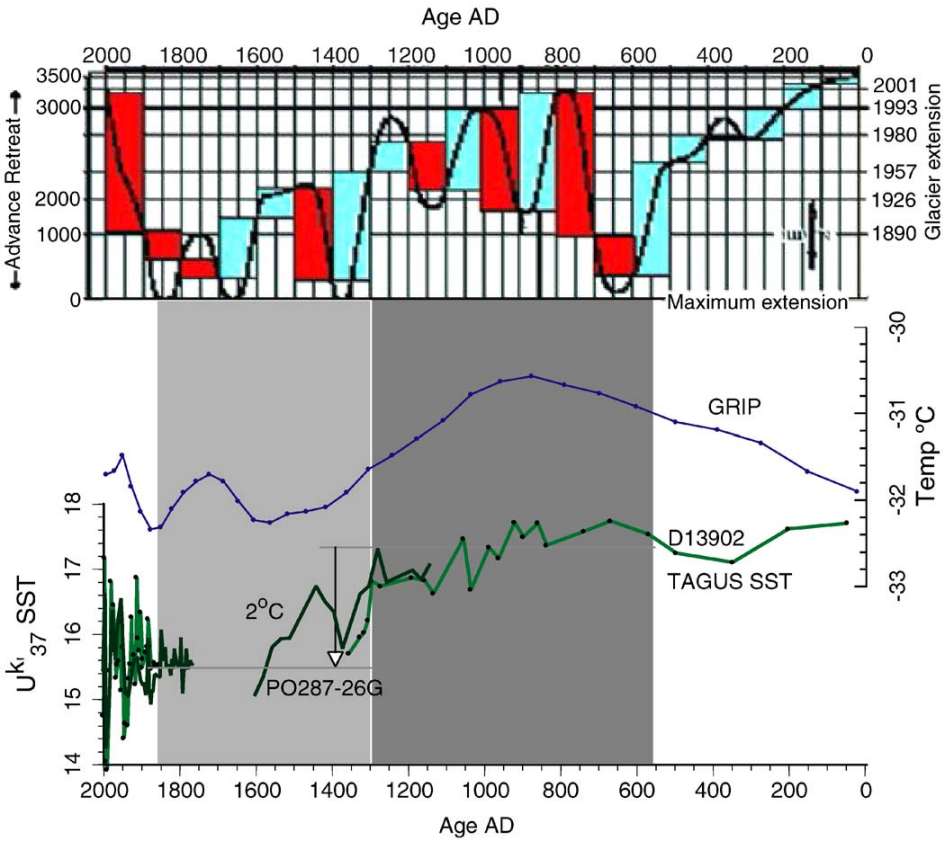

Fig. 7. $U^{k'}_{37}$derived SST anomaly along the Tagus site compared with GRIP borehole and Alpine glaciers advance. SST record with symbols- D13902 and PO287-26B spliced sequence; Line without symbols-PO287-26G. Light Gray Band-LIA; Dark Gray Band-MWP.

Table 5
SST and Phytoplankton data for the Tagus prodelta

	Summer	Winter	Spring	Fall
SST (°C)				
In situ (Instantaneous)[a]	16.0	14.0	14.5	—
Satellite mean (1987–1999)	19.5	15.5	17.5	17.5
Total phytoplankton (# cells/l)[a]	20,000	1000	10,000	—
% Coccolithophores[a]	25–50	50–75	480	—

[a]Data from Moita (2001).

The SST $-U^{k'}_{37}$ off Lisbon (Fig. 7) shows a general decreasing trend for the last 2000 years, marked by the first sharp decline at 1300 AD, but reaching minimum temperatures at ~1600 AD. Although the record is interrupted, between 1759 and 1900 AD, temperatures were still ~15.5°C with a short minima of 15.3°C at 1860 AD. A wide range of climate proxies measured throughout the globe indicate that temperatures were colder than present during the LIA from 1300 to 1900 AD (Stuiver and Braziunas, 1989; Keigwin, 1996; Dunbar and Cole, 1999; Keigwin and Pickart, 1999; deMenocal *et al*., 2000a; McDermott *et al*., 2001; Esper *et al*., 2002; Grudd *et al*., 2002; Gupta *et al*., 2003). This cold period was preceded by warmer temperatures in medieval times. Although less clearly defined and dated in a lower number of sites, the MWP is considered to have occurred between 800 and 1300 AD (Cronin *et al*., 2003; Dahl-Jensen *et al*., 1998; deMenocal *et al*., 2000; Jones *et al*., 2001). In our record, temperatures for this period show a mean value 1.5–2°C higher than the mean temperature observed between 1300 and 1900 AD. This increase in temperatures is in good agreement with both the trend and the magnitude of change observed in the Greenland boreholes (Fig. 7) (Dahl-Jensen *et al*., 1998). However, SST starts to raise around 550 AD, again in good agreement with the GRIP record, but about 100 years earlier than alpine glacier recession (Holzhauser, 1997; Haeberli and Holzhauser, 2003). In addition, most sedimentological parameters indicate that the 550–1300 AD interval was climaticaly and oceanographically different from the climatic and oceanographic conditions before and after this interval.

Within the last 100 years, the mean SST value in the Tagus record equals the mean value for the 1300–1900 AD interval. However, rather stable SSTs are registered between 1759 and 1900 AD, whereas during the last 100 years, rapid variability in SST of broadening amplitude is observed.

4.2.2.River input/continentalclimate

Satellite-derived estimates of the suspended load in the Tagus river plume for a time series between May 1992 and January 1993 (Williams, 1994) indicate that the load of suspended particles, although higher in winter, is large throughout the year. As shown in Fig. 8, from an image of the space shuttle taken in September 1992, sites PO287-26 and D13902 fall within the area of influence of river and sediment discharge. In addition, short but intense rainfall events may lead to floods such as the one observed in February of 1979, causing river flows (12,000m^3/s) 10^6times higher than the months average (0.9 m^3/s) and 30 times higher than the mean-annual flow (400 m^3/s). During these floods the suspended load reaches 300 mg/l whereas the average values are around 20 mg/l (Vale, 1981). Thus, the increase in deposition of fine continental derived material at sites PO287-26 and D13902 can be related with rainfall increases.

At our site, the sediments are composed of terrigenous material with low $CaCO_3$ contents between 4% and 14% (Fig. 9). In terms of grain size, this sequence can be divided into three sections: 0–550 AD, 550–1300 AD and 1300 AD-Present, representing mud (sediment fraction <63 μm, that is, silt+clay—50–60%), sand (47%), and mud (70–80%). This suggests increased river input before 550 AD and after 1300 AD.

Other parameters measured in these cores, MS, Fe, *n*-alkanes, and *n*-alcohols are well-accepted indicators of terrigenous input (Farrington *et al*., 1988; Poynter *et al*., 1989; Lamy *et al*., 1998; Fischer and Wefer, 1999; Ortiz and Rack, 1999). MS shows extremely high values between 76 and 95 cm ccd and 170–174 cm ccd, which most certainly correspond to reworked material (Fig. 4, Section 4.1). If these maxima are excluded, MS shows values between 100 and 700 K 10^{-6} SI units, with highest values above 1300 AD, and a broad minimum between 200 and 1200 AD (Fig. 9). Increases in Fe content (cps) clearly parallel the fine-sediment fraction in the core. The same is observed for the organic carbon (Corg) content, with percentage abundances varying between 0.5% and 1.5% and a tendency to increase in association with the silt and clay content, whereas higher $CaCO_3$ amounts are associated with coarser sediments between 550 and 1300 AD (Figs. 4 and 9).

The lipid composition of this sedimentary sequence is dominated by compounds of terrigenous origin, such as the C_{23}–C_{33} *n*-alkanes and C_{20}–C_{30} *n*-alcohols. The strong correlation of both lipid groups to indicators of alocthonous input and to the presence of fresh water diatoms (Figs. 9 and 10), confirm an increase in sedimentation of continental-derived material during the LIA. Within the last century all parameters show decadal cyclicity, but a decreasing tendency is observable in

the Fe concentration and mean grain-size (Figs. 4 and 9) also accompanied by a decrease in mass accumulation rate (MAR—Fig. 10). The decrease in MAR may be due to the retention of sediments that resulted from the construction of 52 dams along both the Spanish and Portuguese sides of the Tagus. In particular, between 1940 and 1960, when rapid construction of a large number of dams increased the areal surface and water volume of impounded systems increased by a factor of 5 (www.chtajo.es).

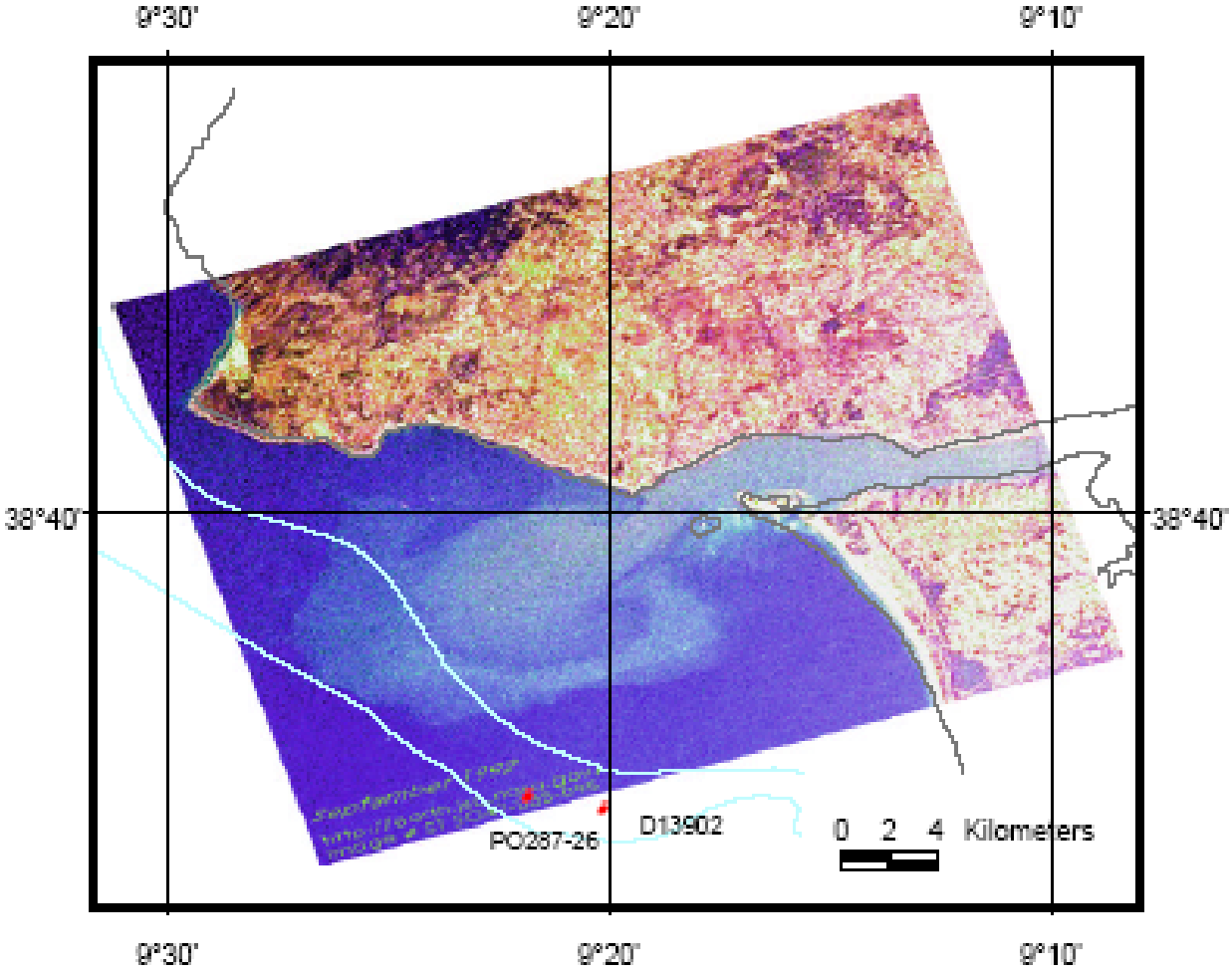

Fig. 8. Space shuttle image of the Tagus River plume (September 1992). http://earth.jsc.nasa.gov/image#SO47-085-095.

4.2.3. Sea-water salinity

The oxygen stable-isotopic composition ($\delta^{18}O$) of the planktonic foraminifera *G.bulloides* and the benthic species *Uvigerina* sp. 221 are shown in Fig. 11. The results show parallel trends for

both records, with an almost constant isotopic offset between 0 and 1300 AD. $\delta^{18}O$ oscillates around 0.5‰ and 1.75‰ for *G. bulloides* and *Uvigerina* respectively. In the last 100 years, the *G. bulloides* record shows a more pronounced variability exhibiting an overall decrease in $\delta^{18}O$ to 0.1‰ for the most recent samples.

Comparison of the variations in terrigenous inputs with past salinities should provide information on the magnitude of river discharge. Salinity in the river plume is generally bellow 35 p.s.u. during Winter and most of Spring (Moita, 2001). $\delta^{18}O$ of foraminifera is mainly determined by $\delta^{18}O$ of ambient seawater and temperature. During the time interval in question no major global-ice-volume-related $\delta^{18}O$ variations have occurred, thus, most of the *G. bulloides* $\delta^{18}O$ signal must reflect regional temperature and salinity conditions, while the *Uvigerina* values are likely to record bottom water (90 m water depth) and oceanic conditions. Lighter $\delta^{18}O$ values of *G. bulloides* appear to be associated with increases in MS and Fe, which are associated with increased precipitation and river runoff (Fig. 9). As $\delta^{18}O$ is linearly related to salinity (dilution by fresh water), sea surface paleosalinities (SSS) can be reconstructed if independent measures of SST are available (Duplessy *et al*., 1984; Rostek *et al*., 1993). In the present study, $\delta^{18}O$ of *G. bulloides* and SST $-U^{k'}_{37}$ are used. Both proxies reflect surface temperatures within the photic zone (Bentaleb *et al*., 1999). Thus, given the shallow depth of the site, no correction for temperature was applied to the *G. bulloides* $\delta^{18}O$ values.

The paleotemperature equation of Shackleton (1974) was used for the reconstruction of $\delta^{18}O$ of ambient seawater:

$$T = 16.9 - 4.38\,(\delta^{18}O_{carb} - (\delta^{18}O_w)$$
$$+0.1\,(\delta^{18}O_{carb} - (\delta^{18}O_w),$$

where T is paleotemperature (°C), $\delta^{18}O_w = \delta^{18}O$ of ambient seawater (per mil versus SMOW), and ($\delta^{18}O_{carb} = \delta^{18}O$ of carbonate (*G. bulloides*) (per mil versus PDB).

The lack of a local $\delta^{18}O$-salinity relationship, prevents the calculation of SSS values, but in the absence of major ice cap changes within the last 2000 years, the anomaly is assumed to be related to changes in salinity driven by river flux.

Calculations can only be done for the levels with foraminifera and alkenone measurements, but the general tendency to lighter $\delta^{18}O$ of ambient waters observed after 1300 AD certainly reflect fresher waters (Figs. 9 and 11). A relation between decreased salinity and lower temperatures is obvious after 1900 AD.

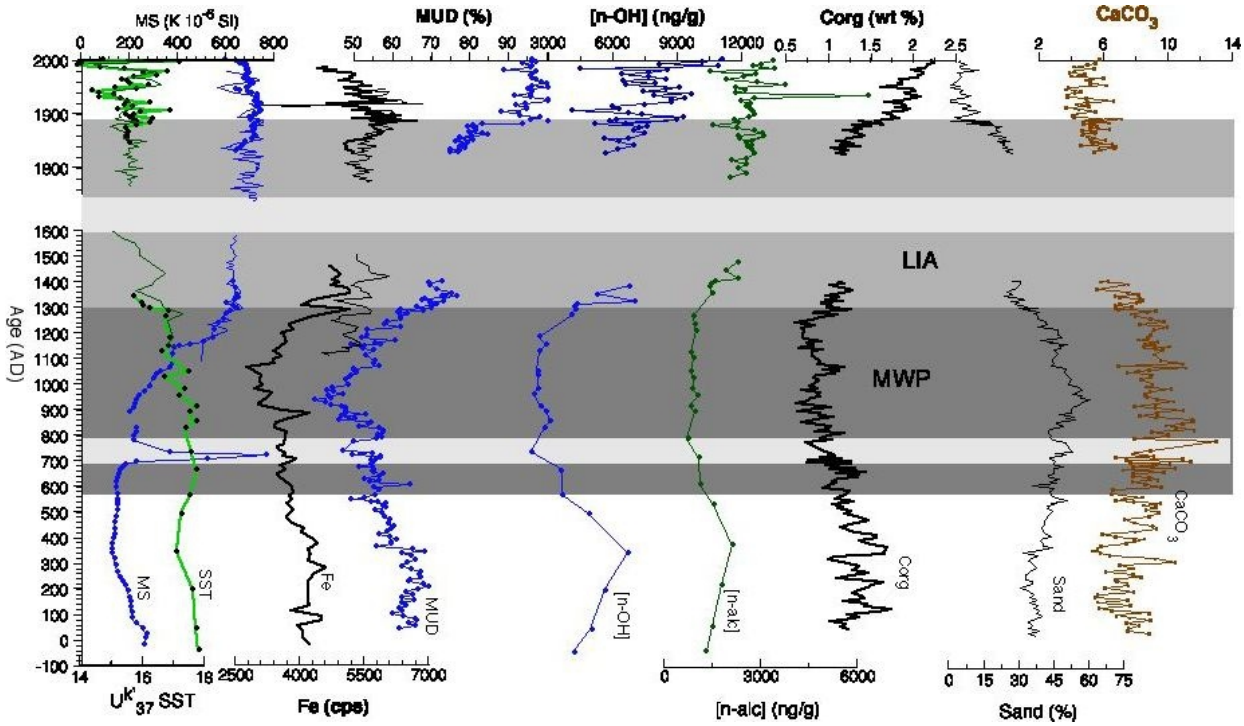

Fig. 9. Continental climate proxies along cores PO287-26 and D13902. MS—magnetic susceptibility (10^{-6} SI units); $U^{k'}_{37}$ derived SST, Fe content as determined by XRF in cps units; Mud—Percent abundance of the sediment fraction <63 μm; [*n*-OH]—alcohols concentration; [*n*-alc]—alkanes concentration; Corg—Organic Carbon content; Percent abundance of Sand; grain-size mean (μm). For MS, SST and Fe thick line represents the data for the D13902 and PO287-26-B spliced sequence, and the thin line the data for core PO287-26G. Medium Gray Band—LIA; Dark Gray Band— MWP; Light Gray bands—Intervals of high MS.

4.2.4.The North Atlantic oscillation and theTagus

The MWP as defined from the alkenone derived temperature (Fig. 7), corresponds to the carbonate maxima positioned between the LIA $CaCO_3$ minima and the earlier $CaCO_3$ minima between 200 and 550 AD. This carbonate increase is accompanied by an increase in mean grain size and minima in continental input indicators.

The relevance of the NAO to the wintertime temperatures, wind speed and direction, and, precipitation across much of the Northern Hemisphere and over the Atlantic/European sector in particular, has been well documented through a number of different studies (Hurrell, 1995, 1996; Rogers, 1997; Osborn *et al*., 1999; Ulbrich *et al*., 1999; Qian *et al*., 2000). Furthermore, the work of Trigo *et al*. (2002) indicates a high correlation between precipitation rate during winter months and low NAO index for the area of the Tagus Basin. A comparison of Hurrel's NAO index (difference between normalized winter sea-level atmospheric pressures between Lisbon, Portugal, and Stykkisholmur, Iceland—Hurrel, 1995) to the Tagus river mean winter

(December–March) discharge between 1900 and 2000 AD is presented in Fig. 12 and reveals a good negative correlation to NAO. Both results support the influence of the NAO on river regime, and are consistent with, though not proof of, a possible long-term association as well. A NAO-like mechanism or the NAO itself, which tended to remain in a low index phase during LIA, and in a high phase during the MWP, could account for the findings in the Tagus prodelta. Further indications of a primarily negative NAO during LIA have been found from the study of sedimentary sequences off Norway (Koç *et al*., 2003) and off Newfoundland (Keigwin and Pickart, 1999), as well as from dendrochronologic summer temperature reconstruction (Grudd *et al*., 2002). An essentially NAO-negative-like phase before 1800 AD is also supported by the Luterbacher *et al*. (2002) multi-proxy reconstruction of the NAO (1400 AD to Present).

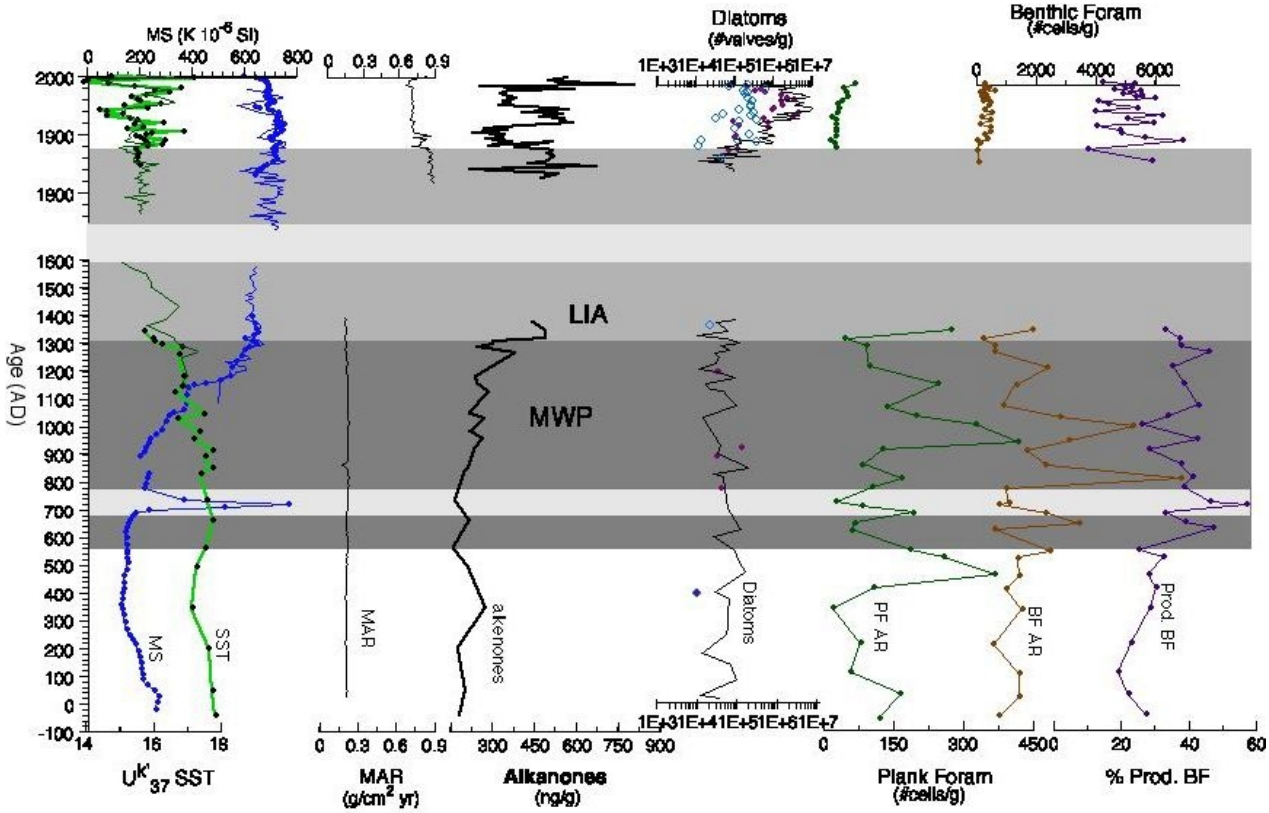

Fig. 10. Productivity proxies along cores PO287-26 and D13902. MS—magnetic susceptibility (data in cgs units 10^6); $U^{k'}_{37}$ derived SST anomaly to the mean; MAR—Mass Accumulation Rate as g/cm^2/yr; Alkenones abundance (ng/g); Diatom abundance as #valves/g of dry sediment, ○—freshwater diatoms, ●—upwelling related diatoms; Planktonic Foraminifera Abundance in #shells/g; Benthic Foraminifera Abundance as #shells/g; % Prod. PF—Percent abundance of the high carbon flux benthic foraminiferal species. Medium Gray Band—LIA; Dark Gray Band—MWP; Light Age (AD) Gray bands—Intervals of high magnetic susceptibility.

4.3.Coastal productivity

Increased primary productivity is generated by the input of new nutrients into the euphotic zone (Dugdale and Goering, 1967; Margalef, 1985). Both coastal upwelling and river runoff can bring new nutrients into coastal regions. However, the water-column conditions generated by these processes are different, involving strong mixing and stratification. Whereas strong mixing caused by upwelling favors the dominance of diatoms, stratification leads to a occolithophore-dominated community (Margalef, 1985; Moita, 2001).

Foraminifera, react to the increase in primary producers. Increases in planktonic foraminifera fluxes, as a response to upwelling pulses, have been observed in sediment-trap experiments (Sautter and Thunell, 1991; Curry and Ostermann, 1992; Ortiz and Mix, 1992; Sautter and Sancetta, 1992; Thunnel and Sautter, 1992; Wefer and Fisher, 1993; Abrantes *et al*., 2002). In addition, increased abundances of benthic foraminifera have been reported as consequence of increases in particle rain to the sea floor (Lutze and Coulbourn, 1984; Altenbach and Sarnthein, 1989; Loubere, 1991; Herguera, 1992; Rathburn and Corliss, 1994).

At our site, diatoms are present in small numbers, an order of magnitude lower than observed in the surface sediments along the rest of the Portuguese coast (Abrantes, 1988) (Fig. 10). Although the evident dissolution indicated by the rapid and important decrease in diatom abundance at about 1940 AD 2000 (~ 30 cm within the sediment), identical abundances in 2005 both coarse and fine sediments, which have a higher sealing effect (Broecker and Peng, 1982), points to initial production as the main control for this diatom record. In terms of assemblages, benthic diatoms are dominant, but upwelling related species (● in Fig. 10) are present between 550 and 1300 AD (MWP) and in the last 100 years, while freshwater forms (○ in Fig. 10) are only present before 500 and after 1300 AD.

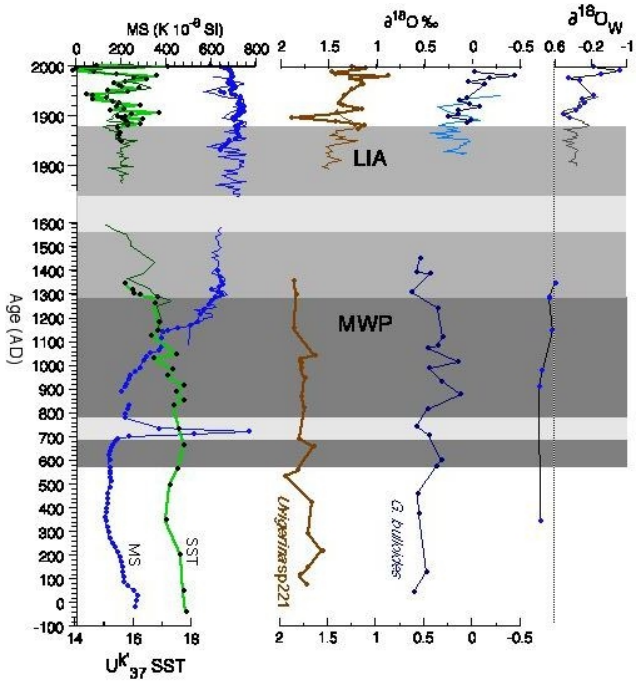

Fig. 11. Isotopic record for ^{18}O on *G. bulloides* and Uvigerina sp. 221 and $^{18}O_w$ anomaly along cores PO287-26B and D13902. Medium Gray Band—LIA; Dark Gray Band—MWP; Light Gray bands—Intervals of high magnetic susceptibility

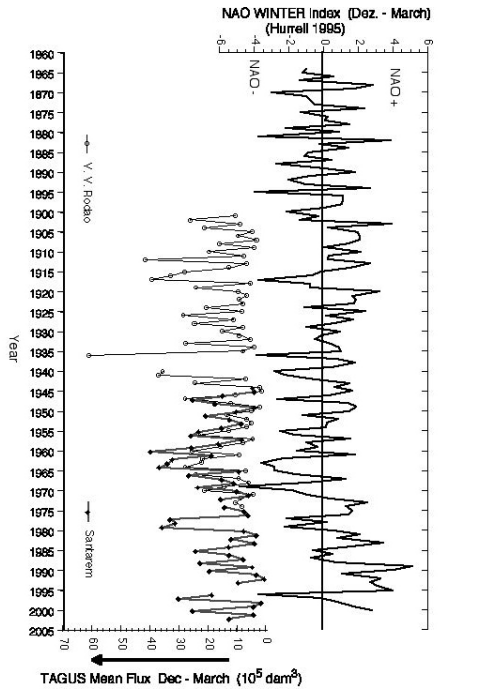

Fig. 12. Comparison of the NAO Index of Hurrell (1995) to the Tagus mean flux during the winter months (December-March) as measured at the Vila Velha de Rodão and Santarém between 1900 and 2003

As for total alkenones, which indicate coccolithophore production (Schubert *et al*., 1998; Schulte *et al*., 1999; Villanueva *et al*., 1997, 2001), concentrations are also lower than those found in cores from the open Atlantic (Bard *et al*., 2000; Villanueva *et al*., 1997, 2001). In this sedimentary sequence, alkenone concentration of 200 ng/g, between 0 and 1300 AD, oscillates from 300 to 600 ng/g after 1300 AD, minimizing increments in continental input indicators, such as Fe and *n*-alkanes or *n*-alcohols (Fig. 9). Based on the work of Cabeçadas *et al*. (2003), winter NO_3 concentrations at the Tagus estuary mouth are about 15 µmol/l decreasing to 4 µmol/l 1.5 nautical miles offshore. The significance of the Tagus River as a source of PO_4^{3-}has also been shown by quantification of the P and N sediment pool sizes (Cabeçadas and Brogueira, 1997). Thus, coccolithophore production during the LIA (1300–1900 AD) is likely to be induced by the riverine input of nutrients.

Planktonic foraminifera have abundances (100–450 shells/g) one order of magnitude lower than benthic foraminifera (500–6000 shells/g), and most of the observed foraminifera are

juvenile. However, the down-core trend in abundance is similar for both planktonic and benthic foraminifera, with higher abundances and amplitude variation observed between 500 and 1300 AD, and lower abundances and less variability observed before 500 AD and at the top of the sequence.

Within the benthic foraminifera species found in these cores, *Bolivina dilatata* (*Bolivina spathulata* in Levy *et al*., 1993), *Bolivina striatula*, and *Hyalinea balthica* have been related to productivity of the overlying waters (Levy *et al*., 1993; Jónsdóttir *et al*., 2003). Besides, the works of Lutze and Coulbourn (1984), Altenbach (1988), Altenbach and Sarnthein (1989) and Schmiedl (1995) have shown that the *Uvigerina* group also respond to high-carbon fluxes. The percent contribution of all these species to the benthic assemblage (Fig. 10) varies between 20% and 60%, with clear cyclicity and higher average values between 550 and 1300 AD.

Increased abundances of foraminifera, both benthic and planktonic, and the presence of upwelling related diatoms during the MWP (Fig. 10), point to the MWP as an interval of stronger upwelling conditions. These results are in good agreement with the results of Diz *et al*. (2003) for a northern Iberian site (Ria de Muros), but in apparent contradiction with the published data for NW Africa by deMenocal *et al*. (2000b). deMenocal *et al*. (2000b) hypothesized an enhanced eastern boundary current delivery of cold subpolar waters or an increase in regional upwelling as a possible explanation for the lower temperatures observed off the NW African coast during the LIA. Iberia and the NW African coasts are influenced by the same eastern boundary current, the Portuguese-Canary current. Nevertheless, significant differences exist between the two sites: (1) at modern times, upwelling favorable conditions occur year round off NW Africa, but only for about 5 months off Portugal; (2) the Tagus site is under the influence of the Tagus river plume and can only feel the Cape Roca filament productivity if and when upwelling conditions are strong. Considering the results of Salgueiro *et al*. (2003) who preformed planktonic foraminifera sensus counts and foraminifera derived SST on four box-cores located along a profile on the SW Portuguese margin, no major changes in upwelling conditions are observed between the LIA and the MWP. This may indicate that even though the eastern boundary system is likely to have persisted, the Portuguese/Canary Current System transported colder subpolar waters during the LIA. The decrease in SSTs by 2° (Tagus) and 4°C off NW Africa (deMenocal *et al*., 2000) is consistent with other data from the Bermuda Rise (Keigwin, 1996) and may reflect the advection of anomalous temperatures by the Gulf Stream/North Atlantic Current system, considered by Visbeck *et al*. (2003) as the reason for

Hemispheric SST variability on multidecadal time scales.

As for the MWP, one could argue that less river input of alochthonous material to the Tagus site, could lead to an apparent increase in productivity indicators by a lower dilution effect. However, MAR does not vary throughout the MWP, but the sediment terrigenous content decreases during this period, as indicated by grain-size and all other river-input indicators. As such, a real increase in carbonate biogenic particles production and sedimentation, certainly caused by more persistent and/or intense coastal upwelling conditions has to be implied (Figs. 9 and 10).

Instrumental data indicate that during positive NAO, precipitation is reduced and the stronger north-Atlantic pressure gradient generates winds favorable to the occurrence of coastal upwelling as well as a strengthening of the North Atlantic current system. Nykjaer and Van Camp (1994) and Oliveira (2000), have calculated the interannual variability of SST, upwelling Index, and Ekman Upwelling Index for the years 1981–1989 and found that the largest anomalies (i.e., more intense upwelling than average occurred in 1982, 1985 and 1988) are in good agreement with positive NAO index (Fig. 10). As for the LIA, modern NAO conditions might also be used as an analogue to explain the Tagus MWP record (drier continental conditions and increased coastal upwelling) if more consistent or extreme positive NAO conditions were maintained during the few centuries that preceded the LIA.

5. Conclusions

Proxy evidence for continental derived material illustrates the high sensitivity of the Tagus river regime to the climatic variability of the last two millennia and reveals a record of a major earthquake felt in the region, as recorded by a large peak in MS centered at 90 cm ccd. The well known 1755 AD Lisbon earthquake and tsunami, is estimated to have eroded 160–355 years of the sedimentary record (most of the LIA) and instantaneously deposited a 19 cm sediment bed consisting of a lower layer of silt sized heavy mineral particles, followed by a coarser layer composed of reworked shell fragments at site D13902.

Within dating uncertainties (50 years) the SST – $U^{k'}_{37}$ for the latest Holocene (2000 years) off Lisbon, can be correlated to the GRIP borehole temperature, allowing the identification of a warm period (MWP) between 550 and 1300 AD, and the LIA.

The marine geological data presented here point to dryer continental conditions and increased coastal upwelling conditions during MWP, and indicate increased river influx and river induced

marine productivity during LIA. Because negative NAO is correlated with precipitation anomaly fields in the Tagus basin, the LIA increased influx of terrigenous material into the studied site is hypothesized to reflect NAO-like variability with more persistent negative state or frequent extreme NAO minima during the LIA. During the milder few centuries of the MWP, coastal upwelling favorable conditions are attributed to more persistently NAO positive state, or, frequent extreme NAO maxima.

Acknowledgements

We thank the captain and crew of RV Discovery and RV Poseidon for their help in collecting the samples. A. Inês, C. Monteiro, M.J. Custódio, A. Silva and C. Trindade of the Institute of Geology and Mining are acknowledged for analytical assistance. The EU PALEOSTUDIES project supported the XRF measurements. Monika Siegel is acknowledged by her help with the isotope measurements, and J. Heinnemeier and W. Boer by the AMS ^{14}C dating and ^{210}Pb measurements respectively. We also thank the Aquário Vasco da Gama for allowing the use of the D. Carlos collection. Thanks are also due to A. Voelker and two anonymous reviewers for the careful review of the initial manuscript. Financial support was provided by the EU projects HOLSMEER (EVK2-CT-2000-00060) and PACLIVA (EVK2-CT2002-00143). Funding for T. Rodrigues was provided by the Fundação para a Ciência e Tecnologia, through the INGMAR project.

REFERENCES

Abrantes, F., 1988. Diatom assemblages as upwelling indicators in surface sediments in Portugal. Marine Geology 85, 15–39.

Abrantes, F., Moita, T., 1999. Water column and recent sediment data on diatoms and coccolithophorids, off Portugal, confirm sediment record as a memory of upwelling events. Oceanologica Acta 22, 319–336.

Abrantes, F., Meggers, H., Nave, S., Bollman, J., Palma, S., Sprengel, C., Hendericks, J., Spies, A., Salgueiro, E., Moita, T., Neuer, S., 2002. Fluxes of micro-organisms along a productivity gradient in the Canary Islands region (29°N): implications for paleoreconstructions. Deep-Sea Research II 49, 3599–3629.

Altenbach, A.V., 1988. Deep sea benthic foraminifera and flux rates of organic carbon. Review Paleobiologie (vol. spéc.) 2, 719–720.

Altenbach, A.V., Sarnthein, M., 1989. Productivity record in Benthic Foraminifera. In: Berger, W.H., Smetacek, V.S., Wefer, G. (Eds.), Productivity of the Ocean: Present and Past. Dahlem Workshop— Life Sciences Research Reports. Wiley, Berlin, pp. 255–270.

Andrade, C., 2002. Assinaturas Geológicas de Inundação Tsunami-génica no Litoral do Algarve. In: 3°Encontro de Professores de Geociências do Algarve.

Appleby, P.G., Oldfield, F., 1992. Applications

of Lead-210 to Sedimentation Studies. Clarendon Press, Oxford.

Baptista, M., Miranda, P., Mendes Victor, L., 1988a. Constraints on the source of the 1755 Lisbon tsunami inferred from numerical modelling of historical data. Journal of Geodynamics 25, 159–174.

Baptista, M.A., Heitor, S., Miranda, J.M., Miranda, P., Victor, L.M., 1988b. The 1755 Lisbon tsunami evaluation; of the tsunami parameters. Journal of Geodynamics 25, 143–157.

Bard, E., Rostek, F., Turon, J.-L., Gendreau, S., 2000. Hydrological impact of Heinrich events in the subtropical northeast Atlantic. Science 289, 1321–1324.

Bentaleb, I., Grimalt, J.O., Vidussi, F., Marty, J.-C., Martin, V., Denis, M., Hatte´ , C., Fontugne, M., 1999. The C37 alkenone record of seawater temperature during seasonal thermocline stratification. Marine Chemistry 64, 301–313.

Bond, G., Showers, W., Cheseby, M., Lotti, R., Almasi, P., deMenocal, P., 1997. A pervasive millenial-scale cycle in North Atlantic Holocene and Glacial climates. Science 278, 1257–1266.

Bond, G., Kromer, B., Beer, J., Muscheler, R., Evans, M., Showers, W., Hoffmann, S., Lotti-Bond, R., Hajdas, I., Bonani, G., 2001. Persistent solar influence on North Atlantic climate during the Holocene. Science 294, 2130–2136.

Broecker, W.S., 2001. Was the medieval warm period global?. Science 291, 1497–1499.

Broecker, W.S., Peng, T.H., 1982. Tracers in the sea. Eldigio Press, New York.

Cabeçadas, G., Brogueira, M.J., 1997. Sediments in a Portuguese coastal area—pool sizes of mobile and immobile forms of nirogen and phosphorus. Marine and Freshwater Research 48, 559–563.

Cabeçadas, G., Rogueira, M.J., Nogueira, M., Cabeçadas, L., Cavaco, H., Nogueira, P., 2003. Coastal phytoplankton productivity associated with different stability and nutrient patterns. EGS-AGU-EUG Joint Meeting, AGU, Nice, France, pp. EAE-A-09277.

Cronin, T.M., Dwyer, G.S., Kamiya, T., Schwede, S., Willard, D.A., 2003. Medieval warm period, little Ice Age and 20th century temperature variability from Chesapeake Bay. Global and Planetary Change 36, 17–29.

Curry, W.B., Ostermann, D.R., 1992. Foraminiferal production and monsoonal upwelling in the Arabian sea: evidence from sediment traps. In: Summerhayes, C.P., Prell, W.L., Emeis, K.C. (Eds.), Evolution of Upwelling Systems Since the Early Miocene. Geological Society Special Publication No. 64, London, pp. 93–106.

Dahl-Jensen, D., Mosegaard, K., Gundestrup, N., Clow, G.D., Johnsen, S., Hansen, A.W., Balling, N., 1998. Past temperatures directly from the Greenland ice sheet. Science 282, 268–271.

de Abreu, L., 2000. High resolution paleoceanography off Portugal during the last two glacial cycles. Unpublished Dissertation Thesis, University of Cambridge.

deMenocal, P., Ortiz, J., Guilderson, T., Adkins, J., Sarnthein, M., Baker, L., Yarusinsky, M., 2000a. Abrupt onset and termination of the African Humid Period: rapid climate responses to gradual insolation forcing. Quaternary Science Reviews 19, 347–361.

deMenocal, P., Ortiz, J., Guilderson, T., Sarnthein, M., 2000. Coherent high-and low-latitude climate variability during the Holocene warm period. Science 288, 2198–2202.

Dingler, J., Anima, R., 1981. Field study of subaqueous avalanching. AAPG Bulletin 65 (5), 918–919.

Diz, P., Francés, G., Pena, L., Nombela, M.A., Alejo, I., 2003. Benthic Foraminifera response to Holocene environmental changes in the Ría de Muros (NW Spain). EGU-AGU-EUG

General Assembly, AGU, Nice.

Dugdale, R., Goering, J., 1976. Uptake of new and regenerated forms of nitrogen in primary productivity. Limnology and Oceanography 12, 196–206.

Dunbar, R., Cole, J., 1999. Annual Records of Tropical Systems (ARTS), recommendations for research. PAGES Workshop Report, 72pp.

Duplessy, J.-C., Laberyie, J., Juillet-Leclerc, A., Maitre, F., Duprat, J., Sarnthein, M., 1984. Surface salinity reconstruction of the North Atlantic Ocean during the Last Glacial maximum. Oceanologica Acta 14, 311–324.

Esper, J., Cook, E.R., Schweingruber, F.H., 2002. Low-frequency signals in long tree-ring chronologies for reconstructing past temperature. Science 295, 2250–2253.

Farrington, H.W., Davis, A.C., Sulanowski, J., McCaffrey, M.A., McCarthy, M., Clifford, C.H., Dickinson, P., Volkman, J.K., 1988. Biogeochemistry of lipids in surface sediments of the Peru upwelling area at 15°S. Organics Geochemistry 13 (4–6), 607–617.

Fischer, G., Wefer, G., 1999. Use of Proxies in Paleoceanography. Springer, Berlin.

Fiuza, A., 1983. Upwelling patterns off Portugal. In: Suess, E., Thiede, J. (Eds.), Coastal Upwelling its Sediment Record. Plenum Press, New York, pp. 85–98.

Fiuza, A., 1984. Hidrologia e Dinamica das Aguas Costeiras de Portugal. Unpublished Dissertation Thesis, University of Lisbon.

Gaspar, L., Monteiro, H., 1977. Matéria Orgânica nos sedimentos da plataforma continental portuguesa entre os cabos Espichel e Raso. Comunicações dos Servic-os Geológicos de Portugal LXII, 69–83.

Goodfriend, G., Flessa, K., 1997. Radiocarbon reservoir ages in the Gulf of California: roles of upwelling and flow from the Colorado River. Radiocarbon 39, 137–148.

Grudd, H., Briffa, K.R., Karlen, W., Bartholin, T., Jones, P.D., Kromer, B., 2002. A 7400-year tree-ring chronology in northern Swedish Lapland: natural climatic variability expressed on annual to millenial timescales. The Holocene 12, 657–666.

Gupta, A., Anderson, D., Overpeck, J., 2003. Abrupt changes in the Asian southwest monsoon during the Holocene and their links to the North Atlantic Ocean. Nature 421, 354–357.

Haeberli, W., Holzhauser, H., 2003. Alpine glacier mass changes during the past two millenia. PAGES News 11, 13–15.

Herguera, J.C., 1992. Deep-sea benthic foraminifera and biogenic opal: glacial to postglacial productivity changes in the western equatorial Pacific. Marine Micropaleontology 19, 79–98.

Holzhauser, H., 1997. Fluctuations of the Grosser Aletsch Glacier and the Gorner Glacier during the last 3200 years: new results. Palaeoclimate Research 24, 35–58.

Hurrell, J., 1995. Decadal trends in the North Atlantic oscillation— regional temperatures and precipitation. Science 269, 679.

Hurrell, J., 1996. Influence of variations in extratropical wintertime teleconnections on Northern Hemisphere temperature. Geophysical Research Letters 23, 665–668.

Hurrell, J., Kushnir, Y., Ottersen, G., Visbeck, M., 2003. An overview of the North Atlantic oscillation. In: Hurrel, J., Kushnir, Y., Ottersen, G., Visbeck, M. (Eds.), The North Atlantic Oscillation: Climatic Significance and Environmental Impact. AGU, Washington, pp. 1–35.

Jansen, J.H.F., Van der Gaast, S.J., Koster, B., Vaars, A.J., 1998. Cortex, a shipboard XRF-scanner for element analyses in split sediment cores. Marine Geology 151, 143–153.

Jones, P.D., Osborn, T.J., Briffa, K.R., 2001. The evolution of climate over the last millenium. Science 292, 662–667.

Jónsdóttir, H.B.B., Knudsen, K.L., Abrantes, F., Heinnemeier, J.E., 2003. Late Holocene climate variability on the Western Iberian Margin: benthic foraminiferal perspective. Newsletter of Micropalaeontology 68, 26.

Keigwin, L., 1996. The little ice age and medieval warm period in the Sargasso Sea. Science 274, 1504–1507.

Keigwin, L., Pickart, R., 1999. Slope water current over the Laurentian fan on interannual to millenial time scales. Science 286, 520–523.

Kissel, C., Laj, C., Labeyrie, L., Dokken, T., Voelker, A., Blamart, D., 1999. Magnetic signature of rapid climatic variations in North Atlantic sediments. In: Abrantes, F., Mix, A. (Eds.), Reconstructing Ocean History: A Window into the Future. Plenum Publishing, London, pp. 419–437.

Koç, N., Andersen, C., Andrews, J., Jennings, A., 2003. Decadal-scale Holocene climate variability in Nordic Seas. EGS-AGU-EUG Joint Meeting, AGU, Nice, France, pp. EAE03-A-14116.

Lamy, F., Hebbeln, D., Wefer, G., 1998. Late quaternary precessional cycles of terrigenous sediment input off the Norte Chico, Chile (27.5°S) and paleoclimatic implications. Palaeogeography, Palaeoclimatology, Palaeoecology 141, 233–251.

Levy, A., Mathieu, R., Poignant, A., Rosset-Moulinier, M., Ubaldo, M.d.L., Ambroise, D., 1993. Recent foraminifera from the continental margin of Portugal. Micropaleontology 39, 75–87.

Little, E., 1993. Radiocarbon age calibration at archeological sites of coastal Massachusetts and vicinity. Journal of Archeological Science 20, 457–471.

Loeblich, A.R., Tappan, H., 1988. Foraminiferal Genera and Their Classification. Van Nostrand Reinhold Company, New York, pp. 1–212.

Loubere, P., 1991. Deep-sea benthic foraminiferal assemblage response to a surface ocean productivity gradient: a test. Paleoceanography 6, 193–204.

Luterbacher, J., Schmutz, C., Gyalistras, D., Xoplaki, E., Wanner, H., 2002. Extending North Atlantic Oscillation reconstructions back to 1500. Atmospheric Science Letters 2, 114–124.

Lutze, G.-F., Coulbourn, W.T., 1984. Recent benthic foraminifera from the continental margin of Northwest Africa: community structure and distribution. Marine Micropaleontology 8, 361–401.

Machado, F., 1966. Contribuição para o Estudo do Terramoto de 1 de Novembro de 1755, Revista da Faculdade de Ciências de Lisbon Series C 14, 19–31.

Margalef, R., 1985. Primary production in upwelling areas. Energy, global ecology and resources. In: Bas, C., Margalef, R., Rubies, P. (Eds.), Simposio International Sobre las areas de Afloramiento mas importantes del oeste Africano (Cabo Blanco Y Buenguela). Instituto de Investigaciones Pesqueras, Barcelona, pp. 225–232.

McDermott, F., Mattey, D., Hawkesworth, C., 2001. Centennial-scale Holocene climate variability revealed by a high-resolution speleothem $\delta^{18}O$ record from SW Ireland. Science 294, 1328–1331.

Moita, T., 2001. Estrutura, Variabilidade e Dinâmica do Fitoplâncton na Costa de Portugal Continental. Unpublished Article Compilation Thesis, University of Lisbon.

Monteiro, H., Moita, I., 1971. Morfologia e sedimentos da plataforma continental e vertente continental superior ao largo da Peninsula de Setúbal. Congresso de Geologia, 301–330.

Müller, P.J., Kirst, G., Ruhland, G., von Storch, I., Rosell-Meré , A., 1998. Calibration of the alkenone paleotemperature index $U^{k'}_{37}$ based on core-pops from the eastern South Atlantic and the global ocean (60°N–60°S). Geochimica et Cosmochimica Acta 62, 1757–1772.

Nykjaer, L., Van Camp, L., 1994. Seasonal and interannual variability of coastal upwelling along northwest Africa and Portugal from 1981 to 1991. Journal of Geophysical Research 99, 14,197–14,207.

Oliveira, P., 2000. Aplicação de Dados de Satélite ao Estudo da Variabilidade da Temperatura da Superfície do Mar no Atlântico Nordeste Subtropical. Unpublished Dissertation Thesis, University of Lisbon.

Ortiz, J., Mix, A., 1992. The spatial distribution and seasonal succession of planktonic foraminifera in the California Current off Oregon, September 1987–September 1988. In: Summerhayes, C., Prell, W., Emeis, K. (Eds.), Upwelling Systems: Evolution Since the Early Miocene. Geological Society Special Publications, London, pp. 197–214.

Osborn, T.J., Briffa, K.R., Tett, S.F., Jones, P.D., Trigo, R.M., 1999. Evaluation of the North Atlantic oscillation as simulated by a climate model. Climate Dynamics 15, 685–702.

Poynter, J.G., Farrimond, P., Robinson, N., Eglinton, G., 1989. Aeolian-derived higher plant lipids in the marine sedimentary record: links with paleoclimate. In: Leinen, M., Sarnthein, M. (Eds.), Paleoclimatology and Paleometerology: Modern and Past Patterns of Global Atmospheric Transport. Kluwer Academic Publishers, Dordrecht, pp. 435–462.

Qian, B., Corte-Real, J., Xu, H., 2000. Is the North Atlantic oscillation the most important atmospheric pattern for precipitation in Europe? Journal of Geophysical Research 105, 11901–11910.

Rathburn, A., Corliss, B., 1994. The ecology of living (stained) deep-sea benthic foraminifera from the Sulu Sea. Paleoceanography 9, 87–150.

Rogers, J.C., 1997. North Atlantic storm track variability and its association to the North Atlantic oscillation and climate variability of northern Europe. Journal of Climatology 10, 1635–1647.

Rostek, F., Ruhland, G., Bassinot, F.C., Mueller, P.J., Labeyrie, L.D., Lancelot, Y., Bard, E., 1993. Reconstructing sea surface temperature and salinity using $\delta\ ^{18}O$ and alkenone records. Nature 364, 319–321.

Salgueiro, E., Abrantes, F., Loncaric, N., Lebreiro, S., Moreno, J., Pflaumann, U., Oliveira, P., Meggers, H., 2003. Productivity changes off Portugal: foraminiferal evidence for the last 1500 years. EGS-AGU-EUG Joint Meeting, AGU, Nice, France, pp. EAE0300488.

Sautter, L.R., Sancetta, C., 1992. Seasonal associations of phytoplankton and planktic foraminifera in an upwelling region and their contribution to the seafloor. Marine Micropaleontology 18, 263–278.

Sautter, L.R., Thunell, R.C., 1991. Planktonic foraminiferal response to upwelling and seasonal hydrographic conditions: sediment trap results from San Pedro Basin, Southern California bight. Journal of Foraminiferal Research 21, 347–363.

Schmiedl, G., 1995. Late Quaternary benthic foraminiferal assemblages from the eastern South Atlantic Ocean: reconstruction of deep water circulation and productivity changes. Berichte zur Polarforschung 160, 207.

Schubert, C.J., Villanueva, J., Calvert, S.E., Cowie, G.L., von rad, U., Schulz, H., Berber, U., 1998. Stable phytoplankton community in the Arabia Sea over the last 200,000 years. Nature 394, 563–566.

Schulte, S., Rostek, F., Bard, E., Rullkötter, J., Marchal, O., 1999. Variations of oxygen-minimum and primary productivity recorded in sediments of the Arabian Sea. Earth and Planetary Science Letters 173, 205–221.

Shackleton, N., 1974. Attainment of isotopic equilibrium between ocean water and the benthonic foraminifera genus *Uvigerina*: Isotopic changes in the ocean during the last glacial. Colloquium International CNRS 219, 203–209.

Shackleton, N., Hall, M., Vincent, E., 2000.

Phase relationships between millenial-scale events 64000–24000 years ago. Paleoceanography 15, 565–569.

Sousa, F.M., 1995. Processos de Mesoescala ao largo da Costa Portuguesa utilizando dados de Satélite e Observações in situ. Unpublished Dissertation Thesis, University of Lisbon.

de Sousa, F.P., 1928. Distritos de Lisboa. Serviços Geológicos de Portugal, Lisboa.

Sousa, F., Bricaud, A., 1992. Satellite-derived phytoplankton pigment structures in the Portuguese upwelling area. Journal of Geophysical Research 97, 11343–11356.

Stuiver, M., Braziunas, T., 1989. Atmospheric ^{14}C and century-scale solar oscillations. Nature 338, 405–408.

Terrinha, P., Pinheiro, L.M., Henriet, J.-P., Matias, L., Ivanov, M.K., Monteiro, J.H., Akhmetzhanov, A., Volkonskaya, A., Cunha, T., Shaskin, P., Rovere, M., 2003. Tsunamigenic-seismogenic structures, neotectonics, sedimentary processes and slope instability on the southwest Portuguese Margin. Marine Geology 195, 55–73.

Thomson, J., Weaver, P.P.E., 1994. An AMS radiocarbon method to determine the emplacement time of recent deep-sea turbidites. Sedimentary Geology 89, 1–7.

Thunnel, R., Sautter, L.R., 1992. Planktonic foraminiferal faunal and stable isotopic indicators of upwelling: results from sediment trap study in the Califoria current. In: Summerhayes, C., Prell, W., Emeis, K. (Eds.), Upwelling Systems: Evolution since the Early Miocene. Geological Society Special Publications, London, pp. 77–92.

Trigo, R.M., Osborn, T.J., Corte-Real, J., 2002. The North Atlantic oscillation influence on Europe: climate impacts and associated physical mechanisms. Climate Research 20, 9–17.

Ulbrich, U., Christoph, M., Pinto, J.G., Corte-Real, J., 1999. Dependence of winter precipitation over Portugal on NAO and baroclinic wave activity. International Journal of Climatology 19, 379–390.

Vale, C., 1981. Entrada de matéria em suspensão no estuário do Tejo durante as chuvas de Fevereiro de 1979. Recursos Hídricos 2, 37–45.

van der Bergh, G.D., Boer, W., Haas, H., van Weering, T., van Wijhe, R., 2003. Shallow marine tsunami deposits in Telik Banten (NW Java, Indonesia), generated by the 1883 Krakatau eruption. Marine Geology 197, 13–34.

Vilanova, S., Nunes, C., Fonseca, J., 2003. Lisbon 1755: a case of triggered onshore rupture?. Bulletin of the Seismological Society of America 93, 2056–2068.

Villanueva, J., 1996. Estudi de les variaciones climàtiques i oceanogràfiques a l`Atlantic Nord Durant els últims 300.000 anys mitjançant l`análisi de marcadores moleculars. Disseration Thesis, Universitat de Barcelona.

Villanueva, J., Grimalt, J.O., 1997. Gas Chromatographic Tuning of the $U^{k'}_{37}$ Paleothermometer. Analytical Chemistry 69, 3329–3332.

Villanueva, J., Pelejero, C., Grimalt, J.O., 1997. Clean-up procedures for the unbiased estimation of C37 alkenone sea surface temperatures and terrigenous *n*-alkane in paleoceanography. Journal of Chromatography A757, 145–151.

Villanueva, J., Calvo, E., Pelejero, C., Grimalt, J.O., Boelaert, A., Labeyrie, L., 2001. A latitudinal productivity band in the central North Atlantic over the last 270 kyr: an alkenone perspective. Paleoceanography 16, 617–626.

Visbeck, M., Chassignet, E., Curry, R., Delworth, T., Dickson, R., Krahmann, G., 2003. The ocean's response to North Atlantic oscillation variability. In: Hurrel, J., Kushnir, Y., Ottersen, G., Visbeck, M. (Eds.), The North Atlantic Oscillation: Climatic Significance and Environmental Impact. AGU, Washington, pp. 113–145.

Voelker, A., Lebreiro, S., Schonfeld, J.,

Abrantes, F., Erlenkeuser, H., 2002. Dansgaard-Oeschger Cyclicity in the Eastern Gulf of Cadiz: Synchroneity between surface and deep water response and Greenland temperature. AGU Fall meeting. AGU, S. Francisco, pp. 47 (OS21A-0183).

Weeks, R., Laj, C., Endignoux, L., Fuller, M., Roberts, A., Manganne, R., Blanchard, E., Goree, W., 1993. Improvements in long-core measurement techniques: applications in paleomagnetism and paleoceanography. Geophysical Journal International 114, 651–662.

Wefer, G., Fisher, G., 1993. Seasonal patterns of vertical flux in equatorial and coastal upwelling areas of the Eastern Atlantic. Deep-Sea Research 40, 1615–1645.

Williams, D., 1994. Satellite study of the Tagus sediment plume. Institute of Geology and Mining, Marine Geology Department Report 21/94, Lisbon.

Zitellini, N., 2001. Source of 1755 Lisbon earthquake and tsunami investigated. EOS Transactions 82

CHAPTER 5:

Climate change and coastal hydrographic response along the Atlantic Iberian margin (Tagus Prodelta and Muros Ría) during the last two millennia

S.M. Lebreiro, G. Francés, F.F.G. Abrantes, P. Diz, H.B. Bartels-Jónsdóttir, Z. Stroynowski, I.M. Gil, L. D. Pena, T. Rodrigues, P. D. Jones, M.A. Nombela, I. Alejo, K. R. Briffa, I. Harris, J. O. Grimalt

The Holocene (in press)

Climate change and coastal hydrographic response along the Atlantic Iberian margin (Tagus Prodelta and Muros Ría) during the last two millennia

S.M. Lebreiro[1], G. Francés[2], F.F.G. Abrantes[1], P. Diz[2], H.B. Bartels-Jónsdóttir[1], Z. Stroynowski[1], I.M. Gil[1], L. D. Pena[3], T. Rodrigues[1], P. D. Jones[4], M.A. Nombela[2], I. Alejo[2], K. R. Briffa[4], I. Harris[4], J. O. Grimalt[5]

[1]INETI, Department of Marine Geology, Estrada da Portela, Zambujal, 2721-866 Alfragide, Portugal
[2]University of Vigo, Facultad de Ciencias, Department of Marine Geosciences, 36200 Vigo, Spain
[3]University of Barcelona, Dept. Stratigraphy, Paleontology and Marine Sciences, Calle Martí Franques, 08028 Barcelona, Spain
[4]University of East Anglia, Climatic Research Unit, Norwich NR4 7TJ, United Kingdom
[5]Institute of Chemical and Environment Research (CSIC), Dept. Environmental Chemistry, Jordi Girona, 18, 08034 Barcelona, Spain

Abstract

The Tagus Prodelta (W Portugal) and the Muros Ría (NW Spain) are areas of high deposition rates registering high-resolution paleoclimatic records for western Iberia. We compare the climatic conditions of the two areas over the last two millennia based on proxies of temperature (sea surface temperatures and oxygen isotopes), continental input (grain size, iron and magnetic susceptibility) and productivity (inorganic and organic carbon, carbon isotopes, benthic foraminifera and diatoms). Biogeochemical changes in the Tagus Prodelta reflect widely recognised North Atlantic climatic periods encompassing the Roman Period (AD 0-350), the Dark Ages (AD 400 – 700), the Medieval Warm Period (MWP) (AD 800 – 1200) and the Little Ice Age (LIA) (AD 1300 – 1750). The atmospheric North Atlantic Oscillation (NAO) drives the Tagus Prodelta multi-decadal, long-term variability in precipitation-river input during cold periods (negative NAO) and marine upwelling during warmer periods (positive NAO), a scheme that is reversed in the Galician region. The Muros Ría shows only local hydrodynamics until AD 1150, including a "suboxic" event in the inner Ría around AD 500-700. Since AD 1150 Atlantic warm upwelled waters have ventilated the outer Ría but only reach the inner Ría at AD 1750. The 20th century records are also interpreted as a reflex of the inverse NAO mode in both areas, resulting in amplification of the LIA biogeochemical water conditions. Centennial-scale solar activity appears to be another important forcing mechanism (or the only one, if solar activity drives the NAO and "Bond-cycles") behind changes in the hydrography of the Tagus Prodelta, and primary production, bottom ventilation and organic carbon degradation in the Muros Ría.

Keywords: Iberia, Tagus River, Muros Ría, NAO, climate, Medieval Warm Period – Little Ice Age

1. Introduction

The Tagus Prodelta and the Muros Ría are representative areas of shallow marine-continental processes in which hydrography is profoundly affected by climatic changes. Only the analysis of high sedimentation rate sequences can provide insights into decadal and (multi-)decadal climate variability characterised by the NAO or solar activity; we do not know yet how widely these affect Earth biogeochemical cycles. Furthermore, regional scale histories of different proxy variables are needed to expand our knowledge on climate variability beyond the instrumental record (Jones *et al*., 2001). Only in this way can we estimate the natural and humain contribution to climate variability and provide more accurate predictions for the future.

Today, the western Iberian climate is mainly determined by the atmospheric North Atlantic Oscillation (NAO), the eastern North Atlantic surface circulation, particularly the Portuguese-Canary boundary current, and the intermediate Eastern North Atlantic Central Water (ENACW). The Portuguese-Canary boundary brings cool water from the northernmost latitudes along the Iberian margin. The ENACW which Fiúza (1983) defined with two origins, subtropical (st) and subpolar (sp), converge at Cape Finisterre. Upwelling of ENACWst (salty and warm) or ENACWsp (fresh and cold) into the Muros Ría depends on favourable northerly winds from late spring to early autumn and the interannual hydrographic position of the front between these two water masses (Álvarez-Salgado *et al*., 1997; Varela *et al*., 2005). In the south, ENACWst upwells along the Tagus Prodelta. The NAO determines the direction and speed of the westerlies and precipitation over Europe and the Atlantic. The NAO Index measures the difference in atmospheric pressure at sea level between the Icelandic and Lisbon poles, mainly in winter (Hurrell, 1995). Close to the Lisbon pole, significant climate anomalies are evidenced by NAO impact on the precipitation anomaly fields (mm/month) determined for a 40 years time series from southern to northern Iberia (Trigo *et al*., 2002a; Trigo *et al*., 2002b).

The Tagus Prodelta is an organic-rich, fine-sediment prism located off the Tagus River on the Portuguese continental shelf (Monteiro and Moita, 1971; Cabeçadas and Brogueira, 1997) (Fig. 1). The Tagus mouth is preceded by a 340 km^2 (at high tide) tidal lagoon estuary-type (Vale and Sundby, 1987). The output of fresh-water to the estuary is 80-720 m^3s^{-1}, occasionally reaching 2200 m^3s^{-1} (Loureiro, 1979). The suspended sediment load entering the estuary is $4x10^5t$ (Vale,

unpublished data), as estimated from catastrophic floods such as the 1979 one, amounting to a volume of sediment sufficient to deposit a 7 mm- thick sheet over its entire surface (Vale and Sundby, 1987). Estuary sediments are mud and sand facies responding to changes in current and river flow regimes. The stronger river flood events are registered in the shelf sediments, alternating with productive episodes due to coastal upwelling enhancement (Abrantes *et al*., 2005a).

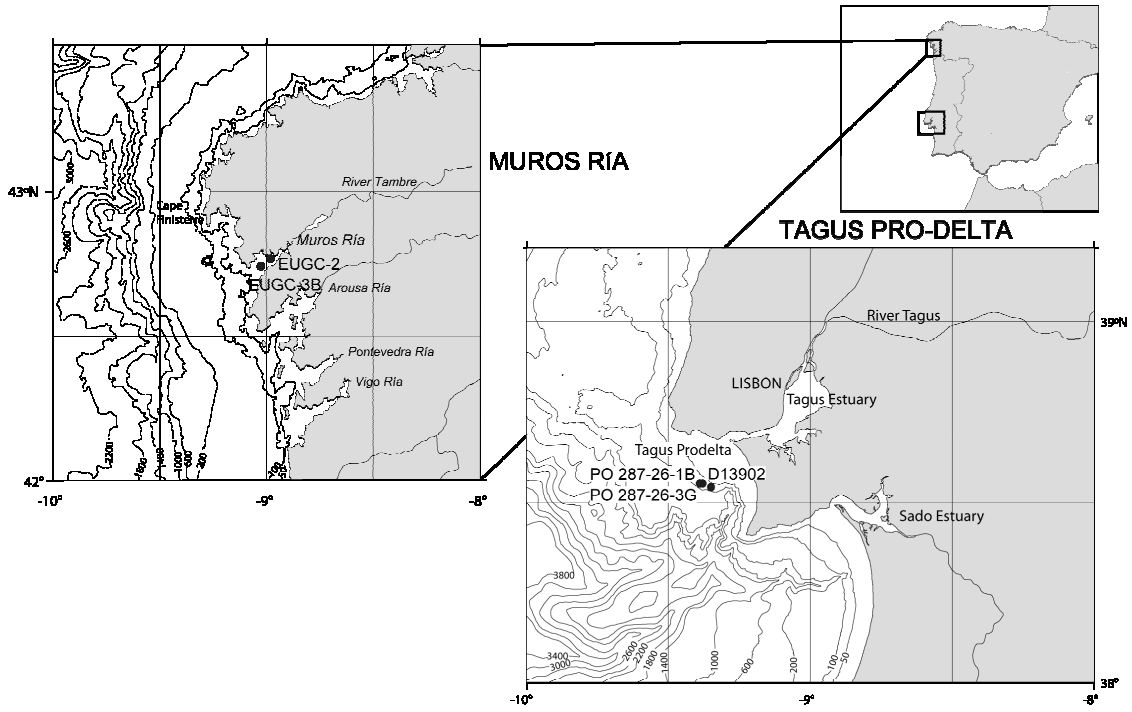

Figure 1. Geographic location of targeted areas in the Iberian Margin. Position of cores studied in the Tagus Prodelta and Muros Ría.

The Muros Ría (97 km^2) is a drowned river system deeply incised into the coastline which traps fluvial material rather than discharging it onto the Spanish continental shelf (Oliveira *et al*., 2002). The most significant freshwater input comes from the River Tambre (54 m^3s^{-1} mean discharge), which mostly influences the estuarine characteristics of the inner Ría. The outer Ría is under strong oceanic control exhibiting a residual circulation in two layers (Fraga and Margalef, 1979; Prego, 1990). Muros is the only Galician Ría without a group of islands at its mouth, which favours oceanic intrusion.

Off Iberia, primary production patterns are mainly conditioned by (1) summer persistent upwelling of cool and nutrient-rich ENACW from 100-300 m depth; (2) water column

stratification; (3) nutrient availability; and (4) the composition and distribution of phytoplankton (Fraga, 1981; Abrantes, 1988; Estrada, 1984; Varela *et al*., 1987; Ríos *et al*., 1992; Abrantes and Moita, 1999). During upwelling conditions (summer), water column chlorophyll *α* concentrations go up to 6 mg m^{-3} in the Tagus (Moita, 2001) and >7 mg m^{-3} in Muros (Nogueira *et al*., 1997). Diatoms are the main contributors at both sites, while coccolitophorids dominate the phytoplankton during non-upwelling, non-productive conditions (winter) (Bode *et al*., 1994; Abrantes and Moita, 1999). On the Tagus shelf, solar irradiation and river discharge results in maximum water stratification in summer, redistributing nutrients in the water column (Moita, 2001). In the two-layer stratified estuary of Muros, with a surface fresh-water outflow and a bottom oceanic inflow circulation, the export of nutrients and phytoplankton to the ocean reinforce the upwelling effect (Estrada, 1984). Furthermore, remineralization of organic matter enriches the subsurface water inflow which brings nutrients back into the Ría (Estrada, 1984). The range of primary production rates off Lisbon (0.6-1.6 g C m^{-2} d^{-1}; Antoine and Morel, 1996; Behrenfeld *et al*., 2001) and NW Spain (0.7-3.7 g C m^{-2} d^{-1}; Nunes *et al*., 1984; Prego, 1993) are similar to those recorded in the Benguela (0.5 g C m^{-2} d^{-1}; Brown and Field, 1986; Brown *et al*., 1991) and Peru upwelling regions (1.9 g C m^{-2} d^{-1}; Barber and Smith, 1981), or the California coastal upwelling system (0.5-2.6 g C m^{-2} d^{-1}; Pilskaln *et al*., 1996). Thus, in the Galician rías, productivity is primarily influenced by shelf winds as well as coastal and estuarine processes (Varela *et al*., 2001; Varela *et al*., 2005). On the Tagus Prodelta, primary productivity can be triggered either by an intensification of coastal upwelling along the Atlantic Iberian margin (Abrantes, 1988; Abrantes and Moita, 1999) or increased input of nutrients by the river into the area.

This paper presents high-resolution paleodata including O and C stable isotopes, benthic foraminifera, diatoms, grainsize and land derived major chemical elements, from two Iberian sedimentary systems: the Tagus Prodelta (Portugal) and the Muros Ría (NW Spain). Our objective is to analyse the regional response to "high-frequency" climate forcing mechanisms, such as the NAO and solar activity.

2: Material and methods

Core description

From the Tagus Prodelta, a spliced sediment sequence composed of box core PO287-26-1B, gravity core PO287-26-3G, and giant piston core D13902, collected during the Portuguese

PALEO1 campaign on board the R/V Poseidon, in 2002, and the British *Discovery* 249 cruise, in 2000, were used for this study. From the Muros Ría, two gravity cores EUGC-2 (inner Ría) and EUGC-3B (outer Ría), were collected during the B/O *Mytilus* cruise, in 2001. Both areas records cover the last 2000 years (Table 1, Fig. 1).

Core number	Core type	Water depth (m)	Core length (m)	Latitude (N)	Longitude (W)
PO287-26-1B	box	96	0.32	38º33.49'	9º21.84'
PO287-26-3G	gravity	96	3.05 (1.50)[i]	38º33.49'	9º21.84'
D13902	piston	90	6.00 (2.10)[i]	38°33.24'	9°20.13'
EUGC-2	gravity	33.3	3.50 (2.00)[i]	42°45.5'	8°59.9'
EUGC-3B	gravity	37.9	4.10 (1.60)[i]	42°45.1'	9°00.2'

(i) Numbers in brackets indicate m of core corresponding to the last 2,000 years.

Table 1. Location, water depth and core length for the five cores in the Tagus Prodelta and Muros Ría.

Although the recovered length of core D13902 is 600 cm, the sediment above 189 cm was disturbed as demonstrated by ^{14}C datings (Abrantes *et al*., 2005a; see samples AAR-7823, OS-37286, AAR-7824, Table 4 in Bartels-Jónsdóttir *et al*., 2006), and discarded, and 0 cm assigned to depth 189 cm. In this study only the interval between 189 and 400 cm, which covers the last 2000 years, is considered. From core PO287-26-3G, located about 2 kilometres from D13902 (Fig. 1), only the section 0-150 cm was considered, in an effort to partially substitute the 350 year hiatus in core D13902 arising from the AD1755 Lisbon earthquake and tsunami (Abrantes *et al*., 2005a). Core EUGC-2 contains modern sediments at its top, but in core EUGC-3B the top has been dated AD 1470. The upper part of the sequence was lost during recovery.

Chronology

For the Tagus Prodelta, accelerator mass spectrometry (AMS) ^{14}C dating of either molluscs or planktonic foraminifera were performed on eighteen samples from the three cores. ^{14}C ages were 400 year reservoir-age corrected after a test on three regional live-colleted pre-bomb mollusc shells (Abrantes *et al*., 2005a) and calibrated using CALIB 4.4 (Stuiver *et al*., 1998a) (Table 2). ^{210}Pb analyses were performed on eighteen samples (sixteen in PO287-26-1B and two in D13902). For the Tagus Prodelta spliced sequence we follow the age model proposed in Abrantes *et al*. (2005a). In this sequence a one cm sampling interval gives a mean time resolution of 1.5 years between AD 2001 to 1759 and 8.4 years between AD 1600 to 0 (Fig. 2).

For the Muros Ría cores, a total of eight samples were dated by AMS ^{14}C (four for each core) on benthic foraminifera and entire articulated bivalve shells (Table 2). Sedimentation rates have been calculated by interpolation between dated points (Fig. 2).

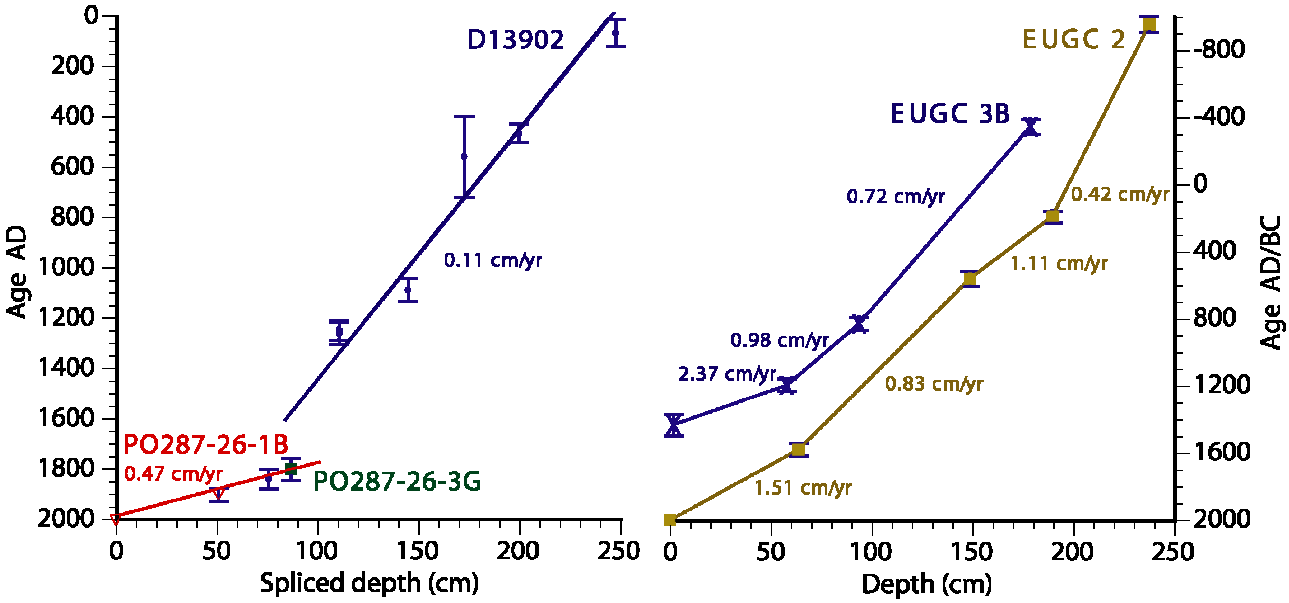

Figure 2. Age models and sedimentation rates for the Tagus Prodelta (left-side; triangles for PO287-26-1B, squares for PO287-26-3G, circles for D13902) and Muros Ría (right-side) cores.

Non destructive physical properties : Low-field magnetic susceptibility of core D13902 was carried out in U-channels at a 4 cm interval resolution at the LSCE/CNRS, Gif-sur-Yvette, France; for the other four cores, magnetic susceptibility was measured using a Multi Sensor Core Logger system at 1 cm interval at the University of Bremen, Germany (ARI-Paleostudies Program). Fe, Ti, K, Ca, Sr abundance in counts per second was measured by means of non-destructive scanning X-ray fluorescence (Jansen *et al*., 1998) at 1 cm resolution for four cores, and 2 cm interval for core D13902, at the University of Bremen, Germany (ARI-Paleostudies Program). Only Fe is shown here.

Textural data

Grain size was determined for the size fraction less than 2 mm using a Coulter LS230 laser particle analyser. Sample treatment consisted of organic matter removal with hydrogen peroxide (H_2O_2) and dispersion with sodium hexametaphosphate (0.033M). Prior to analysis, samples were homogenised and stirred. Resolution is 1 cm for the three Tagus Prodelta cores and 2 cm for Muros core EUGC-3B.

$CaCO_3$ and C_{org}

From an initial volume of 2 mg of dried, ground and homogenised sample, calcium carbonate was calculated by the difference between total carbon and organic carbon (C_{org}) measurements using a CHNS-932 Leco element analyzer. The C_{org} is combusted at 400ºC. Data is presented in weight percentage. The relative precision of two repeated measurements of both samples and standards was 0.03wt%. Sample resolution is 1 cm for cores PO287-26-1B and D13902, 5 cm for core PO287-26-3G, and 2 cm for core EUGC-3.

Core - (Depth) cm	Laboratory code	Spliced Depth (cm)	Species	^{14}C Age BP	Reservoir corr. ^{14}C yr Age	Calendar years BP	STDV (±1 s)	Age AD	δ^{13}C	Sed rate (cm/yr)
PO287-26B (32-33)	AAR-8368.2-K[1]	51	mollusk shell	440	40	51	25	1899	-1.09	0.45
D13902 (27-28)	OS-37286[2]	75.4	mollusk shell	492	92	111	39	1839	0	0.11
D13902 (31-32)	*AAR-8338[1]*	*79.4*	*mollusk shell*	*2150*	*1700*	*1700*	*80*	-	*0*	
D13902 (37-38)	*AAR-7826[1]*	*85.4*	*mollusk shell*	*8955*	*8555*	*8555*	*70*	-	*+0.01*	
D13902 (46-47)	*AAR-8301[1]*	*94.4*	*mollusk shell*	*7075*	*6675*	*6675*	*50*	-	*+0.79*	
D13902 (62-63)	AAR-7207[1]	110.4	mollusk shell	1160	760	691	45	1259	+1.44	0.11
D13902 (62-63)	AAR-7208[1]	110.4	*turritella*	1185	785	704	40	1246	+2.15	0.12
D13902 (96-97)	AAR-7209[1]	144.4	mollusk shell	1370	970	863	45	1087	+2.19	0.13
D13902 (124-125)	OS-37307[2]	172.4	foraminifera[3]	1880	1480	1394	160	556	0	0.14
D13902 (151-152)	AAR-7828[1]	199.4	mollusk shell	2007	1607	1487	37	463	+2.68	0.15
D13902 (199-200)	AAR-7826[1]	247.4	mollusk shell	2340	1940	1885	55	65	+0.71	0.16
PO287-26-3G (86-87)	OS-42381[2]		mollusk shell	545	145	147	45	1801	+0.86	0.17
EUGC-3B (1-2)	AAR-8453[1]		*Nonion commune*	920	520	522	65	1429	-2.53	
EUGC-3B (57-58)	AAR-7966[1]		*Venus nux*	1229	829	799	39	1193	-1.97	2.37
EUGC-3B (93-94)	AAR-7502[1]		*Myrtea spinifera*	1575	1183	1172	40	826	-0.84	0.98
EUGC-3B (178-179)	AAR-7967[1]		*Myrtea spinifera*	2623	2223	2347	45	-349	-0.14	0.72
EUGC-2 (63-65)	AAR-7969[1]		*Lucinoma borealis*	730	330	370	37	1581	+1.00	1.51
EUGC-2 (148-149)	AAR-8508[1]		*Nonion commune*	1855	1455	1390	45	561	-5.33	0.83
EUGC-2 (189-190)	AAR-8662[1]		*Nonion commune*	2170	1770	1761	35	190	-4.08	1.11
EUGC-2 (237-238)	AAR-7970[1]		*Myrtea spinifera*	3136	2736	2904	47	-955	+0.31	0.42

Table 2. Results of ^{14}C AMS datings of the Tagus Prodelta box-core PO287-26B, gravity-core PO287-26G and piston-core D13902 (levels in italic correspond to ages not considered for the age model) (above); and Muros Ría cores EUGC-3B and EUGC-2 (below).

Foraminifera

Samples for foraminiferal counts were wet sieved at 63 μm and dry-sieved at 125 and 2000 μm. Benthic foraminifera were analyzed in the >125 μm fraction. Due to the observation that biogenic carbon from high C_{org} sediments suffers dissolution when the samples are stored in a sodium hexametaphosphate 0.033M solution (unpublished INETI-DGM data), samples were only washed with distilled water. Total benthic foraminiferal assemblages were identified counting at least 300 individuals. Agglutinated foraminifera are excluded in the calculations for the Tagus Prodelta because of their poor preservation potential (Bartels-Jónsdóttir *et al*., 2006), but considered an important part of the assemblage in Muros because no significant taphonomic loss was observed. Sample resolution in the Tagus Prodelta is 1 cm in PO287-26-1B, 2-5 cm in PO287-26-3G, and approximately 3-4 cm in D13902; in Muros, sample resolution is 2 cm for both EUGC-2 and EUGC-3B.

Oxygen and carbon isotopes

Oxygen and carbon stable isotopes were analysed using a Finnigan MAT 251 mass spectrometer at the Department of Geosciences of the University of Bremen (Germany). All samples were measured relative to the VPDB standard with reproducibility of 0.07 ‰ for $\delta^{18}O$ and 0.06 ‰ for $\delta^{13}C$. Measurements were performed on the benthic species *Uvigerina* sp. 221 and planktic *G. bulloides* and *G. inflata* (PO287-26-1B, PO287-26-3G and D13902) at every cm, and on *Nonion commune* (EUGC-2 and EUGC-3B) at 2 cm interval resolution. On average six specimens from the >250 μm fraction were used for the Tagus Prodelta and about 20 specimens from the >125 μm fraction for the Muros Ría.

Diatoms

For diatom slide preparation, a fixed amount of 1-2 gram of fresh sediment from each sample was cleaned following Abrantes *et al*. (2005b) and placed to dry on plates (Battarbee, 1973). To calculate diatom fluxes (number of valves per square centimetre per year), diatom frustules were counted following the counting protocol of Schrader and Gersonde (1978) and Abrantes (1988). Cores PO287-26-1B and EUGC-3B were sampled at 1 cm resolution, PO287-26-3G at 5 cm, and D13902 unevenly between 5-12 cm.

3: Results and discussion

3:1: Major North Atlantic climatic periods

The last two millennia circumscribe five relatively well time-constrained climatic periods, Roman Period (RP) (~AD 0-400; eg. Lamb, 1985), Dark Ages (DA) (~AD 400-700; eg. Keigwin and Pickart, 1999; Mikkelsen and Kuijpers, 2001), Medieval Warm Period (MWP) (AD 800-1300; eg. Hughes and Diaz, 1994; Hass, 1996), Little Ice Age (LIA) (AD 1350-1900; eg. Bradley and Jones, 1993) and a warming 20th century, indicated by instrumental temperature measurements of the last two centuries, extended using proxy records back in time.

Oxygen isotopes have been widely used to infer water temperatures (e.g. Shackleton, 1974; Keigwin, 1996) in marine records. As no significant ice volume changes have occured during the last 2000 years, $\delta^{18}O$ should reflect bottom water temperature at our sites, and deviations from other independently derived temperatures indicate salinity effects.

In the Tagus Prodelta, $\delta^{18}O$ oscillates between 1.9-1.15‰, clearly defining four distinct intervals. Two periods with 1.55‰ average values, AD 0 – 350 (encompassing the Roman Period) and 1.6‰ AD 1250– 1850 (the so-called Little Ice Age); the latter is punctuated by a relatively lighter event centred at AD 1400. Lighter $\delta^{18}O$ values are found between AD 400-650 (corresponding to the Dark Age) and AD 800-1250 (Medieval Warm Period), reaching mean values around 1.4-1.5‰, and during the 20th century, with the lighest oxygen isotope values (1.3‰) (Fig. 3-A). At this location, major fluctuation in the $\delta^{18}O$ is probably related to strong temperature changes at interannual time scale rather than to salinity changes. In the Muros Ría, although the data have a smaller amplitude (1.9-1.6‰), values remain around 1.7-1.8‰ until AD 1750, with the exception of the interval AD 1200-1300 in the outer Ría, becoming gradually lighter towards the present in the inner Ría (Fig. 3-A). In general, the lighter oxygen isotopes at the Tagus Prodelta point to water temperatures reflecting warmer/less saline waters than the Muros Ría (Fig. 3-A, Fig. 4).

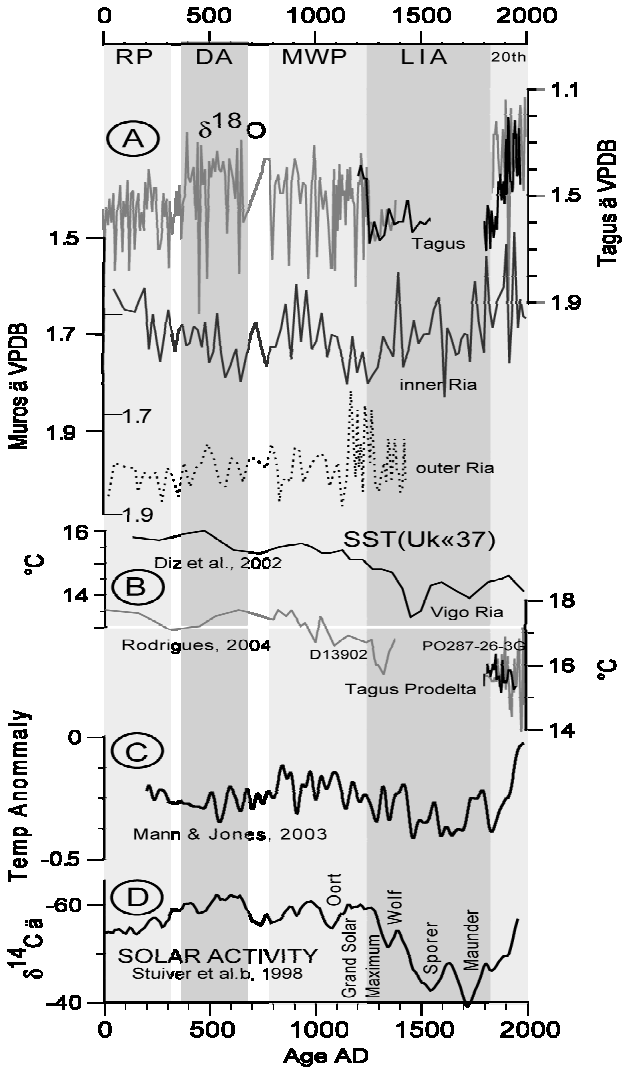

Figure 3. Comparison of temperature indicators between the Tagus Prodelta and the Muros Ría (pannel A-stable oxygen isotopes; B-$U^{k'}_{37}$ Sea Surface Temperatures for the Tagus and the Vigo Ría; C-temperature anommaly; D-^{14}C solar activity). Note different scales in $\delta^{18}O$. RP stands for Roman Period, DA is Dark Ages, MWP is Medieval Warm Period, LIA is Little Ice Age and 20^{th} is the 20^{th} century. See text for details

To support the hypothesis that lighter $\delta^{18}O$ reflects higher water temperature, we compared the $\delta^{18}O$ results from the Tagus Prodelta with SST based on the alkenone $U^{k'}_{37}$ index. High values (17.5ºC) are observed during AD 0-900, with a gradual decrease of 2ºC up to AD 1400. Low temperatures (15ºC) remain until AD 1900, when SST starts to oscillate with high amplitude between 14-17ºC (Rodrigues, 2004; Abrantes *et al*., 2005a) (Fig. 3-B). Clearly, temperature explains the difference in $\delta^{18}O$ in the intervals AD 400-1250 (DA-MWP) and AD 1250-1850 (LIA). The warmings in the RP and the last century, however, are not fully supported by our data. In the Vigo Ría, south of Muros, a similar SST record exists (Diz *et al*., 2002); this is

probably representative for all the Galician region (Fig. 3-B). Here, since AD 1150, relatively warmer/less saline waters came into the Ría (outer site EUGC3B), to only reach and affect the inner Ría much later, around AD 1700.

Additionally, our $\delta^{18}O$ records can be compared to the North Atlantic temperature variability registered by instrumental data, showing that the two major established global temperature climatic periods MWP and LIA (see discussion in Jones and Mann, 2004) are well marked in the Iberian margin (Fig. 3-C). Moreover, the DA is demarcated from the MWP in our records. The Tagus SST do not mirror the rapidly warming 20^{th} century curve of Mann and Jones (2003), hence the very light oxygen isotopes values must indicate lower salinity rather than higher temperature.

3.2 Climatic conditions and the productivity record

C_{org}, $CaCO_3$, $\delta^{13}C$ and micro-organisms provide good indications of past changes in productivity (eg. Broecker and Peng, 1982; Zahn and Sarntheim, 1986; Fisher and Wefer, 1999) (Fig. 5).

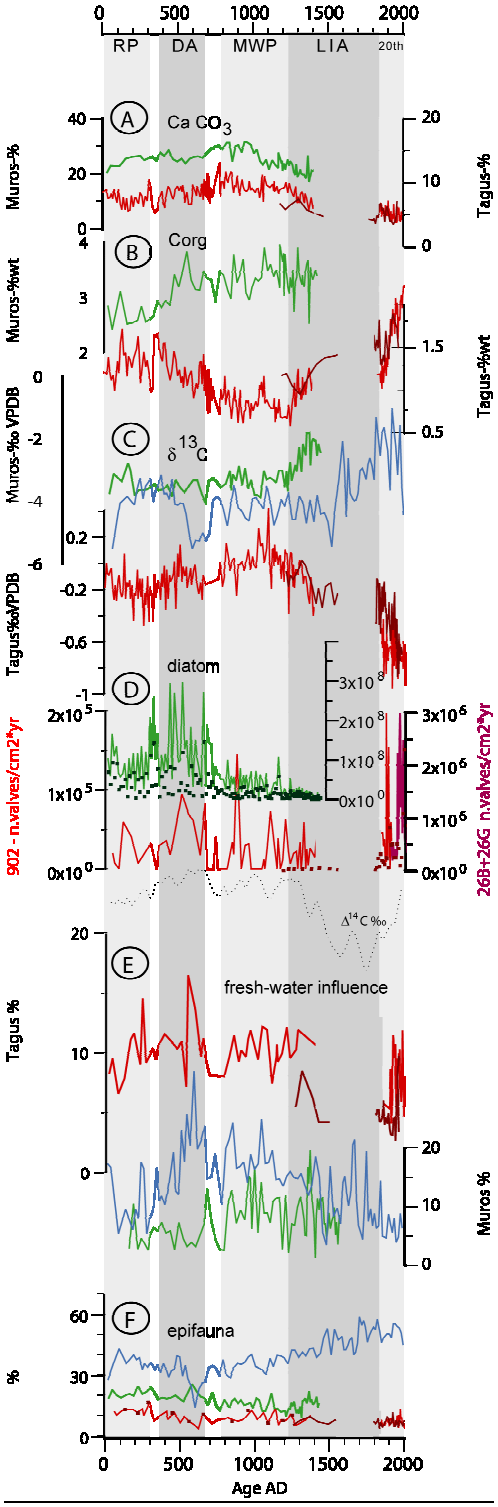

Figure 5. Comparison of productivity indicators between the Tagus Prodelta (red, darker red for PO287-26-3G) and the Muros outer (green) and inner (blue) Ría. Pannel A-calcium carbonate; B-organic carbon; C-carbon stable isotopes; D- diatom Accumulation Rates (*Chaetoceros* in bold squares); E-benthic foraminifera species influenced by fresh-water, and F- benthic foraminifera epifauna. We considered "fresh-water influence" the species driving in estuarine and shelf environments influenced by fresh-water flux from rivers producing brackish water conditions. See text for details. Note change of scales between Tagus and Muros in Corg, $CaCO_3$, $\delta^{13}C$ and diatom AR. Also in the Tagus Prodelta records, change of scale in diatom AR for box PO287-26-1B and gravity core PO287-26-3G. The curve of ^{14}C solar activity from Figure 3-D is given for reference. RP stands for Roman Period, DA is Dark Ages, MWP is Medieval Warm Period, LIA is Little Ice Age and 20th is the 20th century.

Organic carbon in the Tagus core shows very low values (0.5 – 1.5 wt%) for the period AD 500–1250, and relatively higher values between AD 0 - 400 and AD 1250 – 1850 (1-1.7 wt%).

For the last century values increase to near 2.3 wt%, exceeding all previous maxima levels (Fig. 5-B). An inverse correlation exists between organic and inorganic carbon (Fig. 5-A, B). The Muros Ría contains higher than average organic carbon, although within a similar range of variation (2.5 – 3.5 wt%). Nevertheless, organic and inorganic carbon curves follow each other quite closely. The higher content of organic carbon in the Muros Ría relative to the Tagus Prodelta highlights different environments and either stronger productivity or better organic carbon preservation in the Ría (Fig. 5-B).

Comparing both areas, organic carbon in the outer site of the Muros Ría diverges from the Tagus Prodelta between AD 400 – 1300 (DA and MWP), suggesting different water conditions in the two areas. However, the Tagus and Muros inorganic carbon mimic each other (data available only for outer site and AD 0-1400).

$\delta^{13}C$ of benthic foraminifera in the Tagus Prodelta fluctuates between 0.4 and - 0.9‰. It shows relatively low values between AD 100-500, increases until around AD 1300 with a minimum centred at AD 650 (Fig. 5-C). The lowest values are documented during the last century (Suess effect). The Muros Ría presents a higher range variation in $\delta^{13}C$ (-1 to -5.4‰), with the largest fluctuations for the inner Ría, more negative values between AD 100 – 1500, and rapid increase for the last 500 years. Lighter values (-5‰) are evident for the interval AD 550-700, indicating stagnant water conditions. $\delta^{13}C$ is less negative and more constant for the outer Ría, until around AD 1200 when a sharp increase occurs.

More positive $\delta^{13}C$ are indicative of more ventilated, mixed waters, influenced by marine upwelling. In the Tagus Prodelta, $\delta^{13}C$ data validate our previous interpretation of light $\delta^{18}O$ reflecting temperature and not salinity during the DA, MWP and hence suggests intense upwelling during these times. In contrast, river runoff is dominant during the RP, the LIA and the 20th century. However, in the Muros Ría and in light of the carbon isotope results, the same water mass influenced the Ría until AD 1150, although slightly better ventilation and/or less organic matter accumulation characterised the outer Ría (Fig. 5-C). Since AD 1150 the inflow of warmer, oceanic waters caused more intense bottom ventilation in the outer Ría, very likely due to reinforced upwelling. The enhancement of bottom ventilation is delayed in the inner Ría by 400 years. A similar pattern is found in the neighbouring Vigo Ría (Diz *et al*., 2002). Therefore, as opposed to the Tagus Prodelta area, in the Muros Ría the LIA is marked by marine influence. The fact that the Muros Ría records much higher values and variability in the $\delta^{13}C$ data than in

the Tagus Prodelta reflects the importance of organic matter preservation-related processes in the more protected environment of the Ría (Fig. 4).

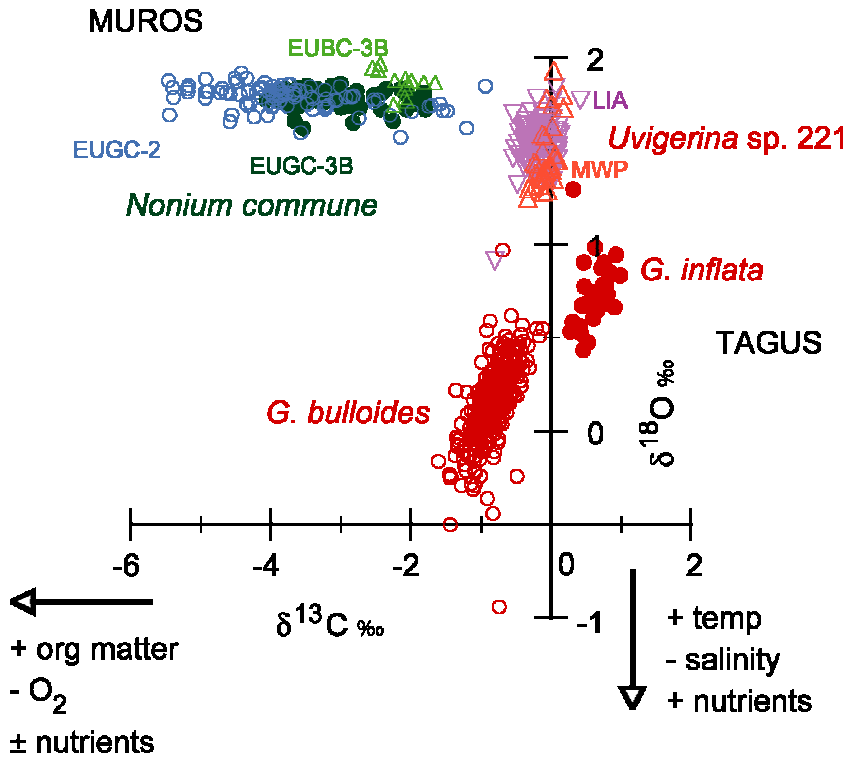

Figure 4. Water masses characterisation on the basis of oxygen and carbon stable isotopes for the Tagus Prodelta (*G. bulloides*, *G. inflata* and *Uvigerina* sp. 221) and Muros Ría (*Nonium commune*). EUBC-3B is a box-core from the Muros Ría at the same position than gravity core EUGC-3B. 0.24‰ in $\delta^{18}O \equiv \Delta 1ºC$ (Shackleton, 1974).

Diatom accumulation rate in the Tagus Prodelta indicates periods of productivity with pulses centred at AD 550, AD 900 and weakly at AD 100 and AD 1100. These four pulses of diatoms, composed by the upwelling-related species (mainly *Paralia sulcata* (Ehrenberg) Cleve and *Chaetoceros* spp.), are tied with the RP, the DA, and the MWP. The four pulses also coincide with heavier $\delta^{13}C$ manifesting ventilation and turbulence. With the onset of the LIA, since AD 1300, diatom concentrations seem to diminish, coeval with a steady decrease in $\delta^{13}C$. This weakening of upwelling conditions is coherent with an increase in phytoliths (I. Gil *et al*., 2006), i.e. a shift to continental river inputs. Much higher fluxes (x10) characterize the last 100 years (Fig. 5-D), partially due to better preservation. It is known that in general, one order of magnitude in the abundance of diatoms is lost by dissolution in the surface sediments, as well as diversity in the fossil assemblage (Bao *et al*., 1997; Abrantes and Moita, 1999). During the last

century, and in particular around AD 1900, brackish diatoms are more frequent, together with less negative $\delta^{13}C$, reaching the lightest values at present. This reinforces the climatic tendency to more continental influence since the onset of the LIA (Fig. 5-C). Spread of brackish diatoms and phytoliths for the last 150 years further confirm the very light $\delta^{18}O$ signal for this period, not only due to lower SST (Fig. 3-A) but also to less saline waters.

In the Muros Ría, a single diatom record exists (EUGC-3B), but diatoms show higher abundances in the Muros Ría (two orders of magnitude) than in the Tagus Prodelta, with accumulation rate peaks over $1.5x10^8$ valves/cm^2 yr. This core, in the outer Ría, reveals a stronger diatom concentration between AD 270 to 670, marking three peak episodes, and a much weaker pulse around AD 50. There is some overlap with the earlier Tagus pulses (Fig. 5-D), encompassing the RP and partially the DA. Contrary to the Tagus Prodelta, light and quite constant $\delta^{18}O$ until AD 1100, poor water ventilation, and an increment in 1 wt% of organic carbon (Fig. 5-B), point to diatom productivity as a result of nutrient input by the Tambre River, in a system which remained isolated from Atlantic influence. Varela *et al.* (2001) stated that although the Tambre fluvial output into the Ría is low, it can still be a significant source of nutrients for phytoplankton blooms. From AD 670 to 1470 (mid-MWP), diatom concentrations decay in Muros. The assemblage itself changes too, from local benthic species, to open ocean centrics (*Thalassiosira* spp., *Rhizosolenia* spp., Stroynowski, pers.comm., 2005) and most notably, the assemblage shows an increase in *Chaetoceros* spp. Lower species diversity and the change in the species assemblage suggests an increase in frequency of upwelling events but the drop in productivity is interpreted as a decrease in preservation (Stroynowski, pers.comm., 2006). This poor preservation could be due to a decrease in bottom waters or surface sediment porewater silica saturation (Bernárdez *et al*., 2006). Unfortunately, we do not have the upper record of EUGC-3B and cannot verify the evolution of diatom concentrations in the Ría after AD 1470.

Benthic foraminifera are grouped, in the two areas, by (1) specific assemblages according to the different environments; (2) species tolerant to salinity changes that are good markers of periods of river discharge (referred to as a "brackish" assemblage in the Tagus and an "inner assemblage" in Muros, and integrated as "fresh-water influence" in Fig. 5-E) or coastal upwelling (shelf assemblage for the Tagus and outer assemblage for Muros); and (3) indicators of labile (epifauna) or refractory organic matter availability at the bottom and, therefore, degree of ventilation of the water masses.

In the Tagus Prodelta, benthic foraminifera assemblages are dominated by typical continental shelf *Cassidulina laevigata*, *Hyalinea balthica*, *Bolivina* spp. and opportunistic species (Bartels-Jónsdóttir *et al*., 2006). *C. laevigata*, *H. balthica*, show an inverse abundance until AD 900 and convergence since then (Bartels-Jónsdóttir *et al*., 2006). Together they denote persistent upwelling for the period AD 400-1300. *H. balthica* and *Nonion commune* (N. *arterizans* according to Bartels-Jónsdóttir *et al*., 2006) have also been related to upwelling by Levy *et al*. (1993), Diz *et al*. (2002) and Diz *et al*. (2006). Both are abundant for AD 0-400, and reflect high flux of fresh labile organic matter related to upwelling and primary productivity (Bartels-Jónsdóttir *et al*., 2006). Around AD 1800 *H. balthica* becomes very rare, being almost absent in the last 100 years. At AD 1330, the onset of the LIA is marked by a significant faunal change to low foraminiferal fluxes and diversity due to reduced quality and quantity of food. *Bolivina* spp., together with *Stainforthia fusiformis*, show rather low values from AD 0 to 1300, after which they increase to the highest values during the last century (Bartels-Jónsdóttir *et al*., 2006). These species show high correlation to the increasing organic carbon content which is, at this location, mainly of terrigenous origin. Species tolerant to salinity changes or brackish environments such as *Ammonia beccarii*, *Haynesina* spp and *Elphidium* spp., compose an important group of the total assemblage (Bartels-Jónsdóttir *et al*., 2006) (Fig. 5-E), showing two times higher average values from AD 0-1300 (includes the RP, DA and MWP) than during AD 1300 – 1850 (LIA). During the last century average abundance increases to similar values as in the MWP (10%). In the Tagus Prodelta, epibenthic foraminifera (species such as *Valvulineria bradyana, Cibicides spp., Cancris auriculus, and Planorbulina mediterraniensis that* live at the surface of the sediment) decrease from 13% during AD 0-500, to 10% until AD 1300 and 8% to AD 1800 (Fig. 5-F). In soft sediments the epibenthic species also live in the top cm of the sediment (shallow infaunal) and are known to respond to good quality food levels at the sediment-water interface (Diz *et al*., 2004). On the basis of benthic foraminiferal assemblage changes, Bartels-Jónsdóttir *et al*. (2006) distinguished four well-defined consecutive phases in the Tagus Prodelta waters for the last 2000 yrs, which fit the four climatic periods. In the RP (AD 0-400) upwelling conditions bring nutrients from deep waters, leading to flux of fresh labile organic matter; in the DA and MWP (AD 400-1400) even more persistent upwelling occurs; at AD1300-1400 a significant climatic change happens with a decrease in the quality of food available in bottom waters presumably caused by river runoff that remains over the LIA (AD 1400-1800); and the last two centuries which are warm and reveal the effect of anthropogenic activities.

In the Muros Ría, the external site (EUGC-3B) is dominated by *Bulimina gibba/elongata*, *Nonion commune*, *Rectuvigerina phlegeri* and *Uvigerina* sp. (referred as the outer Ría assemblage), while in the inner site (EUGC-2) *Eggerelloides scaber* and *Elphidium gerthi* (inner Ría assemblage), as well as epifaunal taxa (*C. refulgens*, *P. mediterranensis*, *Rosalina* spp., *G. praegeri*, *L. lobatula* and *E. pulchella*) are the most abundant. Similar assemblages are found in the neighbouring Vigo Ría (Diz *et al*., 2004; Diz *et al*., 2006). In the Galician rías, *A. beccarii* is considered as a separated marker because its presence could indicate transport processes from shallower areas. EUGC-3B is dominated by high values (40-50%) of the outer Ría assemblage from AD 0 to 600 and between AD 1000 and 1200, low values occur between AD 850-1000, and a sharp decrease around AD 1200 (Fig. 5-E). The inner Ría assemblage in core EUGC-3B shows low amplitude variability around 5% from AD 0 – 500, and higher amplitude centred at 8% between 500 – 1250 AD, followed by a gradual decrease. *A. beccarii* follows a similar pattern, with very low values after the abrupt change at AD 1250. In core EUGC-2, the inner assemblage exhibits increasing values (up to 30%) from AD 0 - 600 (Fig. 5-E), and then a progressive decrease is recorded to present times, on which important fluctuations are superimposed. *A. beccarii* oscillates around 5%, up to AD 1250, when its percentage abundance declines such as at the outer site. In the outer Muros Ría, the epifaunal species are rather stable until around AD 1100 when they increase and the $\delta^{13}C$ becomes heavier (Fig. 5-B). In the inner Ría, the epifauna falls slightly during the first 1000 years of the record collapsing at AD 500-700. This minimum coincides with a well-marked event of lighter carbon isotopes assumed to represent stagnant water. These species increase again during the last millennium reflecting steadily enhanced marine upwelling conditions (Fig. 5-F). The evolution of the assemblages during the last 2000 years emphasizes the different conditions between the outer and the inner sites, with core EUGC-3B and EUGC-2 dominated by the inner assemblage and the epifauna until AD 1100. Thus a widespread inner Ría benthic assemblage, associated with light and quite constant $\delta^{13}C$, and high organic carbon of terrestrial provenance, reveals local conditions until AD 1100 (Fig. 5-E). Progressively, after AD 1250 the outer assemblage becomes more abundant, indicating improved water ventilation, also supported by heavier $\delta^{13}C$ isotopes, suggesting a more active circulation caused by intrusion of upwelling waters that reach the inner part with a delay of 300 years. The Muros Ría behaviour resembles that of the Vigo Ría to the south (Diz *et al*., 2002).

In summary, benthic foraminiferal assemblages are mainly controlled by water mass properties (temperature/salinity), and primary productivity and oxygen concentration in the bottom (Fig. 4). Even in shallow water environments it is difficult to discriminate the effect of these factors in benthic foraminiferal assemblages (van der Zwaan *et al*., 1999). In the Tagus Prodelta, the assemblages show prevailing upwelling conditions until around AD 1300, when they are overtaken by river-induced productivity. Even in the Muros Ría assemblage, which shows only strictly local dynamics until AD 1150, the later period is influenced by the open marine regional Atlantic signal with invasion of upwelled waters. The strong "suboxic" event detected between AD 550 and 700 in the inner Ría, is barely recognized either in the outer Ría, or the Tagus Prodelta.

3.3 Evolution of Tagus Prodelta and Muros Ría sedimentary regimes during major climatic changes

The two sedimentary systems compared in this study are affected by different dominant marine and continental processes at different times. The Tagus Prodelta is situated in a marine domain affected by river discharge (from the Tagus River). The Muros Ría is a semi-enclosed environment dominated by continental input (Tambre River) and processes involving organic matter production and preservation, and is only temporarily influenced by more open coastal processes.

The Tagus Prodelta, between AD 400 and 1300, shows percentages of sand above 45%, corresponding with mean grain size greater than 70 μm. This sand fraction contains mainly biogenic particles such as marine foraminifera (Fig. 6-A, 4-E). Before AD 400 sand values do not exceed 45% and from AD 1100 to present values decrease dramatically to about 10% around AD 1900, pointing to abrupt changes in the regime from dominant marine to fluvial inputs at ~ AD 1300. Magnetic susceptibility variations represent magnetic minerals concentrated in the fine fraction (<63 μm) (Fig. 6-B). Major elements, such as Fe, and Ti, and K, widely considered as continental derived markers (e.g. Adegbie *et al*., 2003) (Fig. 6-C) mimic magnetic susceptibility and finer grain size fractions, supporting evidence for fine continental sediment input from river discharge. Instead, $CaCO_3$ content reflects abundant marine foraminiferal sands (Fig. 5-A). In general terms, low organic carbon coincides with low values of terrigenous markers (Fe, Ti, K) and greater grain size.

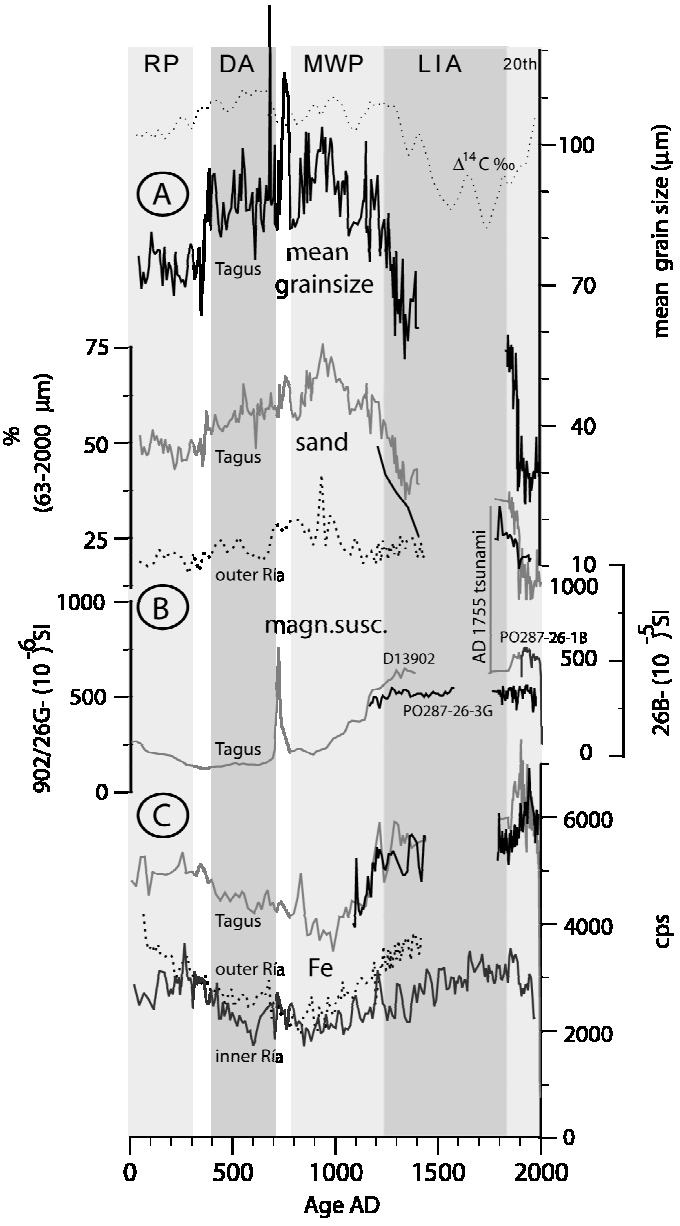

Figure 6. Comparison of land input indicators between the Tagus Prodelta and the Muros Ría (pannel A-mean grainsize and % sand; B-magnetic susceptibility; C- Fe in counts per second, similar to Ti and K). Note change of scale in magnetic susceptibility for the Tagus core PO287-26-1B. The curve of ^{14}C solar activity from Figure 3-D is given for reference. RP stands for Roman Period, DA is Dark Ages, MWP is Medieval Warm Period, LIA is Little Ice Age and 20th is the 20th century. See text for details.

We only have mean grain size data for the outer Muros Ría core (EUGC-3B). Between AD 400 and 1100, sand rises to 27%, with a relative minimum around AD 600 (Fig. 6-A), consisting of biogenic grains, mainly fragmented mollusc shells and agglutinated foraminifera. In this interval Fe concentration is low (Fig. 6-C). A slow increase in the mud content occurs from AD 1100 to 1470 (top sequence is missing) in core EUGC-3B, suggesting the contribution of very fine biogenic components, probably calcareous nannoplankton (Fig. 5-A). Fe and Ti concentrations from AD 0 to 400 and AD 1100 to 1900 in cores EUGC-3B (outer Ría) and

EUGC-2 (inner Ría) are high, corresponding to fine grain sizes. Over the last century, land markers (Fe, Ti, K) mimic the Tagus Prodelta record. Low TOC corrrelates with high terrigenous markers in the outer Ría, the inverse of the Tagus.

Comparing the two areas, there is double the amount of sand in the Tagus record than in the Muros Ría. At first glance, based on grainsize and major land markers, the two sedimentary environments appear apparently similar: finer sediments and high Fe-Ti during the coldest periods and coarse biogenic sands and low Fe-Ti during warm periods. However, assumed correlation between Ca - Sr, and Fe - Ti, with provenance of marine and terrigenous components, respectively (e.g. Arz *et al*., 1999) is correct in the Tagus, but shows an inverse trend in Muros.

Regarding the faunal species as independent indicators, the two sedimentation regimes diverge in their character. During the DA and MWP (AD 400 to 1300) in the Tagus Prodelta, coarse biogenic sand is of marine origin, concurrent with shelf foraminiferal species like *C. laevigata* and upwelling related diatom species, while in the Muros, coarse biogenic sand coincides with brackish foraminifera, the dominant inner assemblage, and more benthic diatoms, likely indicating freshwater discharge of the Tambre River. During the colder LIA (AD 1300 – 1850), high mud accumulation and Fe-land markers, but absence of diatoms in both areas, point to stratified waters. Although productivity is related to increased river-runoff in the Tagus Prodelta (Abrantes *et al*., 2005a) intensification of upwelling conditions with better water ventilation, occurs in Muros. In the neighbouring Vigo Ría, upwelling-related nannoplankton species dominate during the LIA (Álvarez *et al*., 2005). Since AD 1900, the Tagus Prodelta has been under the influence of a strong continental regime, as proved by a 90% mud grain size and higher terrestrial Fe content, as well as high abundance of species dependent on refractory organic matter (*Bulimina marginata*), presence of phytoliths, and lighter C and O isotope values. In Muros, a reinforcement of the upwelling conditions are indicated by heavier C isotopes and higher proportion of marine foraminiferal species. Although we do not have a SST for the Muros Ría, Diz *et al*. (2002) show both δ^{18}Oand SST curves for the Vigo Ría, and taking into account the close similarity between the Tagus and Muros isotope curves, we can assume a comparable SST (western Galicia). The 20th century SST show for both south and north Iberia temperatures similar to those characterizing the LIA.

3.4 Forcing mechanisms of climate variability

The Holocene spectrum of the carbon isotope benthic foraminifera of core EUGC-3B was analysed by Pena *et al*. (submitted) who found a mean periodicity of 1500±500 years (the so-called "Bond events"). The DA and LIA would be the two most recent "cold" isotopic events (Bond *et al*., 1997). At the millennial scale, Pena and co-authors attributed changes in hydrographic conditions to the N-S migration of the ENACWsp/ ENACWst front, and linked the cold episodes (warmer, e.g. MWP) with enhancement of ENACWsp (ENACWst) upwelling, and hence heavier $\delta^{13}C$ (lighter), indicating ventilation at the sea floor, and retention of the organic matter produced in the Ría. Bond *et al*. (2001) demonstrated statistically significant coherence among records in millennial (hematite stained grains) and centennial (^{14}C, ^{10}Be) bands. It seems then that a solar forcing mechanism underlies the North Atlantic millennial scale surface hydrographic changes (Stuiver *et al*., 1997; Chapman and Shackleton, 2000; Bond *et al*., 2001; Mayewski *et al*., 2004). In fact, solar activity, reflected in atmospheric $\Delta^{14}C$ concentrations, forces changes in the oceanic circulation with centennial (the 80 years Gleissberg cycle) scale cyclicity (Keller, 2004). Several other authors have specifically coupled the MWP / LIA to changes in solar activity (Bard *et al*., 2000; Crowley, 2000; Keller, 2004), including workers foccussing on Iberia (Diz *et al*., 2002; Desprat *et al*., 2003). Higher production rates of cosmogenic nuclides are related to reduced solar irradiance (Masarik and Beer, 1999).

If one looks into the higher frequency of curves from our Tagus and Muros sites, both millennial (DA, MWP, LIA) and centennial scale variability is observed. Our proxies for temperature, salinity, primary productivity, and water ventilation (oxygen and carbon isotopes, organic carbon, foraminifera and diatom records) match strikingly the atmospheric $\Delta^{14}C$ swings. This cannot be a coincidence. In the DA and MWP period, the Tagus foraminiferal oxygen isotopes follow closely each maximum/minimum of the solar activity curve (Fig. 3-A, D). In addition, the main concentrations of diatoms match the three solar maxima (Fig. 5-D). High C_{org} (Fig. 5-B) and lower mean grain size values (Fig. 6-A) are, however, tied to reduced solar output. Therefore, indicators of oceanic circulation and dominant upwelling during the DA and MWP seem to have a more direct relationship with maximum solar centennial-scale irradiance. Conversely, indicators of terrestrial inputs coincide with minimum solar activity during the LIA. This is in agreement with our previous hypothesis of an oceanic (terrestrial) influenced MWP (LIA). According to Keller (2004) the magnitude of solar forcing does not necessarily respond to the amount of solar activity, as indirect solar forcings, like biogeochemical intermediate

processes, could account significantly for climate variability. In fact, if we analyse the Muros Ría, for the same DA and MWP period, the primary productivity related proxies are the ones connected with solar maxima. For example, what we called the "suboxic" light $\delta^{13}C$ DA-event, localised in the inner Ría, is contemporaneous with diatom blooms, high C_{org}, reduced epifauna and flux of freshwater (Fig. 5-B-F) and links with the DA highest solar irradiance over the last 2000 years. Thus, in the Ría, solar forcing at a millennial scale seem to influence hydrographic changes, while primary production and organic carbon degradation processes appear to reflect the centennial scale of solar activity.

Most of our records reveal an enhancement of biogeochemical processes during the 20th century not seen during the previous 1900 years. This might be due to less oxidation of sediment given the shorter amount of time passed since deposition. On the other hand, Mayewski *et al*. (2004) might be correct in stating that indirect natural feedbacks amplify the weak forcing related to fluctuations in solar output. Furthermore, Lean and Rind (2001) and Keller (2004) conclude that less than half of the 20th century warming was caused by increase in solar irradiance.

However, hydrography is not only affected by millennial and/or solar activity. At a multi-decadal scale, the atmospheric NAO system with persistent positive (stronger pressure differences) and negative (weaker North-South gradient) modes during the MWP and LIA, respectively, seem to cause biogeochemical changes in the subtropical eastern North Atlantic (Abrantes *et al*., 2005a), and also in the western North Atlantic (Sargasso Sea; Keigwin, 1996). In the Tagus Prodelta, long-term negative NAO characterises the LIA, with storminess, excess precipitation and river discharge while the MWP presents more frequent extreme positive NAO, producing enhanced upwelling (Abrantes *et al*., 2005a). Álvarez *et al*. (2005) presents the opposite scenario for DA-MWP and LIA at the Vigo Ría, in agreement with the climatic changes we propose here for the Muros Ría. After reconstructing precipitations for the last five centuries, Pauling *et al*. (2006) assert that winter precipitation over southern Iberia is mainly maintained by the negative NAO mode, whereas European winter precipitation is rather insensitive to NAO. The northwest of Iberia, Galician Rías Baixas, is positioned between the two NAO poles, explaining the contrary sedimentary conditions compared to the Tagus during the MWP/LIA. The results of Pauling *et al*. (2006) also suggest that the connection of precipitation to large-scale atmospheric circulation over decadal timescales is not stable on its own, requiring complementary patterns, apart from the NAO, to explain precipitation variability. Kirov and

Georgieva (2002) go further, suggesting the influence of long-term solar activity on the NAO, forcing the position and strength of its poles. With respect to the DA, the Tagus light oxygen isotopes, SST and solar irradiance correlate with the North Atlantic low temperatures of Mann and Jones (2003), supposely regulated by the atmospheric NAO (Fig. 3-A,C,D). In detail, however, there are significant discrepancies and biological feedbacks cannot be ignored.

Overall, in the Iberian peninsula, high resolution sedimentary sequences reveal solar irradiance plus the NAO (or maybe the latter is also forced by solar irradiance), as the two (or one) main climatic driving mechanism(s) inducing changes in atmospheric and water circulation, and climate as a whole.

4. Conclusions

Solar activity and the NAO are the two forcing mechanisms behind the changes of temperature/salinity and primary production in the water and the sediment regimes in the Tagus Prodelta and Muros Ría. Our biogeochemical proxies respond to climatic variability at millennial and centennial to the (multi-)decadal scales.

The most distinct change occurs at the transition between the MWP / LIA in both areas, although with opposing hydrographic signals. In the Tagus, ocean circulation (productivity and coastal upwelling) dominates the MWP whereas precipitation (river flux and continental inputs into the shelf) takes over during the LIA. In the Muros, at AD 1200 a fluvial regime switches to an open marine regime. Before AD 1200, local processes related to productivity and organic carbon preservation characterise the Ría. We attribute these climatic changes to long NAO trends, either dominant river runoff mode (NAO^-) or dominant upwelling mode (NAO^+) in the northern and southern sites. The reversal in both areas depends on the latitudinal migration of the persistent position of the Azores/Lisbon and Iceland pressure poles. In the Tagus area it is also possible to distinguish the RP and DA on the basis of hydrographic changes. The DA could have been as warm as the MWP. In the inner Muros Ría, a "suboxic" event is detected in the DA (AD 500-700). Solar irradiance maxima and minima are closely connected to biogeochemical changes in both areas over the last 2000 years.

Acknowledgements

We are grateful to participants and crews of *Discovery* 249, *Poseidon* PALEO I, and B/O *Mytilus* cruises, and for laboratory technical assistance in grainsize, LECO, isotopes,

foraminifera and diatoms at the INETI-Laboratory of Marine Geology. Thanks to C. Kissel for the magnetic susceptibility measurements in Gif-sur-Yvette, to M. Siegl for isotope measurements and the ARI-Program at the University of Bremen, to E. Salgueiro and S. Vaqueiro for XRF measurements at the Bremen Core Repository, to J. Heinemeier for helpful discussions during the construction of age models, to A. Ferreira for data discussion and A.Voelker for comments on the manuscript. The comments of an anonymous reviewer helped to improve the final version of this paper. Financial support was provided by EU project HOLSMEER (EVK2-CT-2000-00060). T. Rodrigues was supported by the Fundação para a Ciência e Tecnologia, INGMAR project.

REFERENCES

Abrantes, F. 1988: Diatom assemblages as upwelling indicators in surface sediments off Portugal. *Marine Geology 85*, 15-39.

Abrantes, F. and Moita, T. 1999: Water Column and Recent Sediment Data on Diatoms and Coccolithophorids, off Portugal, Confirm Sediment Record as a Memory of upwelling Events. *Oceanologica Acta* 22, 319-336.

Abrantes, F., Lebreiro, S., Rodrigues, T., Gil, I., Bartels-Jónsdóttir, H., Oliveira, P., Kissel, C. and Grimalt, J.O. 2005a: Shallow marine sediment cores record climate variability and earthquake activity off Lisbon (Portugal) for the last 2,000 years. *Quaternary Science Reviews* 24, 2477-2494.

Abrantes, F., Gil, I., Lopes, C. and Castro, M. 2005b: Quantitative diatom analyses – a faster cleaning procedure. *Deep-Sea Research* I 52, 189-198.

Adgebie, A.T., Schneider, R.R., Röhl, U. and Wefer, G. 2003: Glacial millennial-scale fluctuations in central African precipitation recorded in terrigenous sediment supply and freshwater signals offshore Cameroon. *Palaeogeography, Palaeoclimatology, Palaeoecology* 197, 323-333.

Álvarez-Salgado, X.A., Rosón, G., Pérez, F.F. and Pazos, Y. 1993: Hydrographic variability off the Rías Baixas (Nw Spain) during the upwelling season. *Journal of Geophysical Research* 98, 14,447-14,455.

Álvarez, M.C., Flores, J.A., Sierro, F.J., Diz, P., Francés, G., Pelejero, C. and Grimalt, J. 2005: Millennial surface water dynamics in the Ría de Vigo during the last 3000 years as revealed by coccoliths and molecular biomarkers. *Palaeogeography, Palaeoclimatology, Palaeoecology* 218, 1-13.

Antoine, D. and Morel, A. 1996: Oceanic primary production 1. Adaptation of a spectral light-photosynthesis model in view of application to satellite chrorophyll observations. *Global Biogeochemical Cycles* 10 (1), 43-55.

Arz, H.W., Patzold, J. and Wefer, G. 1999: Climatic changes during the last deglaciation recorded in the sediment cores from the northeastern Brazilian Continental Margin, *Geo-Marine Letters* 19, 209-218.

Bao, R., Varela, M. and Prego, R. 1997: Mesoscale distribution patterns of diatoms in surface sediments as tracers of coastal upwelling on the Galician Shelf (NW Iberian Peninsula). *Marine Geology* 144, 117-130.

Barber, R. T. and Smith, R. L. 1981: Coastal upwelling ecosystems, In Longhurst, A. R., editor, *Analysis of Marine Systems*: Academic Press, San Diego, 33-68.

Bard, E., Raisbeck, G., Yiou, F and Jouzel, J. 2000: Solar irradiance during the last 1200 years based on cosmogenic nuclides. *Tellus* B 52, 985-991.

Bartels-Jónsdóttir, H. B., Knudsen, K.L., Abrantes, F., Lebreiro, S. and Eiríksson, J. 2006: Climate variability during the last 2000 years in the Tagus Prodelta, western Iberian Margin: benthic foraminifera and stable isotopes. *Marine Micropaleontology* 59, 83-103.

Battarbee, R.W. 1973: A new method for estimation of absolute microfossil numbers with reference especially to diatoms. *Limnology Oceanography* 18, 647-652.

Behrenfeld, M.J., Randerson, J.T., McClain C.R., Feldman, G.C., Los, S.O., Tucker, C.J., Falkowski, P.G., Field, C.B., Frouin, R., Esaias, W.E., Kolber, D.D. and Ollack, N.H. 2001: Biosphere Primary Production during an ENSO transition. *Science* 291, 2594-2597.

Bernárdez, P., Francés, G. and Prego, R. 2006 *in press*: Benthic-pelagic coupling and postdepositional processes as revealed by the distribution of opal in sediments: The case of the Ría de Vigo (NW Iberian Peninsula). *Estuarine, Coastal and Shelf Science.*

Bond, G., Kromer, B., Beer, J., Musceler, R., Evans, M.N., Showers, W., Hoffmann, S., Lotti-Bond, R., Hajdas, I. and Bonani, G. 2001: Persistent solar influence on North Atlantic climate during the Holocene. *Science* 294 (5549): 2130-2136.

Bode, A. Casas, B. and Varela, M. 1994 : Size-fractioned primary productivity and biomass in the Galizian shelf (NW Spain): net plankton versus nanoplankton dominance. *Sciencia Marina* 58, 131-141.

Bradley, R.S. and Jones, P.D. 1993: "Little Ice Age" summer temperature variations: their nature and relevance to recent global warming trends. *Holocene* 3, 367.

Broecker, W.S. and Peng, T.H. 1982: *Tracers in the Sea*, Eldigio Press, New York.

Brown, P. and Field, J. 1986: Factors limiting phytoplankton production in a nearshore upwelling area. *Journal of Plankton Research* 8, 55-68.

Brown, P., Painting, S. and Cochraine, K. 1991: Estimates of phytoplankton and bacterial biomass and production in the northern and southern Benguela ecosystems, *South African Journal of Marine Science* 11, 537-564.

Cabeçadas, G., and Brogueira, M J. 1997: Sediments in a Portuguese coastal area - pool sizes of mobile and immobile forms of nitrogen and phosphorus. *Marine Freshwater Research* 48, 559-563.

Chapman, M.R. and Shackleton I.N. 2000: Evidence of 550-year and 1000-year cyclicities in North Atlantic circulation patterns during the Holocene. *Holocene* 10, 287-291.

Crowley, T. 2000: Causes of climate change over the past 1000 years. *Science* 289, 270-277.

Desprat, S., Sánchez-Goñi, M.F., and Loutre, M.-F. 2003: Revealing climatic variability of the last three millennia in northwestern Iberia using pollen influx data. *Earth and Planetary Science Letters* 213, 63-78.

Diz, P., Francés, G., Pelejero, C., Grimalt, J.O. and Vilas, F. 2002: The last 3000 years in the Ría de Vigo (NW Iberian Margin): climatic and hydrographic signals. *The Holocene* 12, 459-468.

Diz, P., Francés, G., Costas, S., Souto, C. and Alejo, I. 2004: Distribution of benthic foraminifera in coarse sediments, Ría de Vigo, NW Iberian Margin. *Journal of Foraminiferal Research* 34, 258-275.

Diz, P., Francés, G. and Rosón, G. 2006: Effects of contrasting upwelling–downwelling on benthic foraminiferal distribution in the Ría de Vigo (NW Spain). *Journal of Marine Systems* 60, 1-18.

Estrada, M. 1984: Phytoplankton distribution and composition off the coast of Galizia (NW

Spain). *Journal of Plankton Research* 6, 417-434.

Fisher, G. and Wefer, G. (editors) 1999: *Use of proxies in Paleoceanography: examples from the south Atlantic*. Springer-Verlag, Berlin, Heidelberg, 1-68.

Fiúza, A.F.G. 1983: Upwelling pattern off Portugal. In *Coastal Upwelling: its sediment record.* Suess, E. and Thiede, J., editors, Plenum, New York, 85-98.

Fraga, F. and Margalef, R. 1979: Las Rías Gallegas. In Universidad de Santiago, editor, *Estudio y explotación del mar en Galicia*, *La Coruña*, 245-298.

Fraga, F. 1981: Upwelling off the Galician coast, NW Spain. In Richards F.A. (editor), *Coastal Upwelling*. American Geophysical Union, Washington, DC, 176-182.

Gil, I. M., Abrantes, F., Hebbeln, D. 2006 *in press*: The North Atlantic Oscillation forcing through the last 2000 years: spatial variability as revealed by high-resolution marine diatom records from N and SW Europe. *Marine Micropaleontology.*

Hass, H.C., 1996: Northern Europe climate variations during the late Holocene: evidence from marine Skagerrak. *Palaeogeography, Palaeoclimatology, Palaeoecology* 123, 121-145.

Hughes, M.K. and Diaz, H.F. 1994: Was there a "Medieval Warm Period" and if so, Where and When? *Climate Change* 26, 109.

Hurrell, J.W. 1995: Decadal trends in the North Atlantic Oscillation: regional temperatures and precipitation. *Science* 269, 676-679.

Keigwin, L.D. 1996: The Little Ice Age and Medieval Warm Period in the Sargasso Sea. *Science* 274, 1504-1508.

Keigwin, L.D., Pickart, R. S., 1999: Slope water current over the Laurentian Fan on interannual to millenial time scales. *Science* 286, 520-523.

Keller, C.F. 2004: 1000 years of climate change. *Advances in Space Research* 34, 315-322.Kirov, B and Georgieva, K 2002: Long-term variations and interrelations of ENSO, NAO and solar activity. *Physics and Chemistry of the Earth* 27, 441-448.

Kirov, B. and Georgieva, K 2002: Long-term variations of ENSO, NAO and solar activity. *Physics and Chemistry of the Earth* 27, 441-448.

Jansen, J.H.F, van der Gaast, S.J., Koster, B. and Vaars, A.J 1998: CORTEX, a shipboard XRF-scanner for element analysis in split sediment cores. *Marine Geology* 151, 143-153.

Jones, P.D., Osborn, T.J. and Briffa, K. R. 2001: The evolution of climate over the last millennium. *Science* 292, 662-667.

Jones, P.D. and Mann, M.E. 2004: Climate over past millennia. *Reviews of Geophysics* 42, doi:10.1029/2003RG000143.

Lamb, H.H. 1985: Climate history and the future, Princeton University Press, Princeton, NJ, 835 pp.

Lean, J. and Rind, D. 2001: Earth´s response to a variable sun. *Science* 292, 234-236.

Levy, A., Mathieu, R., Poignant, A., Rosset-Moulinier, M., Ubaldo, M.L. and Ambroise, D. 1993: Recent foraminifera from the continental margin of Portugal. *Micropaleontology* 39, 75-87.

Loureiro, J.M. 1979: Curvas de duração dos caudais médios diários no rio Tejo, *Technical Report, Serviço Hidráulico (DGRAH), Lisbon*.

Mann, M.E. and Jones, P.D. 2003: Global surface temperatures over the past two millennia. *Geophysical Research Letters* 30, 5.1-5.4.

Masarik, J. and Beer, J. 1999: Simulation of particle fluxes and cosmogenic nuclide production in the Earth's atmosphere. *Journal of Geophysics Research* 104, D10, 12099.

Mayewski, P.A., Rohling E.E., Stager, J.C., Karlén, W., Maasch K.A., Meeker, L.D., Meyerson, E.A., Gasse. F., van Kreveld, S. Holmgren, K., Lee-Thorp, J., Rosqvist, G., Rack, F., Staubwasser, M., Schneider, R.R. and Steig, E.J. 2004: Holocene climate variability. *Quaternary Research* 62, 243-255.

Mikkelsen, N., Kuijpers, A., 2001: Natural Climate Variations in a geological perspective, Gads Forlag., Copenhagen.

Moita, M.T. 2001: Estructura, variabilidade e dinâmica do fitoplâncton na costa de Portugal continental, *unpublished Ph.D. thesis*, Universidade de Lisboa, 272 pp.

Monteiro, H. and Moita, I. 1971: Morfologia e sedimentos da plataforma continental e vertente continental superior ao largo da Península de Setúbal. *Congresso de Geologia* 301-330.

Nogueira, E., Pérez, F. and Ros, A. 1997: Seasonal patterns and long-term trends in an estuarine upwelling ecosystem (Ría de Vigo, Spain). *Estuarine, Coastal and Shelf Science* 44, 285-300.

Nunes, T., Mariño, J., Iglesias, M., González, N., Campos, M.J. and Cabanas, J.M. 1984: Condiciones ambientales, producción primaria y sucesión de especies fitoplanctónicas en la Ría de Arousa (NW de España). *Cuadernos Area Ciencias Mariñas, Sem. Estudios Galegos* 1, 163-172.

Oliveira, A., Rocha, F., Jouanneau, J., Dias, A., Weber, O. and Gomes, C. 2002: Clay minerals from the sedimentary cover from the Northwest Iberian shelf. *Progress in Oceanography* 52, 233-247.

Pauling, A., Luterbacher, J., Casty, C. and Wanner, H. 2006: Five hundred years of gridded high-resolution precipitation reconstructions over Europe and the connection to large-scale circulation. *Climate Dynamics* 26: 387-405.

Pena , L. D., Francés, G., Diz, P., Nombela, M.A. and Alejo, I. *submitted to Quaternary Science Reviews*: Abrupt climatic changes in NW Iberia during the Holocene: high and low latitude linkage at 1500 yr climatic cycles.

Pilskaln, C., Paduan, J., Chavez, F., Anderson. R. and Berelson, W. 1996: Carbon export and regeneration in the coastal upwelling system of Monterey Bay, central California. *Journal of Marine Research* 54, 1149-1178.

Prego, R. 1990: Las sales nutrientes en las rías gallegas. *Informe Técnico Scientia Mariña* 157, 31.

Prego, R. 1993: General aspects of carbon biogeochemistry in the Ría of Vigo, northwestern Spain. *Geochimica Cosmochimica Acta* 57, 2041-2052.

Ríos, A.F., Pérez and Fraga, F. 1992: Water masses in the upper and middle North Atlantic Ocean east of the Azores. *Deep-Sea Research* 39, 645-658.

Rodrigues, T. 2004: Climatic variation and terrigenous input in the Tagus Prodelta during the last 13.5 kyr. *unpublished Master Thesis*, University of Aveiro, Portugal, pp. 117.

Schrader, H-J. and Gersonde, S. 1978: Diatoms and Silicoflagellates. *Utrecht Micropaleontological Bulletin* 17, 12 – 17.

Shackleton, N.J. 1974: Attainment of isotopic equilibrium between ocean water and the benthonic foraminifera genus *Uvigerina*: Isotopic changes in the ocean during the last Glacial. *Colloques Internationaux du C.N.R.S.* 219, 203–209.

Stuiver, M., Braziunas T.F., Grootes, P.M. and Zielinski, G.A. 1997: Is there evidence for solar forcing of climate in the GISP2 oxygen isotope record? *Quaternary Research* 48, 259-266.

Stuiver, M., Reimer, P.J. and Braziunas, T.F. 1998a: High precision radiocarbon age calibration for terrestrial and marine samples. *Radiocarbon* 40, 1127-1151.

Stuiver, M., Reimer, P.J., Bard, E., Beck, J.W., Burr, G.S., Hughen, K.A., Kromer, B., McCormac, F.G., van der Plicht, J. and Spurk,

M. 1998b: INTCAL 98 Radiocarbon age calibration, 24,000–0 cal BP. *Radiocarbon* 40 (3), 1041–1083.

Trigo, R.M., Osborn, T.J., and Corte-Real, J. 2002: The North Atlantic Oscillation influence on Europe: climate impacts and associated physical mechanisms. *Climate Research* 20, 9-17.

Trigo, R.M., Osborn, T.J., and Corte-Real, J. 2002, *Finisterra* 37 (73), 5-31.

Vale, C. and Sundby, B. 1987: Suspended sediment fluctuations in the Tagus estuary on semi-diurnal and fortnightly time scales. *Estuarine, Coastal and Shelf Science* 25, 495-508.

Van der Zwaan, G.J., Duijnstee, L.A.P., den Dulk, M., Ernest, S.R., Jannink, N.T. and Kouwenhoven, T.J. 1999: Benthic foraminifers, proxies or problems? A review of paleoecological concepts. *Earth Science Reviews* 46, 213-236.

Varela, M., Campos, M.J., Penas, E., Sánchez, J., Larrañaga, A., de Castillejo, F.F., del Río, G.D. and Cabanas, J.M. 1987: Composición y distribución del fitoplacton en la plataforma de Galicia durante la campaña Breogán-684 (junio 1984). *Boletín del Instituto Español de Oceanografía* 4, 75-94.

Varela, M., Prego, R., Belzunce, M.J. and Salas, F.M. 2001: Inshore-offshore differences in seasonal variations of phytoplankton assemblages: the case of a Galician Ría Alta (Ría de A Coruña) and its adjacent shelf (NW Spain). *Continental Shelf Research* 21, 1815-1838.

Varela, R.A., Rosón, G., Herrera, J., Torres-López, S., Fernández-Romero, A., 2005: A general view of the hydrographic and dynamical patterns of the Rias Baixas adjacent shelf area. *Journal of Marine Systems* 54, 97–114.

Zahn, R. and Sarnthein, M. 1987: Benthic isotope evidence for changes of the Mediterranean Outflow during the late Quaternary. *Paleoceanography* 2 (6), 543-559

CHAPTER 6.

The North Atlantic Oscillation forcing through the last 2000 years: spatial variability as revealed by high-resolution marine diatom records from N and SW Europe

Gil, I. M., Abrantes, F., Hebbeln, D.,

Marine Micropaleontology (in press)

ARTICLE IN PRESS

ELSEVIER

Available online at www.sciencedirect.com

SCIENCE DIRECT®

MARINE MICROPALEONTOLOGY

Marine Micropaleontology xx(2006)xxx– xxx
www.elsevier.com/locate/marmicro

The North Atlantic Oscillation forcing through the last 2000 years: Spatial variability as revealed byhigh-resolution marine diatom records from N and SW Europe

Isabelle M.Gil[a,b,*], Fatima Abrantes[a], Dierk Hebbeln[b]

[a]Marine Geology Department, National Institute of Engineering,Technology and Innovation-INETI, Apartado 7586, 2721-866 Alfragide, Portugal

[b]Geosciences, University of Bremen, Klagenfurter Straße, 28359 Bremen, Germany

Received 18 July 2005; received in revised form 22 March 2006;accepted 24 March 2006

*Corresponding author:
email address: isabelle.gil@ineti.pt(I.M.Gil).

Abstract

The Tagus pro-delta (Portuguese Margin) and the Skagerrak (NE of the North Sea) are two marine systems controlled by atmospheric changes, which at Present are mainly determined by fluctuations of the North Atlantic Oscillation (NAO). On the basis of diatom records from marine sediment cores, environmental changes (primary productivity and salinity) are reconstructed for the last 2000 years for both regions. These sites are investigated focusing on the regional response to changing NAO forcing.

Both studied sites are characterized by sedimentation rates in the order of 0.12 cm/yr, and 0.47 cm/yr for the most recent deposits off the Tagus pro-delta, allowing high resolution paleoceanographic reconstructions (8.3 and 2.1 years represented per sample). The last 2000 years are a period covering in Europe the historical climatic periods known as the Dark Ages (DA), the Medieval Warm Period (MWP) and the Little Ice Age (LIA). In the Skagerrak, the cold periods of the DA and LIA are marked by diatom dissolution stages, whereas at the Tagus pro-delta the DA were associated with increased diatom production and possible upwelling and the onset of the LIA corresponded to enhanced flow of the Tagus River. During the MWP, better diatom preservation in the Skagerrak, related to stronger advection of salty Atlantic waters is paralleled by dominant upwelling conditions at the Tagus pro-delta. The two most intense upwelling periods at the Tagus pro-delta, at ~AD 600 and ~AD 900, correspond to a dissolution stage and a slight change in salinity in the Skagerrak, respectively.

Although the comparison of the two study sites suggests a common forcing such as the NAO, the different inferred behaviors for each main climatic period in each region demonstrate that the NAO by its own is not sufficient to explain the climatic variability at a regional scale.

Keywords: Holocene, Diatom, North Atlantic Oscillation, Skagerrak, Iberian Peninsula, Paleoceanography

1. Introduction

The climate variability in the North Atlantic region is largely linked to the North Atlantic Oscillation - NAO (Hurell, 1995; Visbeck, 2002). The NAO is described by the difference between the subpolar-low surface pressure south and east of Greenland and the subtropical high surface pressure around the Azores, the NAO index (Hurrell *et al.*, 2001). The surface pressure difference determines the heat flux associated with the Gulf Stream and the North Atlantic Drift that keeps Northwestern Europe comparatively warm. A strong surface heat flux (i.e. a positive NAO phase) leads to an increase in precipitation over northern Europe. In contrast, a merely zonal flux (i.e. a negative NAO phase) leads to an increase in precipitation over the Iberian Peninsula (Lamb and Peppler, 1987). The NAO is the most important cause for changes in the atmospheric circulation during winter (Jones and Mann, 2004) and although it is less characteristic for the other seasons, it is still the dominant pattern (Hurrell and Van Loon, 1997).

For the Holocene period, paleoclimate reconstructions from the North Atlantic region based on coastal and terrestrial proxy records demonstrated that the observed climatic variability is mainly due to changes in ocean circulation and in the solar radiative budget (e.g. Kristensen *et al*., 2004; Bond, 1997, 2001). The high resolution paleoceanographic reconstructions presented here are an attempt to assess the prevailing factors affecting the climate of southern and northern locations of the West European margin. For the last 2000 yrs in Europe, the main climatic periods are the Dark Ages (DA), the Medieval Warm period (MWP) and the Little Ice Age (LIA). The DA appear to have lasted from ~AD 450 to 650 (over the Laurentian Fan, Keigwin and Pickart (1999); considering several Eurasian locations, Mikkelsen and Kuijpers (2001)); the MWP from ~AD 800 to 1300 (in the Skagerrak, Hass (1996)); and finally the LIA between ~AD 1350 and 1900 (in the Skagerrak, Hass (1996)).

The two investigated marine sediment cores (Fig. 1), one from the Tagus pro-delta (Lisbon latitude) and the other from the Skagerrak (NE North Sea), represent two regional end members with respect to NAO variability. These sites are key locations well suited to assess

changes occurring in the strength of the oceanic heat flux towards Europe, as both are controlled by winds, depending on the position and strength of the pressure cells over the North Atlantic described by the NAO index, with the Tagus pro-delta being more directly influenced by the Azores high, while the Skagerrak is more linked to the Icelandic low. Exploiting the high sedimentation rates of the two cores, detailed records of the oceanographic variability based on diatom analyses for the main climatic periods of the last 2000 years allow to reconstruct the paleoenvironmental conditions at both sites with respect to a common NAO forcing.

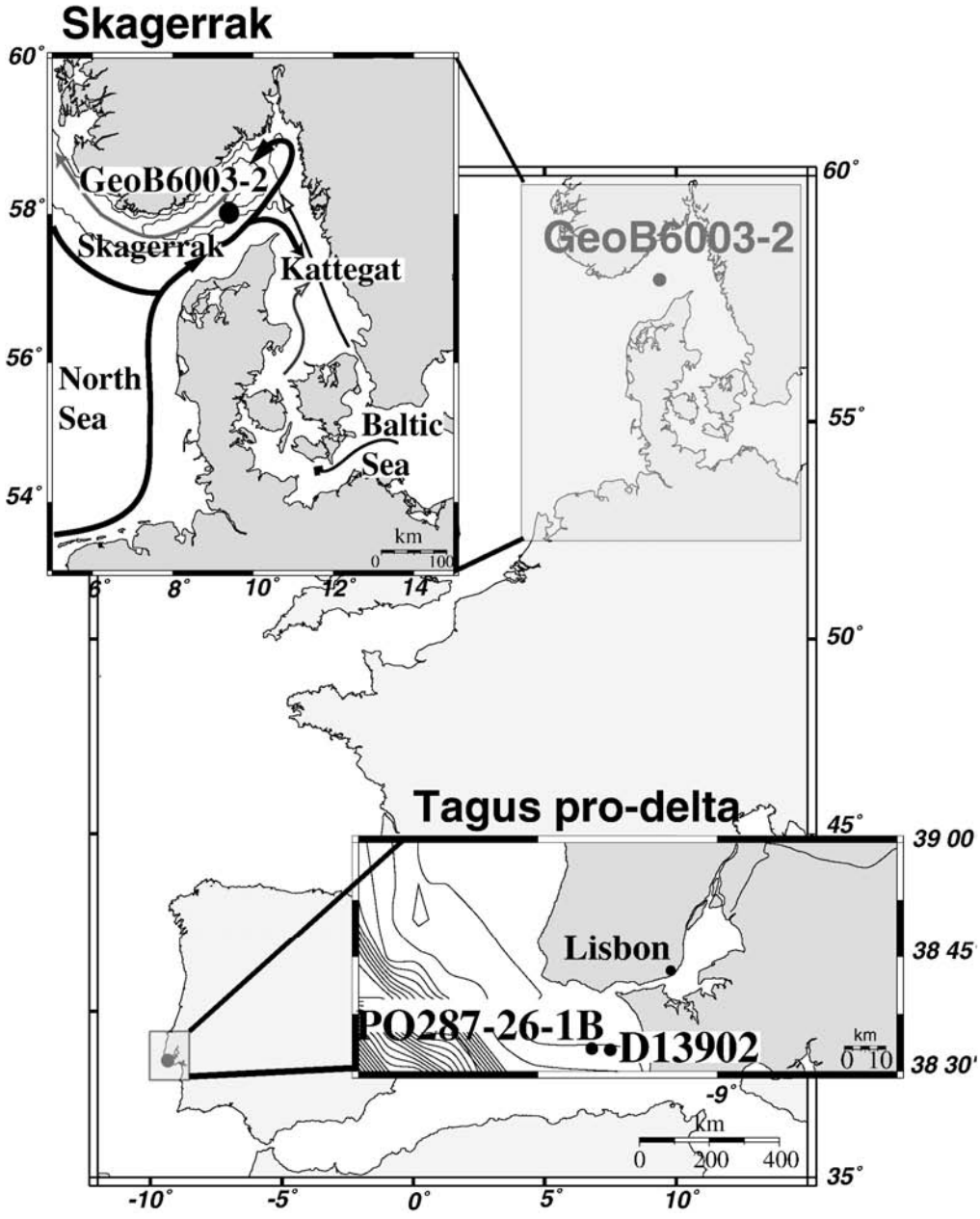

Fig.1. Location of the core sites along the European margin. Surface circulation in the Skagerrak area: thick black arrows represent the Jutland Current, thin black arrows the Baltic Current. The Norwegian Coastal Current is marked by a light grey arrow.

2. Regional settings

2.1 Tagus pro-delta

The Tagus is the longest river of the Iberian Peninsula and the third largest regarding catchment area and outflow. Its flow is strongly influenced by the precipitation over the whole peninsula (Trigo *et al*., 2002a). The precipitation regime over Portugal is described by Trigo and da Camara (2000) based on the period between 1946 and 1990. Throughout the year (except during summer), the anticyclonic circulation dominates. During winter, this circulation type brings only 16% of the precipitation, while the cyclonic, southwesterly and westerly circulation types that are only recorded for 32% of the days deliver all together 62% of the precipitation received. Thus, such cyclonic disturbances are the major contributor for the precipitation over Portugal (Trigo and da Camara, 2000). During summer, the Azores high pressure center is extended, bringing warm and dry air over the continent, and July and August are the driest months. Then, northeasterly and northerly winds prevail and this situation generates coastal upwelling, along the Portuguese margin (Trigo and da Camara, 2000).

In the North Atlantic, off the Tagus River, marine productivity is triggered by two main processes: river discharge and/or coastal upwelling (Moita, 2001), both processes leading to an increase in nutrient availability. The seasonal coastal upwelling affecting the Portuguese margin is instigated by northerly winds during spring and summer (Fiúza *et al.* 1982). The phytoplankton community along the Portuguese margin, is dominated throughout most of the year by coccolithophores (~80% of the phytoplankton), except during the upwelling period, when diatoms take rapidly advantage of the turbulent conditions and clearly dominate (Moita, 2001). The comparison between diatom abundances in the sediment and in the water column during the upwelling season clearly shows that their sediment records traces an intensification of upwelling (Abrantes and Moita, 1999), confirming their use for paleoceanographic reconstructions along the Portuguese margin (Abrantes, 1988, 1991). Furthermore, some diatom species and the mean cell size of the diatoms are good indicators of upwelling occurrence and intensity (Abrantes, 1991), with the diatom flora being also specifically sensitive to changes in salinity.

2.2 Skagerrak

The Skagerrak is the deepest part of the Norwegian Trench, between the North Sea and the Baltic Sea (Fig.1). It is basically characterized by a counter-clockwise circulation with the Jutland Current bringing mainly salty North Sea water (including some coastal waters) from the west and southwest that turn around in the eastern Skagerrak to flow westward again at

its northern margin, now termed the Norwegian Coastal Current (Fig. 1). The advection of North Sea waters is related to the strength of westerly winds and the waters are modified in the easternmost Skagerrak by the addition of brackish waters brought from the Baltic Sea by the Baltic Current (Rodhe, 1996). The hydrological front between the North Sea waters and the Baltic waters resides mainly in the Kattegat, reaching the central part of the Skagerrak only when easterly winds are very strong (Gustafsson and Stigebrandt, 1996).

Presently, during summer, northerly winds prevail in the offshore region and the current velocities in the Skagerrak are low (Rodhe, 1996). The increase in potential energy of the system starts in late summer or early autumn, simultaneously with an increase of southwesterly wind stress (Rodhe, 1996). The stormy winter weather, due to an intensification of the atmospheric low pressure along the polar front, corresponds to stronger southerly winds that result in enforced bottom currents (Rodhe, 1996). Whereas sedimentary deposits in the Skagerrak mainly reflect the strength of the bottom currents induced by climatic conditions (Hass, 1996; Hebbeln *et al*., subm.), the diatom records appear to be quite sensitive to salinity changes (Jiang, 1996).

Sea surface salinities in the Skagerrak are mainly caused by changes in wind forcing with the mixing of North Sea and Baltic waters having a pronounced influence on stratification (Gustafsson and Stigebrandt, 1996). The Baltic waters are mainly confined along the Swedish and Norwegian coasts, but there are strong indications of an occasionally extensive recirculation of those waters within the Skagerrak (Gustafsson and Stigebrandt 1996). Concerning the central part of the Skagerrak (where the investigated core was collected), low saline waters can be brought there by recirculated branches of the Norwegian Coastal Current under westerly wind stirring (Rodhe, 1996). Associated with such a setting, local upwelling might occur in the central Skagerrak, bringing nutrient rich water from deeper layers to the surface and leading to high primary productivity (Fonselius, 1996), marked by a strong spring bloom (Josefson and Hansen, 2003) with at least 33% of the new production made of diatoms (Fonselius, 1996).

2.3 Actual phasing of the sites considering the NAO pattern

Major oceanographic changes in both sites result from the direction of the prevailing winds. Southerly winds are mainly associated to NAO negative phases. These are not dominant along the Portuguese coast, but they bring a major part of the winter precipitation, while in the Skagerrak, they enhance the potential energy of the currents at the end of the summer. The inflow of brackish waters into the Skagerrak is better recirculated under

westerly wind stirring (Rodhe, 1996). Northerly and westerly winds correspond to NAO positive phases. Northerly winds prevail during summer along the Portuguese margin stimulating coastal upwelling and dry conditions on land. At the Skagerrak west to northerly winds block the outflow of low saline water from the central part (Gustafsson and Stigebrandt 1996) and northwesterly wind might intensify the Jutland Current (Hass, 1996).

3. Material and methods

3.1 Material

This study is based on the analysis of two long sediment cores and one short surface core. Core GeoB6003-2 (a long gravity core) from the Skagerrak was collected during RV Meteor cruise M 45 in 1999 (Schott *et al*., 2000). D13902 (long piston-core) and PO287-26-1B (box-core) were collected in the Tagus pro-delta during RV Discovery cruise 249 and RV Poseidon cruise PALEO 1, respectively. The sampling of the box-core was done at one centimeter spacing allowing biennial resolution. The resolution of the long cores is multi-decadal: around 55 years for GeoB 6003-2 (sampling every 5 cm), and variable between 10 and 50 years for D13902 (uneven sample spacing).

3.2 Age control/age models and sedimentation rates

The age model of GeoB 6003-2 from the Skagerrak is based on ^{210}Pb for the more recent sediments and six ^{14}C datings made on benthic foraminifera. The sedimentation rates are in the range of 0.12 cm/yr to 0.165 cm/yr (Scheurle, 2004).

The age model of the box-core PO287-26-1B from the Tagus pro-delta is based on ^{210}Pb measurements and ^{14}C dating on a shell at the base of the box-core and for D13902 on six ^{14}C datings made on shells (Table 4 in Abrantes *et al*., 2005). The reservoir effect used for correction is 400 yrs (verified by ^{14}C dating on three live-collected pre-bomb mollusk shells from the region) and the ages are calibrated using the program CALIB 4.2 (Stuiver and Braziunas, 1989). The sequences are spliced based on ages, magnetic susceptibility and $U^{k'}_{37}$ measurements (Fig.3 in Abrantes *et al*., 2005). The sedimentary sequence exhibits a hiatus likely due to the tsunami generated by the Lisbon earthquake of AD 1755. The sedimentation rate is of 0.12 cm/yr before the tsunami and of 0.47 cm/yr after. Considering unpublished studies of sediment cores from the same area, it appears that the sedimentary dynamic associated with the river discharge deposition center was probably modified by the consequences of the tsunami (Abrantes, pers. comm.).

3.3 Diatom and phytoliths analysis

Diatoms and phytoliths are extracted from $2cm^3$ of bulk sediment, after calcium carbonate removal using HCl, and organic matter oxidation using H_2O_2, according to the method of Fenner (1981). Diatoms and phytoliths are prepared to be mounted on microscope slides in "Norland" mounting medium, after an aliquot of the preparation is dried on cover slips following Battarbee's drying method (1973). Each sample is counted and identified at x 1000 magnification, using the counting protocols of Schrader and Gersonde (1978) and Abrantes (1988).

Total Diatom Accumulation Rates (DAR) and the Phytoliths Accumulation Rates (PhAR) are calculated as number of valves (or phytoliths) per gram of dry bulk sediment x dry bulk density x sedimentation rate. A 5-point smoothing has been applied to the DAR and PhAR data with the Analyseries program (Paillard *et al*., 1996) to better highlight major changes.

Diatom assemblage analysis was only conducted for the Skagerrak core GeoB6003-2 and it is based on the identification of at least 300 valves. The same analysis in core D13902 was not possible as the poor preservation of the diatoms did not allow to readily reach the statistical level of 300 diatoms needed for a reliable assemblage analysis. Nevertheless, the observed diatom species are listed for each sample of D13902 during the counting procedure (cf. Appendix). The mean of the valve diameter of *Paralia sulcata*, based on the measurement of at least 50 well preserved valves was determined only in core GeoB6003-2 due to the same preservation problem.

The preservation index is calculated according to the following ratio: poorly preserved *P.sulcata* / (well preserved *P. sulcata* + poorly preserved *P. sulcata*) (Abrantes, 1991). Grass phytoliths are identified on the basis of the classification of Twiss *et al*. (1969).

3.4 Determination of the Fe content

Fe content is measured by the Bremen CORTEX scanner, a non-destructive XRF system for the logging of split sediment cores (Jansen *et al*., 1998). The long cores are scanned with a resolution of 2 cm (Tagus pro-delta core) and 5 cm (Skagerrak core) and the box-core with a resolution of 1 cm.

4. Results

In general, the low diatom abundances observed in all samples result from strong dissolution, as the diatoms found are mainly heavily silicified forms. Diatom abundance and the preservation status at the Tagus pro-delta are lower compared to the Skagerrak.

4.1 Tagus

The missing top part of D13902 is in part substituted by the box-core PO287-26-1B collected at almost the same location. The splicing of the two sedimentary sequences covers the last 2000 yrs, except from AD 1260 to 1788 due to the previously mentioned hiatus (Fig. 2). In core D13092, 42 diatoms species have been found in the few levels where further diatom assemblage analysis was possible. In box-core PO287-27-1B, 173 diatom species are identified. Most of the species are marine, but 47 are related to fresh water and 25 to brackish waters (cf. Appendix). Diatoms are sparse in D13902 (in the order of $1x10^5$ valves /cm^2/yr and more abundant in the accompanying box-core (in the order of $2x10^6$ valves /cm^2/yr). Phytoliths occur in the order of $2x10^5$ ph. /cm^2/yr in D13902, and $4x10^6$ ph. /cm^2/yr in the box-core. There are three main distinct periods of higher DAR between ~AD 450 and 700 (maximum centered ~AD 550), a period centered ~AD 900 that lasted a century, and a third period from ~AD 1900 to the Present.

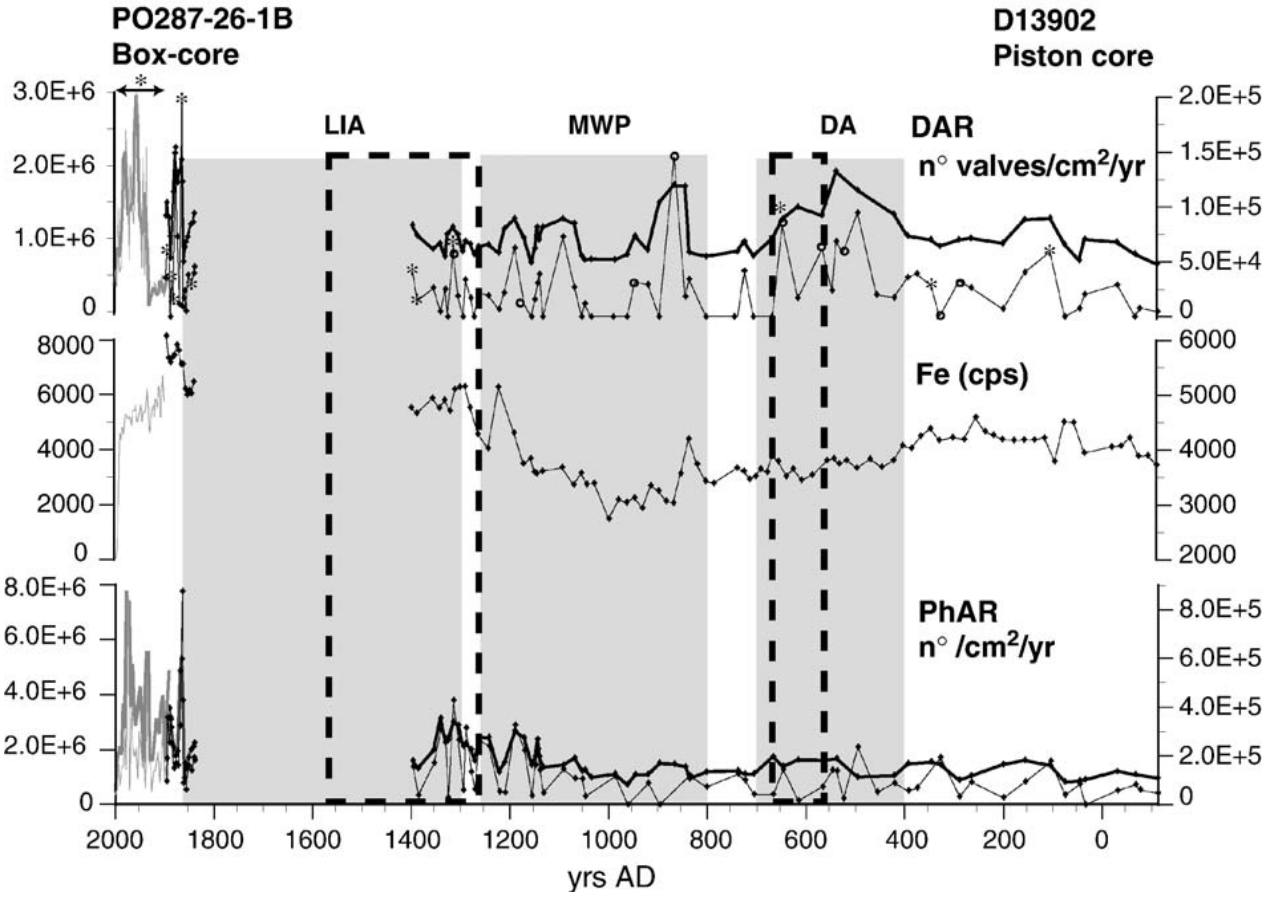

Fig.2. Spliced sequence of PO287-26-1B (box-core–grey curve, left-hand axis) and D13902 (piston core–black curve, right-hand axis) from the Tagus pro-delta: Diatom (DAR) and Phytolith (PhAR) accumulation rates and XRF-derived Fe content. The thicker curves correspond to a smoothing of five points obtained with the Analyseries program (Paillard *et al*., 1996). Open circles and stars indicate the presence of upwelling-related diatoms and fresh water diatoms in core D13902, respectively. Vertical grey bars highlight the main climatic periods and the dashed squares indicate the silica dissolution events in core GeoB6003-2.

Regarding the two older periods, the augmentation of the DAR is not accompanied by an increase in PhAR. The PhAR is roughly constant all along the core until ~AD 1150, when it starts to increase gradually, reaching maximum values between ~AD 1850 and 1970 (Fig. 2). Fresh water diatom species are also better represented during the same time and in particular from ~ AD 1850 to the Present. This rise is closely coupled with variations of the Fe content that starts to increase at ~AD 1100.

4.2 Skagerrak

In core GeoB 6003-2 from the Skagerrak, 114 diatom species have been found. Most of the species are marine, 17 are related to fresh water and 11 to brackish waters (cf. Appendix). The dominant species is *Paralia sulcata* (Ehrenberg) Cleve and its size and preservation state provide indications about productivity conditions and diatom preservation state in general (Fig. 3). The diatom preservation index points to two dissolution events. The first one occurs between ~AD 525 and 675, and a second one between ~ AD 1225 and 1550. Those two stages limit a period of better and continuous preservation of the diatoms, between ~AD 675 and 1225. The dissolution was so strong during the second event that it was not possible to define the diatom assemblage, almost only strongly dissolved valves of *P. sulcata* have been observed. The Fe content remains relatively lower and stable during those events.

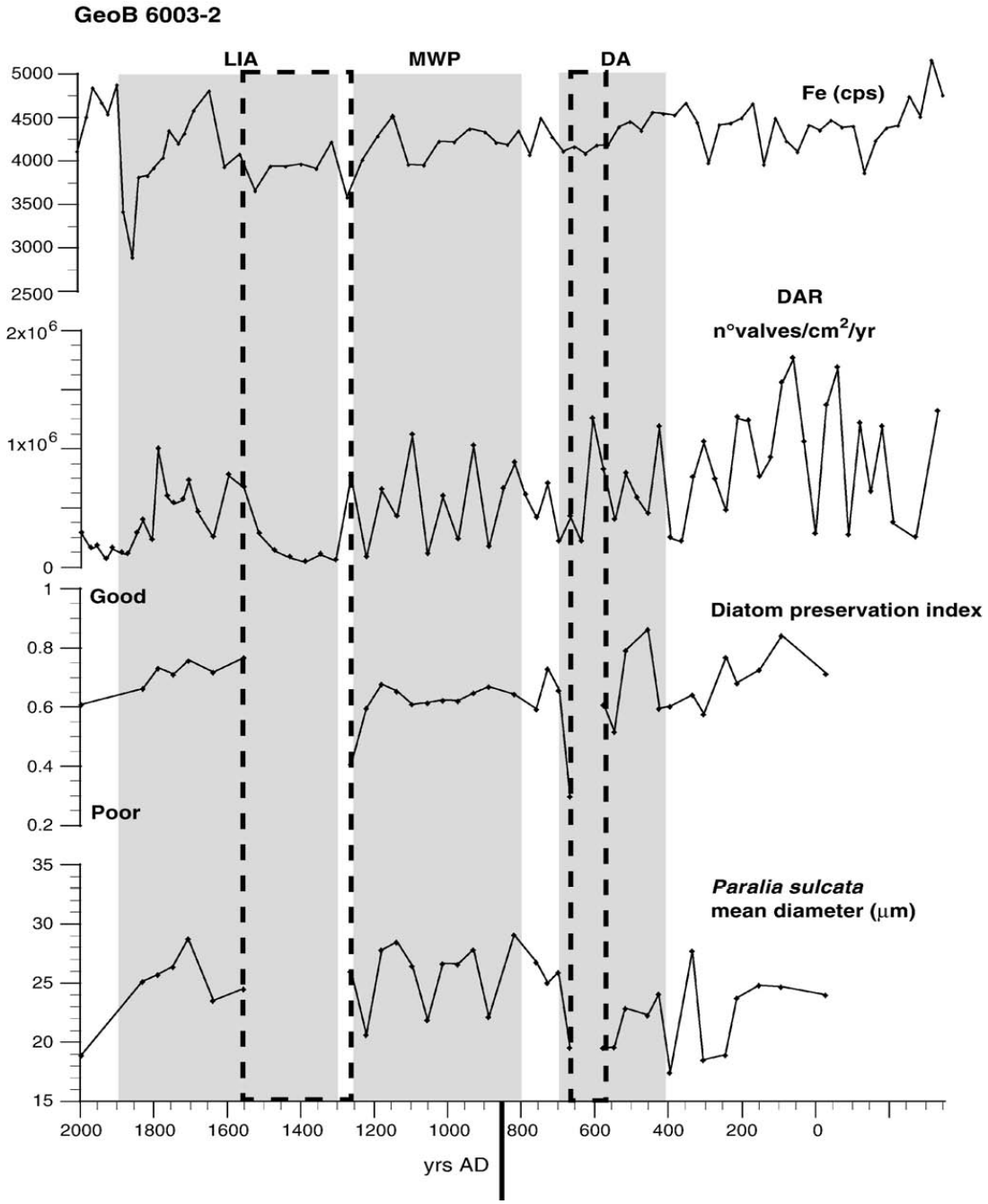

Fig.3. XRF-derived Fe content, diatom accumulation rate (DAR), diatom preservation index –(WPPP/(WPPS+PPPS) with WPPS = well-preserved *P.sulcata* and PPPS = poorly preserved *P.sulcata*)–and *P.sulcata* mean diameter variations within core GeoB6003-2. Grey bars indicate the main climatic periods and the dashed squares demarcate the silica dissolution events; the black tick on the age scale the change in the sedimentation rate from 0.165cm/year to 0.12cm/year (for the more recent sediments).

In general, the DAR shows a continuous decrease, with the lowest rates occurring between AD 1225 and 1550 (during the second dissolution event), and from ~ AD 1800 until present day (Fig. 3). During the period AD 675 - 1225, the mean diameter of *P. sulcata* is almost constant, except at ~AD 900, 1050 and 1225, when an important decrease in size is recorded.

Around AD 900 there is an increase in *Thalassionema nitzschioides* (Grunow) Grunow ex Hustedt and at ~AD 1050 a peak in abundance of *Actinoptychus senarius* (Ehrenberg) Ehrenberg and *Podosira stelligera* (Bailey) Mann (Fig. 4).

From ~ AD 1800 to the Present, the low DAR is associated with changes in the diatom assemblage. *P. sulcata* decreases and *Chaetoceros* spp. becomes the largest contributor to the assemblage. At the same time, *Delphineis surirella* (Ehrenberg) Andrews, *Thalassionema nitzschioides* and *Podosira stelligera* increase. The Fe content registers a decrease from ~ AD 1650 to ~ AD 1850, immediately followed by a rapid increase.

5. Discussion

5.1 Diatom associations in the Skagerrak and their relation to salinity

The environmental interpretation of the Skagerrak diatom assemblages relies mainly on diatom groups (Fig. 4), formed on the basis of Jiang's classification for the Skagerrak-Kattegat surface samples (Jiang, 1996). The groups on that study are mainly related to salinity variations and correspond to different parts of the Skagerrak area, with a group of diatoms related to less saline water (eastern part of the Skagerrak) and another group of diatoms associated to saltier water (area of the Jutland current) (Fig. 4). Additional information about diatom species and ecological preferences was obtained from the monthly monitoring realized in the Skagerrak for the period 1980-1990 (Lange *et al*., 1992).

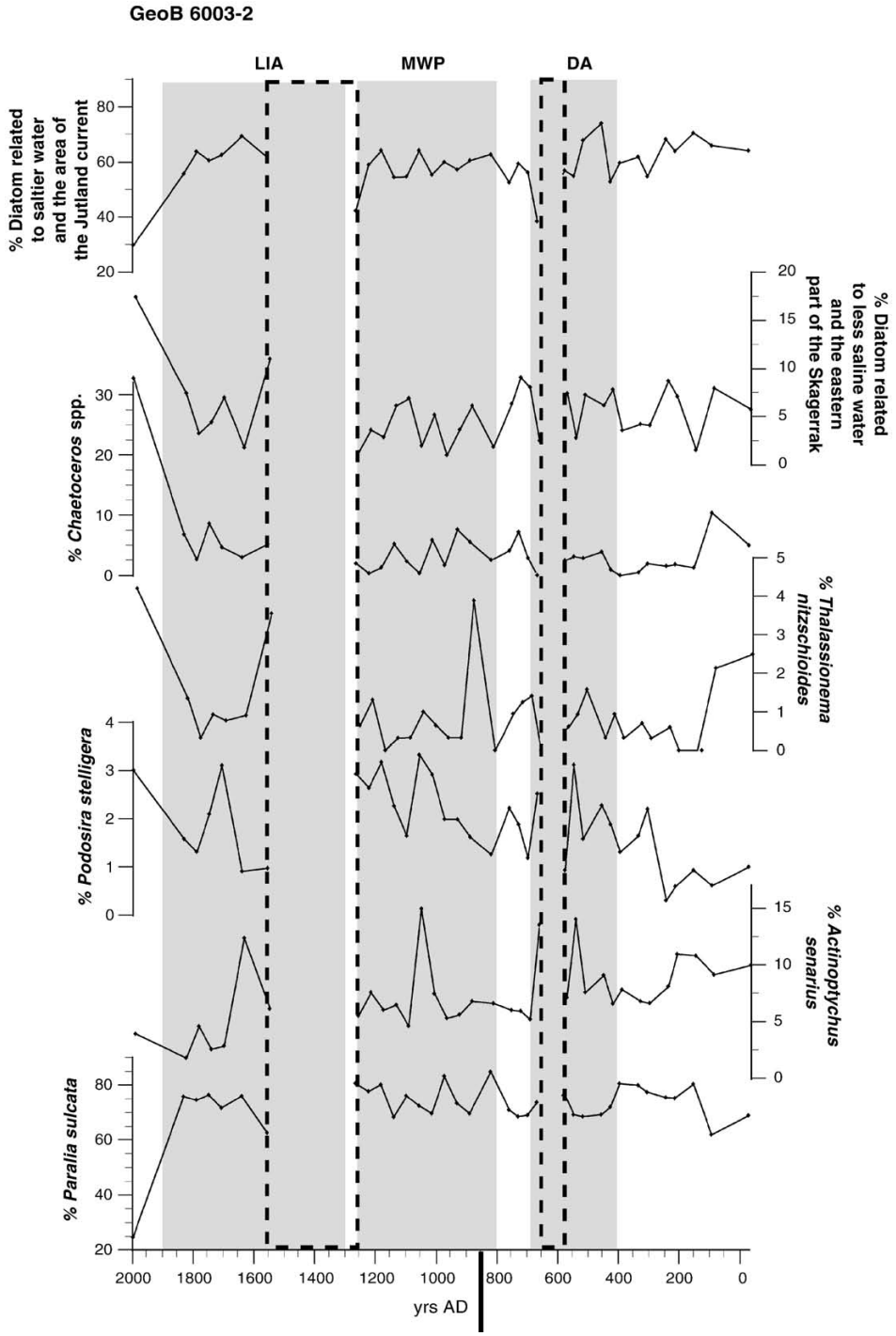

Fig. 4. Relative abundances of the main diatom species and groups along core GeoB6003-2. Grey bars indicate the main climatic periods and the dashed squares demarcate the silica dissolution events; the black tick on the age scale the change in the sedimentation rate from 0.165 cm/year to 0.12 cm/year (for the more recent sediments).

The group related to the less saline waters of the eastern part of the Skagerrak consists mainly of *Delphineis surirella*, *Cymatosira belgica* (Grunow in Van Heurck) and all the fresh water species (listed in the Appendix). The presence of diatoms from this group implies water stratification and freshening of the surface waters. The assumed freshening probably originates from an enhanced influx of waters from the eastern part of the Skagerrak. After a

continuous slight decrease of the contribution of this group until the second dissolution event, it reaches peak values of up to 13% after AD 1600.

The group related to saltier waters (area of the Jutland current) includes *Paralia sulcata*, *Actinoptychus senarius*, *Thalassionema nitzschioides*, *Thalassiosira* spp., *Rhizosolenia* spp., *Actinocyclus octonarius* (Ehrenberg), and other planktonic species (cf. Appendix) (Fig. 4). Although being a coastal species (adapted to lower salinities), *T. nitzschioides* appears to be related to this group. This might be due to the fact that some coastal waters – mainly originated from the mixing of fluvial and marine waters in the German Bight in the Southern North Sea and flowing northward along the Danish coast – contribute to the Jutland Current. Under present day conditions the species of this group are most abundant in winter and early spring (Lange *et al*., 1992). This group clearly dominates for the last 2000 yrs, and generally represents >50% of the identified diatoms. However, the individual evolution of some species, as *Thalassionema nitzschioides*, *Podosira stelligera*, or *Actinoptychus senarius* evidence some slight changes (Fig. 4). *Thalassionema nitzschioides* peaks ~ AD 900 and the contribution of *Podosira stelligera* progressively increases from AD 300, throughout the DA and the MWP. *Actinoptychus senarius* is abundant during the DA and the second part of the LIA. Before and after the dissolution events, the species related to saltier water are relatively better represented.

5.2 Diatom paleoproductivity in the Skagerrak and off the Tagus

The DAR curves present very different pattern for both sites. At the Skagerrak the DAR shows a long-term decrease, however, marked by a high variability and punctuated by two strong silica dissolution events. In contrast, off the Tagus the DAR is rather stable with only three periods of higher values. The general decreasing trend in DAR in the Skagerrak (Fig. 3) matches a slight salinity decrease indicated by a decreasing contribution of the diatom group related to the Jutland Current. Thus, a higher contribution of fresher Baltic Sea waters to the central Skagerrak might be unfavourable for the overall diatom productivity. Such a dependency might also explain the high variability in DAR in the Skagerrak, as even small shifts in the major front between the waters of the Jutland Current and the Baltic Current can strongly affect the oceanographic setting at the core site. Being rather stable in the long-term, the Tagus record is marked by three periods of increased diatom productivity, which will be discussed in detail below.

At the Skagerrak, *Paralia sulcata***,** the dominant diatom species all along the core, is presumably indicative for turbulence and, thus, might trace the upwelling in the central part

of the Skagerrak (Lange *et al*., 1992). This presumption supports other reports showing that this species takes a competitive advantage on unclear waters resulting from mixing and has been considered as an indicator of the initial stage of an upwelling event (Blasco *et al*., 1981; Abrantes and Moita, 1999). Productivity can also be inferred from the valve diameters of well preserved *Paralia sulcata* (Fig. 3). The observed valve diameters range between 17 and 29 μm with an average of ~24 μm. Along the Portuguese coast, Abrantes (1988) described values of 16.5 to 24.2 μm, similar to those from the Skagerrak. Compared to other studies, reporting diameters between 8 and 26 or 29 μm (Roelofs, 1984, McQuoid and Hobson, 1998), the Skagerrak values appear to be in the higher range. Lower DAR in core GeoB6003-2 corresponds to minimum valve diameters and generally to periods when the Jutland Current (i.e. the abundance of the diatom group related to more saline waters) prevails.

However, other studies have shown a negative correlation between *Paralia sulcata* size and productivity (Margalef, 1969; Roelofs, 1984; McQuoid and Nordberg, 2003). Considering the counting procedure (only well preserved valves can be measured), it is possible that the smaller valves that could reflect high productivity conditions have not been measured due to higher dissolution. On the other hand, our data linking minimum valve diameters to enhanced activity of the saltier Jutland Current, is in agreement with Margalef (1969), who suggests that *P. sulcata* valve size is rather linked to salinity changes, with larger valve diameters associated to waters of moderate to low salinity. Variations of *P. sulcata* valve size in the Skagerrak could be rather associated to salinity changes, although a relationship with productivity is not excluded.

Off the Tagus River, the DAR reveals some periods of enhanced productivity and the comparison of the diatom record with the PhAR provides some clues about the forcing behind this increased productivity.

The grass phytoliths result from silica precipitation in continental grass leaves and roots (Twiss *et al*., 1969). They are abundant under dry climatic conditions and transported to the ocean by wind and / or river discharge. At this site, the river input is certainly the main process acting and phytoliths are used as a fresh water proxy. Further comparison of high resolution diatom and phytolith data with instrumental data recording the Tagus river flow substantiate this hypothesis (Gil *et al*., in prep.).

There are three periods (~AD 450 to 700, ~AD 900 and after AD 1850) marked by enhanced DAR and, thus, by enhanced productivity. During the two older periods the PhAR does not change, supporting the interpretation that the increase in DAR is not related to river nutrient input but rather to the improvement of marine productivity conditions possibly

related to upwelling, since the species present during those periods, *Paralia sulcata* and some spores of *Chaetoceros* are upwelling related (Abrantes and Moita, 1999). The combination of the proxies point to improved productivity conditions related to upwelling between ~AD 450 and 700 (with the maximum centered ~AD 550), and also during a period centered ~AD 900. Those periods are within the DA cold period and the MWP, respectively. The gradual increase of PhAR after AD 1150 is closely coupled to the increase in Fe in the core, which can also be interpreted as indicative for enhanced terrigenous sediment input (Wefer, *et al*., 1999). This interpretation is also supported by higher contents of freshwater diatoms, especially after AD 1850. Thus, all these data point to enhanced flow of the Tagus River and, thus, to increasing precipitation on the Iberian peninsula since ~AD 1150. The increase of the PhAR at the end of the MWP and at the onset of the LIA may also reflect higher grass phytoliths production and drier conditions during the MWP and a later transport to the ocean by the increased precipitation and river run-off at the onset of the LIA. Benito *et al*. (2003) has also described evidences for a higher frequency in floods of the Tagus River (central Spain) during several periods of the LIA (highest flood frequency: AD 1540-1640, AD 1730-1760; largest floods: AD 1658-1706 and AD 1870-1900), based on documented historical flood data sets. The large fluctuations in DAR recorded at the Tagus pro-delta for the last century (most of the box-core record) is likely due to a higher resolution of the record (biennial), while the higher DAR might be due (at least in part) to a better preservation of diatom in the top 21 cm sediment column (cf. species list of PO287-26-1B) rather than a proportional increase in productivity conditions.

At the Tagus pro-delta, the DAR appears as an indicator of the major oceanographic changes, delimitating the main climatic periods, while at the Skagerrak the clearest indicators of strong oceanographic changes is not the DAR, but the diatom dissolution events, which are analyzed in detail below. High values of DAR at the Tagus pro-delta registered during the DA and within the MWP indicate upwelling conditions, whereas in recent sediments, DAR increases appear related to enhanced river flow.

5.3 Phasing of the environmental changes registered at both sites

Within the limits of the dating method, the major environmental changes registered at both locations occur at: ~AD 550 / 600, AD 900, from ~AD 1225 to 1550, and from AD 1850 to the Present.

The first increase in productivity conditions at the Tagus pro-delta (accepted as an indication of upwelling) fits within the period of the first dissolution event in the Skagerrak

(~AD 525 - 675). Despite the strong dissolution, many diatom valves remain, as showed by the DAR (Fig. 3). This implies good productivity conditions, however obviously paralleled by strong silica dissolution. Presently, winter conditions correspond to intensified northerly winds, higher current velocities inducing intensified bottom currents, higher frequency of storms and the coarsening of the sediments (Rodhe, 1987; Hass, 1996). These conditions may affect diatom preservation, as a larger grain size of the sediments may increase the silica dissolution rate (Ehrenhauss *et al*., 2004). A slight and a significant increase in grain-size are in fact registered during the first and second dissolution events respectively in the Skagerrak's core (Scheurle, 2004). Both events at the Tagus pro-delta and in the Skagerrak are centered at ~AD 600 well within the DA period. Hass (1996) also detected a colder period in the Skagerrak from AD 400 to AD 700. Regarding the oceanographic changes registered at both locations, the DA appears to spread between ~AD 475 and 675, with dominant upwelling conditions at the Tagus pro-delta and more frequent storminess over the Skagerrak. Those oceanographic and climatic conditions correspond nowadays to NAO positive phases, with a storm track passing over the Skagerrak.

During the MWP, the most significant fact at the Tagus pro-delta is a short productivity event at ~AD 900, corresponding to increased upwelling, as indicated by a better representation of diatoms species related to it. Although saltier waters prevail at the Skagerrak for that period, an increased individual contribution of diatom species associated to less saline water, as *Thalassionema nitzschioides*, *Delphineis surirella* or *Cymatosira belgica* suggest a slight freshening of the surface waters precisely at ~AD 900. An increase in precipitation over the continent leading to the reinforcement of the coastal currents joining the main Jutland current between ~ AD 850 and 1225 is hypothesized, although the Fe record does not show any marked change. In fact, a multiproxy study of the Skagerrak (Hebbeln *et al*., subm.) that includes the same core presented here reveals that the most pronounced change occurred at ~AD 900, with an enhanced advection of Atlantic waters to the North Sea. Nevertheless, good preservation of *P. sulcata* suggests stable conditions associated to the Jutland Current and a positive NAO index during the MWP, although diatom productivity (DAR) presents some variability. According to Hass (1996), the MWP occurred in the Skagerrak between AD 800-1300, in agreement with our diatom record.

The next environmental change starts at ~ AD 1150 at the Tagus pro-delta and at ~ AD 1225 in the Skagerrak which, considering the age uncertainties in both records, might be rather contemporaneous events corresponding to the transition to the LIA. At the Tagus pro-delta, relative increases in DAR (including freshwater diatoms), in PhAR and in Fe content

point to an enhanced river run-off. At the Skagerrak, the second dissolution stage began and productivity is likely to have been lower than during the DA as fewer diatoms have been preserved. Although a major part of the LIA record is missing from the Tagus pro-delta site, at both locations, the LIA appears to last from ~AD 1250 to 1900, accompanied by enhanced storminess in the Skagerrak between ~AD1250 and 1550 as indicated by the second diatom dissolution event. Previous studies already found evidences for a LIA presenting phases of different cooling intensity (Hass, 1996, deMenocal *et al*., 2000). During the winters of the LIA, cyclonic atmospheric situations were more frequent, inducing precipitation over the Iberian Peninsula and stormy conditions in the Skagerrak. Such a climatic situation over the Iberian Peninsula corresponds nowadays to NAO negative phases, while at the Skagerrak it is rather compatible with NAO positive phases.

Since AD 1800, diatom indications suggest different oceanographic conditions at the Skagerrak, with the lowest DAR and a shift in diatom assemblage. While the diatom assemblage related to the Jutland current (and especially the diatom *P. sulcata* included in it) prevails mostly all along the record, diatom assemblages dominated by the diatom genus *Chaetoceros* start to rise and dominate the more recent assemblage, in association with diatom species related to less saline water. The increase in Fe suggests also a terrigenous input for that time, in agreement with the freshening of the surface water indicated by the diatoms. Such a diatom assemblage shift can reflect the end of the LIA with the establishment of new oceanographic conditions. This change could also be associated to new environmental conditions, however it can also be related to human land use or fertilization of the Skagerrak waters via river discharge and resulting eutrophication conditions. Considering the marked decrease in Fe after ~ AD 1850 corresponding precisely to the lowest DAR, it is hypothesized that an higher river input of nutrient (such as Fe) should have lead to water stratification, and so, favored other phytoplanktonic communities, as e. g. coccolithophorids (Moita, 2001). However, the diatom record does not provide further clues to consider this hypothesis.

5.4 Discrepancies in the environmental response of the two regions: climatic implications

It is of particular interest that for the two cold periods, the DA and the onset of LIA, the climatic record at the Tagus pro-delta is different, whereas it is similar at the Skagerrak. At the Tagus pro-delta, an increase in upwelling is observed for the DA, while for the beginning of the LIA, the data point to an increase in precipitation. In contrast, for the Skagerrak an increase in storminess related to a more zonal atmospheric circulation is indicated for both

periods. Indeed, the expansion of the circumpolar vortex implies a southward shift of the cyclone tracks (Lamb, 1977). The diatom dissolution events testify that the storm tracks are passing over Skagerrak.

Although the DA were one of the coldest periods of the last 2000 years (Briffa *et al*., 1990), it was not as long as the LIA. A precise description of the LIA is provided by Lamb (1977), based on several proxies and historical records, and in particular on mean sea level pressure (SLP). Lamb (1977) deduced two different circulation patterns over Western Europe from SLP measurements for the summers AD 1596 and 1695 (both during the LIA) and described the related climatic conditions (Fig. 5). The major difference between these two summers is the location of the main air pressure centers that induce a latitudinal gradient (as the NAO pattern) and lead to different regional climatic responses. Those situations can be used as analogues to explain the discrepancy of our records and suggest that although both DA and LIA were cold periods, they could have been affected by the predominance of different atmospheric circulation patterns.

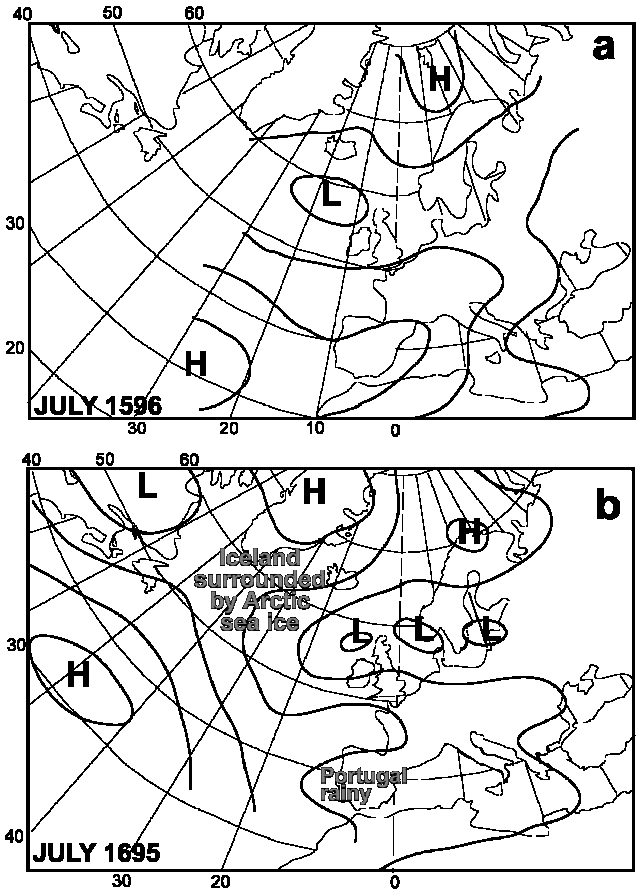

Fig. 5: Reconstruction of the atmospheric circulation patterns for the summers of (a) AD 1596 (considered as analog for DA situation) and (b) 1695 (considered as analog for LIA situation) modified from Lamb (1977). H and L means high and low (center pressure), respectively.

The first reconstructed circulation pattern for AD 1596 presents an anticyclonic pressure center extended over the North East Atlantic, with a low pressure center close to Scotland (Lamb, 1977). Historical records for that time describe stormy weather in the North Sea, severe floods in Scandinavia, and rainy conditions over central Europe. No special situation is recorded over the Iberian Peninsula that is under a clear anticyclonic influence, and the extended high pressure center over most of the Iberian Peninsula likely instigates a coastal upwelling on the western margin. The deduced pressure gradient between the two main pressure centers is high. This atmospheric situation can be taken as a more typical setting for the DA.

The second reconstruction for AD 1695, with marked rainy weather over Portugal can be taken as a more typical setting for our interpretation of the LIA. The atmospheric circulation presents a zonal pattern between the main pressure cells. In this setting, several low pressure centers have been developed in the north between 50° and 60° N, mainly over the North Sea and North of Ireland (Lamb, 1977). Under such conditions, Iceland was surrounded by Arctic sea ice, the summers were cool and frosts frequent in central Europe, strong winds blew frequently south of Ireland and the rain over Portugal was remarkably increased.

The comparison of those two situations within the LIA reveals the high variability of atmospheric patterns that lead to almost similar climatic conditions over Northern Europe (the difference remains mainly in the intensity of the cold that is evidenced by the sea-ice around Iceland in the second situation), while the southern part of Europe experienced major changes, as there the extension of the subtropical Azores anticyclone plays a major role. The Iberian Peninsula appears to be more sensitive to atmospheric conditions connected to southern latitudes. For the last millennium, instrumental records of the Tagus River flow along its catchment area in Spanish territories indicate an increase in the frequency of high floods during parts of the LIA (Benito *et al*., 2003). The intense rainfall over the Iberian Peninsula during the LIA was generated by the passage of Atlantic disturbances, and therefore associated to a zonal atmospheric circulation, including Atlantic cyclones of subtropical origin (Benito at al., 2003). This is in agreement with the Tagus pro-delta record for the LIA.

Furthermore, nowadays, the Iberian Peninsula is marked by a higher sensitivity to the NAO pattern in its southwestern part (Trigo *et al*., 2002b), whereas the eastern and northern parts are more dependent upon the polar or Scandinavian patterns (Gonzales-Hidalgo *et al*., 2003 in Vicente-Serrano *et al*., 2004). It appears that the location of the southern cyclone plays a more important role over southern Europe than over central and northern Europe, where the

SLP gradient appears to be the dominant factor (Castro-Díez *et al*., 2002). As such, not only the NAO phase plays a role, but the location of the pressure centers is also important.

The zonal pattern is also important in southern Europe as a comparison of the Tagus and the Tiber (Italy) discharges for the last millennium shows precisely an opposite pattern (Camuffo, *et al*. 2003). This contrast implies an additional east-west difference in the precipitation pattern that it is not directly in response to the NAO forcing.

The major environmental changes of ~ AD 600 and 900 corresponding to more intense upwelling at the Tagus pro-delta match with arid conditions in the northeast tropical Atlantic (DeMenocal, 2001) and at AD 900 to a warming on the Norwegian coast (Hebbeln *et al*., subm.). Nevertheless, the phasing of the changes suggest a common forcing such as the NAO, but the complex responses of the individual regions stress the importance of a latitudinal gradient. The location of the Polar front or the locations of the pressure centers in the subtropics are factors contributing to the regional European climatic variability.

Conclusions

The present study reveals a similar timing for environmental changes off the Tagus River and at Skagerrak through the last 2000 years, with the DA occurring between AD 400 and 650, the MWP between AD 800 and 1200 and the LIA between AD 1350 and 1900. The cold periods are particularly marked. The discrepancies in the response of these two systems evidence the complexity in relating them to only a single forcing mechanism, such as the NAO. The comparison of the two sites gives a better insight into the distribution and strength of the atmospheric patterns, as it reveals different regional oceanic responses to the same global climatic background and suggests that the mean NAO pattern (positive or negative) alone is not sufficient to assess regional climate variability.

The NAO pattern as the driver of climate variability over Europe does not account for regional scale variations, since the location of the pressure centers associated to the NAO determine the cyclonic tracks and the main storms pathways. Southwestern Iberia reveals a high sensitivity to the location of the subtropical pressure center.

Acknoledgements

This work has been supported by the European Union through funding of the project HOLSMEER – Late Holocene Shallow Marine Environments of Europe (EU - EVK2-2000-00563), the Fundação para a Ciência e Tecnologia - FCT (BD - 18317/2004) and European Social Fund (ESF) through the 3rd EU Framework Program. XRF measurements of core

D13902 and PO287-26-1B were made at the University of Bremen thanks to the funding of PALEOSTUDIES (Contract Nº. HPRI-CT-2001-00124).

We are grateful to A. Inês for laboratory technical support with sample preparation for diatom analysis at the INETI-Laboratory of Marine Geology. We also thank two anonymous reviewers for their valuable comments and suggestions.

REFERENCES

Abrantes, F., 1988. Diatoms assemblages as upwelling indicators in surface sediments off Portugal. Marine Geology, 85: 15-39.

Abrantes, F., 1991. Increased upwelling off Portugal during the last glaciation: diatom evidence. Marine Micropaleontology, 17: 285-310.

Abrantes, F., Lebreiro, S., Rodrigues, T., Gil, I., Bartels-Jonsdottir, H., Oliveira, P., Kissel, C., Grimalt, J. O., 2005. Shallow-marine sediment cores record climate variability and earthquake activity off Lisbon (Portugal) for the last 2000 years. Quaternary Science Reviews, 24: 2477-2494.

Abrantes, F., Moita, M., 1999. Water column and recent sediment data on diatoms and coccolithophorids, off Portugal, confirm sediment record of upwelling events. Oceanologica Acta, 22, 1: 67-84.

Battarbee, R.W., 1973. A new method for estimation of absolute microfossil numbers with reference especially to diatoms. Limno. Oceanogr., 18: 647-652.

Benito, G., Diez-Herrero, A., de Villalta, M. F., 2003. Magnitude and frequency of flooding in the Tagus basin (Central Spain) over the last millennium. Climatic Change, 58(1-2): 171-192.

Blasco, D., Estrada, M., Jones, B.H., 1981. Short Time Variability of Phytoplankton Populations in Upwelling Regions - The Example of Northwest Africa. Am.Geophysical Union, pp. 339-347.

Bond, G., Showers, W., Cheseby, M., Lotti, R., Almasi, P., deMenocal, P., Priore, P., Cullen, H., Hajdas, I., Bonani, G., 1997. A pervasive millenial-scale cycle in North Atlantic Holocene and glacial climates. Science, 278(5341): 1257-1266.

Bond, G., Kromer, B., Beer, J., Muscheler, R., Evans, M. N., Showers, W., Hoffmann, S., Lotti-Bond, R., Hajdas, I., Bonani, G., 2001. Persistent solar influence on North Atlantic climate during the Holocene. Science, 294(5549): 2130-2136.

Briffa, K.R., Bartholin, T.S., Eckstein, D., Jones, P. D, Karlen, W., Schweigruber, F. H., Zetterberg, P., 1990. A 1,400-year tree-ring record of summer temperatures in Fennoscandia. Nature, 346: 434-439.

Camuffo, D., Sturaro, G., Benito, G., 2003. An opposite flood pattern teleconnection between the Tagus (Iberian Peninsula) and Tiber (Italy) rivers during the last 1000 years, Palaeofloods, Historical Floods and Climatic Variability: Applications in Flood risk Assessment (Proceedings of the PHEFRA Workshop), Barcelona.

Castro-Díez, Y., D. Pozo-Vázquez, F.S. Rodrigo and M.J. Esteban-Parra, 2002. NAO and winter temperature variability in southern Europe. Geophysical Research Leters., 29 (8), doi.: 10.1029/ 2001GL014042.

deMenocal, P.B., 2001. Cultural responses to climate change during the Late Holocene. Science, 292: 667-673.

deMenocal, P., Ortiz, J., Guilderson, T., Sarnthein, M., 2000. Coherent high-and-low-latitude climate variability during the Holocene warm period. Science, 288: 2198-2202.

deMenocal, P.B., 2001. Cultural responses to climate change during the Late Holocene. Science, 292: 667-673.

Ehrenhauss, S., Witte, U., Janssen, F., Huettel,

M., 2004. Decomposition of diatoms and nutrient dynamics in permeable North Sea sediments. Continental Shelf Research, 24: 721-737.

Fenner, J., 1981. Diatoms in the Eocene and Oligocene Sediments off NW - Africa. Their Stratigraphic and Paleographic Occurrences. Ph D Thesis, Mathematisch-Naturwissenschaftlichen Fakultat der Christian-Albrechts-Universitat zu Kiel, Kiel, 230 pp.

Fiúza, A., de Macedo, M. E., Guerreiro, M. R., 1982. Climatological Space and Time Variation of the Portuguese Coastal Upwelling. Oceanologica Acta, 5(1): 15.

Fonselius, S., 1996. The upwelling of nutrients in the central Skagerrak. Deep-Sea Research II, 34(1): 57-71.

Gil, I. M., Abrantes, F., Hebbeln, D., in preparation. Instrumental data confirms diatom as upwelling and river discharge indicator off the Tagus pro-delta (Portugal, Lisbon latitude).

Gustafsson, B., Stigebrandt, A., 1996. Dynamics of the freshwater-influenced surface layers in the Skagerrak. Journal of Sea Reserach, 35(1-3): 39-53.

Hass, H.C., 1996. Northern Europe climate variations during the late Holocene: evidence from marine Skagerrak. Palaeogeography, Palaeoclimatology, Palaeoecology, 123: 121-145.

Hebbeln, D., Knudsen, K.-L., Gyllencreutz, R., Kristensen, P., Klitgaard-Kristensen, D., Backman, J., Scheurle, C., Jiang, H., Gil, I., Smelror, M., Sejrup, H.-P., submitted to The Holocene. Late Holocene coastal hydrographic and climate changes in the eastern North Sea.

Hurrell, J.W., 1995. Decadal trends in the North Atlantic Oscillation: Regional temperatures and precipitation. Science, 269: 676-679.

Hurrell, J.W. and VanLoon, H., 1997. Decadal variations in climate associated with the North Atlantic Oscillation. Climatic Change, 36(3-4): 301-326.

Hurrell, J.W., Kushnir Y., Visbeck M., 2001. The North Atlantic Oscillation. Science, 291: 603-605.

Jansen, J.H.F., Van der Gaast, S. J., Koster, B., Vaars, A. J., 1998. CORTEX, a shipboard XRF-scanner for element analyses in split sediment cores. Marine Geology, 151: 145-153.

Jiang, H., 1996. Diatoms from the surface sediments of the Skagerrak and the Kattegat and their relationship to the spatial changes of environmental variables. Journal of Biogeography, 23: 129-137.

Jones, P.D. and Mann, M.E. 2004: Climate over past millennia. *Reviews of Geophysics* 42, doi:10.1029/2003RG000143.

Josefson, A.B., Hansen, J.L.S., 2003. Quantifying plant pigments and live diatoms in aphotic sediments of Scandinavian coastal waters confirms a major route in the pelagic-benthic coupling. Marine Biology, 142(4): 649-658.

Keigwin, L.D., Pickart, R. S., 1999. Slope water current over the Laurentian Fan on interannual to millenial time scales. Science, 286: 520-523.

Kristensen, D.K., Sejrup, H.P., Haflidason, H., Berstad, I.M., Mikalsen, G., 2004. Eight-hundred-year temperature variability from the Norwegian continental margin and the North Atlantic thermohaline circulation. Paleoceanography, 19, PA2007, doi:10.1029/2003PA000960.

Lamb, H.H., 1977. Climate, History and the Modern World, 2. Methuen & Co. Ltd, London, 835 pp.

Lamb, P.J., Peppler R. A., 1987. North Atlantic Oscillation: Concept and an Application. Bulletin American Meteorological Society, 68 (10): 1218-1225.

Lange, C.B., Hasle, G. R., Syversten, E. E., 1992. Seasonal cycle of diatoms in the Skagerrak, North Atlantic, with emphasis on the period 1980-1990. Sarsia, 77: 173-187.

Margalef, R., 1969. Diversidad de fitoplancton de red en dos áreas del Atlántico. Inv. Pesq., 33(1): 275-286.

McQuoid, M.R., Hobson, L. A., 1998. Assessment of palaeoenvironmental conditions on Southern Vancouver Island, British Columbia, Canada, using the marine tychoplankter *Paralia sulcata*. Diatom Research, 13 (2): 311-321.

McQuoid, M.R., Nordberg, K., 2003. The diatom *Paralia sulcata* as an environmental indicator species in coastal sediments. Estuarine, Coastal and Shelf Science, 56: 339-354.

Mikkelsen, N., Kuijpers, A., 2001. Natural Climate Variations in a geological perspective, Gads Forlag., Copenhagen.

Moita, M.T.C.d.J.G., 2001. Estrutura, variabilidade e dinâmica do fitoplâncton na costa de Portugal continental. Ph D Thesis, Faculdade de Ciências da Universidade de Lisboa, Lisbon, 272 pp.

Paillard, D., L. Labeyrie, Yiou, P., 1996. Macintosh program performs time-series analysis. Eos Trans., 77(379).

Rodhe, J., 1987. The large-scale circulation in the Skagerrak; interpretation of some observations. Tellus, 39A: 245-253.

Rodhe, J., 1996. On the dynamics of the large-scale circulation of the Skagerrak. Journal of Sea Research, 35(1-3): 9-21.

Roelofs, A.K., 1984. Distributional patterns and variation of valve diameter of *Paralia sulcata* in surface sediments of Southern British Columbia inlets. Estuarine, coastal and Shelf Science, 18: 165-176.

Scheurle, C. 2004. Climate development and its effect on the North sea environment during the late Holocene. Fachbereich Geowissenschaften. Bremen, Bremen University: 123.

Schott, F., Meincke, J., Meinecke, G., Neuer, S., Zenk, W., 2000. North Atlantic 1999, Cruise nº45, 18 May-4 November 1999. Meteor-Berichte, Universität Hamburg.

Schrader, H.J., Gersonde, R., 1978. Diatoms and Silicoflagellates. Utrecht Micropaleontological Bulletin, 17: 129-176.

Stuiver, M. and Braziunas, T.F., 1989. Atmospheric C-14 and Century-Scale Solar Oscillations. Nature, 338(6214): 405-408.

Trigo, R.M., Da Camara, C. C., 2000. Circulation weather types and their influence on the precipitation regime in Portugal. International Journal of Climatology, 20: 1559-1581.

Trigo, R., Osborn, T. J., Corte-Real, J., 2002a. Influência da oscilação do Atlântico Norte no clima do continente europeu e no caudal dos rios ibéricos atlânticos. Finisterra, XXXVII (73): 5-31.

Trigo, R.M., Osborn, T. J., Corte-Real, J. M., 2002b. The North Atlantic Oscillation influence on Europe: climate impacts and associated physical mechanisms. Climate Research, 20: 9-17.

Twiss, P.C., Suess, E., Smith, R. M., 1969. Morphological classification of grass phytoliths. Soil Science Society of America Proceedings, 33: 109-115.

Vicente-Serrano, S.M., Heredia-Laclaustra, A., 2004. NAO influence on NDVI trends in the Iberian peninsula (1982-2000). International Journal of Remote Sensing, 25(14): 2871-2879.

Visbeck, M., 2002. The ocean's role in Atlantic climate variability. Science, 297: 2223-2224.

Wefer, G., Berger, W. H., Bijma, J., Fischer, G., 1999. Clues to ocean History: a brief overview of proxies. In: G. Fischer, Wefer, G. (Editor), Use of proxies in paleoceanography: examples from the South Atlantic. Springer-Verlag, Berlin Heidelberg, pp. 1-68.

APPENDIX

Diatom species	D13902	PO287-26-1B	GeoB6003-2
			Diatom group
Achnanthes brevipes (Agardh)		X	
Achnanthes ceramii (Hendey)		X	5
Achnanthes clevei (Grunow in Cleve et Grunow)		X	
Achnanthes delicatula (Kützing) Grunow in Cleve et Grunow		X	4
Achnanthes dispar (Cleve)		X	
Achnanthes lanceolata (Brébisson in Kützing) Grunow in Cleve et Grunow		X	
Achnanthes lilljeborgei (Grunow)		X	
Achnanthes minutissima (Kützing)		X	
Achnanthes stroemii (Stroemii) Hustedt		X	
Actinocyclus crenulatus (Grunow)		X	
Actinocyclus octonarius (Ehrenberg)	X	X	5
Actinoptychus senarius (Ehrenberg) Ehrenberg	X	X	1
Amphora binodis (Gregory)		X	
Amphora commutata (Grunow in Van Heurck)		X	
Amphora copulata (Küntzing) Schœman et Archibald		X	4
Amphora crassa (Gregory)		X	
Amphora holsatica (Hustedt)		X	
Amphora laevis (Gregory)		X	
Amphora normanii (Rabenhorst)		X	
Amphora proteus (Gregory)		X	5
Amphora sp.	X		
Amphora spectabilis (Gregory)		X	
Amphora turgida (Gregory)		X	
Amphora valida (Peragallo)		X	
Amphora veneta (Kützing)		X	
Anaulus sp.		X	
Aneumastis tusculus (Ehrenberg) Mann et Stickle		X	
Asteromphalus flabellatus (Brébisson) Greville		X	
Aulacoseira ambigua (Grunow in Van Heurck) Simonsen		X	
Aulacoseira distans (Ehrenberg) Simonsen	X	X	4
Aulacoseira granulata (Ehrenberg) Simonsen	X	X	4
Aulacoseira islandica (Müller) Simonsen			4
Auliscus sp.			5
Bacillaria paxilifer (Müller) Hendey		X	5
Biddulphia pulchella (Gray)		X	
Caloneis leptostoma (Grunow in Van Heurck) Krammer		X	
Caloneis linearis (Grunow) Boyer		X	
Caloneis subsalina (Donkin) Hendey		X	
Campylosira cymbelliformis (Schmidt) Grunow ex Van Heurck		X	

Catacombas gaillonii (Bory) Williams et Round		X	
Catenula adhaerens (Mereschkowsky) Mereschkowsky		X	5
Cerataulus radiatus (Roper) Ross	X	X	
Cerataulus smithii (Ralfs in Pritchard)			5
Chaetoceros diadema (Ehrenberg) Gran		X	5
Chaetoceros lorenzianus (Grunow)			5
Chaetoceros spp.	X	X	5
Chaetoceros wighami (Brightwell)		X	5
Cocconeis costata (Gregory)		X	
Cocconeis disculoides (Hustedt)		X	
Cocconeis disculus (Schuman) Cleve		X	5
Cocconeis grata (Schmidt)		X	
Cocconeis neodiminuta (Krammer)			5
Cocconeis placentula (Ehrenberg)		X	4
Cocconeis pseudomarginata (Gregory)		X	
Cocconeis schmidtii (Cleve-Euler)		X	5
Cocconeis scutellum (Ehrenberg)	X	X	3
Cocconeis scutellum var. parva (Ehrenberg)			3
Cocconeis stauroneiformis (Smith) Okuno		X	
Coscinodiscus marginatus (Ehrenberg)			2
Coscinodiscus radiatus (Ehrenberg)			2
Coscinodiscus sp.			2
Coscinodiscus concinnus (Smith)			2
Coscinodiscus curvatulus (Grunow in Schmidt)		X	
Coscinodiscus marginatus (Ehrenberg)		X	
Coscinodiscus obscurus (Schmidt)		X	
Coscinodiscus oculus-iridis (Ehrenberg)		X	
Coscinodiscus radiatus (Ehrenberg)	X	X	
Coscinodiscus rothii (Ehrenberg) Grunow		X	
Cyclotella atomus (Hustedt)		X	4
Cyclotella bodanica (Eulenstein in Grunow)		X	
Cyclotella choctawatcheeana (Prasad)		X	5
Cyclotella comta (Ehrenberg) Kützing		X	
Cyclotella gamma (Sovereign)		X	
Cyclotella glomerata (Bachmann)		X	4
Cyclotella kurdica (Håkanson)		X	
Cyclotella meneghiana (Kützing)		X	
Cyclotella ocellata (Pantocsek)		X	
Cyclotella striata (Kützing) Grunow in Cleve et Grunow	X	X	5
Cymatosira belgica (Grunow in van Heurck)	X	X	3
Cymbella affinis (Kützing)		X	
Delphineis surirella (Ehrenberg) Andrews		X	3
Dimeregramma minor (Gregory) Ralfs in Pritchard		X	5
Diploneis bombus (Ehrenberg) Ehrenberg ex Cleve	X	X	5
Diploneis coffeaeformis (Cleve)		X	5
Diploneis constricta (Grunow) Cleve		X	5
Diploneis crabro (Ehrenberg) Ehrenberg ex Cleve		X	
Diploneis didyma (Ehrenberg) Cleve		X	5
Diploneis elliptica (Kützing) Cleve		X	

Diploneis incurvata var. dubia (Hustedt)		X	
Diploneis ovalis (Hilse) Cleve		X	
Diploneis smithii (Brébisson ex Smith) Cleve		X	5
Diploneis sp.	X	X	
Diploneis splendida (Gregory) Cleve			5
Diploneis spp.			5
Diploneis suborbicularis (Gregory) Cleve		X	5
Ditylum brightwellii (West) Grunow ex Van Heurck		X	
Epithemia adnata (Kützing) Rabenhorst		X	
Epithemia sp.	X	X	
Epithemia zebra (Ehrenberg) Kützing	X	X	
Eunotia pectinalis (Müller) Rabenhorst		X	
Eunotia sp.	X	X	
Eunotogramma laevis (Grunow in Van Heurck)		X	
Fallacia forcipata (Greville) Stickle et Mann	X	X	5
Fragilaria capucina (Desmazières)	X	X	
Frustulia amphipleuroides (Grunow in Cleve et Grunow) Cleve-Euler		X	
Glyphodesmis distans (Gregory) Grunow in Van Heurck		X	
Gomphonema angustum (Agardh)		X	
Gomphonema truncatum (Ehrenberg)		X	
Grammatophora hamulifera (Kützing)		X	5
Grammatophora marina (Lyngbye) Kützing	X	X	5
Grammatophora oceanica (Ehrenberg)	X	X	5
Grammatophora oceanica var. macilenta (Smith) Grunow		X	
Grammatophora sp.			5
Grammatophora undulata (Ehrenberg)		X	
Gyrosigma sp.	X		
Hantzchia amphioxys (Ehrenberg) Grunow		X	
Hyalodiscus scoticus (Kützing) Grunow			5
Leptocylindricus danicus (Cleve)	X	X	5
Leptocylindricus minimus (Gran)			5
Luticola mutica (Kützing) Mann		X	
Lyrella abrupta (Gregory) Mann		X	
Lyrella atlantica (Schmidt) Mann		X	5
Lyrella hennedyi (Smith) Stickle et Mann		X	
Martyana martyi (Héribaud) Round		X	4
Melosira ambigua (Grunow) Müller			4
Navicula cancellata (Donkin)		X	5
Navicula capitata (Ehrenberg)		X	
Navicula digitoradiata (Gregory) Ralfs in Pritchard		X	
Navicula directa (Smith) Ralfs in Pritchard		X	5
Navicula palpebralis (Brébisson ex Smith)		X	5
Navicula radiosa (Kützing)			4
Navicula salinarum (Grunow in Cleve et Grunow)		X	
Navicula sp.	X	X	
Nitzschia angularis (Smith)		X	
Nitzschia dissipata (Kützing) Grunow		X	
Nitzschia distans (Gregory)		X	

Nitzschia fasciculata (Grunow) Grunow in Van Heurck		X	
Nitzschia lanceolata (Smith)		X	
Nitzschia marina (Grunow) Cleve and Grunow		X	
Nitzschia prolongata (Hustedt)		X	
Nitzschia sigma (Kützing) Smith		X	
Nitzschia sp.		X	
Odontella aurita (Lyngbye) Agardh		X	5
Odontella regia (Schultze) Simonsen		X	
Opephora gemmata (Grunow) Hustedt		X	
Opephora marina (Gregory) Petit		X	5
Paralia sulcata (Ehrenberg) Cleve	X	X	1
Pinnularia borealis (Ehrenberg)		X	
Pinnularia intermedia (Lagerstedt) Cleve		X	
Pinnularia sp.	X		
Plagiogramma interruptum (Gregory) Ralfs in Pritchard		X	
Plagiogramma staurophorum (Gregory) Heiberg			5
Plagiotropis vitrea (Smith) Cleve	X		
Pleurosigma aestuarii (Brébisson ex Kützing) Smith			5
Pleurosigma angulatum (Quekett) Smith			5
Pleurosigma normanii (Ralfs in Pritchard)		X	
Pleurosigma salinarum (Grunow)			5
Pleurosigma sp.		X	5
Podosira stelligera (Bailey) Mann	X	X	1
Psammodictyon panduriforme (Gregory) Mann	X	X	5
Psammodiscus nitidus (Gregory) Round et Mann	X	X	
Pseudostaurosira brevistriata (Grunow in Van Heurck) Williams et Round		X	4
Rhabdonema adriaticum (Kützing)	X		
Rhaphoneis amphiceros (Ehrenberg) Ehrenberg			5
Rhizosolenia bergonii (Peragallo)		X	
Rhizosolenia hebetata forma semispina (Hensen) Gran		X	2
Rhizosolenia spp.		X	2
Rhizosolenia styliformis (Brightwell)		X	2
Rhopalodia gibba (Ehrenberg) Müller		X	
Rhopalodia musculus (Kützing) Müller			5
Roperia tessallata (Roper) Grunow in Van Heurck		X	5
Sellaphora bacillum (Ehrenberg) Mann		X	
Stauroneis phoenicenteron (Nitzsch) Ehrenberg		X	
Staurophora amphyoxis (Gregory) Mann		X	
Staurophora salina (Smith) Mereschkowsky		X	
Staurosira construens (Ehrenberg)	X	X	4
Staurosirella lapponica (Grunow in VanHeurck) Williams et Round	X		
Staurosirella leptostauron (Ehrenberg) Williams et Round			4
Stephanodiscus hantzchii (Grunow)	X	X	
Stephanodiscus rotula (Kützing) Hendey			4
Stephanopyxis turris (Greville et Arnott) Ralfs in Pritchard			5

Surirella fastuosa (Ehrenberg)	X	X	
Synedra rumpens (Kützing)		X	
Synedra sp.	X		
Synedra ulna (Nitzsch) Ehrenberg		X	
Tabellaria flocculosa (Roth) Kützing		X	
Tabularia investiens (Smith) Williams et Round		X	
Terpisinoë americana (Bailey) Ralfs in Pritchard	X		
Thalassionema frauenfeldi (Grunow) Hallegraeff		X	
Thalassionema nitzschioides (Grunow) Grunow ex Hustedt	X	X	2
Thalassiosira angulata (Gregory) Hasle		X	2
Thalassiosira diporocyclus (Hasle)		X	
Thalassiosira eccentrica (Ehrenberg) Cleve	X	X	2
Thalassiosira gravida (Cleve)			2
Thalassiosira lineata (Jousé)		X	2
Thalassiosira nordenskioeldii (Cleve)		X	2
Thalassiosira oestrupii (Ostenfeld) Hasle	X	X	2
Thalassiosira sp.	X	X	
Thalassiosira subtilis (Ostenfeld) Gran			2
Thalassiosira symmetrica (Fryxell et Hasle)		X	2
Thalassiosira tenera (Proschkina-Lavrenko)		X	
Thalassiosira weissflogii (Grunow) Fryxell et Hasle			2
Trachyneis aspera (Ehrenberg) Cleve	X	X	5
Trachysphenia australis (Petit in Folin et Perier)		X	5
Triceratium alternans (Bailey)	X	X	5
Tryblionella acuminata (Smith)		X	
Tryblionella granulata (Grunow) Mann		X	
Frustulia amphipleuroides (Grunow in Cleve et Grunow) Cleve-Euler		X	
Tryblionella navicularis (Brébisson ex Kützing) Ralfs in Pritchard	X	X	5
Tryblionella punctata (Smith)		X	5

For core GeoB6003-2:
1: Diatoms preferring saltier water and related to the Jutland current
2: Oceanic planktonic species (included in the group of saltier water related to the Jutland current)
3: Diatoms related to less saline water and to the eastern part of the Skagerrak
4: Fresh water diatoms (included in the group of less saline water species occurring in the eastern part of the Skagerrak)
5**:** Other diatoms species

CHAPTER 7:

Late Holocene coastal hydrographic and climate changes in the eastern North Sea

Hebbeln, D., Knudsen, K. L., Gyllencreutz, R., Kristensen, Klitgaard-Kristensen, Backman, J., Scheurle, C., Jiang, H., Gil, I., Smelror, Jones, P., Sejrup, H.

The Holocene (in press)

Late Holocene coastal hydrographic and climate changes in the eastern North Sea

Dierk Hebbeln[1], Karen-Luise Knudsen[2], Richard Gyllencreutz [3*], Peter Kristensen[2], Dorthe Klitgaard-Kristensen[4], Jan Backman[3], Carolyn Scheurle[1], Hui Jiang[5], Isabelle Gil[6], Morten Smelror[7], Phil Jones[8] and Hans-Petter Sejrup[9]

[1] Geowissenschaften, Universität Bremen, 28359 Bremen, Germany
[2] Department of Earth Sciences, University of Aarhus, 8000 Århus C, Denmark
[3] Department of Geology and Geochemistry, Stockholm University, 10691 Stockholm, Sweden
[4] Norwegian Polar Institute, 9296 Tromsø, Norway
[5] State Key Laboratory of Estuarine and Coastal Research, East China Normal University, 200062 Shanghai, P.R. China
[6] Marine Geology Department, National Institute of Engineering, Technology and Innovation, 2721-866 Alfragide, Portugal
[7] Geological Survey of Norway, 7491 Trondheim, Norway
[8] Climate Research Unit, University of East Anglia, Norwich NR4 7TJ, United Kingdom
[9] Department of Earth Sciences, University of Bergen, 5007 Bergen, Norway

Abstract

Here we present a high-resolution paleoenvironmental reconstruction covering the Late Holocene from the Skagerrak and other sites in the North Sea area. The data, which are based on the analyses of marine sediment cores, reveal a marked environmental shift taking place between AD 700 and AD 1100 with the most pronounced changes occurring at AD 900. Due to an enhanced advection of Atlantic waters to the North Sea at that time marking the beginning of the Medieval Warm Period (MWP) both surface and bottom waters in the Skagerrak were subject to major circulation and productivity changes. Especially the observed increase in bottom current strength is remarkable as there is hardly any comparable signal in the older part of the record going back to 1000 BC. At the turn to the Little Ice Age (LIA) the bottom current strength remains at a high level, now probably forced by the atmospheric circulation. Thus, as these two consecutive climate scenarios, despite opposite temperature forcing, are apparently able to generate distinctly stronger bottom currents in the Skagerrak than observed in the preceding 2000 years, it might be the strength of the climatic forcing playing a decisive role in shaping the marine environment. Indeed, both the MWP and the LIA are reported as strong climatic signals in northwest Europe, being the warmest (except the late 20th century) and coldest periods, respectively, during at least the last 2000 years.

Keywords: Late Holocene, climate variability, paleoceanography, stable isotopes, benthic foraminifera, grain sizes, North Sea, Skagerrak

Introduction

The assessment of future responses of the Earth's climate system to anthropogenic forcing is most severely inhibited by inadequate understanding of natural climate variability. The latter can be investigated on a number of different time scales reaching e.g., from glacial/interglacial changes, driven by orbital forcing (Imbrie *et al.*, 1984), to decadal variability, as expressed in the North Atlantic Oscillation (Marshall *et al.*, 2001; Hurrell, 1995). An important time frame in this context is the Late Holocene spanning the last approximately 2000 years during which human societies evolved at an ever increasing pace. Besides being affected by significant natural climate variability during this period, humans also started to change their environment, first on local, later on regional and finally on global scales.

The expression of climate change over the past millennia has been a matter of discussion for long time (see e.g., compilations in Jones *et al.*, 2001, and Jones and Mann, 2004). The most often cited and probably most extreme among several explicitly described climate epochs are the relatively warm Medieval Warm Period (MWP) followed by the relatively cold Little Ice Age (LIA). There is an ongoing discussion about the overall nature of these periods and about their global or only regional expression (e.g., Hughes and Diaz, 1994; Jones and Mann, 2004). However, there is some evidence from northern and central Europe for on average warmer conditions during the MWP followed by colder conditions during the LIA (e.g., Grove, 2002; Jones and Mann, 2004), and it appears that these two epochs were the warmest (despite the second half of the 20th century), respectively the coldest periods in the Northern Hemisphere through the last two millennia (Jones and Mann, 2004). Both epochs have been variously dated and, being aware that there are large regional differences in the expression of these epochs (e.g., Huntley *et al.*, 2002), here we use the ranges of AD 800 to AD 1400 and AD 1400 to AD 1900 given by Jones and Mann (2004) to describe periods of generally warmer respectively colder conditions in the Northern Hemisphere. Without adding to the discussion about the overall nature and expression of these climatic epochs, the terms MWP and LIA are used here as they are useful and convenient terms to describe these two intervals characterised by particular patterns of their climatic conditions (Huntley *et al.*, 2002).

Climate variability over the past millennia has been convincingly demonstrated using documentary evidence and historical data, together with terrestrial proxies, notably tree rings, lake records, ice-cores and speleothem, as well as marine proxies. However, marine records

providing a temporal resolution high enough to allow detailed reconstructions of the paleoenvironment over the last 2000 years are scarce, due to the fact that in open marine settings sedimentation rates are mostly too low whereas in shelf settings continuous sedimentation mostly is restricted to very few locations. Nevertheless, such locations exist and, in contrast to open marine records, they bear the potential to provide detailed records (decadal time resolution or better) of both the marine and the terrestrial paleoenvironment.

The North Atlantic plays an important role in the Earth's climate system and, consequently, is a prime target for the reconstruction of Late Holocene paleoenvironments. In this region, a crucial site to study the interaction of the open marine and the more continental setting is the Skagerrak (Figure 1), where the Baltic Sea is connected to the North Sea and, finally, to the North Atlantic. There, almost unaltered North Atlantic as well as modified North Sea waters meet relatively fresh Baltic Sea outflow waters (Rodhe, 1998; Longva and Thorsnes, 1997) strongly affected by precipitation in northern Europe. Most of the sediment load from all these water masses is eventually deposited in the Skagerrak, making this basin the major sink for fine-grained sediments in the North Sea region (Longva and Thorsnes, 1997). Due to the complex circulation system of the North Sea, sedimentary records of environmental changes may be differently manifested in different parts of this area, thus, paleoenvironmental studies of these marine records requires regional consideration. Some paleoenvironmental reconstructions from the Skagerrak covering the last ~2000 years exist (Hass, 1996; Nordberg, 1991) and provide detailed information on specific topics and/or sites. Here, we follow a regional multi-proxy approach focusing on high-resolution marine records from the Skagerrak, but also including data from the Norwegian continental slope and from the southern North Sea. The aim is to reconstruct the interrelationships between climate forcing, oceanic circulation and terrestrial response in this part of the critical North Atlantic region prior to significant anthropogenic forcing of the environment.

Regional settings

The modern circulation pattern in the North Sea is mainly driven by the inflow of Atlantic waters between Scotland and Norway (Figure 1). This inflow stimulates a counter-clockwise circulation in the North Sea, with parts of the Atlantic water following the depth contours in the northern North Sea, namely as the Tampen Bank Current (TBC) and the Southern Trench Current (STC) (Rodhe, 1998). Part of the Atlantic water flows around the entire North Sea, where its properties are modified e.g., by freshwater supplied by numerous large rivers such as e.g., the Thames, Rhine, Elbe, and Weser. Finally, this modified North Sea water runs up the Danish coast as the South Jutland Current (SJC) and continues as the North Jutland Current (NJC) into the Skagerrak. In the eastern Skagerrak, the North Jutland Current and Southern Trench Current waters are supplemented by less saline Baltic outflow water, the Baltic Current (BC). These combined waters turn towards northwest and west and form the Norwegian Coastal Current (NCC), which continues northward along the Norwegian coast (Rodhe, 1998; Longva and Thorsnes, 1997) (Figure 1).

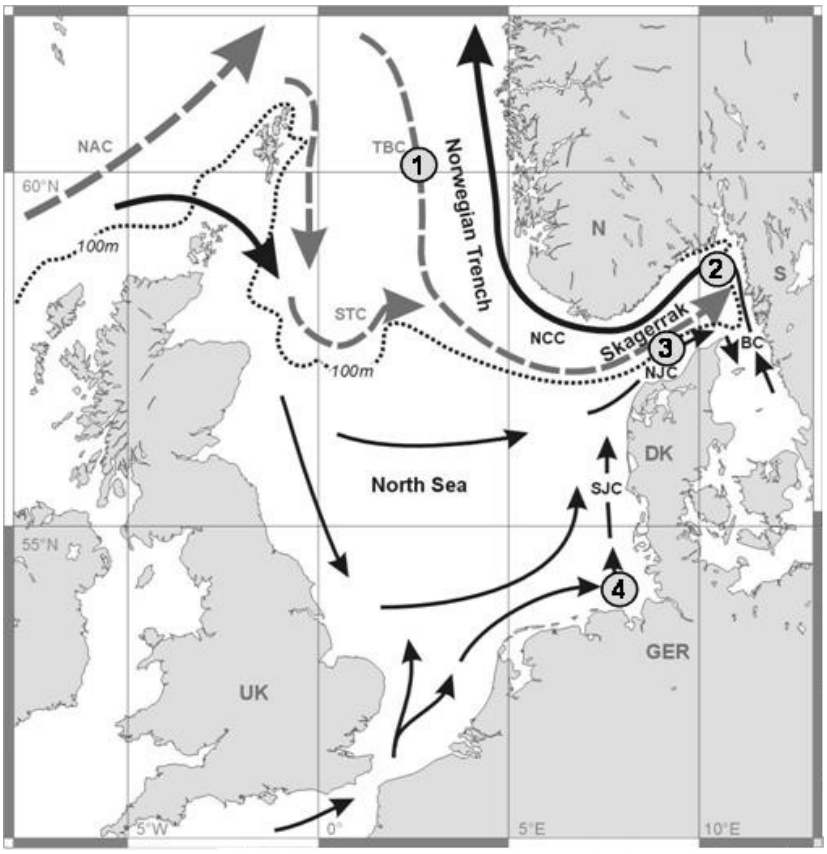

Figure 1 Selected core locations for this study: (1) HM115-16 from the Norwegian margin, (2) MD99-2286 and (3) GeoB 6003-2 from the Skagerrak, and (4) GeoB 4801-1 from the Helgoland mud area. The map also shows a general circulation pattern for the North Sea with the major currents abbreviated as NAC – Norwegian Atlantic Current, STC – Southern Trench Current, TBC – Tampen Bank Current, SJC – South Jutland Current, NJC – North Jutland Current, BC – Baltic Current, and NCC – Norwegian Coastal Current. Modified from Danielssen *et al.* (1991) and Nordberg (1991)

This North Sea circulation pattern is also related to the large scale atmospheric circulation system. For example, strong westerly winds enhance the currents, whereas easterly wind directions hamper the water mass circulation (Dooley and Furnes, 1981). This is even more obvious for the Skagerrak, where (i) the strength of the South Jutland Current, and thus the supply of sediment-laden North Sea waters, is largely dependent on the regional wind stress over the southern North Sea (Rodhe, 1996), and where (ii) also the bottom current velocities respond to changing wind fields (Longva and Thorsnes, 1997). Thus, the atmospheric forcing also plays an important role in the dynamics of the North Sea.

The shallow North Sea (on average <100 m water depth, Figure 1) is characterised by high tidal and wave energy levels and consequently, continuous sediment redistribution is a dominant process. There are only a few depo-centers where sustained sediment deposition, the precondition for any meaningful paleoenvironmental reconstruction, occurs (Lohse *et al.*, 1995). Among these, the Skagerrak with a maximum depth of about 700 m is the most important depo-center in the entire North Sea and its sediment sequences have been used for many paleoenvironmental studies (e.g., Stabell and Thiede, 1985; Nordberg, 1991; van Weering *et al.*, 1993; Conradsen and Heier-Nielsen, 1995; Knudsen *et al.*, 1996), however, with only a few focusing on the Late Holocene (e.g., Hass, 1993, 1996).

The current system in the Skagerrak forms an anticlockwise circulation pattern that is part of the North Sea circulation pattern as described above. Both the surface and bottom currents in the Skagerrak generally follow this pattern, however, with lower bottom current velocities compared to the surface waters (Dahl, 1978; Qvale and Van Weering, 1985; Rodhe, 1987). Most of the bottom waters are of North Atlantic origin with only a minor contribution of dense winter water formed in the shallow northern North Sea during very cold winters (Ljøen and Svansson, 1972). In general, the highest bottom current velocities occur on the convex southern slope of the Skagerrak (Rodhe, 1987), to which the inflowing water masses are constrained.

A second, but less important depo-center in the North Sea is the Helgoland mud area in the German Bight (von Haugwitz *et al.*, 1988). Its potential as an archive for paleoenvironmental reconstructions has been proved by Hebbeln *et al.* (2003) and Scheurle *et al.* (2005).

Material and methods

This study focuses on the Skagerrak in the NE North Sea with two strategically chosen sediment core sites, one in the southern Skagerrak (GeoB 6003-2) reflecting merely the advection of Atlantic waters to the area, and one in the north-eastern Skagerrak (MD99-2286) situated in the path of the Baltic outflow (Figure 1, Table 1). Additional information is taken from core sites in the German Bight (GeoB 4801-1) and at the Norwegian margin (HM115-16) (Figure 1, Table 1).

Core	Latitude	Longitude	Water Depth	Reference
GeoB 4801-1	54°06.7´N	08°02.2´E	25 m	1
GeoB 6003-2	57°58.3´N	09°23.2´E	312 m	2
HM115-16	60°52.0´N	03°44.0´E	338 m	3
MD99-2286	58°43.8´N	10°12.3´E	225 m	4

Table 1 Overview about the sediment cores used for this study. References: (1) Hebbeln *et al.* (2003), (2) Scheurle (2004), (3) Klitgaard-Kristensen *et al.* (unpublished), (4) Gyllencreutz *et al.* (2005).

Most analyses concentrated on the two cores from the Skagerrak. Core GeoB 6003-2 was analysed for its chemical composition using the Bremen X-ray fluorescence (XRF) Core Scanner, which allows a semi-quantitative determination of the contents of major and minor elements by scanning split sediment cores in a non-destructive way (e.g., Jansen *et al.*, 1998; Röhl *et al.*, 2000). Here we use Ca and K contents measured in 1 cm resolution. The semi-quantitative data (given in *counts per second*) are displayed here as the Ca/K ratio and used as an indicator for the composition of the sediments. Whereas Ca is often used as a proxy for the content of biogenic carbonate (e.g., foraminifera, coccoliths, see e.g., Jennerjahn *et al.*, 2004), K can be used as a proxy for its main mineralogical carrier illite (e.g., Kuhlmann *et al.*, 2004).

Diatom preparation and counting were conducted following standard procedures as described by Battarbee (1973), Schrader and Gersonde (1978), Fenner (1981) and Abrantes (1988). For both cores in the Skagerrak the summer sea surface salinity (SSS) has been reconstructed based on diatom transfer functions that rely on a diatom-environmental variable dataset from the Skagerrak-Kattegat showing that the distribution of the surface sediment diatom assemblages is clearly correlated with modern environmental parameters, especially with the summer SSS (Jiang, 1996). For our reconstructions, an extended dataset with additional samples from the northern part of the Skagerrak and from the Baltic Sea has

been used (Jiang, unpubl. data). In addition, for core GeoB 6003-2, also the diatom accumulation rate has been calculated as valves per cm^{-2} yr^{-1}, according to Abrantes (1988).

For grain-size analyses, the sediment samples were wet-sieved over a 63 μm sieve. For core MD99-2286 more detailed analyses were performed on the untreated fine fraction (1-63 μm) using the sedigraph technique, as described in detail for this core by Gyllencreutz (2005). Organic carbon and carbonate were not removed from the samples, but their contents were measured. No significant correlation was found between the grain-size parameters discussed here and carbonate content (Gyllencreutz, 2005) or organic carbon content (Gyllencreutz, unpubl.data).Shown here is the median of the sortable silt fraction (10-63 μm), which according to McCave *et al.* (1995) can be used as a proxy for relative bottom current speed.

In order to obtain the best possible comparison with previous foraminiferal analyses in the area, the samples were sieved over a 100 μm sieve, and foraminifera in the size fraction >100 μm were concentrated using the heavy liquid CCl_4 ($\rho = 1.59$ g/cm^3) as described by Meldgaard and Knudsen (1979). Calcareous benthic foraminifera, which were generally well preserved, form the major part of the fauna. The planktic foraminifera fauna consists of small-sized specimens of only a few species. Where possible, at least 300 specimens of benthic calcareous foraminifera were identified and counted in each sample. Only the most interesting species with respect to the paleoenvironment in the Skagerrak are discussed here. The accumulation rates (or fluxes) of all benthic and planktic foraminifera are calculated from the total number of individuals >100 μm per gram sediment, the dry bulk density of the sediment and the estimated sedimentation rates.

Stable oxygen ($\delta^{18}O$) and carbon ($\delta^{13}C$) isotopes have been analysed on all the cores listed in Table 2. The measurements of benthic as well as planktic foraminifera shells have been conducted in the laboratories in Bergen, Bremen, and Stockholm following standard procedures described elsewhere (e.g., Klitgaard-Kristensen *et al.*, 2001; Scheurle and Hebbeln, 2003). The basic parameters of the analyses discussed here are summarised in Table 2. The use of different species of benthic foraminifera is linked to the different settings of the investigated cores ranging from very shallow habitats (e.g., 25 m water depth for core GeoB 4801-1) via a basin setting in the Skagerrak (cores GeoB 6003-2 and MD99-2286) to an open slope setting along the Norwegian margin (core HM115-16) resulting in very different benthic foraminiferal assemblages.

Core	Species	No. of tests	Size	Lab	Reference
GeoB 4801-1	*Elphidium excavatum f. selseyensis*	10-20	>150 µm	Bremen	5,6
GeoB 6003-2	*Globigerinita uvula*	~150	>100 µm	Bremen	2
GeoB 6003-2	*Melonis barleeanus*	10-20	>100 µm	Bremen	2
HM115-16	*Uvigerina mediterranea*	1-2	>125µm	Bergen	3
MD99-2286	*Melonis barleeanus*	3-8	>100 µm	Stockholm	4

Table 2 Overview of the stable isotope analyses carried out for this study. Analytical standard deviations for these measurements are about ±0.07‰ PDB for $\delta^{18}O$ and ±0.06‰ PDB for $\delta^{13}C$ for the three Isotope Laboratories at the Bremen, Bergen and Stockholm Universities). References: (2) Scheurle (2004), (3) Klitgaard-Kristensen *et al.* (unpublished), (4) Knudsen *et al.* (unpublished), (5) Scheurle and Hebbeln (2003), (6) Scheurle *et al.* (2005).

Furthermore, for the Norwegian margin core (HM115-16) sea surface temperature (SST) and salinity (SSS) reconstructions have been carried out using dinoflagellate transfer functions (Smelror *et al.*, unpubl. data). This reconstruction is based on the dinoflagellate database consisting of 439 samples from the North Atlantic compiled by Rochon *et al.* (1999). WAPLS (Weighted Average Partial Least Square) in the software program C2 (http://www.campus.ncl.ac.uk/staff/Stephen.Juggins/software) has been used as the statistical method combining sea surface salinity and temperature for both February and August. Statistically, the August salinity and surface temperature presented here have error estimates of 1.9 psu and 2.7°C degrees. We are aware that the amplitudes of the reconstructed salinity and temperature changes in the dinoflagellate record are within the same range as the error estimates from the transfer function calculations, hence it seems that no significant changes can be extracted from the record. However, the large error estimates may be related to the transfer function method. One issue that could explain this is the database used (Rochon *et al.*, 1999) that only has a low density of samples from our study region and thereby lacks good analogues. Improving the database with better coverage from the North Sea region probably would enhance the statistical performance. Nevertheless, as the data reveal a clearly structured record through time that also fits to e.g., the benthic $\delta^{18}O$ record of the same core, we are confident, that the SST and SSS data can be used as indicators for past water mass variability off Norway.

Age models

The age models of the cores used here are principally based on AMS ^{14}C as well as ^{210}Pb analyses. Some of these have already been published (GeoB 4801-1: Hebbeln *et al.*, 2003; MD99-2286: Gyllencreutz, 2005). For the other cores, the ^{210}Pb-based age estimates were obtained by measuring the ^{210}Pb activity via it's α-particles emitting grand daughter ^{210}Po, following the method described by Van Weering *et al.* (1987). The AMS ^{14}C datings were made at the Leibniz Laboratory for Age Determinations and Isotope Research at the University of Kiel (Nadeau *et al.*, 1997) and at the Poznań Radiocarbon Laboratory at the Adam Mickiewicz University in Poland (Table 3). The ^{14}C ages of core HM115-16 were calibrated by using CALIB vers. 5.0 (based on marine INTCAL04 (Hughen *et al.*, 2004)), whereas for the dates from core GeoB 6003-2 the CALIB4 programme (Stuiver *et al*., 1998), applying the marine model calibration curve has been used. For all ^{14}C ages a marine reservoir age of 400 years has been used as described for Danish waters by Heier-Nielsen *et al.* (1995).

Core depth (cm)	Lab. ident.	Material	^{14}C ages (BP)	Err. (+/-)	Reservoir corrected ages (BP)	Calibrated ages (cal yr BP)	Min/Max range; 1σ	$\delta^{13}C$
GeoB 6003-2								
283	KIA 18238	mix. benth. for.	2400	35	2000	2020	+53/-40	-9.8
343	KIA 18236	mix. benth. for.	2690	30	2290	2345	+22/-14	-2.6
403	KIA 13694	mix. benth. for.	2875	30	2475	2692	+15/-30	0.1
446	KIA 18926	shell fragment	3190	30	2790	2968	+55/-34	+1.1
HM 115-16 BC								
18.9–19.8	Poz-6403	*N. pachy*. (dex.)	1150	150	750	690	95/-180	
20.4–21.6	KIA 20091	*N. pachy*. (dex.)	1005	30	605	585	+35/-35	-0.32
28.2-29.1	Poz-6404	*N. pachy*. (dex.)	990	30	590	580	+40/-35	
35.7-36.6	KIA 20092	*N. pachy*. (dex.)	1115	30	715	665	+25/-35	-3.72
HM 115-16 GC								
18-19	Poz-6405	*N. pachy*. (dex.)	1040	35	640	630	+40/-20	
39-42.5	Poz-6487	*N. pachy*. (dex.)	2035	45	1635	1600	+60/-70	

Table 3 AMS ^{14}C dates for the cores GeoB 6003-2 from the southern Skagerrak and HM115-16BC and HM115-16GC from the Norwegian margin. The measurements made in Kiel (KIA) and in Poznań (Poz) are based on samples consisting of mixed benthic foraminifera (mix. benth. for.), of shell fragments or of monospecific assemblages of the planktic foraminifera *Neogloboquadrina pachyderma* (dextral).

The ^{210}Pb activity in the upper 40 cm of core GeoB 6003-2 decreases significantly downcore, enabling an estimation of the sedimentation rate (1.8 mm/yr) for the last ~200 years characterised by rather unconsolidated sediments. (Figure 2). Further downcore the

AMS ^{14}C dates obtained between 283 cm and 446 cm core depth line up nicely and indicate a constant sedimentation rate of ~1.65 mm/year. The extrapolation of the sedimentation rate of 1.65 mm/yr towards the core top points to a decrease in sedimentation rate in the younger part of the core, as the ^{210}Pb data indicating recent sediments at the core top exclude a core top hiatus. The presumed drop in sedimentation rate has been aligned with a significant increase in coarse fraction (>63 µm wt.-%) in 135 cm core depth (Figure 2). This increase is interpreted as an indicator for the enhancement of bottom currents resulting in enhanced winnowing and, thus, in a lower sedimentation rate. Consequently, from this level, with an extrapolated age of *c*. 1050 cal yr BP, towards the core top a lower sedimentation rate of 1.2 mm/yr has been estimated.

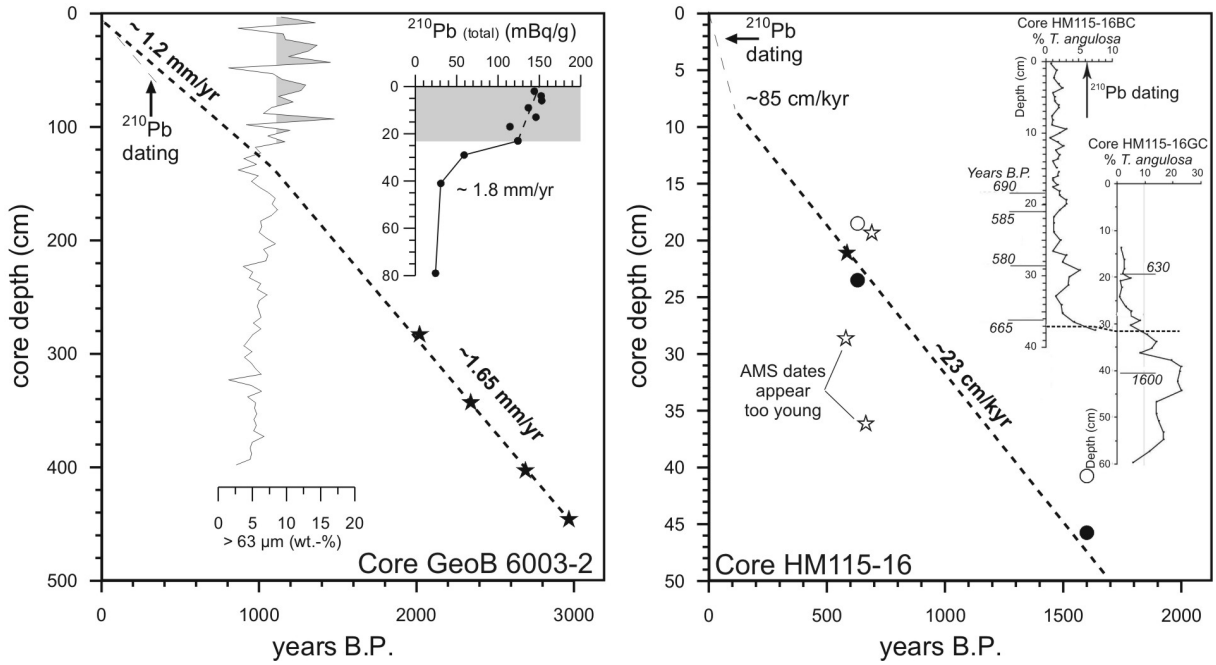

Figure 2 Left panel: Age model for core GeoB 6003-2 from the southern Skagerrak. The inset in the upper right shows the ^{210}Pb data versus core depth. The shading in the upper ~20 cm indicates the mixed layer at the surface. The decrease in ^{210}Pb further downcore indicates a sedimentation rate of ~1.8 mm/yr. The stars indicate the AMS ^{14}C dates obtained for the lower part of the investigated section that line up resulting in a sedimentation rate of ~1.65 mm/yr. The increase in the >63 µm fraction at ~135 cm core depth is assumed to mark a decrease in sedimentation rate. Right panel: Age model for core HM115-16 from the Norwegian margin. The inset in the upper right shows the *Trifarina angulosa* records in both, the box core (BC) and the gravity core (GC) from this site, used for correlation. The marked decrease in *T. angulosa* at 37 cm core depth in the BC and at 32 cm in the GC points to a depth offset of 5 cm, probably due to coring disturbance in the course of the gravity corer deployment. The AMS 14 dates are marked by stars for the BC and by circles for the GC. The open circles indicate the original data whereas the filled circles represent the GC dates shifted by 5 cm to align with the BC dates to the same depth scale. The final age model is based on linear interpolation using the filled circles and the filled star (see text).

The chronology of site HM115-16 is based on a combination of the box core HM115-16BC and the gravity core HM115-16GC (Table 3). In core HM115-16BC, it is clear that the four AMS radiocarbon dates overlap by one standard deviation making any stratigraphic interpretation difficult. In core HM115-16GC, the two AMS ^{14}C dates point to a sedimentation rate of ~23 cm/kyr. The two cores have been correlated by the relative abundance of the benthic foraminifera *Trifarina angulosa* (Figure 2). The change in the relative abundance of *T. angulosa* at 37 cm in HM115-16BC is regarded similar to the change at 32 cm in HM115-16GC. Considering an offset in core depth of 5 cm between the box core and the gravity core, it appears that the AMS dates in the gravity core line up with the AMS date at 21 cm core depth in the box core (Figure 2) resulting in an average sedimentation rate of ~23 cm/kyr for both cores. Only for the very core top of the box core, higher sedimentation rates of ~85 cm/kyr are estimated based on ^{210}Pb dating for these rather unconsolidated sediments. This interpretation requires exclusion of the remaining AMS dates in the box bore, with the upper one being too old and the two lowermost dates being too young. Whereas the 18 cm date has a high standard deviation due to a small sample size, it is not clear what might have caused the seemingly too young ages for the dates at 29 cm and 36 cm core depth. However, the similar pattern of the *T. angulosa* record, found also in other near-by cores (Klitgaard-Kristensen *et al.*, 2001), strongly supports the age model adopted here.

Results and discussion

Surface water conditions in the Skagerrak

Sea surface salinity (SSS) reconstructions from the southern Skagerrak show a trend towards decreasing SSS through the last 2000 years (Figure 3), although the record is incomplete due to two core sections marked by strong diatom dissolution prohibiting a meaningful interpretation of the diatom data. In this record the trend towards lower SSS is punctuated by a step at *c.* AD 900. Before this change the SSS in the southern Skagerrak was on average 2 psu higher compared to the north-eastern site, while afterwards at both sites SSS varied around a similar level of 28.5 to 29 psu. In the north-eastern Skagerrak, the salinity remained basically on a stable level of ~28.5 psu through the last 2000 years. However, two events marked by very low SSS (AD 1000 to AD 1200 and AD 1400 to AD 1520) are recorded and most likely reflect enhanced outflow of low saline Baltic Sea water.

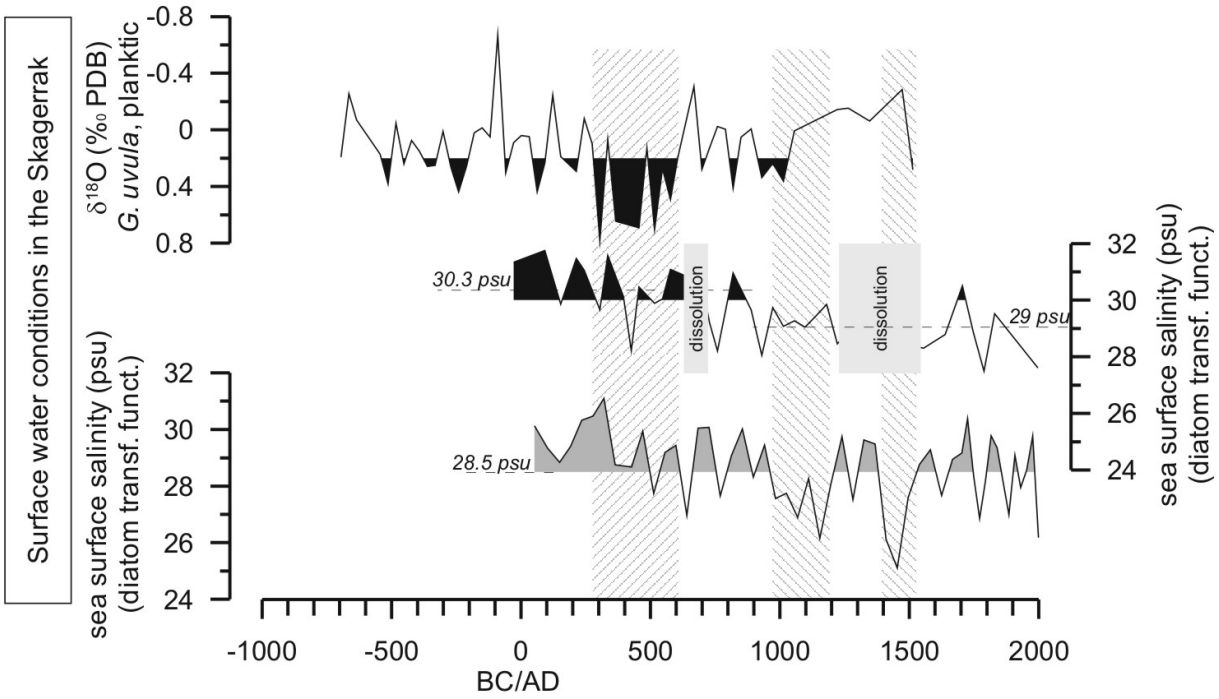

Figure 3 Proxies for the surface water conditions in the Skagerrak through the last 3000 years. Black curves display data from core GeoB 6003-2 in the southern and grey curves from core MD99-2286 in the north-eastern Skagerrak. Hatched fields mark periods discussed in the text.

The stable oxygen isotope ($\delta^{18}O$) data measured on planktic foraminifera are also linked to SSS, but in addition they depend on sea surface temperatures (SST). At site GeoB 6003-2 the $\delta^{18}O$ record obtained on the planktic foraminifera species *G. uvula* (Ehrenberg) shows rather heavy values (i.e., high SSS and/or low SST) between AD 300 and AD 600 (Figure 3). As the diatom based SSS reconstructions do not indicate higher salinities, the high $\delta^{18}O$ data probably point to lower SSTs during this interval. This is in principal agreement with an alkenone-based SST record from the southern Skagerrak indicating a slight cooling (0.7°C) slightly later at AD 500 (Emeis *et al.*, 2003). After AD 1000, light isotope data parallel the lowered SSS obtained from the diatom transfer functions and, thus, support these data. However, only a few data points are available for this period as the number of planktic foraminifera in the core became too low to allow any $\delta^{18}O$ measurements. Interestingly, very low amounts of planktic foraminifera in core MD99-2286 prevented any such measurements at this site. As planktic foraminifera are sensitive to salinity, it appears that in the Skagerrak planktic foraminifera cannot thrive any longer at salinities below ~30 psu (e.g., Johannesen *et al.*, 1994). The data imply that such conditions prevailed in the north-eastern Skagerrak at least through the last 2000 years and in the southern Skagerrak since AD 1000.

Paleoproductivity in the Skagerrak

The paleoproductivity can be assessed by qualitative (e.g., stable carbon isotopes, $\delta^{13}C$) as well as by quantitative (e.g., flux rates) proxies. In the southern Skagerrak the $\delta^{13}C$ data of planktic as well as benthic foraminifera show a coherent pattern pointing to a significant long-term decrease in productivity as indicated by increasing $\delta^{13}C$ values between AD 700 and AD 1500 with the most significant changes occurring between AD 700 and AD 900. In contrast, in the north-eastern Skagerrak the available benthic $\delta^{13}C$ data display relatively little variability (Figure 4). However, at both sites the flux rates of benthic foraminifera show a marked drop, also between AD 700 and AD 900 with a subsequent increase back to higher values at AD 1700. The diatom flux rates available for the southern Skagerrak also reveal a long-term trend towards lower fluxes. Also the planktic foraminifera flux mainly shows a long-term decrease. However, this might rather reflect a salinity effect than represent a paleoproductivity signal (see above). In all flux records (and partly also in the $\delta^{13}C$ data) there are two events marked by a sudden decrease in paleoproductivity. These events occurred between 300 BC and 100 BC and around AD 400.

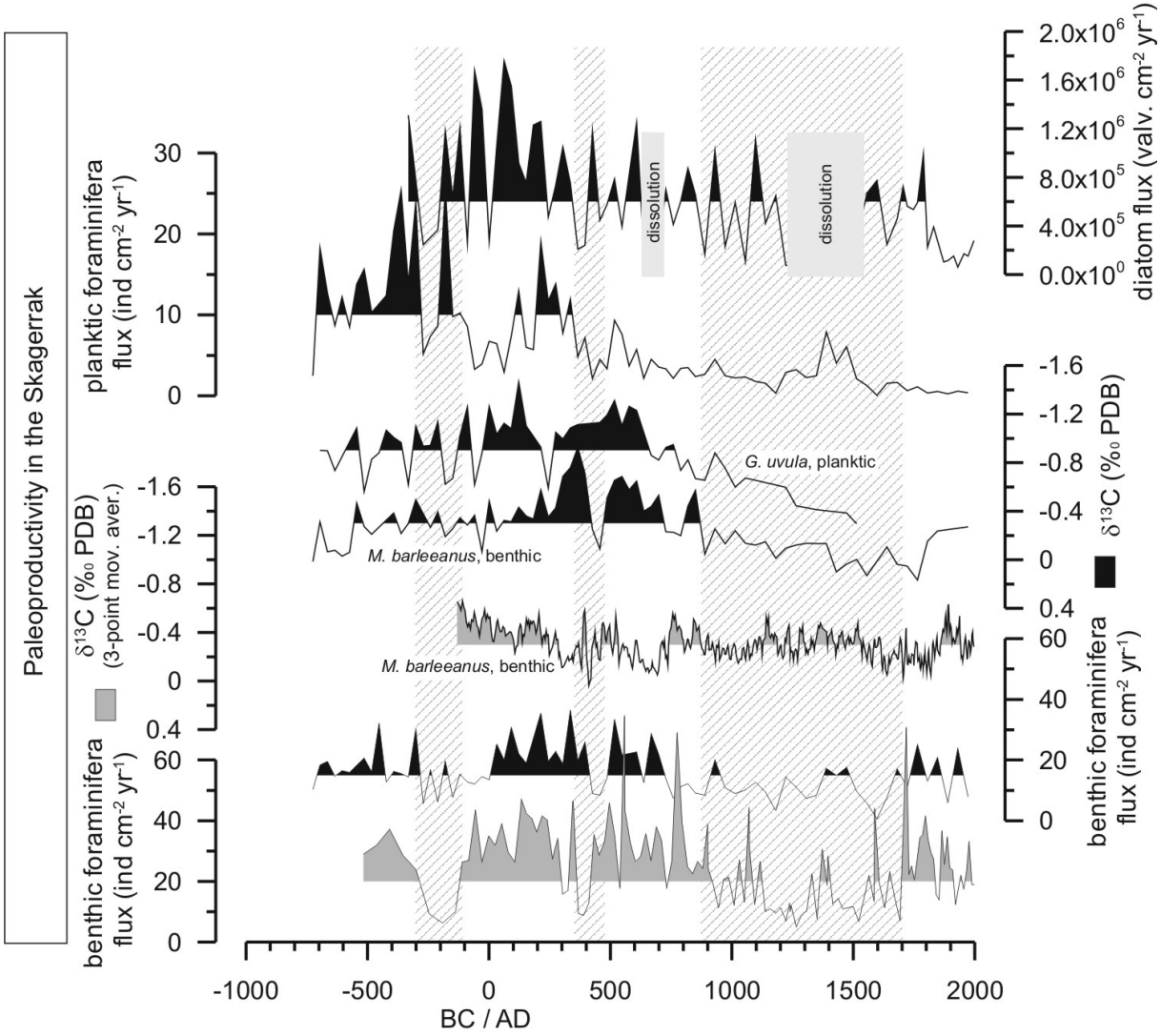

Figure 4 Proxies for the paleoproductivity in the Skagerrak through the last 3000 years. Black curves display data from core GeoB 6003-2 in the southern and grey curves from core MD99-2286 in the north-eastern Skagerrak. At both sites the benthic $\delta^{13}C$ data are obtained on *M. barleeanus*. Hatched fields mark periods discussed in the text.

Bottom water conditions in the Skagerrak

Grain-size distributions and the composition of the sediments can provide information about the environmental setting at the sea floor with the strength of the prevailing bottom currents often leaving the most significant impact. Analyses of the sortable silt fraction in the north-eastern Skagerrak core MD99-2286 reveal a clear step towards a coarser median of the sortable silt at AD 600 (Figure 5) which is accompanied by short-term maxima in the content of the >63 µm fraction. After AD 600, the sortable silt median stays almost continuously at a high level, while the sand content (>63 µm) reaches almost persistently higher values only after AD 900. Enhanced bottom current strength in the younger part of the record at this site, as indicated by the coarser sediments, is in agreement with data from the southern Skagerrak, also showing significantly increased percentages of the >63 µm fraction after AD 1000. At

that site, the coarsening of the sediments comes along with a shift in composition, exemplified by increasing Ca/K elemental ratios, which are supposed to reflect changes in the composition of the sediments, as e.g., a decrease in very fine grained K-rich clay minerals after AD 900-1000. Also these data sets indicate short events prior to the major paleoenvironmental shift around AD 900. At around 200 BC and between AD 600 and AD 750 at both sites there are indications for short-term enhancements of the bottom currents.

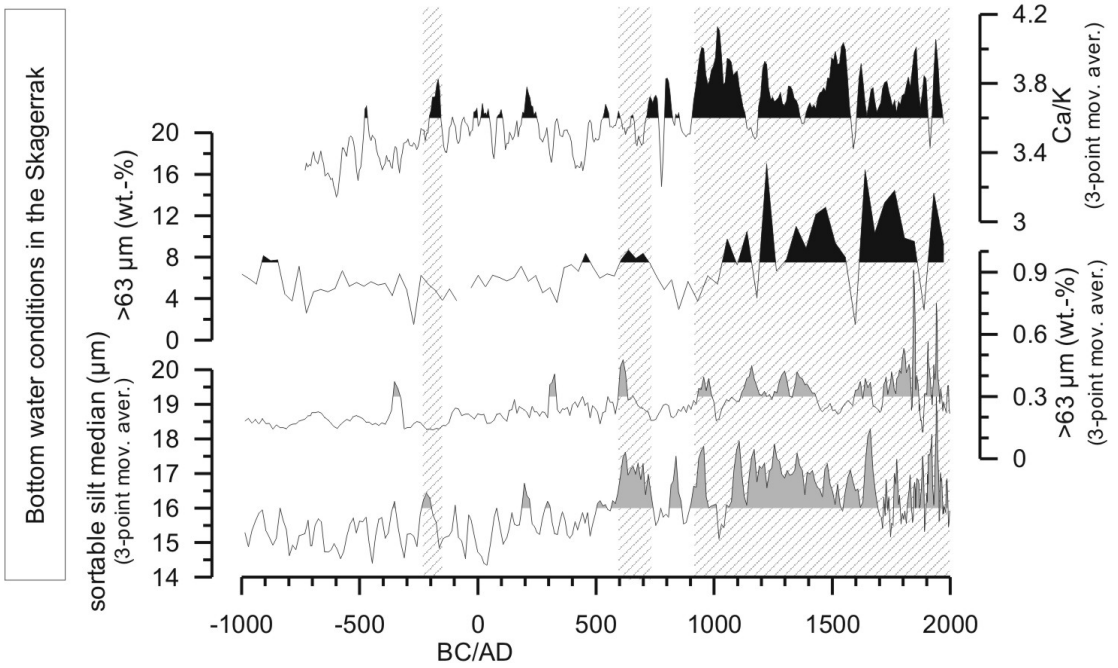

Figure 5 Proxies for the bottom water conditions in the Skagerrak through the last 3000 years. Black curves display data from core GeoB 6003-2 in the southern and grey curves from core MD99-2286 in the north-eastern Skagerrak. Hatched fields mark periods discussed in the text.

Variability in the bottom water conditions is also reflected in the species composition of the benthic foraminiferal fauna. Once more, the records indicate one major paleoenvironmental shift and a number of abrupt events. However, the major paleoenvironmental shift at around AD 900 occurs at different times for different species at the two sites.

The first indication of this "series of shifts", altogether reflecting the major paleoenvironmental shift, is a sudden drop in the contribution by *Hyalinea balthica* (Schroeter) in the southern Skagerrak at around AD 750. This is followed in the north-eastern Skagerrak by a major decrease in *Bulimina marginata* (d'Orbigny) and a considerable increase in *Melonis barleeanus* (Williamson) at around AD 850, and in *Cassidulina laevigata* d'Orbigny at AD 1000 (Figure 6). Another significant transition occurs at AD 1150, when, in the southern Skagerrak, the decrease in the contents of *Pullenia osloensis* (Feyling-Hanssen) and *C. laevigata* is balanced by an increase in *Stainforthia fusiformis* (Williamson) and the

temperate forma *selseyensis* (Heron-Allen and Earland) of *Elphidium excavatum* (Terquem). Over the last 100 years, another strong shift is indicated at the north-eastern site by increasing percentages of *B. marginata* and decreasing contents of *C. laevigata*. Although both cores are from relatively near-by settings, the differences in water depth and in the environmental setting in the southern and in the north-eastern Skagerrak result in partly opposite records in the relative abundances of individual species of benthic foraminifera as exemplified here for *C. laevigata* (Figure 6). Thus, these differences hamper a direct comparison of the long-term development of individual species.

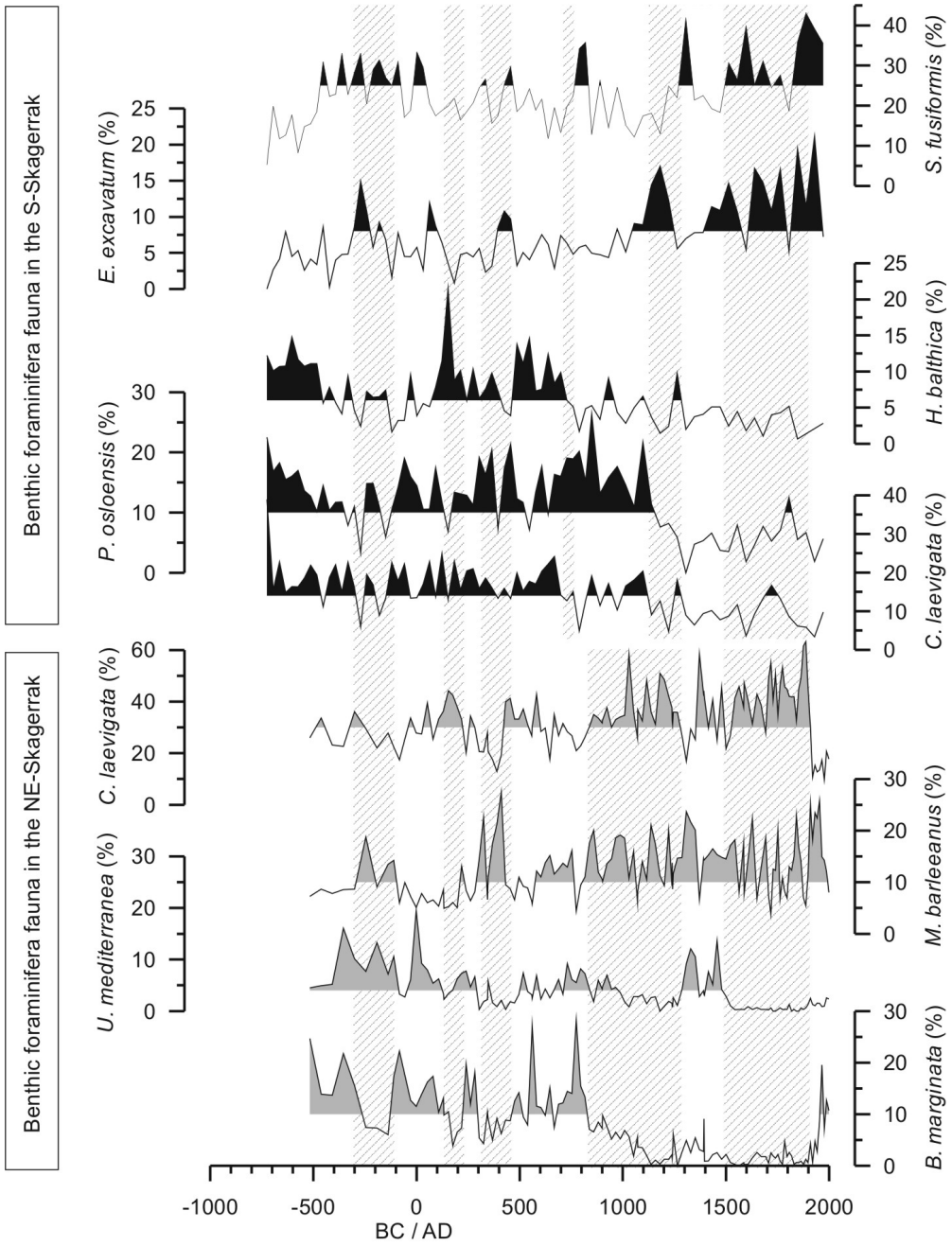

Figure 6 Relative abundances of selected benthic foraminifera in the Skagerrak through the last 3000 years. Black curves display data from core GeoB 6003-2 in the southern and grey curves from core MD99-2286 in the north-eastern Skagerrak. Hatched fields mark periods discussed in the text.

The general indication of the faunal shifts in the Skagerrak is associated with changes in the water masses of the area. The assemblages in the lower part of the record in the southern Skagerrak reflect relatively stable bottom water conditions under the influence of deeper Skagerrak water masses of Atlantic origin. The faunal composition found in this part of the record corresponds to modern assemblages living on the deeper parts of the southern slope of the Norwegian Trench (e.g.,. *C. laevigata*, *P. osloensis* and *H. balthica*; see Conradsen *et al.*, 1994; Bergsten *et al.*, 1996). The subsequent change in assemblage at around AD 900 is a result of increased environmental instability, presumably due to an intensification of the North Jutland Current. This is indicated by high amounts of the species *S. fusiformis* together with an increase in shallow water species such as *E. excavatum*, a species which is suggested to be reworked from the North Sea and Danish shelf areas (cf. Alve and Murray, 1995, 1997). In general, the assemblages in the upper part of the record correspond to the present-day faunas at the core site, which is in an area that is characterised by a relatively high influence of North Sea waters compared to the deeper part of the slope (e.g., Bergsten *et al.*, 1996).

In the north-eastern Skagerrak core, the faunal compositions are quite different from those in the southern Skagerrak, but the faunal shift at around AD 900 is clearly a result of the same general environmental change in the area. The assemblages in the lower part of the north-eastern Skagerrak record, characterised by an important contribution of *B. marginata*, correspond to modern faunas found further to the east along the Swedish west coast today (Conradsen *et al.*, 1994). The faunal distribution in the lower part of the record shows that previous to AD 1000, this *B. marginata* province covered a wider area along the Swedish coast than at present. This is in agreement with results by Gyllencreutz and Kissel (in press). They found that magnetic properties of core MD99-2286 indicate stronger influence of the Baltic current and the currents along western Sweden and southern Norway before an abrupt change at about AD 900 than after. From AD 900 until the present, the sedimentation in the north-eastern Skagerrak was totally dominated by southern North Sea and Atlantic Ocean sources (Gyllencreutz and Kissel, in press).

After these major shifts (and despite the most recent shift after AD 1900) the mid-term variability in the faunal composition of the benthic foraminifera is comparably low with only one strong signal between AD 1300 and AD 1500, best indicated by a sudden increase in *Uvigerina mediterranea* (Hofker) in the north-eastern Skagerrak before this species vanished from the area. This event is probably also reflected in the diatom record resulting in enhanced biogenic opal dissolution, which most likely took place at the sea floor. In addition, before

AD 750 some events leaving strong signals in the species composition at both sites occurred. The most pronounced events took place at 300 to 100 BC, around AD 200 and between AD 300 and AD 450, however, all of these have different responses of the benthic fauna preventing a straightforward interpretation of their causes.

Paleoenvironmental conditions along the Norwegian margin and in the German Bight

Core HM115-16 from the Norwegian margin represents the "Atlantic end-member" in this compilation. Especially the benthic record, expected to be unaffected by the relatively fresh and shallow Norwegian Coastal Current reaching the core site occasionally, should be related to the strength of Atlantic water advection. After a smaller event centered around AD 500, the benthic foraminifera $\delta^{18}O$ data show a shift towards sustained lighter (i.e., "warmer") values around AD 900 (Figure 7) indicating an increase in the advection of Atlantic waters. After AD 1450 the isotope data returned to variable, but on average "colder" values before they display a marked increase through the last 50 years. Interestingly, this pattern is largely mirrored in surface water temperature and salinity reconstructions based on dinoflagellate transfer functions. These show, for the period AD 900 to AD 1450, marked by the light benthic $\delta^{18}O$ data, relatively warm and saline surface waters also compatible with an increased strength of the North Atlantic Current. Subsequently, this appears to have been considerably weaker, as indicated by low SSS and SST values, probably related to further westward extension of the Norwegian Coastal Current. During the last 50 years, when the benthic isotope data reach the lightest values, especially the SSS record is marked by a strong increase possibly related to another intensification of the Atlantic water advection.

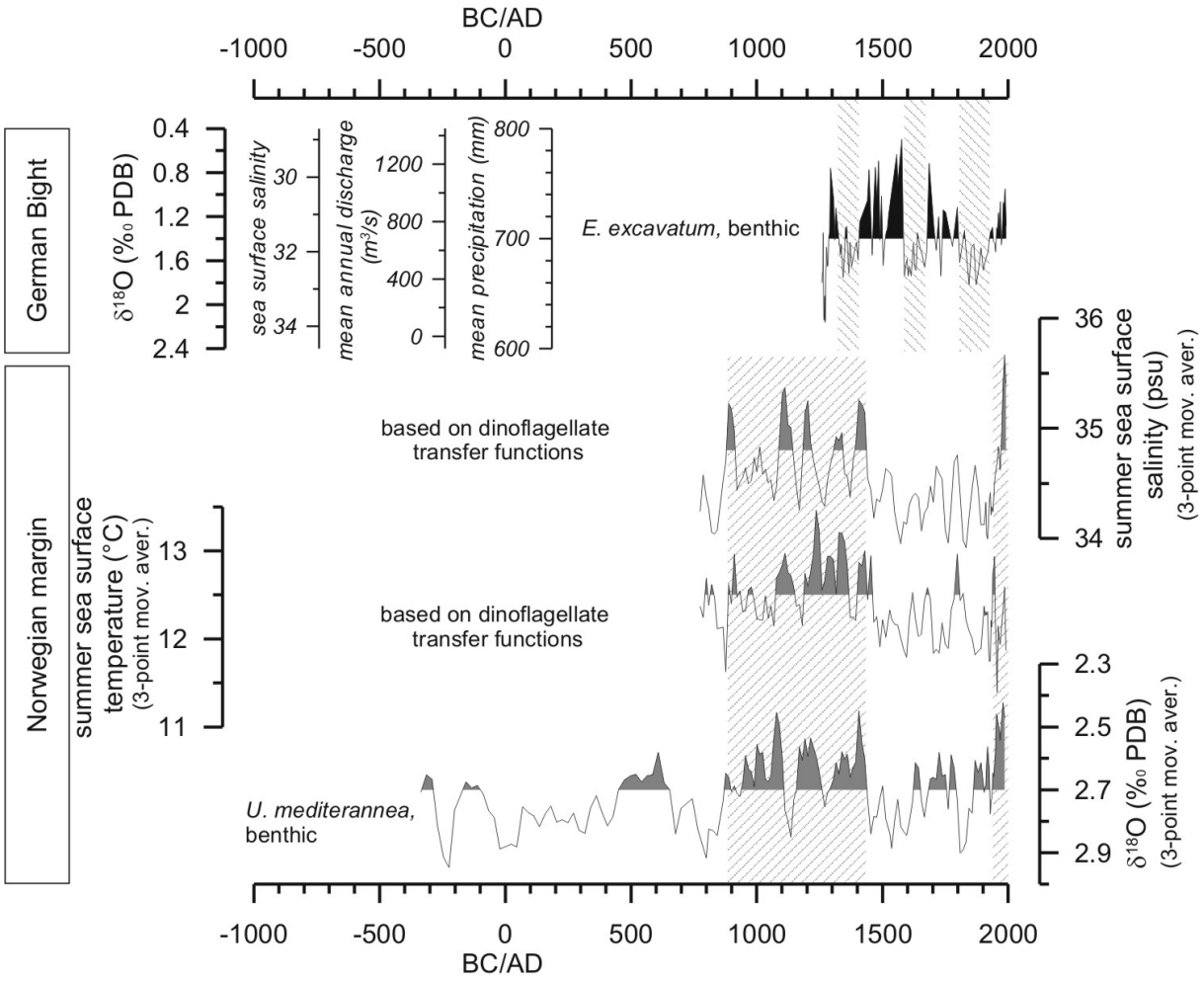

Figure 7 Proxies for the paleoenvironmental conditions at the Norwegian margin (core HM115-16) and in the German Bight (core GeoB 4801-1). Hatched fields mark periods discussed in the text.

In the German Bight the $\delta^{18}O$ data are almost exclusively related to salinity variations as has been deduced from detailed correlations with instrumental records (Scheurle and Hebbeln, 2003). Thus, the $\delta^{18}O$ data of core GeoB 4801-1 provide a detailed salinity reconstruction for the German Bight with salinity in this area being mainly dependent on the Elbe river discharge, which in turn gives a good integration of the precipitation in Central Europe (Scheurle *et al.*, 2005). The available record spans the last 800 years and indicates three periods of relatively high salinities (i.e., low discharges and low precipitation): AD 1300-1400, AD 1590-1650, and AD 1800-1920 (Figure 7).

Regional integration of proxy data

Apparent in all data sets covering the last 2000 years is a major environmental shift that took place between AD 600 and AD 1100, with most of the changes taking place around AD 900 (Figure 8). At this time there is a strong increase in the advection of Atlantic waters

recorded at the Norwegian margin site. As to be expected, this coincided with an intensification of the circulation in the North Sea as evidenced by a significant increase in bottom current strength in the Skagerrak. Although the sortable silt median gives an early indication for such an increase at AD 600, the increase in sand content and the change in sediment composition reflected in changing Ca/K ratio point to AD 900 as the time of the most pronounced increase in bottom current strength. In addition, changes in the wind forcing over the North Sea can affect the bottom current strength along the slopes of the Skagerrak, which will increase in response to strong south-westerly winds (Longva and Thorsnes, 1987).

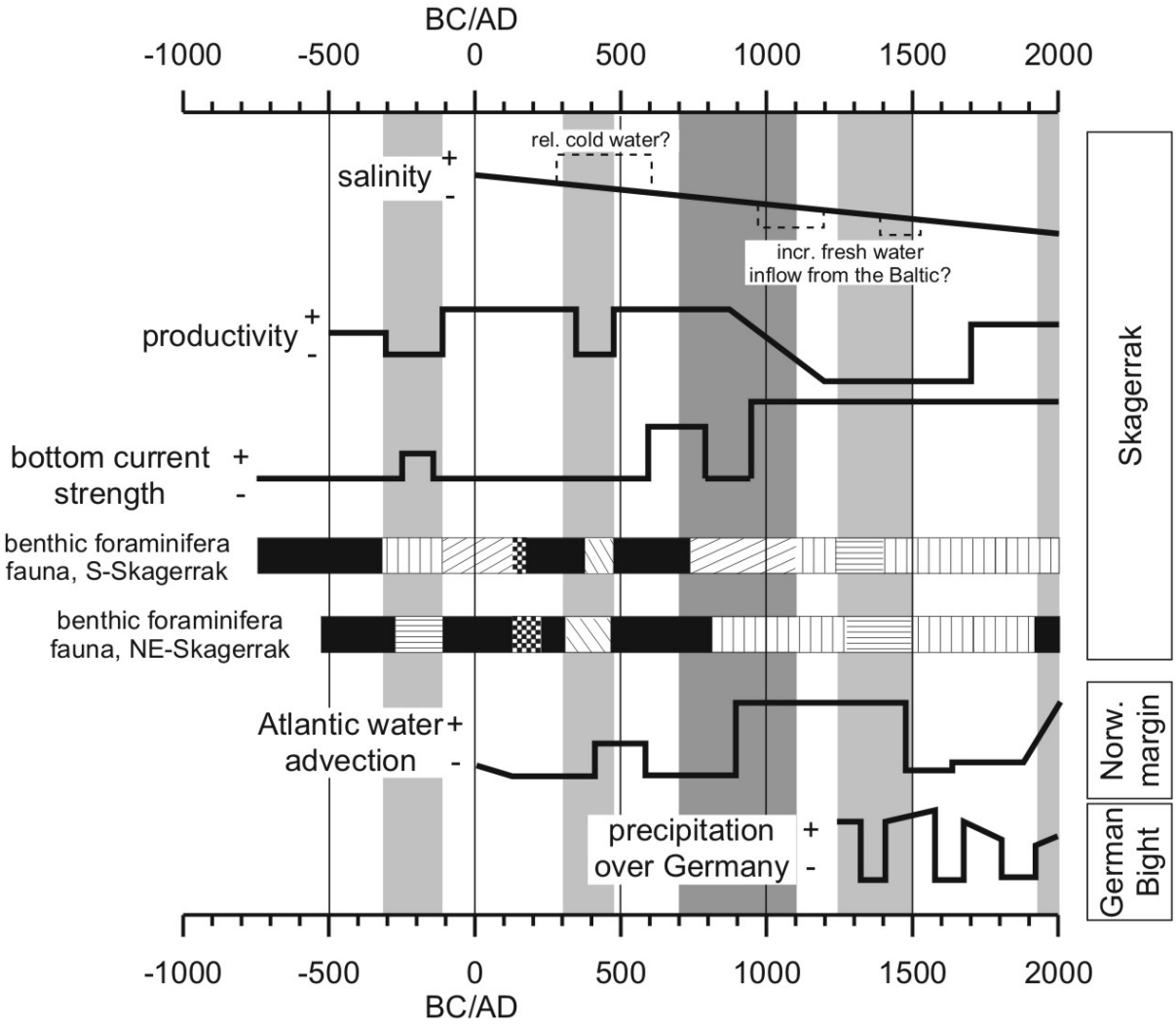

Figure 8 Schematic overview of the environmental changes in the North Sea region through the last 3000 years (see text for background). The coding for the two benthic foraminifera records is not linked as the assemblages are quite different. Vertical bars indicate events/periods in the environmental history (see text) and the major paleoenvironmental shift between AD 700 and AD 1100.

Both forcing factors that most likely caused the coarsening of the sediments (Atlantic water advection and/or changes in the wind field) would also result in a strengthening of the South

Jutland Current (Rodhe, 1996). This current, that flows northward along the shallow, sand-dominated Danish west coast, is the most erosive of the currents contributing to the Skagerrak sediments, and transports the highest concentrations of suspended sediment and, in particular, bedload (Eisma and Kalf, 1987). Thus, also an enhanced South Jutland Current could have contributed to the observed changes in grain size distribution and sediment composition. In a previous study of Late Holocene sediments from the southwestern flank of the Skagerrak, Hass (1996) has also observed a distinct increase in the coarse fraction between AD 700 and AD 1000, which he explained to reflect the onset of modern circulation conditions in the North Sea during the early part of the Medieval Warm Period.

The environmental change centered at AD 900 also resulted in a most pronounced change in the benthic foraminifera communities at both sites in the Skagerrak through the last 2500 years. In the southern Skagerrak, the benthic foraminifera fauna shows a shift from a stable, Atlantic water bound community, nowadays only present in deeper parts of the Skagerrak, to a more unstable community, often related to North Sea waters (Bergsten *et al.*, 1996). Although counterintuitive at first glance, an intensification of the advection of Atlantic waters will not necessarily result in a larger body of true Atlantic water in the deep Skagerrak. Instead, the related overall enhancement of the North Sea circulation would stimulate a strengthening of the North Jutland Current that would push the boundary between North Sea water and true Atlantic water at the southern slope of the Skagerrak to a greater water depth. This would also explain the increasing numbers of probably reworked benthic foraminifera (e.g., *E. excavatum*) originating from shallower settings (i.e., Alve and Murray, 1995, 1997). In addition, the community change in the north-eastern Skagerrak, marked by a drastic reduction of *B. marginata*, also would be in line with the interpretation of an enhanced circulation that probably pushed the *B. marginata* zone closer towards the Swedish coast and assemblages from more westerly areas of the Skagerrak immigrated into the core site area.

Also at around AD 900 there is a clear decrease in the productivity in the Skagerrak, showing that not only the bottom but also the surface waters are affected by this shift. In addition, these surface waters are also affected by a long-term decrease in SSS.

Interestingly, the bottom current strength in the Skagerrak stays at a rather high level until the present, while the Atlantic water advection to the Norwegian margin (AD 1450), as well as the productivity in the Skagerrak (AD 1700), almost return to pre-AD 700 levels. The

decreasing advection of Atlantic waters only leaves an enhanced wind forcing to explain the continued high bottom current velocities after AD 1450.

In addition to this major environmental shift, there are several smaller events that leave their traces in a number of proxies. The first observed event occurred between 300 BC and 100 BC and is recorded in all proxies available for that period. At that time, a drop in productivity is associated with an increase in bottom current strength and a change in the benthic foraminifera fauna. The next event (AD 300 to AD 500) is also marked by a lowered productivity, a change in the benthic foraminifera fauna and possibly colder surface waters in the Skagerrak, whereas the bottom current strength remains unaltered. An increase in the Atlantic water advection to the Norwegian margin commences slightly later, which could possibly be due to stratigraphic uncertainties.

After the major shift at AD 900, such events continue to happen although later on they are mostly reflected in the benthic foraminifera fauna, as e.g., between AD 1250 and AD 1500, when the return of *U. mediterranea* to the north-eastern site might be associated with an increase in temperature (cf. Murray, 1991), possibly due to a change in the water mass structure. The termination of this event coincides with the end of the period with very strong advection of Atlantic waters to the Norwegian margin, while at the same time a low salinity pulse in the Skagerrak points to enhanced Baltic Sea outflow, possibly associated with high continental precipitation as indicated in the German Bight core. Finally, at AD 1950 another increase in Atlantic water advection to the Norwegian margin goes along with a change in the benthic foraminifera fauna in the north-eastern Skagerrak. However, the increase of *B. marginata* during the last 100 years in the Skagerrak is suggested to be a result of anthropogenic influence in the area (Seidenkrantz, 1993).

Inferred environmental forcing

In a previous assessment of the Late Holocene paleoenvironmental history of the Skagerrak, Hass (1996) concluded that climate changes associated with well known climatic periods such as the Medieval Warm Period (MWP, AD 700-1350, according to Hass, 1996) or the Little Ice Age (LIA, AD 1350-1900, according to Hass, 1996) are the driving forces behind the observed changes in the Skagerrak. He relates warm periods (the MWP and the Roman Climate Optimum, 320 BC – AD 380) to weaker bottom currents, less Atlantic water advection and less wind forcing resulting from more northerly located cyclone tracks. Opposite conditions are assumed to dominate the colder phases (LIA and the Dark Ages, AD

400-700). These conclusions are drawn using subtle changes in grain size distributions and stable oxygen isotope data. In addition, this data set also shows a marked and sustained coarsening of the sediments between AD 700 and AD 1000 (Hass, 1996), very similar to that described here. Hass (1996) related this to an intensified circulation system in the Skagerrak, however, without finding a relation to any climatic forcing.

Based on the results presented above, a different view on the interrelation of the different forcing factors as well as on their temporal development can be developed. Basically, the climate in northern Europe and particularly in the North Sea is closely related to the strength of the advection of warm and saline Atlantic waters to the region. Consequently, our records from the Norwegian margin should give an indication of this "Atlantic-type" forcing. From the Norwegian margin record, it is clear that for most of the MWP (since AD 900) the region was affected by strong Atlantic water advection that continued well into the LIA (until AD 1450, see also Koç and Jansen, 2002). The onset of this event is in agreement with other records from the NE-Atlantic and from the Icelandic shelf (e.g., Eirikson *et al.*, in press). However, at these sites a significant cooling, probably related to decreasing advection of Atlantic waters, began already at AD 1300, roughly at the turn from the MWP to the LIA.

As pointed out before, the onset of this Atlantic water advection event at AD 900 coincides with the permanent enhancement of bottom currents in the Skagerrak. Due to a more northerly position of the Northern Hemisphere subtropical anticyclones during the MWP, westerly winds at latitudes between 40^{o} and 60^{o}N were presumably weaker and less prevalent (Lamb, 1977). Therefore, the enhanced bottom current strength most likely resulted from the intensification of the North Sea circulation as outlined above, and not from wind stress. At first glance, one might also expect an associated temperature and salinity increase in the Skagerrak, however, the response appears to be much more complex. Almost at the same time when the bottom water circulation in the Skagerrak intensified, the salinity in the surface waters decreased. The latter can only be explained by taking into account the consequences for the atmospheric circulation resulting from a warming of the North Atlantic. Indeed, in addition to the data shown in Figure 8, increased Atlantic sea surface temperatures have also been documented for other cores from the Norwegian margin in the time interval between about AD 1100 and AD 1450 (Koç and Jansen, 2002; Andersson *et al.*, 2003, Klitgaard Kristensen *et al.*, 2004).

This warming probably resulted in enhanced evaporation over the ocean and enhanced precipitation over the continent. Much of the precipitation falling over northern Europe is

flowing directly into the North Sea or into the Baltic Sea, from where the fresh water is canalised through the Kattegat and the Skagerrak to finally return to the Atlantic. Thus, a warming of the North Atlantic would result in enhanced fresh water flow to the North Sea and especially to the Skagerrak. Such a link between enhanced heat flux from the North Atlantic to the atmosphere and increased precipitation over the Baltic Sea catchment area has also been described by Emeis *et al.* (2003). Actually, such a pattern is indicated by the decreasing salinities in the Skagerrak surface waters and, even more pronounced, by the salinity minimum between AD 1400 and 1550, which coincides with increased precipitation over Germany (Figure 8).

The associated decrease in productivity in the Skagerrak might result from increased stratification of the water column between the fresher surface water and the deeper fully marine waters. Such stratification would hamper the delivery of nutrients from the deeper waters to the photic zone and thereby decrease the productivity. In addition, the much lower nutrient content of the low saline Baltic Sea outflow water (Rasmussen and Gustafsson, 2003) may also have contributed to the reduction in productivity.

At AD 1450, already well within the LIA, the advection of Atlantic waters to the Norwegian margin and consequently to the North Sea decreased. Interestingly, the response of the paleoenvironment in the Skagerrak appears to be rather weak. The bottom sediments as well as the benthic foraminifera continue to indicate strong bottom currents and also the productivity remains at a low level, returning to a somewhat higher level not until AD 1700. Under such a weak Atlantic water advection scenario only enhanced atmospheric forcing (i.e., stronger winds; Longva and Thorsnes, 1987) could explain the high bottom current velocities in the Skagerrak. And indeed, a southward shift of the cyclone tracks due to the expansion of the circumpolar vortex during the LIA, as suggested by Lamb (1977, 1979), would have resulted in stronger westerly winds and increased storm activity over the North Sea. This is supported by data from Björck and Clemmensen (2004) who interpreted aeolian sand influx in raised bogs in south-western Sweden as an indication of increased winter storminess from *c.* AD 1450 to AD 1900, preceded by about 700 years of low values. Thus, although forced by different factors before (the advection of Atlantic waters) and after (stronger winds and increased storminess) AD 1450, the strong bottom currents in the Skagerrak after AD 1000 can be related to the prevailing environmental conditions at the respective periods.

Of course, the next question is what caused the principal difference between the environmental setting prior to AD 700-1000 (weak bottom currents) and afterwards (strong bottom currents). At first glance a climatic forcing appears unlikely, as e.g., the strong bottom currents persisted through a warm period (MWP) as well as through a cold stage (LIA). However, if both settings are able to produce such strong bottom currents it might be the strength of the climatic variability playing the decisive role. Indeed, the two periods mentioned here are known as the warmest and coldest periods at least of the last 2000 years in this region (ignoring the period since the 1970s). Thus, it is possibly the strength of the respective forcing (MWP – oceanic vs. LIA – atmospheric) that regulates bottom current velocities in the Skagerrak. Under a less extreme forcing as e.g., during the Roman Climate Optimum or the Dark Ages the energy provided was probably insufficient to accelerate the bottom currents in the Skagerrak in a significant way. Looking beyond the MWP, our records show only one short period at the onset of the Roman Climate Optimum (300-100 BC, Figure 8), when probably a warm climate forcing was strong enough to enhance the North Sea circulation in a way similar as during the MWP.

At the present stage other causes for the observed paleoenvironmental changes in the Skagerrak cannot be excluded. For instance, the sustained change in sediment composition at AD 900 might reflect a more local, climate-independent change e.g., in sediment source area, sediment transport pathways or coastal erosion intensity. According to Nordberg (1981), enhanced coastal erosion might have resulted in coarser sediments and in enhanced sedimentation rates in the Skagerrak at some time between AD 1000 and AD 1500. However, at these times we found coarser sediments associated with lower sedimentation rates indicative of increased winnowing by enhanced bottom currents. To the knowledge of the authors there are no independent hints for any local trigger of environmental variability in the Skagerrak region. In contrast, the evidence put together here from different sites in the North Sea all point to a major environmental shift at AD 900 affecting surface as well as bottom waters in the Skagerrak and at the Norwegian margin and are, thus, supportive of a more regional, i.e., climatic trigger.

Finally, although the strong winds of the LIA are suggested to cause strong bottom currents in the Skagerrak after AD1450, when the advection of Atlantic waters to the Norwegian margin decreased, it has to be noted that none of the records from the Skagerrak gives any clear hint indicating the transition from the MWP to the LIA. In contrast, increasing productivity in the Skagerrak at AD 1700, coinciding with an increase in northern Fennoscandian summer temperature anomalies (Briffa *et al.*, 1992), might indicate the end of

the LIA in the Skagerrak, although there is no related signal found in the Norwegian margin cores. Thus, despite the available data, further studies are needed to finally unravel cause and effects of paleoenvironmental changes in the Skagerrak region through the last two millennia.

Acknowledgements

This work has been supported by the European Union through funding of the project HOLSMEER - Late Holocene Shallow Marine Environments of Europe (EVK2-CT-2000-00060). We are grateful to the *Institut Paul-Emil Victor* (IPEV) for IMAGES coring operation onboard the *R/V Marion Dufresne*. This manuscript benefited greatly from the reviews by Christian Hass and Kay-Christian Emeis.

REFERENCES

Abrantes, F. 1988: Diatom productivity peak and increased circulation during latest Quaternary: Alboran basin (Western Mediterranean). *Marine Micropaleontology* 13, 79-96.

Alve, E. and Murray, J. 1995: Benthic foraminiferal distribution and abundance changes in Skagerrak surface sediments: 1937 (Höglund) and 1992/93 data compared. *Marine Micropaleontology* 25, 269-288.

Alve, E. and Murray, J. 1997: High benthic fertility and taxonomy of foraminifera: a case study of the Skagerrak, North Sea. *Marine Micropaleontology* 31, 157-175.

Andersson, C., Risebrobakken, B., Jansen, E. and Dahl, S.O. 2003: Late Holocene surface ocean conditions of the Norwegian Sea (Vøring Plateau). *Paleoceanography* 18, 1044, doi:10.1029/2001PA000654.

Battarbee, R.W. 1973: A new method for estimation of absolute microfossil numbers with reference especially to diatoms. *Limnology and Oceanography* 18, 647-652.

Bergsten, H., Nordberg, K. and Malmgren, B. 1996: Recent benthic foraminifera as tracers of water masses along a transect in the Skagerrak, north-eastern North Sea. *Journal of Sea Research* 35, 111-121.

Björck, S. and Clemmensen, L.B. 2004: Aeolian sediment in raised bog deposits, Halland, SW Sweden: a new proxy record of Holocene winter storminess variation in southern Scandinavia? *The Holocene* 14, 677-688.

Conradsen, K. and Heier-Nielsen, S. 1995: Holocene paleoceanography and paleoenvironments of the Skagerrak-Kattegat, Scandinavia. *Paleoceanography* 10, 801-813.

Conradsen, K., Bergsten, H., Knudsen, K.L., Nordberg, K. and Seidenkrantz, M.-S. 1994: Recent benthic foraminiferal distribution in the Kattegat and the Skagerrak, Scandinavia. *Cushman Foundation Special Publication* 32, 53-68.

Dahl, F.E. 1978: On the existence of a deep countercurrent to the Norwegian Coastal Current in the Skagerrak. *Tellus* 30, 552-556.

Danielssen, D.S., Davidsson, L., Edler, L., Fogelquist, E., Fonselius, S.H., Føyn, L., Hernroth, I., Håkansson, B., Olsson, I. and Svendsen, E. 1991: SKAGEX: Some preliminary results. *International Council for the Exploitation of the Sea* CM 1991, C:2, 14 pp.

Dooley, H.D. and Furnes, G.K. 1981: Influence of the wind field on the transport of the northern North Sea. In Saetre, R. and

Mork, M., editors, *The Norwegian coastal current.* University of Bergen 1, 57-71.

Eiríksson, J., Bartels-Jónsdóttir, H.B., Cage, A.G., Gudmundsdóttir, E.R., Klitgaard-Kristensen, D., Marret, F., Rodrigues, T., Abrantes, A., Austin, W.E.N., Jiang, H., Knudsen, K.L. and Sejrup, H. in press: Variability of the North Atlantic Current during the last 2000 years based on shelf bottom water and sea surface temperatures along an open ocean shallow marine transect in western Europe. *The Holocene* in press.

Eisma, D. and Kalf, J. 1987: Dispersal, concentration and deposition of suspended matter in the North Sea. *Journal of the Geological Society* 144, 161-178.

Emeis, K.-C., Struck, U., Blanz, T., Kohly, A. and Voss, M. 2003: Salinity changes in the central Baltic Sea (NW Europe) over the last 10000 years. *The Holocene* 13, 411-421.

Fenner, J. 1981: Diatoms in the Eocene and Oligocene Sediments off NW - Africa. Their Stratigraphic and Paleoceanographic Occurrences. *PhD Thesis*, *University of Kiel* 230 pp.

Grove, J.M. 2002: Climatic Change in Northern Europe over the last two thousand years and its possible influence on human activity. In Wefer, G., Berger, W.H., Behre, K.-E., Jansen, E., editors, *Climate development and history of the North Atlantic realm*. Springer Verlag Berlin Heidelberg, 313-326.

Gyllencreutz, R. 2005: Late Glacial and Holocene paleoceanography in the Skagerrak from high-resolution grain size records. *Palaeogeography, Palaeoclimatology, Palaeoecology* 222, 344-369.

Gyllencreutz, R., Jakobsson, M. and Backman, J. 2005: Holocene sedimentation in the Skagerrak interpreted from chirp sonar and core data. *Journal of Quaternary Science* 20, 21-32.

Gyllencreutz, R., and Kissel, C. in press: Late Glacial and Holocene paleoceanographic variability in north-eastern Skagerrak interpreted from grain size and magnetic properties in IMAGES core MD99-2286. *Quaternary Science Reviews*.

Hass, H.C. 1993: Depositional processes under changing climate: Upper Subatlantic granulometric records from the Skagerrak (NE-North Sea). *Marine Geology* 111, 361-378.

Hass, H.C. 1996: Northern Europe climate variations during late Holocene: evidence from marine Skagerrak. *Palaeogeography, Palaeoclimatology, Palaeoecology* 123, 121-145.

Hebbeln, D., Scheurle, C. and Lamy, F. 2003: Depositional History of the Helgoland Mud Area, German Bight, North Sea. *Geo-Marine Letters* 23, 81-90.

Heier-Nielsen, S., Heinemeier, J., Nielsen, H.L. and Rud, N. 1995: Recent reservoir ages for Danish fjords and marine waters. *Radiocarbon* 37, 875-882.

Hughen, K.A., Baillie, M.G.L., Bard, E., Bayliss, A., Beck, J.W., Bertrand, C., Blackwell, P.G., Buck, C.E., Burr, G., Cutler, K.B., Damon, P.E., Edwards, R.L., Fairbanks, R.G., Friedrich, M., Guilderson, T.P., Kromer, B., McCormac, F.G., Manning, S., Bronk Ramsey, C., Reimer, P.J., Reimer, R.W., Remmele, S., Southon, J.R., Stuiver, M., Talamo, S., Taylor, F.W., van der Plicht, J., and Weyhenmeyer, C.E. 2004: Marine04 Marine Radiocarbon Age Calibration, 0–26 cal kyr BP. *Radiocarbon* 46, 1059-1086

Hughes, M.K. and Diaz, H.F. 1994. Was there a `Medieval Warm Period´, and if so, where and when? *Climatic Change* 26, 109-142.

Huntley, B., Bailie, M., Grove, J.M., Hammer, C.U., Harrison, S.P., Jacomet, S., Jansen, E., Karlén, W., Koç, N., Luterbacher, J., Negendank, J. and Schibler, J. 2002. Holocene paleoenvironmental changes in North-West Europe: Climatic implications and the human dimension. In Wefer, G., Berger, W.H., Behre, K.-E., Jansen, E., editors, *Climate development and history of the North Atlantic realm*. Springer Verlag Berlin Heidelberg, 259-298.

Hurrell, J. 1995: Decadal trends in the North Atlantic Oscillation: regional temperatures and precipitation. *Science* 269, 676-679.

Imbrie, J., Hays, J.D., Martinson, D.G., McIntyre, A., Mix, A.C., Morley, J.J., Pisias, N.G., Prell, W.L. and Shackleton, N.J. 1984: The orbital theory of Pleistocene climate: support from a revised chronology of the marine $\delta^{18}O$ record. In Berger, A.L., Imbrie, J., Hays, J.D., Kukla, G., Saltzman, B., editors, *Milankovitch and Climate*. D. Reidel Publishing Company, Part 1, 269-305.

Jansen, J.H.F., van der Gaast, S.J., Koster, B. and Vaars, A.J. 1998: CORTEX, a shipboard XRF-scanner for element analyses in split sediment cores. *Marine Geology* 151, 143-153.

Jennerjahn, T.C., Ittekkot, V., Arz, H.W., Behling, H., Pätzold, J. and Wefer, G. 2004: Asynchronous terrestrial and marine signals of climate change during Heinrich events. S*cience* 306, 2236-2239.

Jiang, H. 1996: Diatoms from the surface sediments of the Skagerrak and the Kattegat and their relationship to spatial changes of environmental variables. *Journal of Biogeography* 23, 129-137.

Johannesen, T., Jansen, E., Flatøy, A. and Ravelo, A.C. 1994: The relationship between surface water masses, oceanographic fronts and paleoclimatic proxies in surface sediments of the Greenland, Iceland and Norwegian Seas, pp 61-85. In Zahn, R. and Kaminski, M., editors, *Carbon Cycling in the Glacial Ocean*. NATO ASI Series I, 17, Springer, Berlin.

Jones, P.D., Osborn, T.J. and Briffa, KR. 2001: The evolution of climate over the last millennium. *Science* 292, 662-667.

Jones, P.D. and Mann, M.E. 2004: Climate over past millennia. *Reviews of Geophysics* 42, doi:10.1029/2003RG000143.

Klitgaard-Kristensen, D., Sejrup, H.P. and Haflidason, H. 2001: The last 18 kyr fluctuations in Norwegian Sea surface conditions and implications for the magnitude of climatic change: Evidence from the North Sea. *Paleoceanography* 16, 455-467.

Klitgaard Kristensen, D., Sejrup H.P., Haflidason, H. and Berstad, I.M. 2004: Eight-hundred-year temperature variability from the Norwegian continental margin and the North Atlantic thermohaline circulation. *Paleoceanography* 19, PA2007, doi:10.1029/2003PA000960.

Knudsen, K.L., Conradsen, K., Heier-Nielsen, S. and Seidenkrantz, M.-S. 1996: Paleoenvironments in the Skagerrak-Kattegat basin in the eastern North Sea during the last deglaciation. *Boreas* 25, 65-77.

Koç, N. and Jansen, E. 2002: Holocene evolution of the North Atlantic ocean and the Nordic Seas – a synthesis of new results. In Wefer, G., Berger, W.H., Behre, K.-E., Jansen, E., editors, *Climate development and history of the North Atlantic realm*. Springer Verlag Berlin Heidelberg, 165-173.

Kuhlmann, H., Meggers, H., Freudenthal, T. and Wefer, G. 2004: The transition of the monsoonal and N Atlantic climate system off NW Africa during the Holocene. *Geophysical Research Letters* 31, 22, L22204.

Lamb, H.H.1977: *Climate: present, past and future*, *Volume 2: Climatic history and the future*. Methuen & Co Ltd, London, 1-853.

Lamb, H.H. 1979: Climatic variation and changes in the wind and ocean circulation: the Little Ice Age in the Northeast Atlantic. *Quaternary Research* 11, 1-20.

Ljøen, R. and Svansson, A. 1972: Long-term variations of subsurface temperatures in the Skagerrak. *Deep-Sea Research* 19, 277-288.

Lohse, L., Malschaert, J.F.P., Slomp, C.P., Helder, W. and van Raaphorst, W. 1995: Sediment-water fluxes of inorganic nitrogen compounds along the transport route of organic matter in the North Sea. *Ophelia* 41, 173-197.

Longva, O. and Thorsnes, T., editors, 1997: Skagerrak in the past and at the present - an integrated study of geology, chemistry, hydrography and microfossil ecology. *Geological Survey of Norway, Special Publication* 8, 1-100.

Marshall, J., Kushnir, Y., Battisti, D., Chang, P., Czaja, A., Dickson, R., Hurrell, J., McCartney, M., Saravanan, R. and Visbeck, M. 2001: North Atlantic climate variability: phenomena, impacts and mechanisms. International *Journal of Climatology* 21, 1863–1898.

McCave, I.N., Manighetti, B. and Robinson, S.G. 1995: Sortable silt and fine sediment size/composition slicing: Parameters for paleocurrent speed and paleoceanography. *Paleoceanography* 10, 593-610.

Meldgaard, S. and Knudsen, K.L. 1979: Metoder til indsamling og oparbejdnung af prøver til foraminifer-analyser. *Dansk Natur Dansk Skole Årsskrift 1979*, 48-57.

Murray, J. 1991: *Ecology and Paleoecology of Benthic Foraminifera*. Longman Scientific & Technical, 397 pp.

Nadeau, M.J., Schleicher, M., Grootes, P.M., Erlenkeuser, H., Gottolong, A., Mous, D.J.W., Sarnthein, J.M. and Willkomm, N. 1997: The Leibniz-Labor AMS facility at the Christian-Albrechts University, Kiel, Germany. *Nuclear Instruments and Methods in Physics Research* 123, 22-30.

Nordberg, K. 1991: Oceanography in the Kattegat and Skagerrak over the past 8000 years. *Paleoceanography* 6, 461-484.

Qvale, G. and van Weering, T.C.E. 1985: Relationship of surface sediments and benthic foraminiferal distribution patterns in the Norwegian Channel (Northern North Sea). *Marine Micropaleontology* 9, 469-488.

Rasmussen, B. and Gustafsson, B.G. 2003: Computation of nutrient pools and fluxes at the entrance to the Baltic Sea, 1974–1999. *Continental Shelf Research* 23, 483-500.

Rochon, A., de Vernal, A., Turon, J.L., Matthiessen, J. and Head, M.J. 1999: Distribution of dinoflagellate cyst assemblages in surface sediments from the North Atlantic Ocean and adjacent basins and quantitative reconstruction of sea-surface parameters, *Special Contribution Series, American Association of Stratigraphic Palynologists* n° 35.

Rodhe, J. 1987: The large-scale circulation in the Skagerrak; interpretation of some observations. *Tellus* 39A, 245-253.

Rodhe, J. 1996: On the dynamics of the large-scale circulation of the Skagerrak. *Journal of Sea Research* 35, 9-21.

Rodhe, J. 1998: The Baltic and North Seas: A process-oriented review of the physical oceanography. In Robinson, A.R. and Brink, H.H., editors, *The Sea*. John Wiley & Sons, 699-732.

Röhl, U., Bralower, T.J., Norris, R.D. and Wefer, G. 2000: New chronology for the late Paleocene thermal maximum and its environmental implications. *Geology* 28, 927-930.

Scheurle, C. 2004: Climate development and its effect on the North Sea environment during the Late Holocene. PhD Thesis, University of Bremen, 121 pp.

Scheurle, C. and Hebbeln, D. 2003: Stable oxygen isotopes as recorders of salinity and river discharge in the German Bight, North Sea. *Geo-Marine Letters* 23, 130-136.

Scheurle, C., Hebbeln, D. and Jones, P. 2005: An 800 year record of salinity and river discharge in the German Bight. *The Holocene* 15, 429-434.

Schrader, H.J. and Gersonde, R. 1978: Diatoms and Silicoflagellates. *Utrecht Micropaleontological Bulletin* 17, 129-176.

Seidenkrantz, M.-S. 1993: Subrecent changes in the foraminiferal distribution in the Kattegat and the Skagerrak, Scandinavia: anthropogenic influence and natural causes. *Boreas* 22, 383-395.

Stabell, B. and Thiede, J. 1985: Upper Quaternary marine Skagerrak (NE North Sea) deposits: Stratigraphy and depositional evnironment. *Norsk Geologisk Tidsskrift* 65, 9-149.

Stuiver, M., Reimer, P.J., Bard, E., Beck, J.W., Burr, G.S., Hughen, K.A., Kromer, B., McCormac, F.G., v.d. Plicht, J. and Spurk, M. 1998: INTCAL98 Radiocarbon Age Calibration, 24.000-0 cal BP. *Radiocarbon* 40, 1041-1083.

van Weering, T.C.E., Berger, G.W. and Kalf, J. 1987: Recent sediment accumulation in the Skagerrak, northeastern North Sea. *Netherlands Journal of Sea Research* 21, 177-189.

van Weering, T.C.E., Rumohr, J. and Liebezeit, G. 1993: Holocene sedimentation in the Skagerrak: A review. *Marine Geology* 111, 379-391.

von Haugwitz, W., Wong, H.K. and Salge, U. 1988: The mud area southeast of Helgoland: A reflection seismic study. *Mitteilungen Geologisch-Paläontologisches Institut Universität Hamburg* 65, 409-422

.

CHAPTER 8:

1750 yrs of rapid oceanographic changes over the Laurentian Fan (South of Newfoundland) as revealed by high resolution diatom record

Gil, I. M., Keigwin, L. D., Abrantes, F., Hebbeln, D.

Submitted to Paleoceanography

Diatom evidence for rapid oceanographic change over the Laurentian Fan (South of Newfoundland) since 1750 years B.P.

Gil, I. M.[1, 2], Keigwin, L. D.[3], Abrantes, F.[1], Hebbeln, D.[2]

[1] Marine Geology Department, National Institute of Engineering, Technology and Innovation, 2721-866 Alfragide, Portugal
[b] MARUM – Center for Marine Environmental Sciences, University of Bremen, Leobener Straße, 28359 Bremen, Germany
[3] McLean Laboratory, Woods Hole Oceanographic Institution, Woods Hole, Massachusetts, USA.

Abstract

Diatom analyses on a multicore from the Laurentian fan show the occurrence of warm spells between 1750 and 1100 yr BP and between 500 and 150 yr BP, coinciding with the Dark Ages and the Little Ice Age. A northward migration of the Warm Slope Water Current generates such a local warming. In general, this result supports previous inferences based on the planktonic foraminiferal fauna.

However, the diatoms reveal additional cold phases centred at ~800 and ~300 yr BP, while *Neogloboquadrina pachyderma* (s), a cold water planktonic foraminifera species, does not register so significant changes. It suggests that such cold events recorded by the diatoms may be limited to the surface water. The timing of those events overlaps historical changes in solar activity, the Medieval Maximum and the Maunder Minimum, and the centennial-scale variability of the record is in agreement with the centennial-scale solar cycle.

1. Introduction

Climate changes are documented by human societies for the historical periods such as the Little Ice Age (LIA), the Medieval Warm Period (MWP) and the Dark Ages (DA) in particular. Of the several millennial and centennial scale climate events of the Holocene, these are the major climatic periods of the last two Millennia (Keigwin, 1996, Broecker, 2001, McDermott *et al*., 2001, Cronin *et al*., 2003, Gil *et al*., *in press*). Most of the information available (reports of famine or warm spells for example) is largely developed for the European continent and the major climatic anomalies found there have been considered to have a worldwide expression.

Recent insights into the mechanisms of climate change demonstrate the importance of the North Atlantic as a main regulator of present day climate (Dickson, 1996; Visbeck, 2002). Impacts of oceanographic changes affect directly both sides of the North Atlantic and the balance is illustrated by the North Atlantic Oscillation (NAO) that determines the distribution

of the meridional heat transport associated with the Gulf Stream and the surface water circulation. The NAO index is defined as the atmospheric pressure difference at sea level between the subtropical high and the subpolar low (Hurrell, 1995). Recent studies of late Holocene sedimentary sequences document a coupling between the estimated climatic variability and NAO related changes at centennial scale (Appenzeller *et al*., 1998; Kristensen *et al*., 2004). Rapid warming and cooling periods on longer (millennial) time scales have been assumed as a result of changes in the solar radiative budget (Andersen *et al*., 2004) and in the thermohaline circulation (THC). Bond *et al*. (2001) additionally suggest a 1-2 kyr cycle in Holocene climate driven by solar activity and amplified by the variability of the THC, which is possibly reduced during cold events. A diatom based reconstruction of Holocene Sea Surface Temperatures (SST) for the Nordic Seas also shows that the sites under the direct influence of currents derived from Atlantic water (Norwegian and Irminger currents) record more intensely the cooling over for the last 10 000 years than the other sites (Andersen *et al*., 2004). Such results suggest that the oceanographic variability resulting from changes in insolation is particularly marked in the North Atlantic.

The location of the Laurentian fan is particularly interesting since it is at the confluence of waters from clearly opposite origin, and, has a high St Lawrence River sediment supply which results in detailed high resolution sediment records. At Present, the Slope Water system oscillates in phase with the NAO, but in the temperature signal, it is in antiphase with other North Atlantic locations such as the Sargasso Sea (Keigwin, 1996) or tropical West Africa (deMenocal *et al.,* 2000). Instrumental records show that during the negative phase of the NAO in the 1960s, weaker winds were associated with higher temperatures over Newfoundland, while coastal areas of the Scotian shelf registered lower temperatures (Loder *et al*., 2001).

The strength of the Labrador Current with its high amounts of nutrients has a major role in the productivity of the region (Dutkiewicz *et al*., 2001). Diatoms clearly dominate the phytoplanktonic communities over the Newfoundland area: during the spring bloom that occurs in the uppermost 50 m, they represent 80% of the primary productivity of the first 10 m depth and 92% of the next 25 m (McKenzie *et al*., 1997).

Where opal is well preserved on the seafloor, diatom abundance is a good indicator of productivity conditions and the assemblage composition records temperature and salinity of surface water (Abrantes, 1988). Although many diatom species can be low light adapted and bloom below the pycnocline (Gallager *et al*. 1996), they mostly live in the photic zone and

therefore reflect the features of the upper surface water layer. In comparison, the planktonic foraminifera *N. pachyderma* (s) prefers deeper waters. In the high latitude North Atlantic under the influence of Atlantic Water, this species has its highest abundance between 50 and 200 m water depth and the food supply has been proposed as the main factor controlling its vertical distribution, with the highest abundances found below the phytoplankton biomass maximum (Stangeew, 2001). This points to a preferential habitat of *N. pachyderma* (s) below the diatoms. At the Laurentian fan large SST variability in the top 50 m of the slope waters north of the Gulf Stream may be instigated by the influence of waters from the Gulf of St Lawrence and the inshore Labrador Current (Umoh, 1992). The diatoms are therefore considered as reflecting the high variable water masses of the upper 50 m, while *N. pachyderma* (s) thrives mainly in deeper waters. Therefore, the different habitats of foraminifera and diatoms may express the structure of the near-surface water column.

Holocene SST over the Laurentian fan sediments has been investigated by Keigwin and Pickart (1999), using the abundance of the planktonic foraminifera *Neogloboquadrina pachyderma* (s), a species present in waters colder than 10˚C, as a proxy. The results indicate that the cold climatic periods over Europe of the DA and the LIA (Jones *et al*., 2001) correspond to warm conditions over the Laurentian fan (Keigwin and Pickart, 1999). This record was interpreted as a result of a northward migration of Warm Slope Water Current over the Laurentian fan, associated with a NAO minimum phase (Pickart *et al*. 1999). Furthermore, Keigwin and Pickart (1999) suggest that the NAO can be a model for climate variability during the Holocene, although results off West Africa do not support that suggestion (deMenocal *et al.*, 2000).

A more precise assessment and characterization of the surface waters is attained from the diatom analyses carried out on the same levels used for the 1750 yrs *N. pachyderma* (s) record of Keigwin and Pickart (1999) and evidently, no diatom paleoceanographic reconstructions have been carried out before at this location to investigate the variability of the Slope water. This allows us to better define the oceanographic changes occurring at this specific location to finally examine their relationship with the principal climatic factors suggested for the Holocene: the NAO and solar variability.

2. Regional settings

The Laurentian fan is located south of Newfoundland (Fig. 1). The modern distribution of surface currents over the Laurentian fan is characterized by the close juxtaposition of warm saline water masses of subtropical origin, and the flow of cold and relatively low saline water

of subpolar and Arctic origins. Therefore a strong temperature and salinity front results from the competing influence of water masses from opposite origins. The Slope Water Current (SWC) is a bifurcation of the Gulf Stream, a well mixed water found between 0 and 400 m depth, flowing primarily eastward (Gatien, 1976). Its border to cold waters from the North varies in response to changes in intensity of the Gulf Stream and of the Labrador Current. The SWC is therefore a major component of the circulation system over the area (Pickart *et al*., 1999). We can also infer more intense Labrador Slope current during NAO negative phases (Pickart, 1999).

The zone under the influence of the warm water of the Gulf Stream is nutrient limited, while the area under the influence of the Labrador Current is rather light limited (Afanasyev *et al*., 2001). Therefore, the physical and biological gradients are pronounced in this region: cold water rich in nutrients flows southward, whereas the warm water masses of the Gulf Stream flow northward.

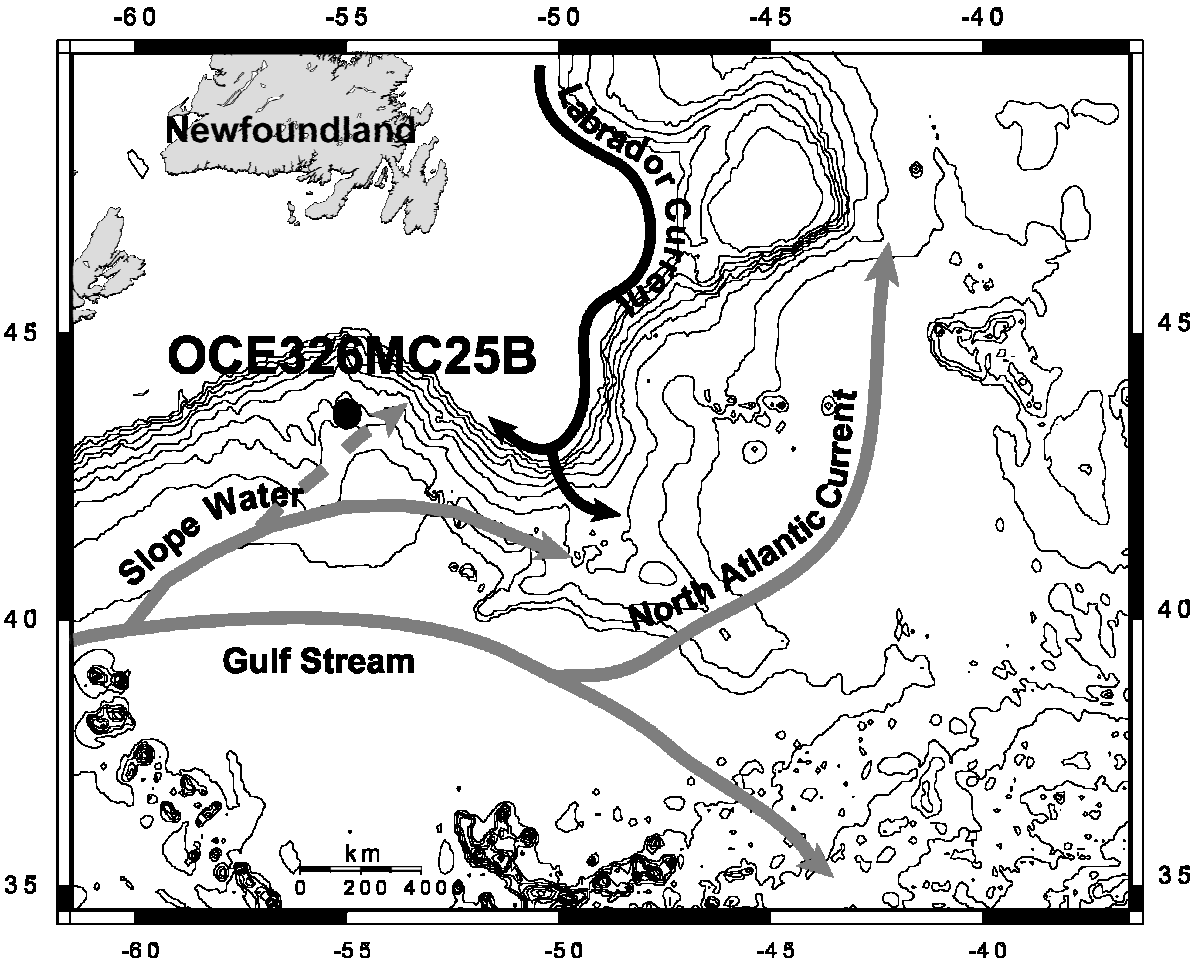

Figure 1: Schematic circulation in the region of the Grand Banks of Newfoundland after Pickart *et al*. (1999) and location of multicore OCE3026MC25B. Cold and warm currents are represented by black and grey arrows, respectively. The grey dashed arrow indicates the orientation that the Slope Water takes during a NAO-negative, in response to the strengthening of the Labrador Currrent.

3. Material and methods

The study is carried out on multicore OCE326 MC25B, retrieved from 3890 m water depth at the Laurentian deep sea fan (43º29'001N – 54º52'019W) in July 1998, on board the R/V Oceanus. The core is 48 cm long and was sampled every centimeter. We use an age model based on four radiocarbon dates, including zero age at the core top, made on mixed planktonic foraminifera (Keigwin and Pickart, 1999).

3.1 Organic Carbon

For the determination of the organic carbon content, 1 cm^3 of bulk sediment is dried and milled before being processed with a CHN-932 LECO elemental analyzer. The organic carbon content is calculated by the difference between total carbon and inorganic carbon determined in the same set of samples, before and after being subjected to combustion through a predefined stepwise temperature increase up to 400˚C. Analyses are performed on two replicates of 1 mg of dried and homogenized sediment per level. The accumulation rate of organic carbon ($mg/cm^2/yr$) is used.

3.2 Sample preparation for diatom analyses

Diatoms are extracted from ~ 1 g of bulk sediment, after calcium carbonate removal using HCl and organic matter oxidation using H_2O_2, according to the method of Abrantes *et al*. (2005). A variable aliquot of sample is sedimented on cover slips following Battarbee's method (1973). The cover slips are mounted on microscope slides using the optical adhesive "Norland" and diatoms are counted and identified at 1000 X magnification, using the counting protocol of Schrader and Gersonde (1978) and Abrantes (1988). At least 300 specimens are identified to define the diatom assemblage.

Diatom Accumulation Rates (DAR) are calculated as number of valves per cm^2/yr, according to Abrantes (1988), applying the following formula: total diatom abundance (number of valves per gram) x dry bulk density x sedimentation rate. Diatom quantification is realized for every sample, while diatom assemblage determination is roughly done for every other sample.

3.3 Diatom data

3.3.1 Definition of diatom groups

The diatom assemblages determined in this multicore are composed of taxa from very distinct environments: from subtropical water masses to sea-ice. 118 diatom species (45

genera) are identified; nine of those are fresh water species, but only few specimens were found. A few *Chaetoceros* resting spores as *Chaetoceros debilis* Cleve and *Chaetoceros furcellatus* Bailey, related to cold waters (Hasle *et al*., 1996) have been identified and are presented as "% of cold *Chaetoceros*". Diatom taxa are grouped as subtropical, sea-ice and cold water, based on the species related ecological data found in the literature and, in particular, on previous diatom studies conducted on surface sediments from the North Atlantic that demonstrate the relationship between diatom assemblages and surface hydrography (Maynard, 1976; Karpuz and Schrader, 1990; Kohly, 1998).

The group of diatoms related to subtropical environments does not include species considered as related to warm water in the previously mentioned studies, such as *Thalassionema nitzchioides* (Grunow) Grunow ex Hustedt and *Thalassiosira oestrupii* (Ostenfeld) Hasle. In this way, it is possible to separate species related to warmer subtropical waters of the Gulf Stream from the less warm water derived from it (like the North Atlantic Drift, as stated in the previous diatom studies from the North Atlantic). The subtropical group is composed of several species belonging to the following genera: *Asterolampra*, *Asteromphalus*, *Azpeitia*, *Bacteriastrum*, *Nitzschia*, *Rhizosolenia*, *Thalassionema*, and *Thalassiosira*. The sea-ice related group is mainly composed by resting spores of *Thalassiosira gravida* (Cleve) and several species of *Fragilariopsis*. Finally, the cold water group is composed by species of the genus *Thalassiosira* (vegetative cells of *T. gravida* / *T. antarctica*, *T. trifulta*, *T. poroseriata*, *T. nordenskioeldii*). Full species list is available in the PANGAEA data base under XXXXXX.

3.3.2 Temperature index

To assess changes in SST, a semi-quantitative temperature index based on the contribution of the different diatom groups is calculated as the ratio (% cold + % sea-ice diatoms) / (% warm + (% cold + % sea-ice diatoms)). A decrease in the index values indicates increasing temperatures. The total abundance of *Chaetoceros* spores is not included in the ratio calculation.

3.4 Lithic grains (IRD)

Quantification of lithic grains in the fraction of the sediment >150 µm has been done with a binocular microscope. Grains are classified according to their nature and shape and expressed in number of grains per gram. We refer to these grains as the ice-rafted debris (IRD) in Fig. 2.

3.5 Spectral Analysis

To facilitate the identification of periodic oscillations in the DAR record, the computer program REDFIT (Schulz and Mudelsee, 2002) has been used. This program helps to estimate if peaks in the power spectrum of the DAR are significant despite the red-noise background of relative short time series that register large variability.

4. RESULTS

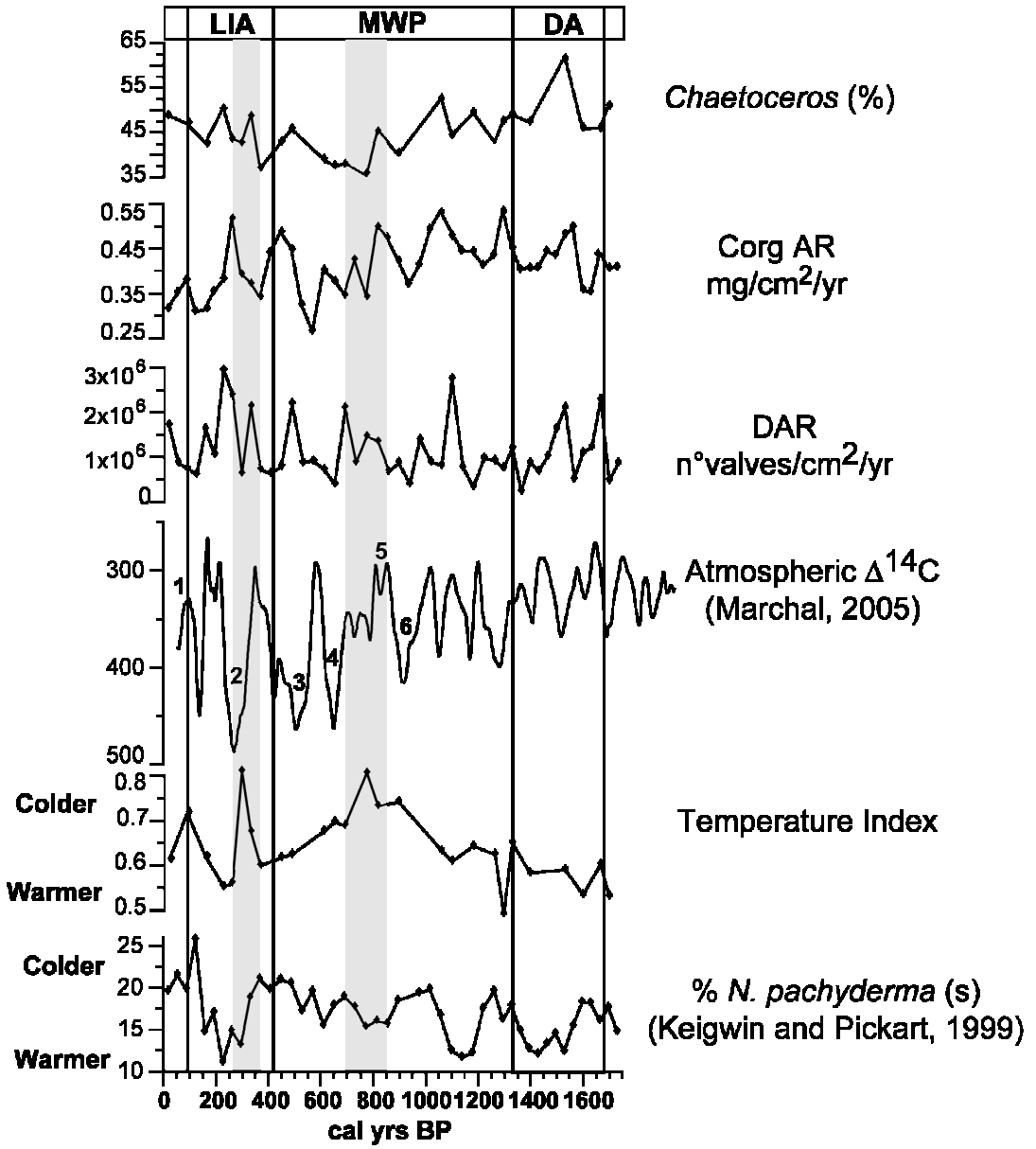

Figure 2: Paleoceanographic data from OCE326MC25B: Contribution of *Chaetoceros* (spores and vegetative cells), the most common genus in productive surface waters (Hustedt, 1930); Organic carbon accumulation rate (Corg AR), Diatom Accumulation Rate (DAR); Atmospheric $\Delta^{14}C$ (Marchal, 2005) with 1- Modern Maximum, 2-Maunder Minimum, 3-Spörer Minimum, 4-Wolf Minimum, 5-Medieval Maximum, 6-Oort Minimum (Dean, 2000); Diatom derived Temperature index (cold water taxa/(cold+warm taxa)); Contribution of *N pachyderma* (s) (Keigwin and Pickart, 1999).

4.1 Productivity

Diatom Accumulation Rate (DAR) shows centennial-scale variability with oscillations of two orders of magnitude between 0.33 x 10^5 and 2.93 x 10^6 valves /cm^2/year (Fig. 2) and points to three principal periods of relatively high productivity conditions as compared to surface sediment conditions (1.71x10^6 valves /cm^2/year): a period between 1700 and 1450 yr BP (with a maximum 2.28x10^6 valves /cm^2/year), including a pronounced decrease around 1600 yr BP (minimum of 5.05x10^5), a period between 850 and 700 yr BP (with DAR maximum of 2.09 x10^6), and finally a period between 250 and 150 yr BP (with DAR maximum of 2.93x10^6). In between, DAR levels are relatively low except at ~1100 yr BP (with 2.74x10^6 valves /cm^2/year).

The organic carbon accumulation rate (Corg AR) is also an indicator of productivity conditions (Wefer *et al*., 1999). The Corg AR oscillates between 0.02 and 0.05 mg/cm^2/year (Fig. 2). There are three periods of higher values: between 1550 and 1400 yr BP, between 1110 and 950 yr BP, and between 500 and 400 yr BP. From 1100 to 550 yr BP, the Corg AR decreases until reaching the minimum value of the entire record. Other marked minima in Corg AR are registered at ~1600 and at ~150 yr BP. Both proxies agree in the indication of an increase in productivity around 1100 yr BP and between 500 and 150 yr BP, and marked minima at ~1600 and 150 yr BP.

4.2 Temperature trends, lithic grains and temporal evolution of the diatom species and groups

The diatom temperature indications are mainly compared with the abundance of the lithic grains. These grains observed with a binocular microscope are angular quartz and are considered as ice-rafted debris (IRD), however down slope transport could have delivered them to the Laurentian fan from the point which they were originally ice rafted.

- From 1700 to 1100 yr BP, the diatom temperature index points to relatively warm surface waters (Fig. 3) determined by a higher contribution of *T. oestrupii* at ~1600 yr BP (Fig. 3) and by *T. nitzchioides* and *Rhizosolenia bergonii* (Peragallo) at ~1300 yr BP (Fig. 3). Between ~ 1550 and 1350 yr BP, the highest abundances of IRD in association with a better representation of fresh water diatoms marks an extreme event (Fig. 3).
- From 1100 to 800 yr BP, the diatom temperature index indicates a broad cooling (after a minor warm phase ~ 1100 yr BP indicated by a peak in *Rhizosolenia bergonii*), culminating precisely at ~800 yr BP, when a major peak in sea-ice diatom taxa (in particular

of resting spores of *Thalassiosira gravida* (Cleve)) is registered immediately followed by simultaneous peaks of IRD and fresh water diatoms.

- From 800 to 150 yr BP, surface waters warmed again progressively and this warming is only interrupted by a significant cold event at ~300 yr BP. This SST warming is closely linked to the rise of the warm water diatom *Thalassiosira oestrupii* and paralleled by a decrease in cold *Chaetoceros* (Fig. 3). The contribution of the subtropical diatom group is also relatively high and stable during this period.
- The cold event at ~300 yr BP is divided into three steps according to the diatom record (Fig. 3): first, the abundance of cold *Chaetoceros* increases, then, the groups of the cold and sea-ice related taxa (in particular, resting spores of *Thalassiosira gravida* and *Rhizosolenia styliformis* (Brighwell)) increase in association with a modest peak in IRD (without the occurrence of fresh water diatom), and finally the subtropical diatom group rises again. This event spanned almost a century.
- The temperatures started again to decline from 250 yr BP until ~100 yr BP, when a new cold event is expressed by an increase in IRD and a higher contribution of cold water diatoms. Since that time, temperatures rose until the Present.

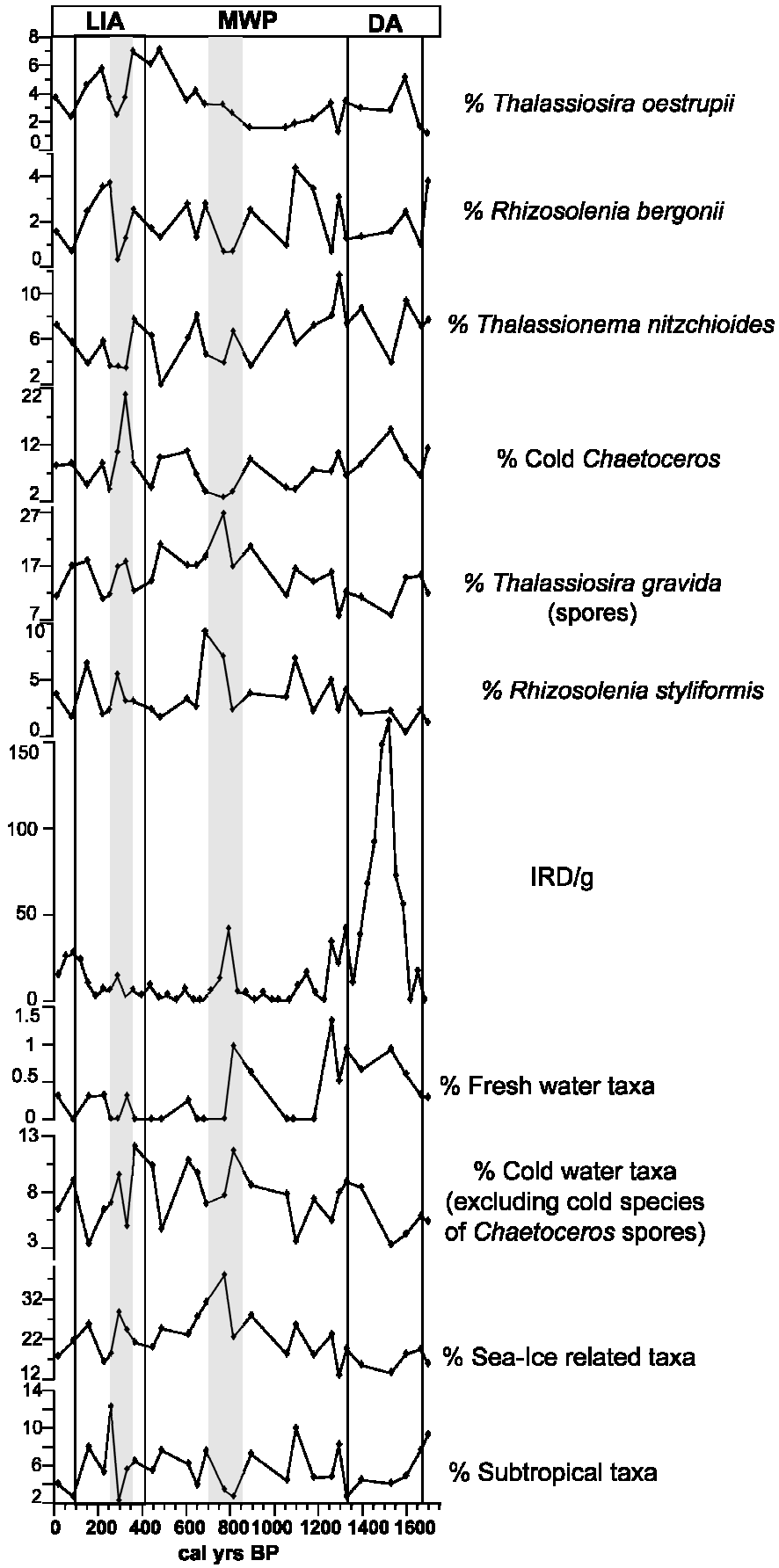

Figure 3: Distribution of diatom species and groups (in %) and IRD abundance along OCE326MC25B

5. Discussion

5.1 Main temperature changes indicated by the diatoms

The diatom record agrees with the *N. pachyderma* (s) indication of warm periods during the DA and the LIA (Keigwin and Pickart, 1999), through the increase in subtropical diatom species mainly during the LIA, and through the presence of warmer water indicated by *T. oestrupii* and *T. nitzchioides* during the DA. The warm signal during the DA is less clear because there are also evidences for cold water conditions: a major peak in IRD is registered at the same time of notable contributions of cold *Chaetoceros* species and fresh water taxa. Such data suggest the occurrence of a high productivity period triggered by the input of nutrients by melt water. Interestingly, this major peak in IRD is not clearly associated with the progression of the sea-ice related diatom group as it would be expected, suggesting that the IRD and fresh water diatom peaks are the expression of a turbidite derived from the Gulf of St Lawrence or the nearby continental slope. Indeed, this event is also associated with common benthic foraminifera of the nearshore genus *Elphidium* (L. Keigwin, unpublished data), a common genus in shallow water areas. Besides, the general shape of the fresh water diatom and IRD records (Fig. 3) present a similar pattern all along the core, suggesting a link between these two data sets, although the contribution of the fresh water diatom group never reaches the statistically significant level of 2% (highest contribution ~1250 and 800 yr BP with 1.3 % and 1 % respectively, always matching an IRD peak) and their concomitant rise frequently precedes a peak in abundance of sea-ice related diatoms. The coupling between IRD and fresh water diatom can be interpreted as strong evidence for a down slope flow during the DA. Furthermore, between 1600 and 150 yr BP, the waters on the Scotian Shelf were cold (Keigwin *et al*. 2003), confirming that the cold Labrador current flowed strong on the shelf, when the WSWC moved northward as it occurs during NAO negative phases (Pickart, 1999). Albeit the evidences for cold melt water input, this turbidite could also be a consequence of storminess or even seismic activity (regional seismic activity is e.g. reflected by the AD 1929 Grand Banks earthquake).

The diatom record additionally indicates two cold events at ~800 and 300 yr BP. The event at ~800 yr BP corresponds to a slight drop in the abundance of *N. pachyderma* (s) and at ~300 yr the event is even not perceived by the foraminifera data, suggesting strong water column stratification. Besides, those events have different oceanographic expressions. While the event at ~800 yr BP appears as a transitional phase in the record (from a cooling trend towards a centennial scale warming) and as the midpoint of a colder period, at ~300 yr BP the cold phase is in phase with the general climatic situation of the northern hemisphere, as it

is one of the two coldest periods of the last 600 yrs along the southern Norwegian continental margin (Berstadt *et al*., 2003) and it also corresponds to the maximum advance of the Swiss glaciers and the increase of sea-ice around Iceland in particular (Grove, 2001). Moreover, if the diatom temperature index is compared to the solar activity record (Fig. 2), both cold events correspond to particular solar activity phases: the Medieval Maximum and a period close to the Maunder Minimum (MM), considered as the climax of the LIA. A correlation that suggests that opposite solar intensities could have lead to similar oceanographic conditions (cold surface waters South of Newfoundland) and suggests also that the solar forcing has a great influence on the upper water column, with the Medieval Maximum implying warm conditions that possibly triggered the melting of the sea ice edge (evidences for melt water input, with maximum contribution of sea-ice diatoms preceded by a relative higher abundance of fresh water taxa associated to a peak in IRD) that increased the water flux from the Gulf of St Lawrence. In fact, although the first reports of ice drift passing through the Northern North Atlantic maritime routes appeared in 753 yr BP (Lamb, 1977), there is no evidence for an increased ice drift in this area at that time (Marchitto and Demenocal, 2003; Bond *et al*. 2001) which argues for a Gulf of St Lawrence origin for this water. Likewise, the reduced solar activity around 300 yr BP seems to have produced similar oceanic circulation changes, but the diatom record (higher contribution of sea-ice related diatoms in association with a modest abundance in IRD without fresh water diatom record preceded by a peak in the cold water diatom genus *Chaetoceros*) suggests rather a brief southward migration of the front, between cold nutrient rich water (supplied by a more intense supply of Labrador Slope water) and the more saline WSWC over the cored site. The different succession of environmental conditions suggested by the diatom record itself points to multidecadal scale variability. The MM (275 - 235 yr BP) is mainly caused by the conjunction of reduced solar activity (Eddy, 1976) and amplified volcanic activity (Briffa *et al*., 1998), what has lead to a significant cooling in various regions surrounding the North Atlantic Ocean (Luterbacher, 2001; Shindell *et al*., 2001). However, it is just one cold event and the Laurentian fan experienced warm conditions during most of the LIA. Besides, other historical changes in solar activity are not registered by the diatom record.

The warm periods over the Laurentian fan are a consequence of the strengthening of the Labrador Slope Water that displace in response the WSWC northward (Fig. 1) and corresponds to NAO negative phases (Pickart, 1999). A relationship between the solar forcing and the NAO has been suggested, with a reduced solar activity combined with an anthropogenic forcing generating negative phases of the NAO (Rind *et al*., 2004). Our

diatom derived water temperature changes over the Laurentian fan reflect oceanographic changes generated by the NAO (considering that a northward migration of warm water over the Laurentian fan occurs during NAO negative phases) and changes in solar activity.

5.2 Periodicity of the DAR

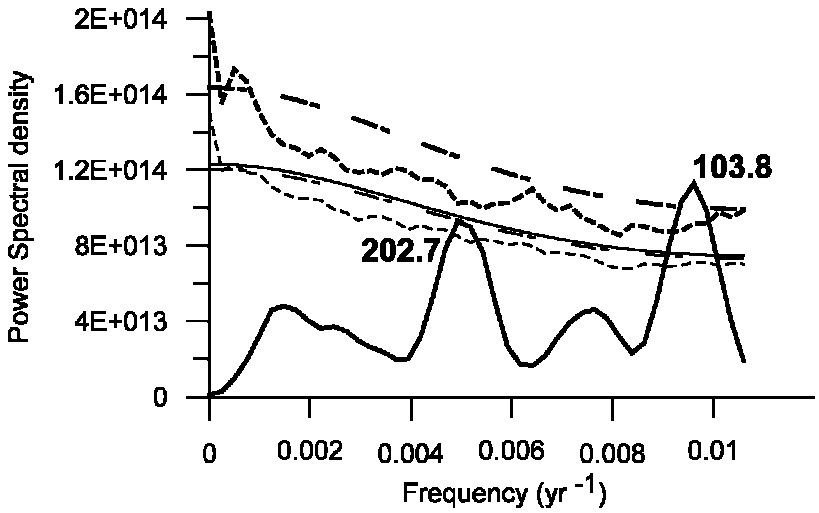

Figure 4: Power spectra of DAR with different confidence levels: bold solid line represents the spectrum estimate; dashed line 95% (regular) and 99% (bold) Monte-Carlo test; dash and point line 95% (regular) and 99% (bold) Chi-square test; solid line indicates the false alarm level.

Periodic fluctuations of the DAR (Fig. 4) are identified by spectral analyses realized by REDFIT (Schulz and Mudelsee, 2002). The most prominent cyclicity is 103.9 yrs, reaching a confidence level 99% in the Chi-square and Monte-Carlo probability tests, and a critical false-alarm level of 97.77 %. When the spectral peak exceeds this critical false-alarm level, it is considered significant (Schulz and Mudelsee, 2002). A second peak of 202.7 yrs is also noticed, but it is slightly too weak to exceed the critical false-alarm level and, it only reaches the confidence level of 95% with the Chi-square and Monte-Carlo probability tests.

The major periodicity of 103.9 yrs is in the range of the Gleissberg cycle (Gleissberg, 1944), a cycle that has a wider frequency band than initially thought, with frequencies between 60-130 yrs (Ogurtsov *et al*., 2002) or 80-120 yrs over the last two and a half centuries (Henkel, 1971; Garcia and Mouradian, 1998). The second notable (but weaker) periodicity of 202.7 years is also in the range of another solar periodic fluctuation of ~208-212 years, the Suess cycle (Suess and Linick, 1990). Considering the uncertainties of the dating method (± 25 to 45 years), it is plausible that the registered frequency peaks correspond to those solar cycles.

The main century scale variability discerned in the Laurentian fan DAR record is also found in other marine records from the Great Bahama bank (Roth and Reijmer, 2005), the

Caribbean and tropical North Atlantic (Black *et al*., 2004) as well as in lakes of the Yucatan Peninsula (Hodell *et al*., 2001). Most of those records come from tropical latitudes and the two last mentioned records suggest that the solar forcing interfere in the balance of the ITCZ and in the strength and position of the Hadley circulation cell. The minor warm phase at ~1100 yr BP (especially perceived by *N. pachyderma* (s) this time) over the Laurentian fan corresponds also to a period of drought in Yucatan between 925-1200 yr BP and that might reflect a southward migration of the Intertropical Convergence Zone (ITCZ) (Hodell *et al*., 2001), evidencing a weakening of the Gulf Stream, in agreement with a NAO negative phase and the present record. Between the subtropical areas of the North Atlantic and the Laurentian fan area, the link could be made through the NAO and its relationship with the ITCZ. The link between changes in the intensity and position of the ITCZ and the NAO would be at a decadal time scale (Rajagopalan *et al.*, 1998; Bojariu and Reverdin, 2002), and even though the NAO is not a condition for the Tropical Atlantic variability, it appears as a factor that could significantly influence it (Wu and Liu, 2002), with the NAO likely interfering with the trade winds of the tropical North Atlantic (George and Saunders, 2001).

In conclusion, the SST changes inferred from the diatom record are synchronous with changes occurring in the tropical zone and it suggests that the NAO and its relation to insolation are important factors affecting the circulation of the North Atlantic, on a basin-wide scale.

Conclusions

Over the past 1750 yr BP, foraminifera and diatom studies highlight two warm periods over the Laurentian fan between 1700 and 1100 yr BP and from 500 to 150 yr BP. Periods evidenced by a clear decrease in abundance of *N. pachyderma* (s) and an increase in warm water diatom species that coincide with the DA and the LIA, respectively.

Diatom evidence seems to provide a better record of the upper surface layer relatively to the *N. pachyderma* (s), revealing additional cold events centered at ~800 and 300 yr BP. Short cold events that appear to only affect the upper surface layers (around the upper 50 m) and are associated to the Medieval Maximum and the MM, respectively.

The local warm periods are interpreted as due to a northward migration of Slope Water Current in response to the intensification of the Labrador Current during the cold historic episodes (especially during the LIA) and related to the NAO negative phase as suggested before by Keigwin and Pickart (1999).

The high-resolution record over the Laurentian fan apparently presents the imprints of oceanic circulation changes induced by the NAO, but also the impact of the solar forcing. The periodicities of the record also sustain the hypothesis that solar variability can be a forcing mechanism for the climate at a centennial time scale, by interfering directly on the circulation of oceanic superficial water.

Acknowledgments

This work has been supported by the Fundação para a Ciência e Tecnologia - FCT (BD - 18317/2004) and European Social Fund (ESF) through the 3rd EU Framework Program. We are grateful to A. Inês and Cremilde Monteiro for laboratory technical support in the sample preparation for diatom and organic carbon analysis at the INETI-Laboratory of Marine Geology and to Michael Schulz for help and explanations when using REDFIT program.

APPENDIX
Diatom species found in OCE326MC25B

Cold water species:
Asteromphalus hookeri (Ehrenberg)
Asteromphalus hyalinus (Karsten)
Chaetoceros debilis (Cleve)
Chaetoceros furcellatus (Bailey)
Coscinodiscus undulosus (Mann)
Fragilariopsis rhombica (Hustedt)
Grammatophora arcuata (Ehrenberg)
Probosciaia alata (Brightwell) Sundström
Rhizosolenia hebetata (Bailey)
Thalassiosira antarctica (Comber)
Thalassiosira angulata (Gregory) Hasle
Thalassiosira kushirensis (Takano)
Thalassiosira maculata (Fryxell et Johansen)
Thalassiosira nordenskioeldii (Cleve)
Thalassiosira perpusilla (Kozlova)
Thalassiosira poroseriata (Ramsfjell) Hasle
Thalassiosira trifulta (Fryxell)
Thalassiotrix longissima (Cleve et Grunow)

Ice related species:
Bacteriosira fragilis (Gran) (Syn.: *Bacteriosira bathyomphala* (Cleve))
Fragilariopsis cylindrus (Gnunow) Krieger in Helmcke et Krieger
Fragilariopsis oceanica (Cleve) Hasle (Syn.: *Nitzchia grunowii* (Hasle))
Porosira glacialis (Grunow) Jörgensen
Rhizosolenia styliformis (Brightwell)
Thalassiosira gravida (Cleve) - spore
Thalassiosira guillardii (Hasle)

Subtropical species:
Asterolampra marylandica (Ehrenberg)
Asteromphalus flabellatus (Brébisson) Greville
Azpeitia africana (Janisch ex Schmidt) Fryxell et Watkins
Azpeitia neocrenulata (Van Landingham) Fryxell et Watkins
Azpeitia nodulifera (Schmidt) Fryxell et Sims
Bacteriastrum comosum (Pavillard)
Cymatosira lorenziana (Grunow in Van Heurck)
Fragilariopsis doliolus (Wallich) Medlin et Sims
Grammatophora hamulifera (Kützing)
Hemidiscus cuneiformis (Wallich)
Nitzschia capsuspaleae (Simonsen)
Nitzschia cuspidata (Hasle)
Nitzschia interruptestriata (Simonsen)
Nitzschia kolaczeckii (Grunow)

Nitzschia marina (Grunow in Cleve et Grunow)
Nitzschia sicula (Castracane) Hustedt
Rhizosolenia bergonii (Peragallo)
Rhizosolenia fallax (Sundström)
Roperia tessalata (Roper) Grunow in Van Heurck
Thalassionema frauenfeldii (Grunow) Hallegraeff
Thalassiosira aestivalis (Gran)
Thalassiosira ferelineata (Hasle et Fryxell)
Thalassiosira leptopus (Grunow) Hasle et Fryxell
Thalassiosira lineata (Jousé)
Thalassiosira punctifera (Grunow) Fryxell

Other warm water species:
Thalassionema nitzchioides (Grunow) Grunow ex Hustedt
Thalassiosira oestrupii (Ostenfeld) Hasle

Coastal species
Coscinodiscus rothii (Ehrenberg) Grunow
Cyclotella striata (Kützing) Grunow
Nitzschia lacunarum (Hustedt)
Nitzschia ovalis (Arnott in Cleve et Grunow)
Psammodyction panduriforme (Gregory) Mann
Rhaphoneis amphiceros (Ehrenberg)
Rhizosolenia pungens (Cleve-Euler)
Thalassiosira baltica (Grunow) Ostenfeld
Thalassiosira conferta (Hasle in Hasle and Fryxell)
Thalassiosira eccentrica (Ehrenberg) Cleve

Fresh water species
Cyclotella bodanica var. affinis (Grunow) Cleve-Euler
Fragilaria capucina (Kützing) Lange-Bertalot
Nitzschia capitellata (Hustedt)
Nitzschia linearis (Agardh) Smith
Nitzschia rosenstoeckii (Lange-Bertalot)
Martyana martyi (Héribaud) Round
Melosira ambigua (Grunow) Müller
Sellaphora bacillum (Ehrenberg) Mann
Thalassiosira delicatula (Hustedt)

Marine species not giving information about the temperature
Actinocyclus octonarius (Ehrenberg)
Actinoptychus senarius (Ehrenberg) Ehrenberg
Amphora lybica (Ehrenberg)
Chaetoceros spp.
Chaetoceros atlanticus (Cleve)
Chaetoceros diadema (Ehrenberg) Gran (syn. *Chaetoceros subsecundus* (Grunow) Hustedt)
Chaetoceros radicans (Schütt)
Chaetoceros vixvisibilis (Schiller)
Cocconeis aff. peltoides (Hustedt)
Cocconeis disculus (Schumann) Cleve in Cleve et Jentzsch
Cocconeis scutellum (Ehrenberg)
Coscinodiscus asteromphalus (Ehrenberg)
Coscinodiscus divisus (Grunow)
Coscinodiscus marginatus (Ehrenberg)
Coscinodiscus oculus-iridis (Ehrenberg)
Coscinodiscus radiatus (Ehrenberg)
Coscinodiscus vetustissumus (Pantocsek)
Cymatosira belgica (Grunow)
Delphineis surirella (Ehrenberg) Andrews
Delphineis sachalinensis (Shehshukova-Poretskaya)
Denticulopsis sp.
Diploneis bombus (Ehrenberg) Ehrenberg ex Cleve
Diploneis smithii (Brébisson) Cleve
Diploneis suborbicularis (Gregory) Cleve
Diploneis weissflogii (Schmidt) Cleve
Fragilariopsis sublinearis (Heurck) Heiden
Leptocylindrus danicus (Cleve) - spore
Lyrella atlantica (Schmidt) Mann
Navicula cancellata (Donkin)
Navicula directa (Smith) Ralfs in Pritchard
Navicula jamalinensis (Cleve in Cleve et Grunow)
Nitzschia dietrichii n.sp.
Nitzchia pseudonana (Hasle)
Odontella aurita (Lyngbye) Agardh
Odontella mobiliensis (Bailey) Grunow
Paralia sulcata (Ehrenberg) Cleve
Plagiogramma tesselatum (Greville)
Pleurosigma normanii (Ralfs in Pritchard)
Podosira stelliger (Bailey) Mann

Psammodiscus nitidus (Gregory) Round et Mann
Rhizosolenia imbricata (Brightwell)
Rhizosolenia setigera (Brightwell)
Surirella fastuosa var. cuneata (Peragallo et Peragallo)
Thalassiosira aff. plicata (Schrader)
Thalassiosira anguste lineata (Schmidt) Fryxell et Hasle
Trachyneis aspera (Ehrenberg) Cleve
Triceratium alternans (Bailley) Mann

Note: *Paralia sulcata* (Ehrenberg) Cleve is not included in any thermal group as it is considered by Maynard (1976) as a subpolar species, while Karpuz Koç and Schrader (1990) associate it to the warm waters of the North Atlantic.

References

Abrantes, F. (1988), Diatoms assemblages as upwelling indicators in surface sediments off Portugal, *Marine Geology*, *85*, 15-39.

Abrantes, F., Gil, I., Lopes, C., Castro, M. (2005), Quantitative diatom analyses-a faster cleaning procedure, *Deep-Sea Research I*, *52*, 189-198.

Afanasyev, Y. D., Nezlin, N. P., Kostianoy, A. G. (2001), Patterns of seasonal dynamics of remotely sensed chlorophyll and physical environment in the Newfoundland region, *Remote Sensing of Environment*, *76*, 268-282.

Andersen, C., Koç, N., Jennings, A., Andrews, J. T. (2004), Nonuniform response of the major surface currents in the Nordic Seas to insolation forcing: Implications for the Holocene climate variability, *Paleoceanography*, 19 doi: 10.1029/2002PA000873.

Appenzeller, C., Stocker, T. F., Anklin, M. (1998), North Atlantic Oscillation dynamics recorded in Greenland ice cores, *Science*, *282*, 446-449.

Battarbee, R. W. (1973), A new method for estimation of absolute microfossil numbers with reference especially to diatoms, *Limnography and Oceanography*, *18*, 647-652.

Berstad, I., Sejrup, H. P., Klitgaard-Kristensen, D., Haflidason, H. (2003), Last 600 years variability in temperature and geometry of the Norwegian current: stable isotope and grain size evidence from the Norwegian Margin, *Journal of Quaternary Science*, *18*, 591-602.

Black, D. E., Thunell, R. C., Kaplan, A., Peterson, L. C., Tappa, E. J. (2004), A 2000-year record of Caribbean and tropical North Atlantic hydrographic variability, *Paleoceanography*, *19*, PA2022, doi:10.1029.

Bojariu, R. and G. Reverdin (2002), Large-scale variability modes of freshwater flux and precipitation over the Atlantic, *Climate Dynamics*, *18*, 369-381.

Bond, G., Kromer, B., Beer, J., Muscheler, R., Evans, M. N., Showers, W., Hoffmann, S., Lotti-Bond, R., Hajdas, I., Bonani, G. (2001), Persistent solar influence on north Atlantic climate during the Holocene, *Science*, *294*, 2130-2136.

Briffa, K. R., Jones, P. D., Schweingruber, F. H., and T. J. Osborn (1998), Influence of volcanic eruptions on Northern Hemisphere summer temperature over the past 600 years, *Nature*, *393*, 450-455.

Broecker, W. S. (2001), Was the Medieval Warm Period global?, *Science*, *291*, 1497-1499.

Cronin, T. M., Dwyer, G. S., Kamiya, T., Schwede, S., Willard, D. A. (2003), Medieval Warm Period, Little Ice Age and 20th century temperature variability from Chesapeake Bay, *Global Planet Change*, *36*, 17-29.

Dean, W. E. (2000), The sun and climate, *U. S. Geological Survey Fact Sheet*.

deMenocal, P., Ortiz, J., Guilderson, T., Sarnthein, M. (2000), Coherent high-and-low-latitude climate variability during the

Holocene warm period, *Science*, *288*, 2198-2202.

Dickson, R., Lazier, J., Meincke, J., Rhines, P., Swift, J. (1996), Long-term coordinated changes in the convective activity of the North Atlantic, *Progress in Oceanography*, *38*, 241-295.

Dutkiewicz, S., Follows, M., Marshall, J., Gregg, W. W. (2001), Interannual variability of phytoplankton abundances in the North Atlantic, *Deep-Sea Research II*, *48*, 2323-2344.

Eddy, J. A. (1976), The Maunder Minimum, *Science*, *192-4245*, 1189-1202.

Gallager, S. M., Davis, C. S., Epstein, A. W., Solow, A., Beardsley, R. C. (1996), High-resolution observations of plankton spatial distributions correlated with hydrography in the Great South Channel, Georges Bank, *Deep-Sea Research II*, *43 (7-8)*, 1627-1663.

Garcia, A. and Z. Mouradian (1998), The Gleissberg cycle of minima, *Solar Physics*, *180*, 495-498.

Gatien, G. (1976), A study of the Slope Water region south of Halifax, Journal of the Fisheries Research Board of Canada, *33*, 2213-2217.

George, S. E. and M. A. Saunders (2001), North Atlantic Oscillation impact on tropical north Atlantic winter atmospheric variability, *Geophysical Research Letters*, *28*, 1015-1018.

Gil, I., Abrantes, F., Hebbeln, D. (in press), The North Atlantic Oscillation forcing through the last 2000 years: spatial variability as revealed by high resolution marine diatom records from N and SW Europe, *Marine Micropaleontology*.

Gleissberg, W. (1944), A secular change in the shape of the spot-frequency curve, *The Observatory*, *65*, 244.

Grove, J. (2001), The onset of the LIA, in *History and Climate - Memories of the Future?*, edited by P. D. Jones, Ogilvie, A. E. J., Davies, T. D., Briffa, K. R., pp. 153-186, Kluwer Academic/Plenum Publishers, New York.

Hasle, G. R., Syversten, E. E., Steidinger, K. A., Tangen, K. (1996), Marine diatoms, in *Identifying marine diatoms and dinoflagellates*, edited by C. R. Tomas, Academic Press, Inc., San Diego, 598 pp.

Henkel, R. (1971), A feature of the secularly smoothed maxima of sunspot frequency, *Solar Physics*, *20*, 345-347.

Hodell, D. A., Brenner, M., Curtis, J. H., Guilderson, T. (2001), Solar forcing of drought frequency in the Maya lowlands, *Science*, *292*, 1367-1370.

Hurrell, J. W. (1995), Decadal trends in the North Atlantic Oscillation: Regional temperatures and precipitation, *Science*, *269*, 676-679.

Hustedt, F. (1930), Die Kieselalgen. Deutschlands, Österreichs und der Schweiz, edited, p. 920, Otto Koeltz Science Publishers, Koenigstein.

Jones, P. H., Osborn, T. J., Briffa, K. R. (2001), The evolution of climate over the last Millenium, *Science*, *292*, 662-667.

Karpuz Koç, N., Jansen, E. (1992), A high-resolution diatom record of the last deglaciation from the SE Norwegian Sea: documentation of rapid climatic changes, *Paleoceanography*, *7*, 499-520.

Keigwin, L. D. (1996), The Little Ice Age and Medieval Warm Period in the Sargasso Sea, *Science*, *274*, 1504-1508.

Keigwin, L. D. and R. S. Pickart, (1999), Slope water current over the Laurentian Fan on interannual to millenial time scales, *Science*, *286*, 520-523.

Keigwin, L. D., Sachs, G. A., Rosenthal, Y. (2003), A 1600-year history of the Labrador Current off Nova Scotia, *Climate Dynamics*, *21*, 53-62.

Kohly, A. (1998), Diatom flux and species composition in the Greenland Sea and the Norwegian Sea in 1991-1992, *Marine Geology*, *145*, 293-312.

Kristensen, D. K., Sejrup, H. P., Haflidason, H., Berstad, I. M., Mikalsen, G. (2004), Eight-hundred-year temperature variability from the Norwegian continental margin and the North Atlantic thermohaline circulation, *Paleoceanography*, 19, PA2007, doi:10.1029/2003PA000960.

Lamb, H. H. (1977), *Climate, History and the Modern World*, 835 pp., Methuen & Co. Ltd, London.

Loder, J. W., Shore, J. A., Hannah, C. G., Petrie, B. D. (2001), Decadal-scale hydrographic and circulation variability in the Scotia-Maine region, *Deep-Sea Research II*, *48*, 3-35.

Luterbacher, J. (2001), The Late Maunder Minimum (1615-1715) - Climax of the "Little Ice Age" in Europe, in *History and Climate - Memories of the Future?*, edited by P. D. Jones, Ogilvie, A. E. J., Davies, T. D., Briffa, K. R., pp. 29-54, Kluwer Academic/Plenum Publishers, New York.

Marchal, O. (2005), Optimal estimation of atmospheric C-14 production over the Holocene: paleoclimate implications, *Climate Dynamics*, *24*, 71-88.

Marchitto, T. M., deMenocal, P. B. (2003), Late Holocene variability of upper North Atlantic Deep Water temperature and salinity, Geochemistry, Geophysics, Geosystems, 4 (12), 1100, doi 10.1029/2003GC000598.

Maynard, N. G. (1976), Relationship between diatoms surface sediments of the Atlantic Ocean and the biological response and physical oceanography of overlying waters, *Paleobiology*, *2*, 99-121.

McDermott, F., Mattey, D. P., Hawkesworth, C. (2001), Centennial-scale holocene climate variability revealed by a high-resolution speleothem delta O-18 record from SW Ireland, *Science*, *294*, 1328-1331.

McKenzie, C. H., Deibel, D., Thompson, R. J., MacDonald, B. A., Penney, R. W. (1997), Distribution and abundance of choanoflagellates (acanthoecidae) in the coastal cold ocean of Newfoundland, Canada, *Mar Biol*, *129*, 407-416.

Ogurtsov, M. G., Nagovitsyn, Y. A., Kocharov, G. E., Jungner, H. (2002), Long-period cycles of the Sun's activity recorded in direct solar data and proxies, *Solar Physics*, *211*, 371-394.

Okumura, Y., Xie, S. P., Numaguti, A., Tanimoto, Y. (2001), Tropical Atlantic air-sea interaction and its influence on the NAO, *Geophysical Research Letters*, *28*, 1507-1510.

Pickart, R. S., McKee, T. K., Torres, D. J., Harrington, S. A. (1999), Means structure and interannual variability of the Slopewater system South of Newfoundland, *Journal of Physical Oceanography*, *29*, 2541-2558.

Rajagopalan, B., Kushnir, Y., Tourre, Y. M. (1998), Observed decadal midlatitude and tropical Atlantic climate variability, *Geophysical Research Letters*, *25*, 3967-3970.

Rind, D., Shindell, D., Perlwitz, J., Lerner, J., Lonergan, P., Lean, J., McLinden, C. (2004), The relative importance of solar and anthropogenic forcing of climate change between the Maunder Minimum and the present, *Journal of Climate*, *17*, 906-929.

Roth, S. and J. J. G. Reijmer (2005), Holocene millennial to centennial carbonate cyclicity recorded in slope sediments of the Great Bahama Bank and its climatic implications, *Sedimentology*, *52*, 161-181.

Schrader, H. J., Gersonde, R. (1978), Diatoms and Silicoflagellates, *Utrecht Micropaleontological Bulletin*, *17*, 129-176.

Schulz, M., Mudelsee, M. (2002), REDFIT: estimating the red-noise spectra directly from unevenly spaced paleoclimatic time series, *Computers and Geosciences*, *28*, 421-426.

Shindell, D. T., Schmidt, G. A., Mann, M. E., Rind, D., Waple, A. (2001), Solar forcing of regional climate change during the Maunder Minimum, *Science*, *294*, 2149-2152.

Stangeew, E. (2001), Distribution and isotopic composition of living planktonic foraminifera *N. pachyderma* (sinistral) and *T. quinqueloba* in the high latitude North Atlantic, Ph. D thesis, 90 p. Christian-Albrechts-Universitat zu Kiel, Kiel.

Stuiver, M., Reimer, P. J., Bard, E., Beck, W., Burr, G. S., Hughen, K. A., Kromer, B., McCormac, G., van der Plicht, J., Spurk, M. (1998), INTCAL98 radiocarbon age calibration, 24,000-0 cal BP, *Radiocarbon*, *40*, 1041-1083.

Suess, H. E. and T. W. Linick (1990), The C-14 Record in Bristlecone-Pine Wood of the Past 8000 Years Based on the Dendrochronology of the Late Ferguson,C.W., *Philosophical Transactions of the Royal Society of London* A, *330*, 403-412.

Umoh, J. U. (1992), Seasonal and interannual variability of sea temperature and surface heat fluxes in the Northwest Atlantic, 237 pp, PhD thesis, Dalhousie University, Halifax.

Visbeck, M. (2002), The ocean's role in Atlantic climate variability, *Science*, *297*, 2223-2224.

Wefer, G., Berger, W. H., Bijma, J., Fischer, G. (1999), Clues to ocean History: a brief overview of proxies, in *Use of proxies in paleoceanography: examples from the South Atlantic*, edited by G. Fischer, Wefer, G., pp. 1-68, Springer-Verlag, Berlin Heidelberg.

Wu, L. X. and Z. Y. Liu (2002), Is Tropical Atlantic Variability driven by the North Atlantic Oscillation?, *Geophysical Research Letters*, *29*, 10.1029/ 2002GL016492.

CHAPTER 9:

CONCLUSIONS

The comparison of the three regions considered in this study provides important information for the spatial reconstruction of the oceanographic circulation, and in particular of the effects of spatial and temporal variable climatic forcing over the last 2000 yrs. The NAO pattern appears as a good analog to explain the main climatic periods (DA, MWP and LIA). However, at the regional scale, the observed variability could not always be explained by the NAO, which implies that at specific sites part of the variability is due to more regional dynamics.

The historical cold periods (DA and LIA) left a better imprint in the diatom records than the warmer periods, as only the MWP is registered and there is no specific evidence for general record of the RWP. At all sites, the cold periods are evidenced by a clear and strong change in the environmental conditions: at the Skagerrak, diatom dissolution occurred and over the Laurentian fan, new diatom assemblages prevailed. At the Tagus pro-delta, the records of the DA and the LIA differ and are explained on the basis of its latitudinal position, on the limit of direct subtropical influence (Azores high pressure center), that is also important in determining climate at this latitude. On the other side, the Laurentian fan record reveals a temperature signal in anti-phase with the eastern North Atlantic locations: the historical cold periods are recorded here as a warming of the surface waters, a situation that at Present occurs during NAO negative phases. Such results appeal for higher resolution studies to determine the response of the oceanic system at a more precise scale.

Nevertheless, the timing of major oceanographic changes for each record suggests indeed a common forcing of wide expression. At the European margin, the DA spread from AD 400 to 650, the MWP from AD 800 to 1200 and the LIA from 1350 to 1900. Over the Laurentian fan, the DA occur between AD 350 and 600, the MWP between AD 750 and 1550 and the LIA between AD 1550 and 1850.

The diatom records also present the imprints of solar forcing. Not only by reflecting some specific changes in solar activity as the Medieval Maximum or the Maunder Minimum, over the Laurentian fan, but also by the frequencies registered in the record. Changes in the oceanic circulation are linked to solar variability and the relationship between NAO and solar forcing has also been established, with negative solar forcing generating negative phase of the NAO.

Diatoms reflect the conditions in the upper oceanic surface layer and they are a good proxy to assess changes in oceanographic circulation, especially in terms of water masses that have a specific salinity and / or thermal signature. The detection of periodicities in the record makes the acquisition of longer diatom records for the late Holocene an interesting perspective, as it will permit to check the presence of longer periodicities, such as the millennial solar periodicity already found in marine records or the 512 yrs cycle linked to the thermohaline circulation. High-resolution records will allow to confirm and / or precise shorter periodicities, already identified.

Besides the diatom paleoreconstructions presented in this thesis, some methodological aspects of diatom analyses are investigated by trying to ameliorate the slide preparation method (mainly speeding up the cleaning procedure) and by testing the reliability of the diatom record in an area subjected to silica dissolution. The new cleaning procedure elaborated reduces the time that sediment samples need to stay in the laboratory and was used afterwards on the studied material. The improvement of this new method resides in not drying the bulk sediment and in dispersing it before removing the carbonates and the organic matter. Such a gain in time permits to treat more samples and to have more time to analyze more samples, what is of major interest to provide high resolution records. The second methodological aspect aiming in demonstrating the reliability of the diatom proxy, even in area of important silica dissolution, relies in the comparison of very high-resolution paleorecords with instrumental data. The results obtained from two box-cores from the Tagus pro-delta demonstrated that the presence of diatoms by itself in the sediment is a signal of productivity. Furthermore, the comparison of fresh water diatom and *Chaetoceros* abundances with the total diatom abundance permits to discriminate the trigger of the productivity recorded, that might be generated either by higher river flow or by upwelling events. Finally, another methodological aspect examined is the diatom valve size variation in the Skagerrak material. Its relationship with salinity and productivity is still to be defined, but the observation of *Paralia sulcata* (Ehrenberg) Cleve valve size in the Skagerrak core in comparison with productivity and salinity indicators provides more evidence for a negative correlation between diatom valve size and salinity, without excluding a link to productivity.

Finally, comparison of diatom records with other proxy records from the same sample material demonstrated that diatoms better record changes in surface water properties and provide more information about environmental conditions as they cover a very wide range of

environmental conditions (temperature and salinity). Over the Laurentian fan, they confirm temperatures changes indicated by the foraminifera record, but also reveal cold events in the surface waters not perceived by the foraminifera.

In conclusion, diatom analyses offer a wide range of possibilities for paleoreconstructions (additionally to the elaboration of diatom temperature and preservation indices), allowing to address a variety of paleoenvironmental parameters. Their reliability as a proxy for paleoenvironmental reconstructions has been demonstrated, thereby support for their use for further paleoreconstructions.